Characterizing the Load Environment of Washington State Ferry and Alaska Marine Highway Ferry Landings

WA-RD 804.1

Andrew T. Metzger
Jason Kwiatkowski
Jonathan Hutchinson

May 2013

Washington State Department of Transportation
Office of Research & Library Services

WSDOT Research Report

TECHNICAL REPORT STANDARD TITLE PAGE

1. REPORT NO.	2. GOVERNMENT ACCESSION NO.	3. RECIPIENTS CATALOG NO
WA-RD-804.1		

4. TITLE AND SUBTILLE	5. REPORT DATE
Characterizing the Load Environment of Washington State Ferry and Alaska Marine Highway Ferry Landings	May 2013
	6. PERFORMING ORGANIZATION CODE AUTC # 309001
7. AUTHOR(S) Andrew T. Metzger, Ph.D., P.E., Jason Kwiatkowski, EIT, Jonathan Hutchinson, EIT	8. PERFORMING ORGANIZATION REPORT NO. INE/AUTC 13.04
9. PERFORMING ORGANIZATION NAME AND ADDRESS Alaska University Transportation Center P.O. Box 755900 Fairbanks, AK 99775-5900	10. WORK UNIT NO.
	11. CONTRACT OR GRANT NO. DTRT06-G-0011
12. CPONSORING AGENCY NAME AND ADDRESS Alaska Department of Transportation, Research, Development, and Technology Transfer 2301 Peger Road,Fairbanks, AK 99709-5399 Office of Research and Library Services, Washington State Department of Transportation PO Box 47372, Olympia WA 98504-7372	13. TYPE OF REPORT AND PERIOD COVERED Final Report (9/09-3/13)
	14. SPONSORING AGENCY CODE

15. SUPPLEMENTARY NOTES

This study was conducted in cooperation with the U.S. Department of Transportation, Federal Highway Administration and Alaska Dept. of Transportation and Public Facilities

16. ABSTRACT

Anybody riding a ferry wants it to dock safely — and for port managers, having passengers and goods in the water is never a good thing. This project aims to mitigate uncertainty and assumptions about load demands on ferry terminal structures, specifically, ferry landing structures. The project will provide information needed to safely and efficiently design ferry berthing and landing facilities, decrease the uncertainty in design criteria, and remove assumptions associated with procedures traditionally used to design these structures. For Alaska Marine Highway System facilities, loads imposed on dolphin structures and mooring line loads are of most concern. Due to a lack of information about the magnitude of these loads or how they may be determined, AMHS engineers are forced to make (sometimes gross) design assumptions. The Washington State Ferry System also confronts these uncertainties, specifically in the design of wingwall structures that accept vessels during loading/unloading of passengers and vehicles. While the structures used by AMHS and WSFS have fundamental differences, the metrics needed to determine appropriate design criteria are the same. Thus, the instrumentation used to monitor these facilities in operation is also similar. These similarities present an opportunity for a cost-sharing project in which the ADOT&PF and Washington State DOT are able to leverage research funding and benefit from a much more comprehensive project than either might be able to support individually. To achieve this project's goals, the research team will acquire a robust statistical sample of the metrics (strains and displacements) needed to define the design criteria (loads from vessels and waves). The data will be gathered via in situ monitoring of in-service acilities, specifically, the AMHS terminal at Auke Bay near Juneau, Alaska, and the WSF Seattle terminal in Washington.

17. KEY WORDS	18. DISTRIBUTION STATEMENT
Berthing facilities (Pmhbmpmbrf), Docking (Dcnbscsd), Ferries (Qbhdht), Marine transit (Aetw)	

19. SECURITY CLASSIF. (of this report)	20. SECURITY CLASSIF. (of this page)	21. NO. OF PAGES	22. PRICE
None	None		

SI* (MODERN METRIC) CONVERSION FACTORS

APPROXIMATE CONVERSIONS TO SI UNITS

Symbol	When You Know	Multiply By	To Find	Symbol
		LENGTH		
in	inches	25.4	millimeters	mm
ft	feet	0.305	meters	m
yd	yards	0.914	meters	m
mi	miles	1.61	kilometers	km
		AREA		
in^2	square inches	645.2	square millimeters	mm^2
ft^2	square feet	0.093	square meters	m^2
yd^2	square yard	0.836	square meters	m^2
ac	acres	0.405	hectares	ha
mi^2	square miles	2.59	square kilometers	km^2
		VOLUME		
fl oz	fluid ounces	29.57	milliliters	mL
gal	gallons	3.785	liters	L
ft^3	cubic feet	0.028	cubic meters	m^3
yd^3	cubic yards	0.765	cubic meters	m^3
		NOTE: volumes greater than 1000 L shall be shown in m^3		
		MASS		
oz	ounces	28.35	grams	g
lb	pounds	0.454	kilograms	kg
T	short tons (2000 lb)	0.907	megagrams (or "metric ton")	Mg (or "t")
		TEMPERATURE (exact degrees)		
^oF	Fahrenheit	5 (F-32)/9 or (F-32)/1.8	Celsius	^oC
		ILLUMINATION		
fc	foot-candles	10.76	lux	lx
fl	foot-Lamberts	3.426	$candela/m^2$	cd/m^2
		FORCE and PRESSURE or STRESS		
lbf	poundforce	4.45	newtons	N
lbf/in^2	poundforce per square inch	6.89	kilopascals	kPa

APPROXIMATE CONVERSIONS FROM SI UNITS

Symbol	When You Know	Multiply By	To Find	Symbol
		LENGTH		
mm	millimeters	0.039	inches	in
m	meters	3.28	feet	ft
m	meters	1.09	yards	yd
km	kilometers	0.621	miles	mi
		AREA		
mm^2	square millimeters	0.0016	square inches	in^2
m^2	square meters	10.764	square feet	ft^2
m^2	square meters	1.195	square yards	yd^2
ha	hectares	2.47	acres	ac
km^2	square kilometers	0.386	square miles	mi^2
		VOLUME		
mL	milliliters	0.034	fluid ounces	fl oz
L	liters	0.264	gallons	gal
m^3	cubic meters	35.314	cubic feet	ft^3
m^3	cubic meters	1.307	cubic yards	yd^3
		MASS		
g	grams	0.035	ounces	oz
kg	kilograms	2.202	pounds	lb
Mg (or "t")	megagrams (or "metric ton")	1.103	short tons (2000 lb)	T
		TEMPERATURE (exact degrees)		
^oC	Celsius	1.8C+32	Fahrenheit	^oF
		ILLUMINATION		
lx	lux	0.0929	foot-candles	fc
cd/m^2	$candela/m^2$	0.2919	foot-Lamberts	fl
		FORCE and PRESSURE or STRESS		
N	newtons	0.225	poundforce	lbf
kPa	kilopascals	0.145	poundforce per square inch	lbf/in^2

*SI is the symbol for the International System of Units. Appropriate rounding should be made to comply with Section 4 of ASTM E380.
(Revised March 2003)

Table of Contents

Pagination error: Gap in page numbering from 149 through 190, but NO CONTENT IS MISSING.

List of Figures

List of Tables

Author Acknowledgments

The research reported herein was performed under AUTC Project Number 309001 by the Department of Civil and Environmental Engineering at the University of Alaska Fairbanks (UAF). The Institute of Northern Engineering was the contractor for this project with AUTC serving as the Fiscal Administrator. The Alaska Department of Transportation and Public Facilities and the Washington State Department of Transportation provided match funding for this project. The AUTC matched the funds provided by Alaska and Washington State, funding 50% of the total project budget.

Dr. Andrew T. Metzger, Assistant Professor of Civil Engineering at UAF was the Project Director and Principal Investigator. The other authors of this report are Jonathan Hutchinson and Jason Kwiatkowski. Both Jonathan and Jason functioned as Research Associates and Master of Science Candidates during the project.

Abstract

This report documents and presents the results of a study on the impact load demands at in-service ferry landings. Two ferry landings were instrumented to measure and determine several metrics used in characterizing berthing demands (impact demands) on the two structures. One structure was the Auke Bay ferry terminal in Juneau, Alaska; the other was Slip 1 at the Seattle ferry terminal in Seattle, Washington. The field campaign for this project included a one-year field study at each site. Measurements of a number of berthing metrics were collected and used to characterize the magnitudes of impact load demands on the structures. Measurements of marine fender displacement, vessel approach distance with respect to time, and pile strain were used to determine berthing demands. Data collected from the field campaign were characterized, compiled, and analyzed statistically. Probability theory was used to provide design value recommendations for berthing energy, impact force, approach velocity, and berthing factor at each location. These results are presented here as well as in a number of design aids intended to quantify the berthing load environment for each site. Design aids should facilitate immediate implementation of the results.

Executive Summary

Two ferry landings were instrumented to measure and determine several metrics that are used in characterizing the berthing demands (impact demands) on structures that are impacted by vessels. Two wingwalls at the Seattle site and three mooring dolphins at the Auke Bay site were instrumented. Both wingwalls were contacted during each berthing maneuver in Seattle. At Auke Bay, vessels could contact one, two, or all three of the dolphins instrumented at the site.

At the conclusion of each field campaign, all events were analyzed. Following filtering and event characterization, the dataset for the Auke Bay site consisted of approximately 486 data points. The dataset for the Seattle site consisted of approximately 3448 impact events at the north wingwall and 3504 impact events at the south wingwall, for 6952 vessel impact events.

Results were obtained for five parameters at both sites: approach velocity, berthing energy, berthing force, berthing coefficient, and berthing factor. Point of contact was estimated for each impact at the Seattle site.

For each parameter, results are portrayed as follows:

Histograms provide a graphical representation of the frequency distribution of each parameter, such as approach velocity or berthing energy, and the frequency of occurrence. The purpose of the histograms is to display the relative frequencies of each parameter by displaying the number of times magnitudes within a certain range occur over the sample size.

Probability density functions (pdf), fitted to the corresponding histograms, attempting to match a well-defined pdf to the empirical data. Using probability distributions that correlate with the experimental data, a probability of occurrence can be associated with the experimentally determined results.

Probability plots are another method of visualizing the fit of data to a particular probability density function. The vertical axis represents the probability that a given parameter value will not occur or be exceeded during any one berthing event.

Design charts provide a convenient means of determining the appropriate value for a parameter, given a number of vessel impacts and the desired level of *reliability*, that is, the probability that the parameter will not be met or exceeded in a given number of berthing events.

Presented here in the Executive Summary are statistics of the parameters as well as the probability-of-non-exceedance values, and the design charts along with the conclusions from each site's study. Details of how the values were determined and the plots described above are found in the body of the report.

Velocity Results

Approach velocity was determined using the sonic distance sensor data with respect to time. The change in distance over change in time 1 second prior to impact was used to determine the velocity. Velocity for the initial impact during each event at each instrumented structure[1] was used for analysis.

[1] For Auke Bay, measurements of impact velocity were measured at Dolphins E1 and E2, thus providing one or two velocity data points for each berthing maneuver.

Energy Results

Berthing energy is the most common parameter used by engineers for the design of berthing structures. Berthing energy was determined from measurements of the deflected structure. With the measurements, the elastic potential energy of the deformed structure was calculated, which represents the energy actually absorbed by the structure.

Equations to calculate the elastic potential energy for both sites were formulated. Direct measurements of the rubber fenders at each site were used to infer deflection from the backing structure. The deflection of the backing structure represented a fraction of the total elastic potential energy (e.g., about 15% at Auke Bay). Structural analysis software, as-built drawings, and soil information were used to model the backup structures at both locations. With this information, the stiffness of the backup structures was estimated.

Force Results

With knowledge of the stiffness of the system and displacement, the force applied to the system can be determined. Based on this information, equations for determining the force of impact at each site were formulated. These equations are based on known force-displacement relationships of the fenders, stiffness of the support structure, and beam theory. While energy values are generally applicable, impact force values presented here are only applicable to the respective structures studied in this project.

Berthing Coefficient Results

Using direct measurements of berthing events allows for berthing energy to be quantified and provides an opportunity to estimate berthing coefficients. Berthing coefficients are commonly used in practice, where they are multiplied by the apparent kinetic energy of the incoming vessel. Historically, the purpose of the factors is to account for uncertainties associated with the berthing maneuver and mechanisms of energy absorption.

The berthing coefficients were calculated as the ratio of the elastic potential energy of the deformed structure to the apparent kinetic energy of the vessel.

The results of this study are not in line with berthing coefficient values customarily used in practice. At both sites, much larger-than-expected berthing coefficients were calculated; this was explained by observing actual berthing events and studying distance versus time plots.

The majority of velocities observed were small: less than 0.5 feet/second. During a berthing event, vessel controls are used to maneuver the ship, adding energy to the system and changing the kinetic energy in real time. This condition is in conflict with the dead-drift assumption commonly used in the Kinetic Energy Method of determining berthing energy, which makes use of berthing coefficients. It was observed that at velocities more consistent with design velocities—about 1.2 feet/second—berthing coefficient values were more consistent with values found in associated literature. However, there are so few of these higher-velocity data points that meaningful statistics were not possible.

Berthing coefficient values are presented in this report for completeness only. The authors do not recommend using berthing coefficient values presented in the Seattle study for design purposes.

Berthing Factor Results

For this study, the berthing factor is defined as the energy-per-unit mass of the vessel. This berthing factor may be used to estimate the berthing energy of other classes of vessels (having different displacements) not observed in this study. Obtaining the berthing factor is accomplished by dividing the elastic energy of the deformed structure by the mass of the vessel. The mass of the vessel was determined using the published vessel displacement.

Additional Information

This study resulted in two successfully defended Master of Science theses, each corresponding to a study site. The authors of these theses provided additional discussion, results, and commentary on implementation not presented in this report. For additional information on both studies, the reader is referred to Hutchinson (2011) for the Auke Bay study and Kwiatkowski (2012) for the Seattle study.

Please note that Hutchinson (2011) considered only the first 192 impact events. Data from subsequent events were incorporated in the database and results, and all data are reflected in this report. Some of the results from Hutchinson (2011) changed significantly when updated with the remaining data, mostly from the summer season; but the manuscript contains additional discussion that should prove beneficial to Alaska Marine Highway engineers and others.

Summary of Results

Auke Bay Results

Velocity Summary Tables

Velocity			
	Max (ft/s)	Mean (ft/s)	# of Measurements
All Vessels	0.83	0.16	350
Columbia	0.5	0.14	39
Kennicott	0.5	0.17	52
Malaspina	0.83	0.16	178
Matanuska	0.46	0.10	82

Probability of Non-exceedance: Velocity (ft/sec)					
	Columbia	Kennicott	Malaspina	Matanuska	All Vessels
(1-*p*)%					
90	*	*	0.30	0.23	0.29
95	*	*	0.38	0.28	0.36
98	*	*	0.49	0.36	0.46
99	*	*	0.58	0.42	0.54
99.9	*	*	0.92	0.65	0.87
99.99	*	*	1.34	0.94	1.27
99.995	*	*	1.49	1.03	1.42
99.999	*	*	1.87	1.28	1.78
99.9995	*	*	2.06	1.40	1.96
99.9999	*	*	2.52	1.70	2.41
# of events			178	81	350

* Not enough data points to fit a pdf to the data

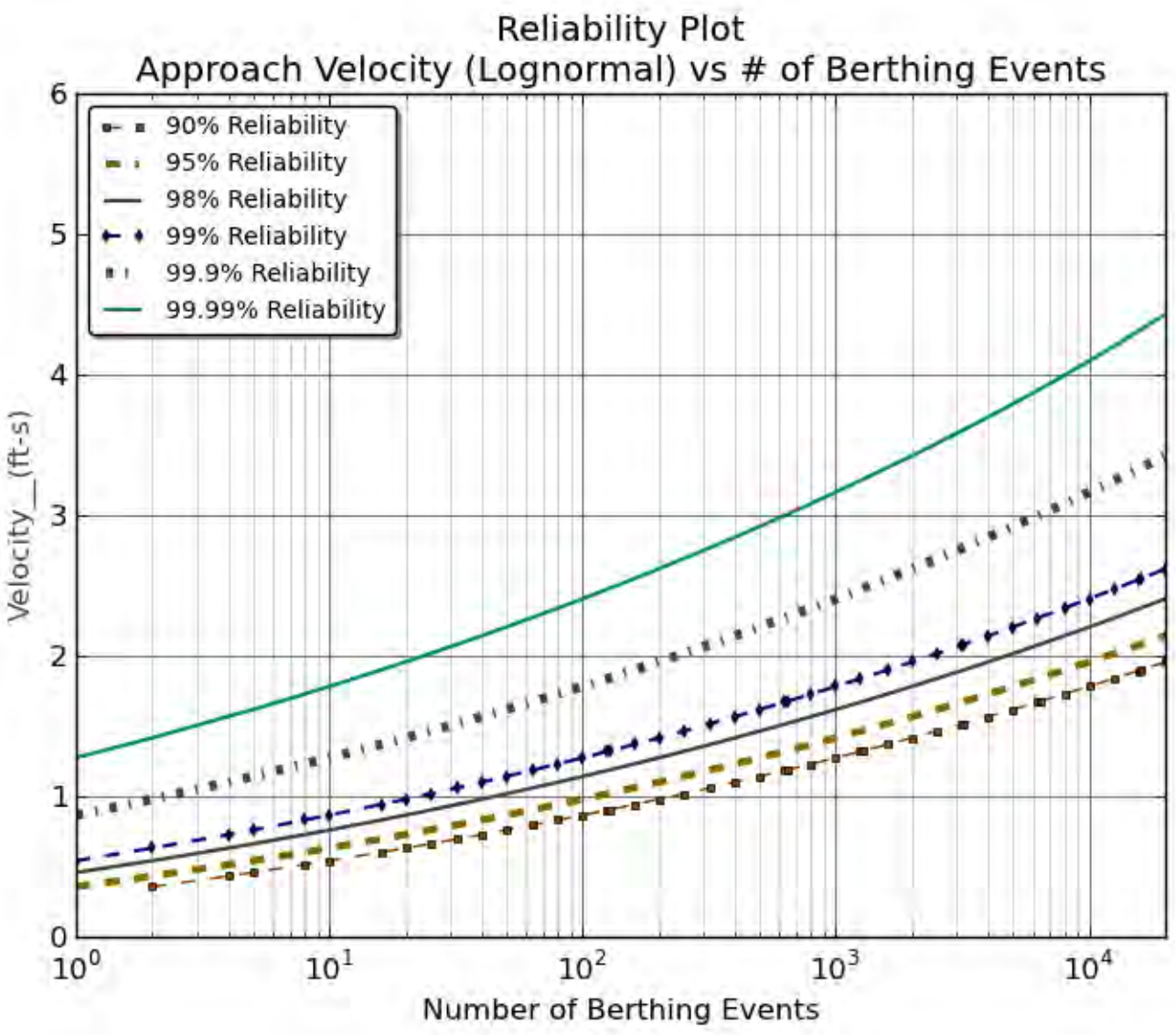

Velocity Design Chart

Energy Summary Tables

Energy			
	Max (kip-ft)	Mean (kip-ft)	# of Measurements
All Vessels	47	3.9	486
Columbia	43	5.1	54
Kennicott	26.5	3.8	62
Malaspina	47	4.2	253
Matanuska	28.3	2.8	117

Probability of Non-exceedance: Energy (kip-ft)					
	Columbia	Kennicott	Malaspina	Matanuska	All Vessels
(1-*p*)%					
90	13	11	11	7	11
95	21	18	18	11	17
98	33	30	29	18	27
99	43	40	38	23	35
99.9	86	83	78	45	72
99.99	139	139	130	73	118
99.995	157	158	147	82	134
99.999	203	207	192	106	175
99.9995	224	230	213	117	194
99.9999	276	288	265	143	240
# of events	54	62	253	117	486

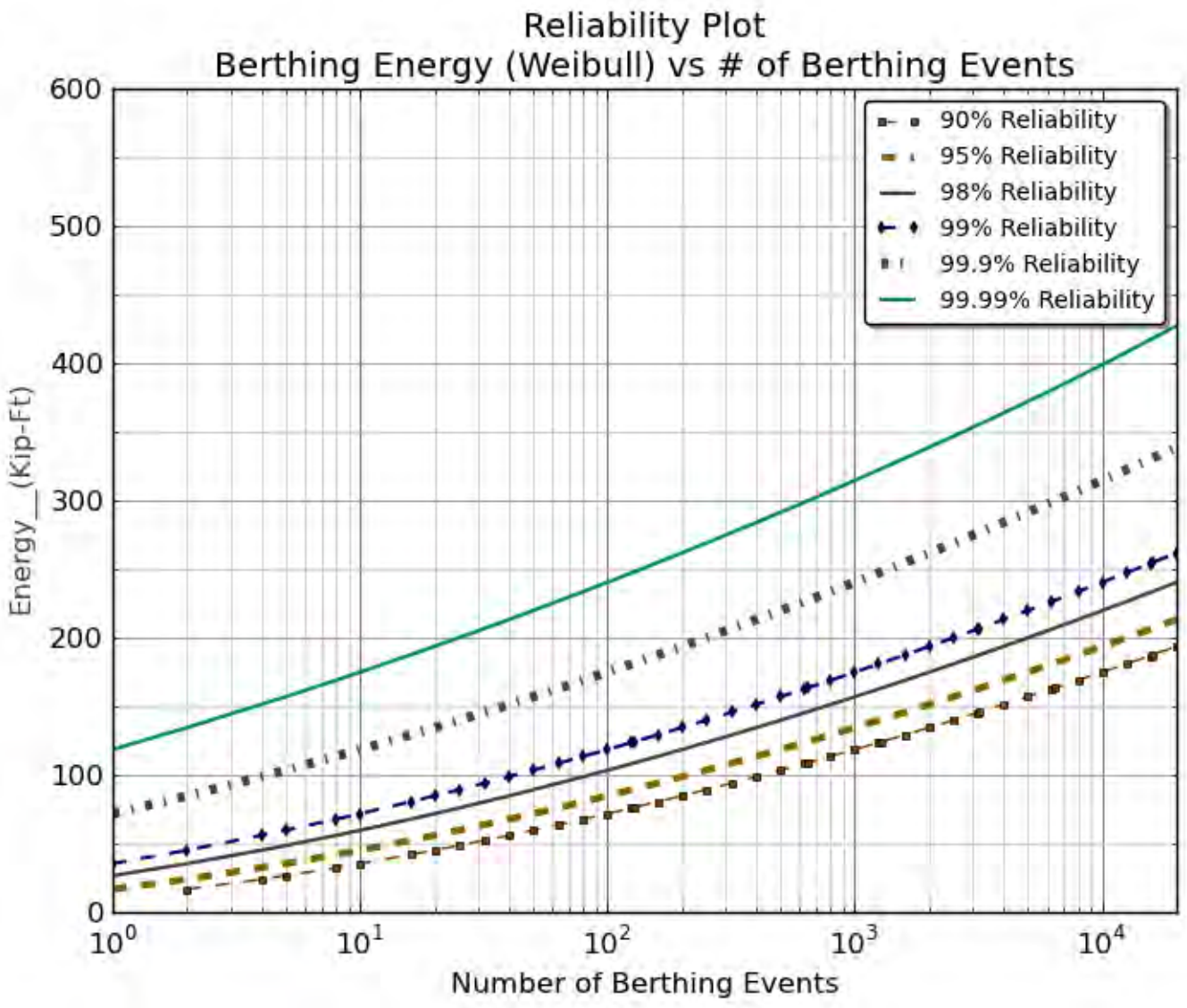

Energy Design Chart

Force Summary Tables

Berthing Force			
	Max (kip)	Mean (kip)	# of Measurements
All Vessels	77.3	16.3	485
Columbia	77.3	19.0	54
Kennicott	26.5	15.3	62
Malaspina	64.6	16.9	253
Matanuska	65.1	14.2	116

Probability of Non-exceedance: Force (kips)					
	Columbia	Kennicott	Malaspina	Matanuska	All Vessels
(1-*p*)%					
90	41	34	37	30	35
95	51	44	46	38	45
98	64	57	58	47	56
99	73	67	67	54	65
99.9	103	99	96	76	93
99.99	131	130	124	97	120
99.995	139	139	132	103	128
99.999	158	161	150	117	146
99.9995	166	170	158	123	154
99.9999	184	191	176	137	171
# of events	54	62	253	116	485

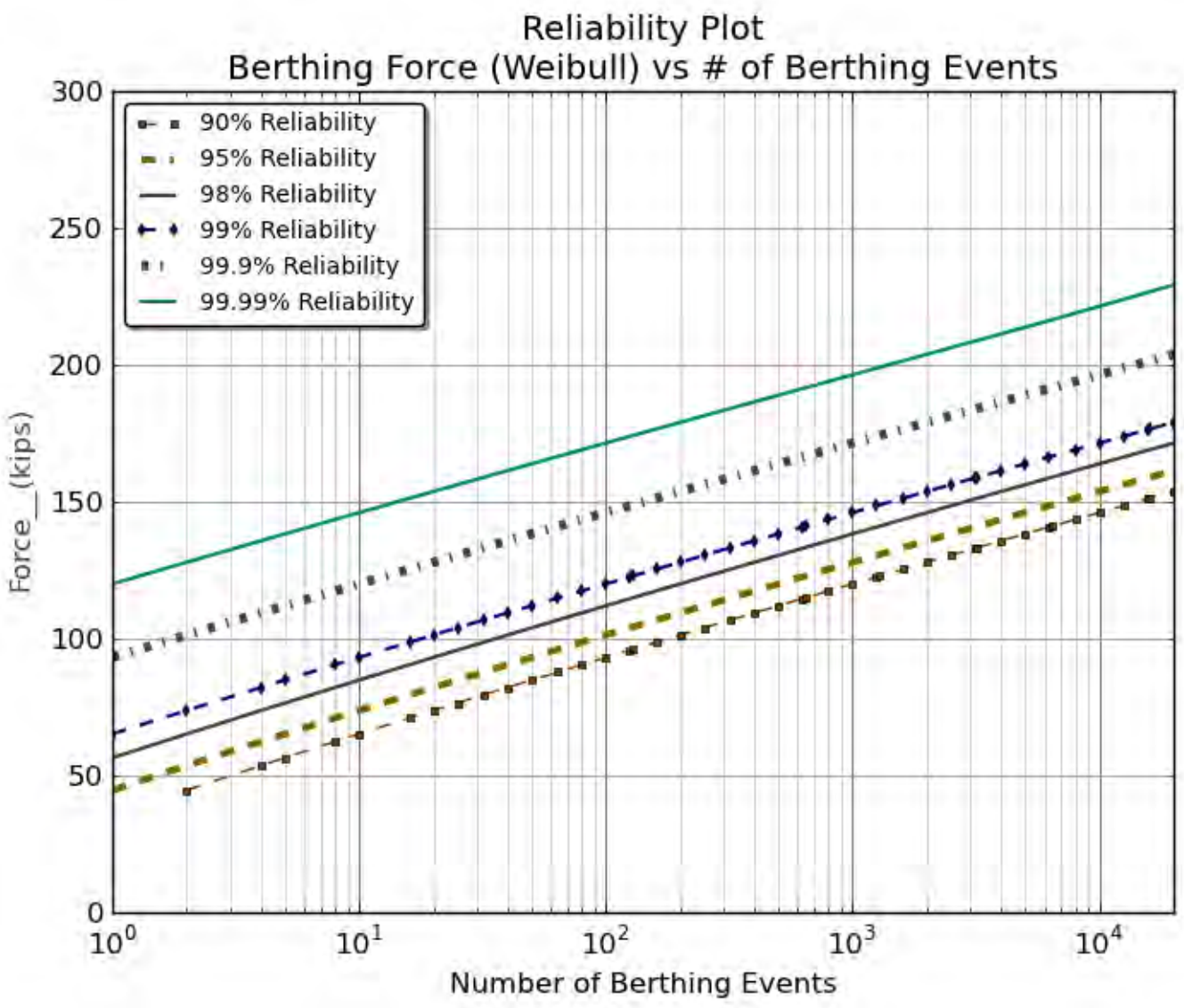

Force Design Chart

Berthing Coefficient Summary

Berthing Coefficient (C_b)			
	Max	Mean	# of Measurements
All Vessels	1.22	0.32	293
Columbia	1.22	0.48	30
Kennicott	0.59	0.28	44
Malaspina	1.16	0.33	151
Matanuska	0.91	0.26	68

Berthing Factor Summary

Berthing Factor			
	Max	Mean	# of Measurements
All Vessels	0.1217	0.0093354	486
Columbia	0.0805	0.0096176	54
Kennicott	0.0508	0.0072696	62
Malaspina	0.1217	0.010792	253
Matanuska	0.0731	0.0071509	117

Probability of Non-exceedance: Berthing Factor (ft^2/s^2)					
	Columbia	Kennicott	Malaspina	Matanuska	All Vessels
(1-*p*)%					
90	0.03	0.02	0.03	0.02	0.03
95	0.04	0.04	0.05	0.03	0.04
98	0.06	0.06	0.07	0.05	0.06
99	0.08	0.08	0.10	0.06	0.08
99.9	0.16	0.16	0.20	0.12	0.17
99.99	0.26	0.27	0.34	0.19	0.28
99.995	0.29	0.30	0.38	0.21	0.32
99.999	0.38	0.40	0.50	0.27	0.42
99.9995	0.42	0.44	0.55	0.30	0.46
99.9999	0.52	0.55	0.69	0.37	0.57
# of events	54	62	253	117	486

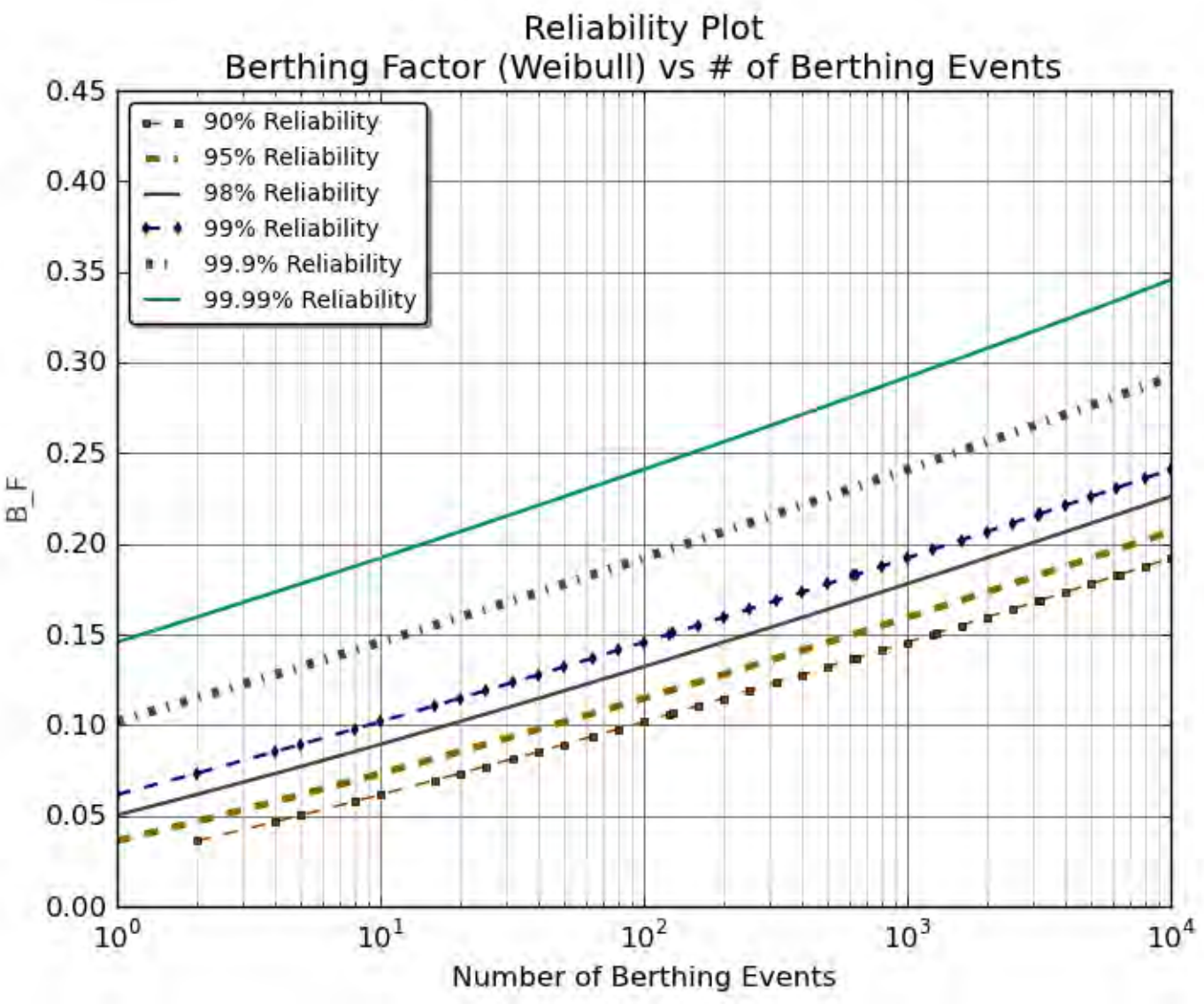

Berthing Factor Design Chart

Design Load/Parameter Summary Tables

Nominal/Service Loads, 90%, 30events		
Berthing Energy	51	kip-ft
Berthing Force	78	kip
Approach Velocity	0.68	ft/sec
Berthing Factor	0.121	ft^2/s^2

Nominal is a 99.65 percentile per event, which is a 90% probability of non-exceedance in 30 events

Ultimate Loads, 90%, 3500 events		
Berthing Energy	147	kip-ft
Berthing Force	134	kip
Approach Velocity	1.53	ft/sec
Berthing Factor	0.354	ft^2/s^2

99.997% percentile per berthing event, a 90% probability of non-exceedance in 3500 events

Ultimate Loads, 98%, 10,500 events		
Berthing Energy	220	kip-ft
Berthing Force	164	kip
Approach Velocity	2.2	ft/sec
Berthing Factor	0.525	ft^2/s^2

99.9998% percentile per berthing event, a 98% probability of non-exceedance in 10,500 events

Seattle Results

Velocity Summary Table

Approach Velocity, feet/second				
Wall	Mean	Standard Deviation	Max	# of Events
North	0.32	0.19	1.65	2672
South	0.32	0.20	1.64	2455
Combined	0.32	0.92	1.65	5127

Probability of Non-exceedance: Approach Velocity			
One Event	Complete Set	North Wingwall	South Wingwall
Probability of Non-exceedance, %	feet/second	feet/second	feet/second
98	0.79728	0.78845	0.80652
99	0.87558	0.86443	0.88728
99.9	1.1051	1.0866	1.1248
99.99	1.3037	1.278	1.3309
99.999	1.4819	1.4494	1.5165
99.9995	1.5325	1.498	1.5693
99.9999	1.6455	1.6064	1.6872
99.99995	1.6924	1.6513	1.7362
99.99999	1.7978	1.7523	1.8464
99.999999	1.9411	1.8894	1.9965
99.9999999	2.0769	2.0192	2.1389

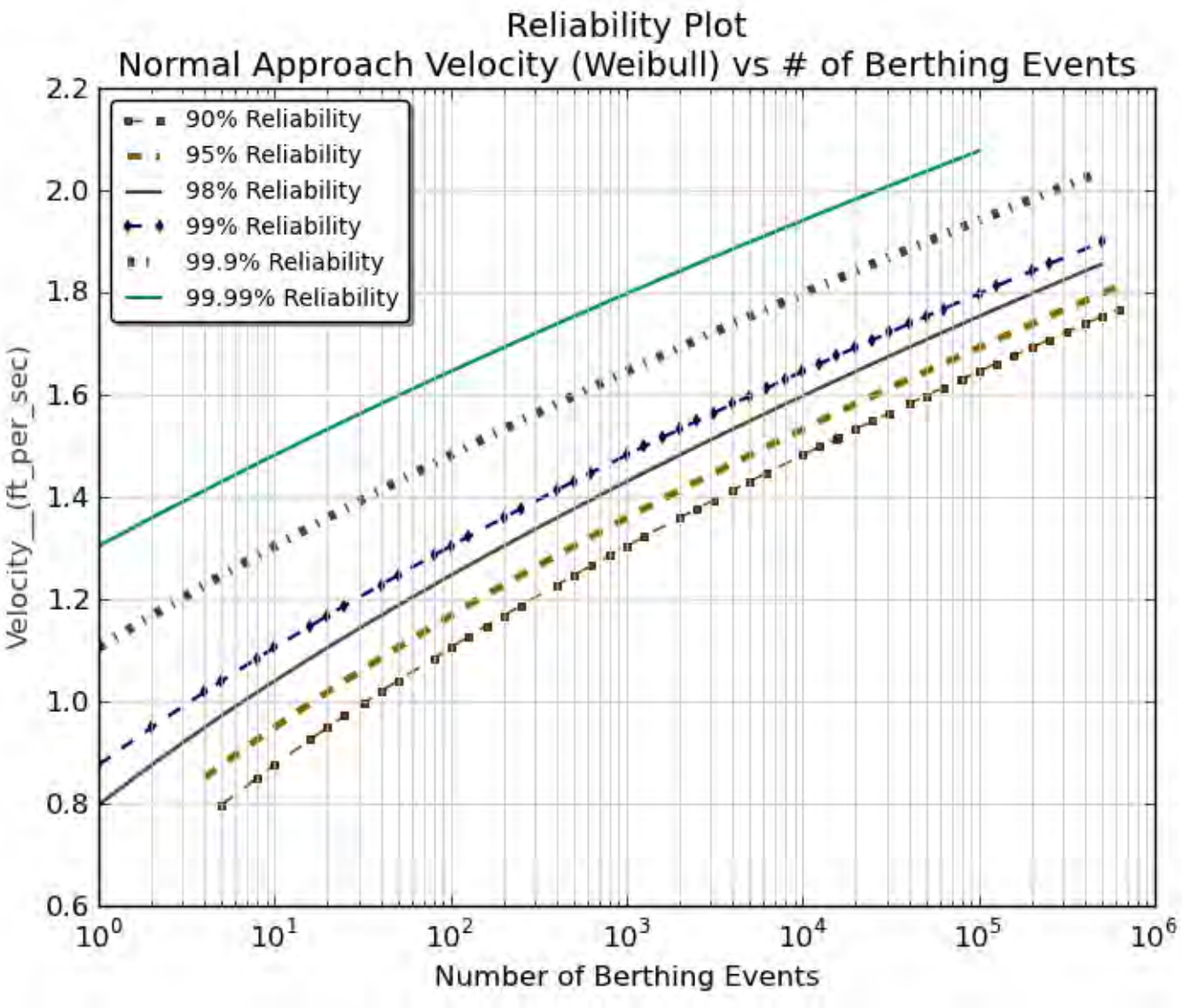

Velocity Design Chart

Energy Summary Tables

Energy Absorbed by Wingwalls, kip feet				
Wall	Mean	Standard Deviation	Max	# of Events
North	12.74	9.095	146.17	3448
South	11.946	8.287	80.476	3484
Combined	12.341	8.707	146.17	6932

Probability of Non-exceedance: Kinetic Energy			
One Event	Complete Set	North Wingwall	South Wingwall
Probability of Non-exceedance, %	kip-ft	kip-ft	kip-ft
98	38.03	38.34	37.57
99	45.37	45.58	44.96
99.9	74.38	73.99	74.32
99.99	111.74	110.24	112.41
99.999	159.09	155.85	161.00
99.9995	175.57	171.65	177.98
99.9999	218.26	212.46	222.06
99.99995	238.68	231.92	243.20
99.99999	291.28	281.89	297.79
99.999999	380.45	366.22	390.71
99.9999999	488.36	467.75	503.65

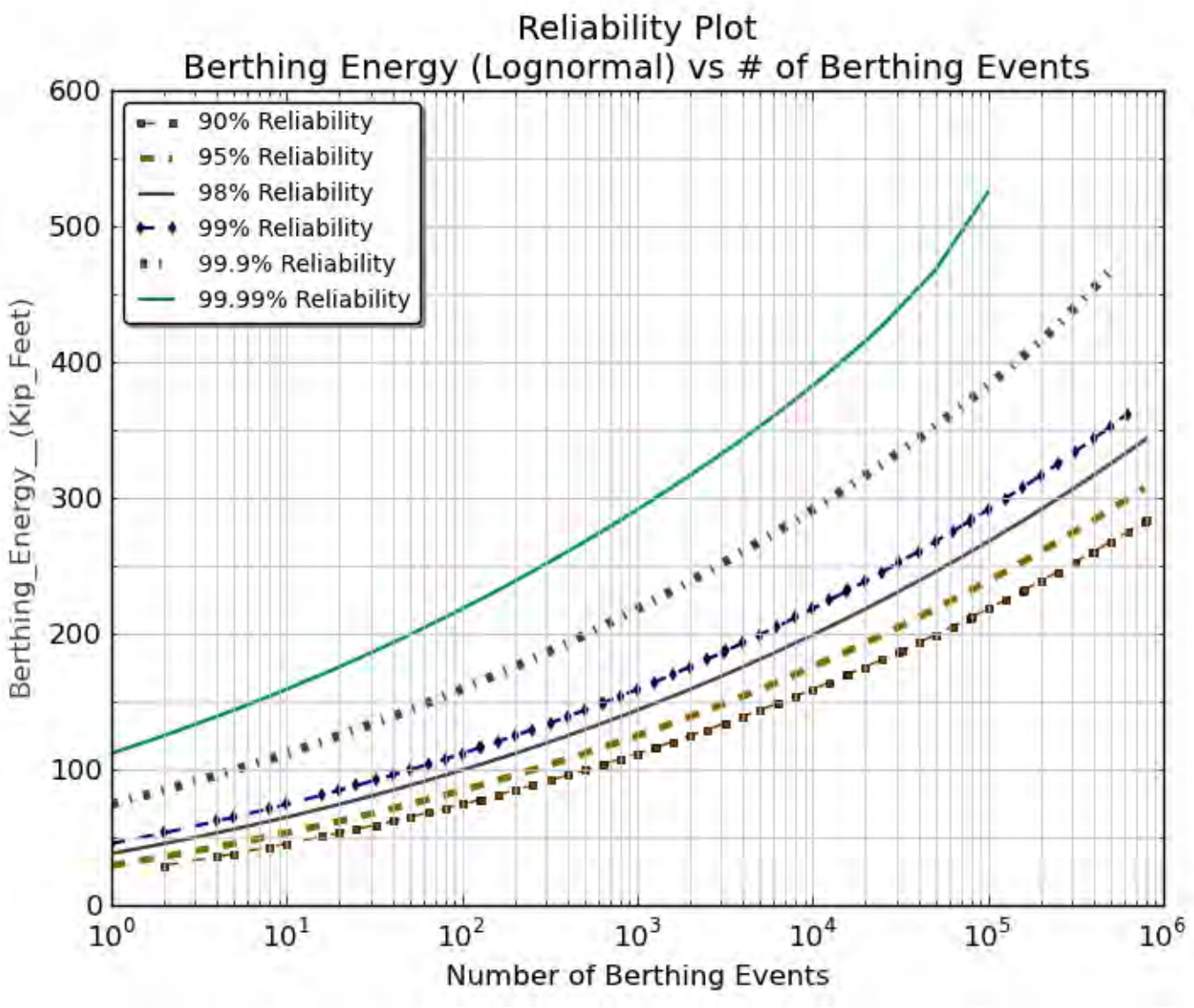

Berthing Energy Design Chart

Berthing Force Summary

Berthing Force at Wingwalls, kips				
Wall	Mean	Standard Deviation	Max	# of Events
North	74.272	41.7	413.139	3448
South	75.725	40.302	307.286	3484
Combined	75.002	41.01	413.139	6932

Probability of Non-exceedance: Berthing Force, Gamma Distribution			
One Event	Complete Set	North Wingwall	South Wingwall
Probability of Non-exceedance, %	kips	kips	kips
98	177.25	176.44	177.98
99	196.90	196.12	197.59
99.9	258.86	258.21	259.39
99.99	317.71	317.22	318.04
99.999	374.69	374.37	374.80
99.9995	391.58	391.31	391.62
99.9999	430.41	430.27	430.29
99.99995	446.99	446.91	446.80
99.99999	485.21	485.27	484.85
99.999999	539.31	539.58	538.71
99.9999999	592.87	593.34	592.01

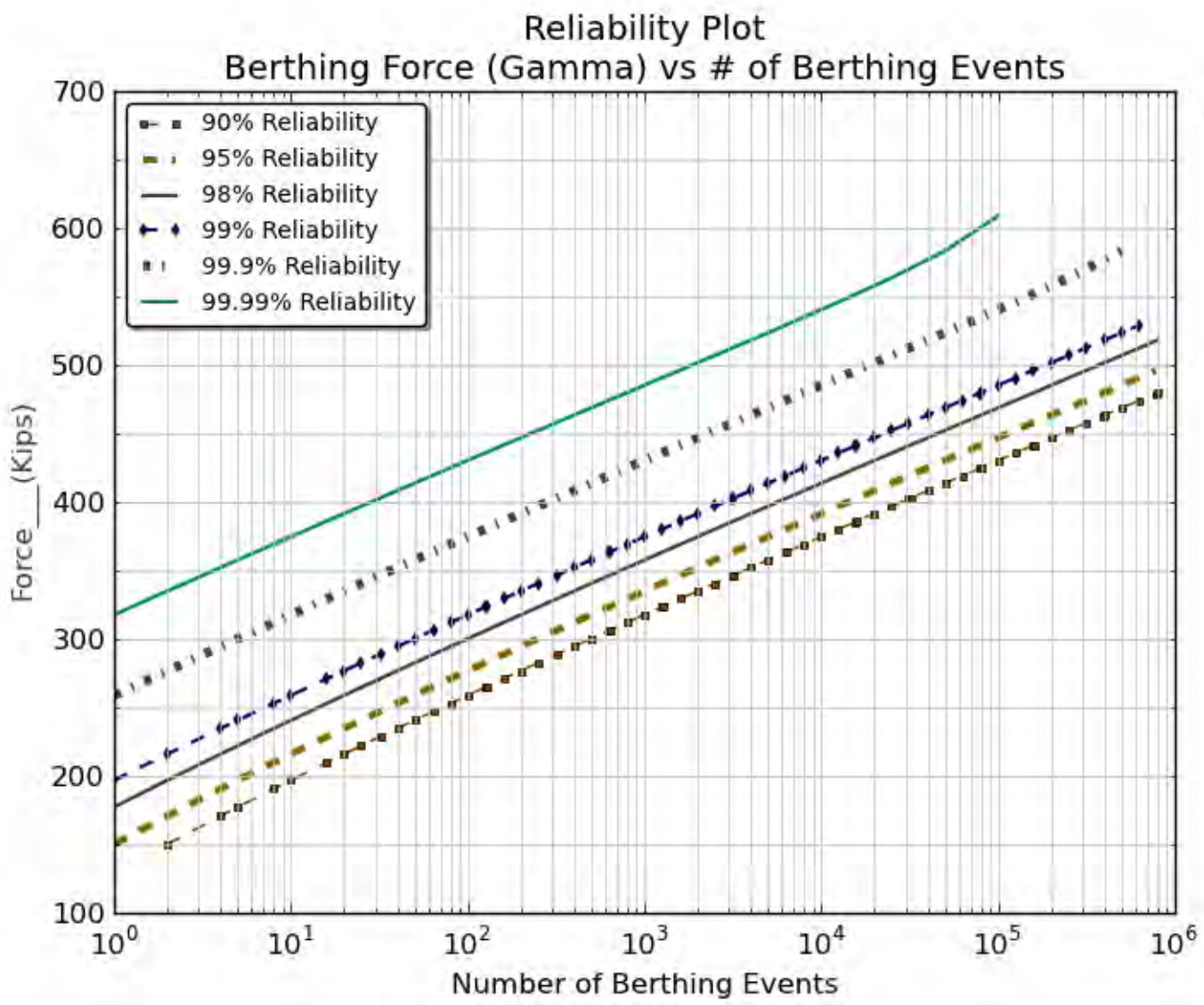
Reliability Plot
Berthing Force (Gamma) vs # of Berthing Events
90% Reliability
95% Reliability
98% Reliability
99% Reliability
99.9% Reliability
99.99% Reliability
Force__(Kips)
Number of Berthing Events
700
600
500
400
300
200
100
10^0
10^1
10^2
10^3
10^4
10^5
10^6

Probability of Non-exceedance Berthing Force, Lognormal Distribution			
One Event	Complete Set	North Wingwall	South Wingwall
Probability of Non-exceedance, %	kips	kips	kips
98	209.48	202.66	216.31
99	244.82	236.19	253.47
99.9	378.95	362.75	395.26
99.99	542.94	516.41	569.80
99.999	741.87	701.71	782.73
99.9995	809.38	764.37	855.22
99.9999	980.99	923.27	1039.96
99.99995	1061.68	997.81	1127.01
99.99999	1265.95	1186.06	1347.89
99.999999	1602.92	1495.45	1713.55
99.9999999	1998.64	1857.32	2144.63

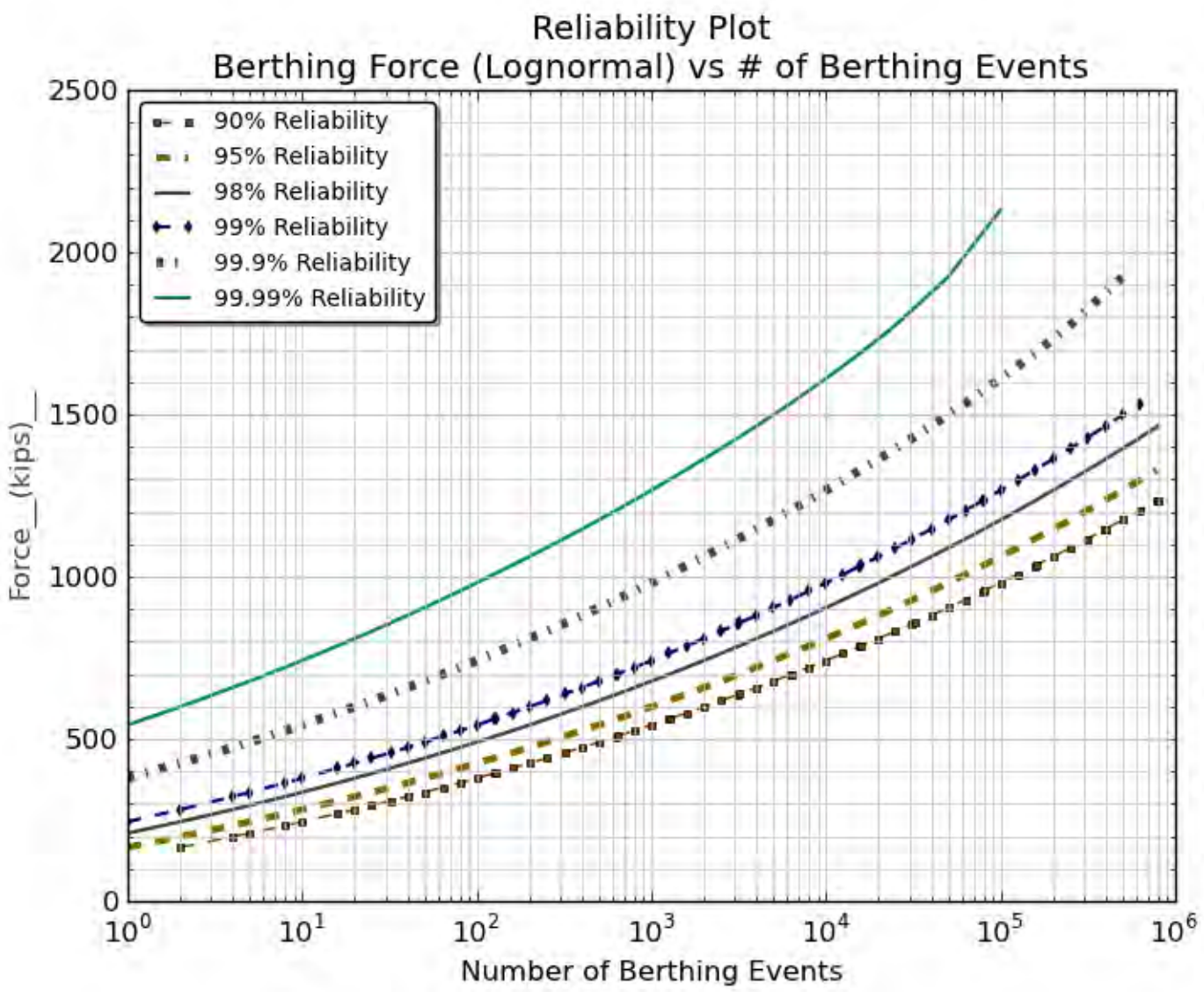
Reliability Plot
Berthing Force (Lognormal) vs # of Berthing Events
90% Reliability
95% Reliability
98% Reliability
99% Reliability
99.9% Reliability
99.99% Reliability
Force__(kips)__
Number of Berthing Events
0
500
1000
1500
2000
2500
10^0
10^1
10^2
10^3
10^4
10^5
10^6

Berthing Factor Results Summary

Berthing Factor, f_b				
Wall	Mean	Standard Deviation	Max	# of Events
North	0.586	0.0429	0.675	2648
South	0.548	0.0377	0.372	2417
Combined	0.568	0.0405	0.675	5065

Probability of Non-exceedance: Berthing Factor			
One Event	Complete Set	North Wingwall	South Wingwall
Probability of Non-exceedance, %	ft^2/sec^2	ft^2/sec^2	ft^2/sec^2
95	0.1319	0.1352	0.1282
98	0.1711	0.1750	0.1664
99	0.2035	0.2079	0.1981
99.9	0.3307	0.3370	0.3225
99.99	0.4933	0.5014	0.4819
99.999	0.6980	0.7079	0.6827
99.9999	0.9522	0.9640	0.9326
99.99995	1.0397	1.0520	1.0186
99.99999	1.2643	1.2779	1.2397
99.999999	1.6436	1.6586	1.6134
99.9999999	2.1006	2.1167	2.0640

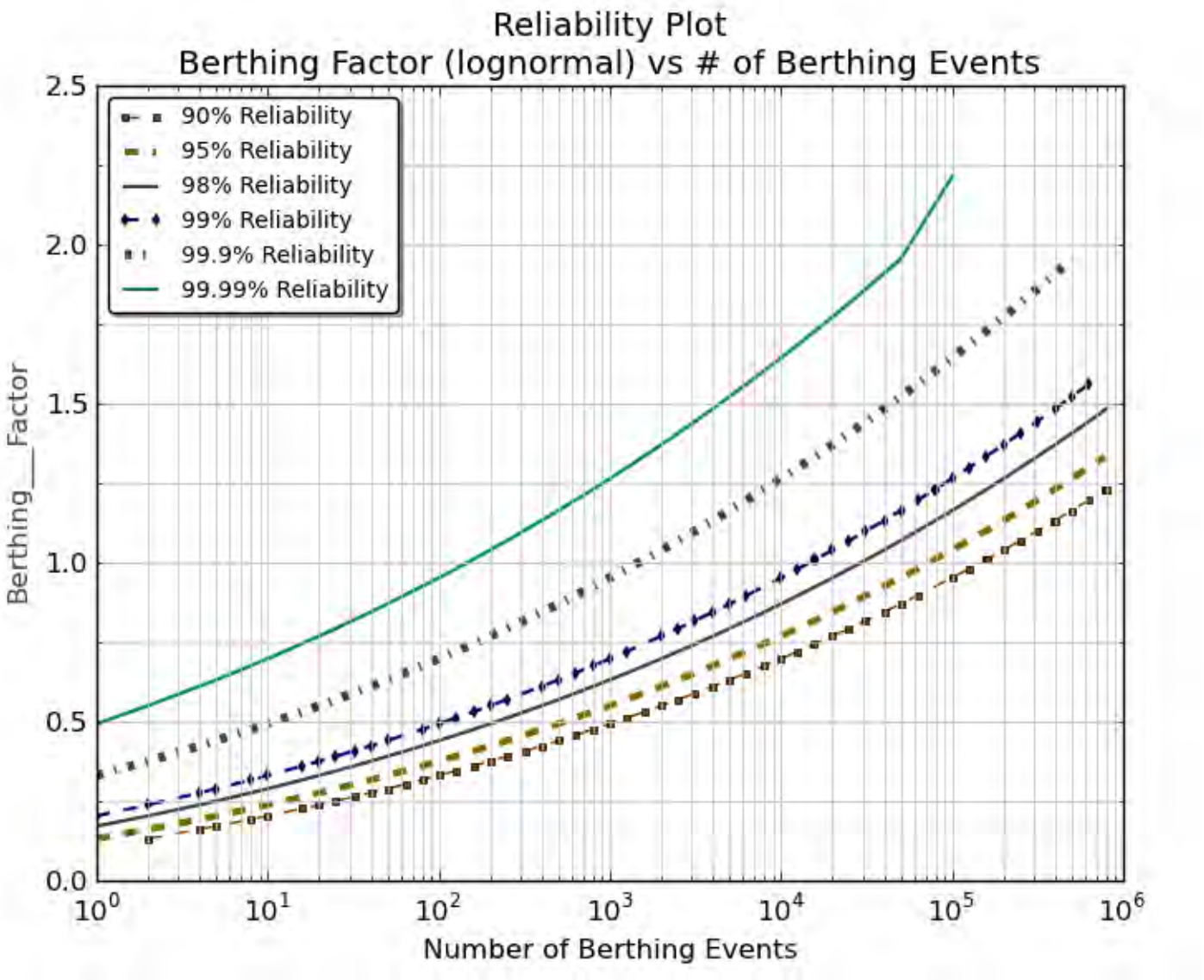

Berthing Factor Design Chart

Point of Impact Results

The instrumentation of all wingwall fenders allows for determination of where the vessel is contacting the impact face. The point-of-impact results were determined as the location of the resultant force of all the fender forces. Results from all impacts are summarized below:

Mean Point of Impact Summary		
	North	**South**
Lateral distance from “throat” of wingwall (feet)	5.84	8.61
Elevation with respect to bottom edge of wingwall (feet)	16.18	14.54

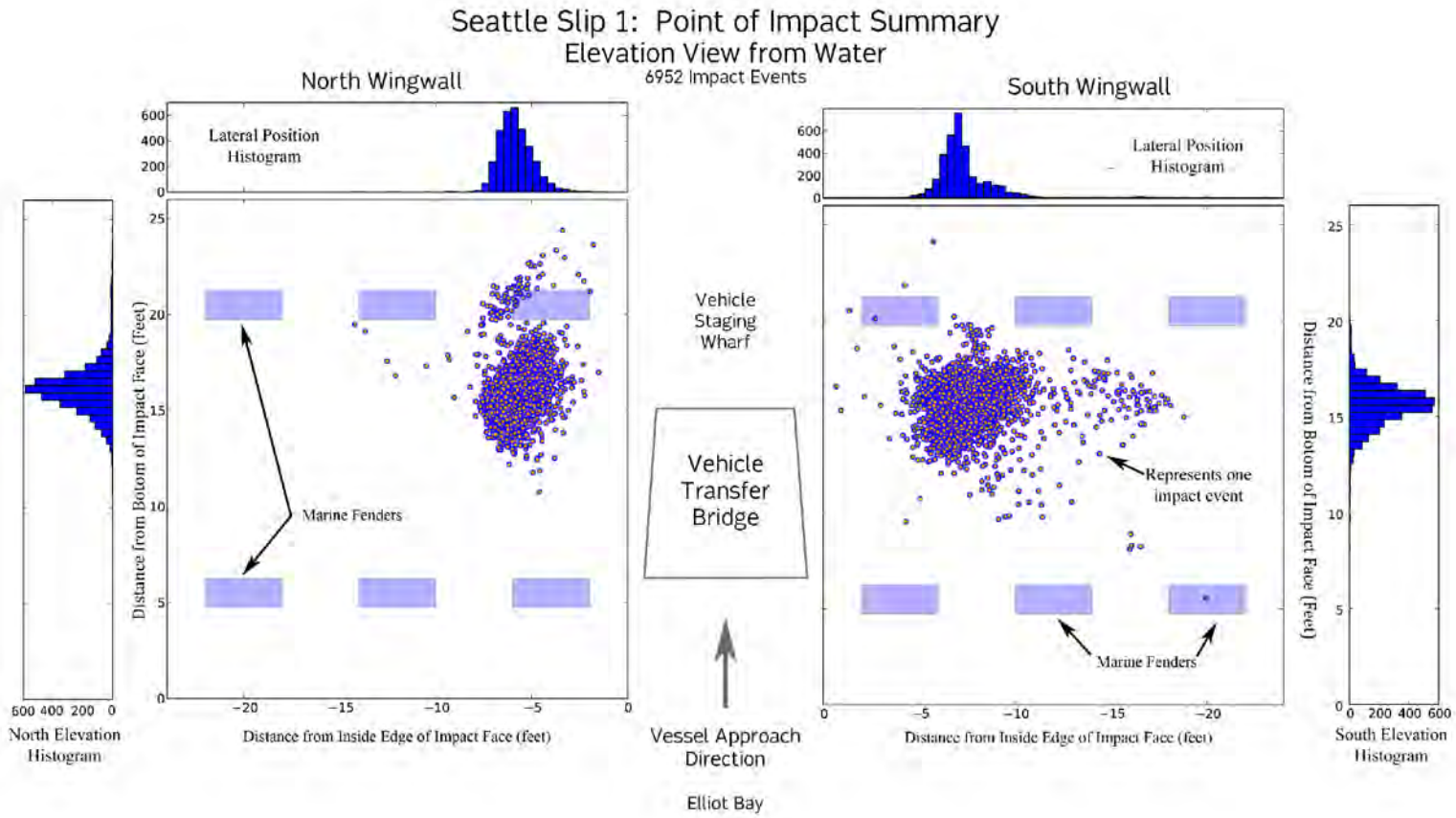

Point of Impact Summary Graphic

Conclusions

Auke Bay Study

Understanding vessel impact loads is crucial to the design of cost-effective and reliable berthing structures. When a berthing structure is designed, a certain level of uncertainty exists that is typically accounted for by using a simple factor of safety. Even with a factor of safety applied, there always exists the potential for design energy, force, or velocity to be exceeded. Engineers have developed their own design guidelines through trial and adjustment over many operation/failure cycles, and have developed factors of safety that compensate for assumptions in load. However, precisely quantifying berthing loads remains a challenge, with limited information often leading to the design of structures rooted in assumption and discretion.

A number of statistical studies were conducted in the late 1960s and early 1970s, giving valuable design energy recommendations based on vessel displacement and berthing frequency. The studies, however, were limited to tanker-type vessels, which vary significantly in size and geometry from ferry vessels. Additionally, published load values such as energy and approach velocity are site specific, and cannot always be interchangeably used with confidence.

The use of analytical models and programs is valuable in handling the complex ship-fluid interactions of a berthing vessel, particularly when information is limited for the particular vessel type, size, and location. However, even the most advanced analytical models cannot fully account for all aspects associated with a berthing vessel, including factors such as vessel maneuverability and vessel approach variations due to environmental and human influence. For this reason, non-empirical design values are often confirmed or used in conjunction with full-scale measurements, which inherently account for all variables.

A particular challenge associated with berthing structures is the large variation in load. Extreme events must be considered in addition to typical service loads. It is understood that certain extreme events such as “accidents” can never be fully accounted for, and to attempt to do so would result in an overly conservative design. However, extreme events can be framed as having a probability of occurring. Reliability engineering is a powerful tool when dealing with highly variable loads, because it allows engineers to develop rational designs based on anticipated extreme events and their associated risk levels.

This study analyzed the berthing events of four different vessels at the Auke Bay ferry landing in Juneau, Alaska. The results from this study provide a broad set of parameters to the Alaska Marine Highway’s information base; they also provide a probability-based option for the design of future landings.

Results were compared with current design values for the berthing structures at Auke Bay. In general, the dolphins at Auke Bay have performed adequately. Conversely, of the total sample of captured berthing events, loads (demands) in excess of the design values (although rare) were observed. Recommendations on nominal and service load values have been provided.

Nominal load recommendations were selected to approximate the maximum values measured at Auke Bay. Nominal loads represent the maximum service loads that the berthing structures are subject to on a regular basis. These values are similar to *design* values used by the ADOT&PF Marine Highway Department for the berthing structures at Auke Bay. Alaska Marine Highway System engineers apply factors of safety to the structures in anticipation of working

stresses being exceeded due to extreme events. While this design approach has proven adequate, the present study provides an alternative design option, in which factors of safety in load demand are rationally quantified based on probability of exceedance.

Ultimate load recommendations represent extreme events that the berthing structure must be expected to resist over a specified design life or number of berths. It is left to the designer to decide what level of risk (probability of exceedance) is acceptable.

Regarding the fenders currently used at Auke Bay, the fenders themselves are potentially adequate for resisting nominal loads in their linear range as well as ultimate loads in their non-linear range. However, the fenders are physically limited to a maximum displacement of 14 inches. This limits the allowable absorption capacity of the fenders. Loads in excess of the *limited* fender's capacity are absorbed by the backing structure, imparting substantial loads to the tripod piling.

Overall, the complex and variable load environment on berthing structures implies the advantages of a probability-based approach in which fenders and backing structures can be rationally designed for exceptional events.

The following is a summary of recommendations and comments:

- Fenders should be designed to resist ultimate loads from extreme events that are expected to occur over their design life, or design number of berths. An overload allowance (load factor) on the order of 2.10 to 2.55 times the largest service energy is recommended.
- A vessel‘s initial kinetic energy does not always reflect the maximum energy per berthing event. Care must be taken when using the Kinetic Energy Method.
- Design velocity recommendations (service level and ultimate) apply to all four vessels. No definitive distinction between vessel displacement and approach speed was observed.
- Use Design Example 1 (Chapter 6) for landings that are similar to Auke Bay in terms of vessel displacement and environmental/approach conditions.
- Use Design Example 2 for vessels with displacements other than those in this study.
- Berthing and fender force values are a function of fender stiffness and thus are unique to Auke Bay. Use design energy values from Examples 1 or 2 to derive the required force.

Seattle Study

Selection of an appropriate design berthing energy is reliant on subjective decisions made by engineers with years of experience in marine structural design. Structures that prove to be resilient over their lifespan provide little information regarding the actual amount of energy they are absorbing. Without evidence regarding the loading conditions experienced by the structure, design is based on trial and adjustment. In traditional methods, it is customary to account for uncertainties regarding loading conditions and vessel-structure interaction using berthing coefficients. Providing engineers with information regarding the actual demands placed on the structure allows for less reliance on subjectivity and results in more reliable and efficient designs.

There is substantial research available to assist facility designers in the shipping industry. This information corresponds to vessels with displacements of approximately 20 to 100 times the vessel displacements of the Washington State Ferries fleet. Although these studies may expand analytical techniques and provide for increased understanding of the berthing process, they are of limited applicability to engineers designing for high-frequency ferry landings.

Advanced mathematical techniques and the use of software to analyze vessel-fluid-structure interactions allow a range of options when considering specific berthing situations. The use of these techniques, however, requires highly trained individuals, is expensive, and has practical limitations for design professionals. The berthing maneuver of a ship represents a complicated action that is dependent on many difficult-to-model systems such as vessel piloting, the environment, and hydrodynamic effects.

Measurements of the berthing process capture all aspects of the berthing ship and provide the designer with a representation of the actual energy absorbed by the structure, which ultimately is the metric of concern to the design engineer. Compiling information for a sample of statistical relevance allows for a more complete picture of the berthing demand placed on the structure. In the presence of a statistically significant sample of berthing events, the traditionally employed Kinetic Energy Method is obsolete. Empirical and statistical techniques provide a comprehensive understanding of the load environment and a rational basis for an engineer to implement a reliable and efficient design.

This study investigated and characterized thousands of ferry berthing events at the Bremerton slip of the Seattle ferry terminal (Slip 1). The findings of this research further the understanding of vessel-structure interaction and the load environment at the Bremerton slip. Due to the challenges of obtaining pertinent berthing demand data for ferries, this information will serve to bridge the gap between design assumptions and operational realities. Another component of the analysis is to present design utilities based on statistical techniques and reliability engineering principles. Application of probability distributions to a large empirical sample allows extreme-event parameters to be quantified by a probability of occurrence. The development of reliability-based tools is intended to quantify the likelihood of extreme events and provide designers with a methodology to rationally determine service and ultimate berthing load parameters.

The wingwall structures at the Bremerton slip have handled berthing demands without issue over the past 20 years, and have significant excess capacity. The maximum berthing energy recorded was less than 40% of the current design criteria.

This report focuses on the development of probability-based occurrences of berthing load demand, and facilitates transition to a design methodology based on load and resistance factors when coupled with material codes. The major assumptions associated with this approach are (1) that the extreme values are, in fact, approximated reasonably well by the selected probability density function, and (2) that the empirical data represent a stationary random process; that is, the year the facility was monitored is considered a typical year, and the associated statistical properties do not vary from year to year. The service and ultimate loads presented are based on probabilities associated with design values occurring or being exceeded. Service loads represent the maximum loads that the wingwalls experience on a regular basis. Ultimate loads represent the maximum loads the wingwalls are expected to experience over their service life. Both service and ultimate loads represented in this study are based on reliability levels arbitrarily chosen by the authors, and may not reflect the desired reliability level of the Washington State Ferries (WSF) system.

Dissipation of kinetic energy associated with a berthing vessel is a complex process in which there is significant uncertainty associated with the load environment. Quantifying this load environment with the characterization of nearly 7000 impact events provides information that can be confidently used by a design engineer to refine future structural designs.

The following is a compilation of findings, comments, and recommendations from the project:

- The arrangement of WSF terminals is often characterized as "end berthing" as opposed to "side berthing." The WSF terminals are similar to a pocket-shaped berth, with the wingwalls oriented 40 degrees to the berthing vessel. This arrangement allows for vessel landings that share characteristics of side-berthing and end-berthing maneuvers or something completely different.

- The current WSF design assumption is based on the premise that the vessel contacts both wingwalls simultaneously and loads both wingwalls with approximately the same energy or, alternatively, the vessel impacts one wingwall farther from the throat but loses energy as it slides/rotates into the other wingwall . In either case, it is assumed that half the total berthing energy is imparted to each wingwall.

  After characterizing events over the course of the past year, it is has been observed that each wingwall is subject to independent impacts, and the impact energy associated with the north and south wingwalls is rarely equal.

- Analysis of berthing events reveals that a vessel impacts each wingwall multiple times per berthing event, and the initial impact may, or may not, be the most significant.

- Approach velocity is a quantity that is challenging to measure accurately. It is most relevant at the point of impact, and may be misleading when measured at even small distances from the impact location. Rotational velocity effects are present and may have significant effects on the kinetic energy of the berthing vessel. Eccentricity coefficients from the literature may not be appropriate for the berthing scenario common at the Bremerton slip.

- Kinetic energy estimates (based on the Kinetic Energy Method), which use small approach velocities, tend to substantially underestimate the amount of kinetic energy a structure absorbs, suggesting that the combination of a vessel's propulsion and

environmental and rotational velocity components contributes significant amounts of energy to the berthing process.

- The wingwall system installed at the Bremerton slip contains substantial excess capacity based on the observation of this study.
- Each berthing event has a unique transfer of energy to the wingwalls due to the use of the propeller, rudder, effects of weather, etc.
- The empirically determined kinetic energy data used in conjunction with the reliability-based approach represent a logical paradigm for developing design energies.
- Reliability design charts and tables offer a concise method of approximating design berthing energy demands over a given service life.
- Berthing factor results allow empirical energy data to be used for vessels of different classes (displacements) than were recorded at the Bremerton slip.
- The berthing coefficient recommendations are general in nature, because the maximum energy absorbed by the berthing structure often includes additional effects unrelated to the initial kinetic energy of the vessel. A few examples that have effects that are impossible to isolate are the use of the ship's controls (rudder[s]), the propulsion system, and wind, wave, and tidal effects. *Therefore, it is recommended that the berthing coefficient results be used for preliminary inquiries only and not for design purposes*.
- Point-of-impact results provide information that could be used to refine the geometry and placement of the wingwall impact face.
- The existence of a statistically significant sample of energy absorbed by the structure renders the Kinetic Energy Method obsolete

Chapter 1 – Introduction

The Alaska Marine Highway and the Washington State Ferries are vital components of the U.S. highway system, providing a necessary transportation service that supports local communities and economies as well as national interests.

The Alaska Marine Highway (AMH) is a vital part of the transportation system in southern Alaska, connecting over 33 ports, many of which are only accessible by air or sea. The AMH provides service from Bellingham, Washington, to Dutch Harbor, Alaska, along the Aleutian Chain. The Auke Bay ferry terminal alone serves over 150,000 passengers and 30,000 vehicles each year.

Washington State Ferries (WSF) is the largest ferry system in the United States, comprising 22 vessels, 10 routes, and 20 terminals. In terms of vehicles carried, it is the largest ferry system in the world. Annual ridership for 2011 exceeded 22 million passengers and approached 10 million vehicles. Washington State Ferries is a critical link between the highly developed economies of eastern Puget Sound and the growing communities on the Kitsap and Olympic Peninsulas and the San Juan Islands. The Seattle terminal serves as the departure point for ferries bound for Bremerton and Bainbridge Island (Transportation 2012).

Although marine highways are part of the U.S. highway system, they are often overlooked in transportation studies. Consequently, the knowledge base for this type of infrastructure (e.g., vessel impact forces on landing structures, the structures that receive ferry vessels) is less developed than the knowledge base for other modes of transportation. The present standard of practice for designing these structures equates the kinetic energy of the approaching vessel to the elastic potential energy of the deformed structure. In this approach, assumptions must be made regarding approach velocity, vessel mass, and energy transferred to the structure. These assumptions have historically resulted in uncertainty in design or intentional overdesigning of the structure, which has a negative effect on the economy of design.

To help address this gap in knowledge, this research project ("Characterizing the Load Environment of Ferry Landings for Washington State Ferries and the Alaska Marine Highway System") was initiated to study forces from ferry vessels on ferry landing structures. The objective was to collect information needed for reliable yet economical structural designs. This objective was accomplished by measuring vessel approach velocity, displacement, and internal forces as vessels impacted a landing structure. The ultimate goal was to provide probability-based design criteria for vessel berthing demands. To facilitate this goal, measurements were taken each time a vessel landed. The instrumentation deployed for this project was designed to measure a number of parameters of interest to engineers:

- Acoustic distance sensors to measure the distance between the dock and vessel at a rate of five times per second. The velocity at the time of impact was estimated with this information.
- Marine vessel landings are often equipped with rubber fenders designed to cushion the impact and lessen the force experienced by the structure and the vessel. Fenders that are too stiff or too soft can result in damage to the structure or vessel. Having well-defined force-displacement relationships, measurements of how much a fender compresses during impact, allows determination of the force in the fender. Fenders at both sites were

instrumented with linear motion transducers (LMTs) to measure their displacement during impact.

- Support piling, consisting of both vertical and battered piles, were instrumented with strain gauges. The strain gauges were configured to determine the axial force in the piling.
- At each study site, another distance sensor oriented toward the water served as a tide gauge. Both locations experience extreme tidal variation, and this information was needed to determine the elevation of the ship's sponson, a projection from the vessel that makes contact with the structure (i.e., the point of impact).
- The instrumentation was driven by dataloggers onsite. Digital wireless modems connected to the dataloggers allowed remote control of the system and downloading of data over the cellular network.

The Auke Bay terminal in Juneau, Alaska, and the Seattle-Bremerton terminal in Seattle, Washington, were chosen for study. Each location was monitored continuously for about a year. An algorithm was programmed into the dataloggers whereby, when the vessel was at a predetermined distance from the motion sensor, the loggers would begin recording data. Velocity at the time of impact, maximum fender displacement, and pile force were identified and inserted into a database. The database was used to generate a number of histograms for developing engineering design aids.

The force imparted to the structure depends on the vessel mass, impact velocity, and other factors. The mass and velocity can be expected to differ between berthing events, resulting in uncertainty when choosing engineering design parameters. Statistics of the data, taken over numerous berthing events, were used to identify approach velocities, forces, and impact energies that have a low probability of being exceeded. Using criteria in this format should result in a design with a quantifiable degree of reliability (based on loads with a known probability of not being exceeded).

Although standard structural design procedures apply to port-related marine structures, these structures tend to be unique in terms of location, loading conditions, constructability, and configuration (Tsinker 2004). Because of the challenges associated with developing marine infrastructure, the design of these facilities has, to date, defied standardization. Engineers have typically applied basic concepts and lessons learned from similar structures to best achieve the objectives of a project. This approach often results in facilities that are one of a kind. The design process for berthing structures usually begins with a determination of the maximum design berthing load. The design load for a wingwall can be determined by using several methods, including the kinetic energy method, statistical method, and analytical method. Little information is available for ferry-class vessels that serves to validate any of these methods directly. The statistical approach involves direct measurements of berthing events and provides information specific to the location being studied. However, the downside of this method is cost, and the data obtained may not apply to other facilities directly.

Objective

A vessel moving toward a berthing facility approaches with some momentum and associated kinetic energy. The berthing facility must be designed to safely absorb the kinetic energy while

protecting the vessel, cargo, and berthing structure. The goal of this study is to characterize the load environment experienced at each study site and to provide several design aids that will inform the planning of future Alaska Marine Highway and Washington State Ferries terminals.

Field Campaign

Auke Bay Study

Over the course of 11½ months, approximately 480 significant impact events were observed at the Auke Bay ferry landing. Measurements from berthing events at Auke Bay were collected and recorded using an automated system that consisted of motion sensors, strain gauges, tide gauges, and LMTs, all connected to two on-site dataloggers. The three most active side-berthing dolphins on the east berth were instrumented and monitored for berthing loads. Statistical samples of berthing parameters were collected with this system.

Ten-minute time histories were recorded for every berthing event. The motion sensors recorded vessel position as a function of time, from which the vessel velocity for each berthing event was estimated just prior to impact. Berthing forces for each event were determined based on the displacement of the side-loaded cylindrical fenders and the estimated point of impact of the vessel on the fender face at time of impact. The approximate height of impact was determined by measuring tide levels relative to the top of each dolphin for each event. Berthing energy was extrapolated from the relationship between the overall deflection and stiffness of the structure-fender system. The stiffness for each dolphin was estimated separately using structural analysis software.

Seattle Study

Over the course of 11 months, measurements from approximately 6950 impact events were recorded and analyzed. Impact events refer to discrete vessel-structure interactions at each wingwall; each ferry berthing event contains two impact events. An integrated and automated system consisting of distance sensors, LMTs, strain gauges, and tidal gauges was used to capture berthing events. Both the north and south wingwalls at the Bremerton slip were instrumented. Each wingwall instrumentation consisted of the following: a distance sensor to activate the recording of the event and measure the approaching vessel's position as a function of time; six LMTs to measure the deflection at each of the marine fenders; and two full bridge strain gauges on each support pile (for a total of 18 gauges per wingwall). This system was then connected via instrumentation wire to a datalogger that recorded the events to a memory card. The datalogger was connected to a cellular modem controlled by a laptop computer in Fairbanks, Alaska.

Two-minute time histories were recorded for each berthing event. The vessel's approach velocity was calculated using a sonic distance sensor that recorded the ferry position every 0.2 seconds. Berthing forces and energies were estimated using deflection data provided by LMTs that were mounted adjacent to the marine fenders of the system. Tidal data were recorded using an ultrasonic distance sensor that allowed estimation of the elevation of impact. Strain gauges were installed on all piles to measure axial strain in the support structure.

Data Processing

Raw data from the dataloggers were first split into berthing event files. Next, berthing events were presented graphically to ensure they represented actual vessel berthing events and to enable

the selection of the data points that characterize berthing events. The key data points used to inform the analysis were point of maximum vessel impact, the point just prior to vessel impact (in order to have baseline information concerning the initial state of the system), and a point 1 second prior to impact (used to calculate the approach velocity). After the event file was appended to the information that characterized the primary vessel impact, all subsequent calculations were performed using this information. The approach velocity, berthing force, energy, and tidal data were all written to a summary file that accumulated the statistics from each event. The stiffness of the system was estimated separately using SAP2000, a structural analysis software package.

Presentation of Results

The results for both studies are displayed in multiple formats intended to provide as much information to practicing engineers as possible. Recorded and estimated parameter values are presented in tables, histograms, probability distribution fits, and probability plots. A probability-based design approach is presented as a foundation for rationally determining the value of design parameters. The probability-based data are presented in tables as a function of reliability level, as service and ultimate values, and in plots that are based upon the number of vessel berthing events a structure is expected to receive during its service life.

Chapter 2 – Literature Review

Overview

The load environment of vessel berthing structures has been studied primarily as it relates to vessels of relatively large displacements, such as tankers and cargo ships. Ferry-class vessels have seen little direct study, with a few exceptions noted in the following sections.

Understanding the load environment of a marine fender system is of critical importance to berthing facility design, and leaves much to the engineer's judgment. A summary of berthing energy, applicable research, and current methods to assess berthing energy is presented in this chapter.

Berthing Energy

For a vessel to unload its contents, it must come to a stop in a manner that safely dissipates its kinetic energy. Some portion of the vessel's energy can be dissipated by the use of the vessel's propeller, thrusters, or tugboats. However, most berthing procedures require that the dock structure absorb the remainder of the energy applied by the vessel as it comes to rest. The interface between the approaching vessel and the dock is where energy-absorbing marine fenders are used to protect shore side infrastructure from approaching vessels (Gaythwaite 2004; Tsinker 2004).

Designing a marine fender system must begin with an assessment of the kinetic energy of vessels that will be landing at the site. There are four accepted methods to calculate this energy: the kinetic energy method, the statistical method, the empirical approach, and mathematical modeling. Berthing energy is a function of vessel size, approach velocity, configuration of the structure, environmental conditions, and hydrodynamic effects. In practice, it is assumed that all berthing energy will be absorbed by the fender system, though in theory, some of the energy will be absorbed by the structure supporting the fender system. Fenders mounted on flexible structures are an exception; these configurations absorb 10% to 25% of the total energy to be absorbed. The common procedure is to develop an approximation of the incoming vessel's kinetic energy and then evaluate how the berthing facility will respond (deflect) based on load-deflection characteristics of the structure and fender system (Gaythwaite 2004).

Kinetic Energy Method

The most widely used method for estimating berthing demands on marine facilities is the Kinetic Energy Method. This method is prescribed by PIANC – the World Association for Waterborne Transport Infrastructure (PIANC 2002), the Unified Facilities Criteria (DOD 2005), the British Standard for Maritime Structures (BSI 1994), and others. The kinetic energy method (Equation 2.1) assumes that the displacement tonnage is known and that the energy to be absorbed by the fender system is the product of the vessel's apparent kinetic energy and a number of coefficients that describe various aspects of the system. These coefficients are collectively referred to as berthing coefficients, and they describe aspects such as the eccentricity of the vessel approach, geometric configuration of the ship at point of impact, deformation characteristics of the ship's hull, configuration of the berthing structure, and effective mass of the vessel (DOD 2005).

$$E_w = \frac{W}{2g} v^2 C_m C_g C_d C_c C_e$$ Equation 2.1

$$C_b = C_m C_g C_d C_c C_e$$ Equation 2.2

where

E_w = Berthing energy to be absorbed by wingwall system

C_b = Berthing coefficient, a product of coefficients

W = Weight of vessel in pounds

g = Acceleration of gravity

v = Berthing velocity normal to the berth

C_m = Effective mass or virtual mass coefficient (accounts for added mass due to entrained water, water that moves with the vessel)

Model and prototype experiments were used to develop Equation 2.3. This equation is referenced in Costa (1964), DOD (2005), and Gaythwaite (2004).

$$C_m = 1 + \frac{2D}{B}$$ Equation 2.3

where

D = Maximum draft of ship

B = Beam width of ship

C_g = Geometry coefficient; dependent on geometric configuration of ship at point of impact

C_d = Deformation coefficient (this accounts for the energy reduction effects due to deformation of the ship's hull and deflection of the ship along its longitudinal axis)

C_c = Configuration coefficient (this accounts for the difference between an open and solid pier or wharf, and the "cushioning" effect of water when berthing occurs at solid structure, when it has been shown that the water cushion absorbs significant portions of the berthing energy)

C_e = Eccentricity coefficient (this accounts for the vessel's rotation dependent on angle of approach and point of contact with the berthing structure). See Equation 2.4 (DOD 2005) and Figure 2.1:

$$C_e = \frac{k^2}{(a^2 + k^2)}$$ Equation 2.4

where

k = Radius of longitudinal gyration of the ship, feet

a = Distance between ship's center of gravity and the point of contact on the ship's side, projected onto the ship's longitudinal axis

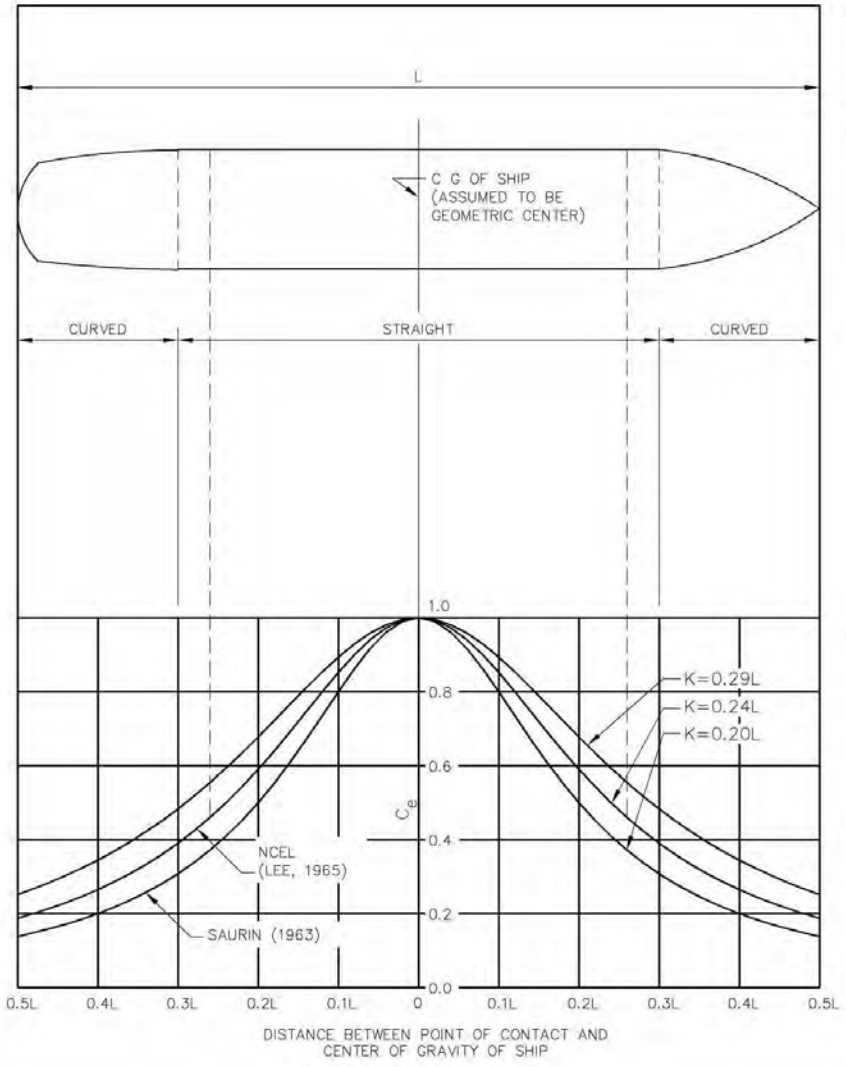

Figure 2.1: Eccentricity coefficient, C_e (DOD 2005)

The kinetic energy method uses the vessel's approach velocity, and choosing a suitable value can be a challenge for ferry designers, since berthing conditions can vary widely among facilities in terms of approach conditions, vessel size, and exposure. The published data on approach velocities primarily focus on tankers and cargo ships utilizing the assistance of tugs

during berthing maneuvers. Much of this information is provided by fender manufacturing companies (Gaythwaite 2004).

Research performed in the early 1990s in Washington State (Jahren and Jones 1993) is particularly useful, as it involves measurements at the Edmonds terminal and provides the basis for much of WSF terminal design standards. Using video analysis techniques, 568 berthing events at the Edmonds terminal were recorded and analyzed to describe the distribution of approach velocities of WSF vessels between 2095 and 3335 long tons. The mean perpendicular velocity found in this study was 0.44 feet per second. A methodology for defining a design approach velocity is introduced in Equation 2.5 (Jahren and Jones 1993).

$$v_{design} = FS_v * v_n \qquad \text{Equation 2.5}$$

where

v_{design} = Design approach velocity, feet per second

FS_v = Factor of safety for approach velocity, based upon a review of safety factors for various materials; suggested to be 2.0

v_n = Approach velocity that exceeds *n* percent of observations in empirical approach velocity distribution; *n* is chosen as 95% in both Jahren and Jones (1996) and Jahren and Jones (1993)

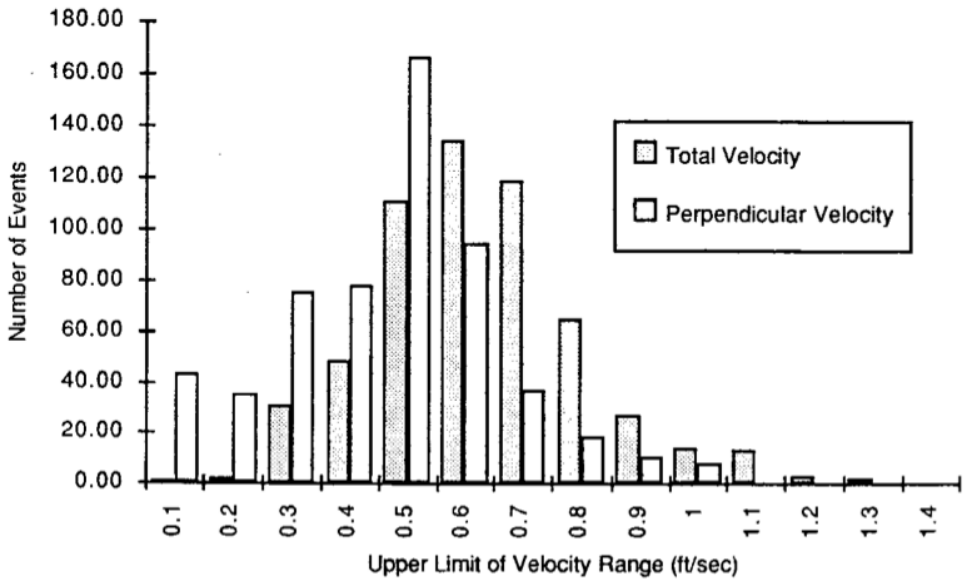

Figure 2.2: Velocity histogram (Jahren and Jones 1993)

Depending on the berthing maneuvers, several design approach velocities are recommended, the largest value of which could be considered the design approach velocity for a Super-class vessel of 2.0 feet per second in the surge direction and 1.6 feet per second in the direction normal to the wingwalls. This velocity is in agreement with the British Standard (BSI 1994) and with information found in (Gaythwaite 2004), which prescribe approach velocities for ferry and roll-on/roll-off (RORO) vessels of 1.6 to 3.3 feet per second. Both of the previously mentioned sources cite Brolsma's approach velocity curves (Figure 2.3) as a starting point for selection of vessel approach-velocity values. Brolsma used probability distributions to derive vessel approach velocity curves (Brolsma 1977). However, Beckett-Rankine (2010) investigated the development of these velocity curves and found that they have serious statistical deficiencies; the author also found that historical revision of the velocity standards has been accomplished without supporting explanation. The report recommends an update to reflect more modern berthing procedures and more maneuverable vessels (Beckett-Rankine 2010). The Beckett-Rankine report provides some insight into the discrepancy between recorded data at WSF terminals and the literature.

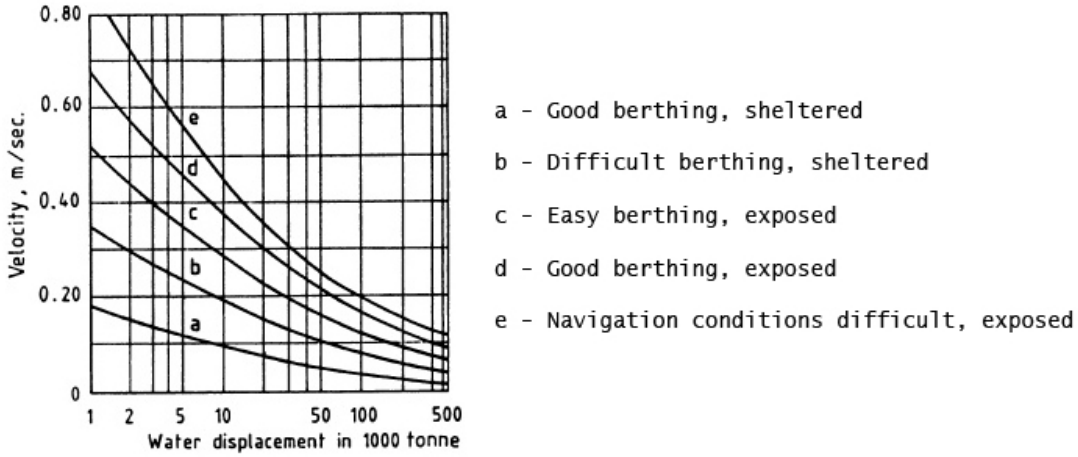

Figure 2.3: Brolsma approach velocity curves (BSI 1994)

The kinetic energy method is used widely in practice, despite the challenges associated with selecting suitable berthing coefficients and approach velocities. Without data collected from a berthing facility site, the accuracy of the design assumptions is subjective in nature and can lead to designs grossly over- or under-designed (Gaythwaite 2004).

One of the goals of this study is to provide information regarding a berthing coefficient that can be used in WSF design procedures, and approach velocities to improve the accuracy and efficiency of future wingwall designs. The current state of practice for the Washington State structural engineers working on marine projects is to use the kinetic energy method (Equation 2.1). The approach velocity currently used for design of WSF terminals is 2.53 feet per second (WSF 2012). Berthing coefficients currently employed are an amalgamation of empirical evidence and published information from published literature.

Analytical Approach

Highly developed analysis techniques are becoming more common as software and computational techniques evolve to handle the complex interaction of wind, wave, vessel, and mooring systems. These techniques are particularly useful for certain scenarios, where testing several possible configurations is desired because no site information is readily available (Gaythwaite 2004).

Traditionally, mathematical simulation of ship berthing has been accomplished by using frequency domain analysis or time domain analysis. Frequency domain analysis is widely used due to its relative simplicity when compared with time domain analysis. Frequency domain analysis is based in mechanical vibration theory, and involves a separate equation for each degree of freedom of a vessel's motion and several coefficients (Gaythwaite 2004).

$$\big(M + a(\omega)\big)\ddot{x} + \ b(\omega)\dot{x} + \ cx = F(t) \qquad \text{Equation 2.6}$$

where

M = Vessel mass

ω = Vessel motion frequency

$a(\omega)$ = Added mass coefficient

x = Vessel displacement

$\dot{x}$ = Vessel velocity, at vessel's center of mass

$\ddot{x}$ = Vessel acceleration, at vessel's center of mass

$b(\omega)$ = Damping coefficient

c = Linear spring constant

$F(t)$ = Time varying forcing function

The frequency domain technique has some fundamental shortcomings that can provide misleading results, and it has given way to time domain analysis (Gaythwaite 2004). Time domain analysis, which arose in the 1960s, involves the convolution integral over the past history of the exciting force with the impulse response function (Cummins 1962).

$$(M + m^{'})\ddot{x} + \int_{-\infty}^{t} K(t-\tau)\dot{x}d\tau + \ cx = F(t) \qquad \text{Equation 2.7}$$

where

M = Vessel mass

$m^{'}$ = Constant inertial coefficient

x = Vessel displacement

$\dot{x}$ = Vessel velocity

$\ddot{x}$ = Vessel acceleration

$K(t-\tau)$ = Impulse response function, τ represents variable integration time of earlier vessel position

c = Hydrostatic restoring force coefficient

$F(t)$ = Arbitrary varying forcing function

From this methodology, a time history of vessel motion in response to an arbitrary force (or system of forces) is derived. Values for the constant inertial coefficient and the impulse response coefficient cannot be determined directly and are derived from frequency-dependent hydrodynamic coefficients (Gaythwaite 2004).

This procedure, further elaborated in Fontijn (1980), describes the behavior of a ship berthing to a jetty. To facilitate solving, assumptions are made that include idealizing the ship as a rigid prismatic body. Only sway and yaw are considered, the water is calm, the fluid exists unbounded in the horizontal direction, and the bottom is flat. Experimental results agreed satisfactorily with predictions made from time domain analysis, with hydrodynamic coefficients adapted from a three-dimensional situation.

The Naval Facilities Engineering Service Center (NFESC) uses a model that employs a computational fluid mechanics approach. The model combines a Reynolds-Averaged Navier–Stokes (RANS) numerical method with a six-degrees-of-freedom motion program for time domain simulation of ship and fender reactions. The model has been verified with small-scale models and full-size model tests (DOD 2005).

Software Packages:

Currently, at least three software packages are capable of time domain simulation of the dynamic behavior of mooring vessels: TERMSIM, BeAn, and AQWA. Use of these software packages requires highly trained individuals who have a background in the analytical techniques used by the software programs. These programs allow a more rigorous analysis of berthing facility alternatives than the kinetic energy method. The use of advanced software packages is most common when designers are faced with unusual and/or complicated vessel-structure interactions that are not easily addressed by the kinetic energy method.

TERMSIM is produced by the Maritime Research Institute Netherlands (MARIN) and is targeted at the export tanker industry. Model tests are carried out in a wave and current basin to assist in calibration of the model, and the software contains extensive databases relating to ship berthing in the marine environment (MARIN 2012).

BeAn is a software package for berthing analysis that employs a simplified mathematical model that calculates time histories of fender forces, deflections, and vessel motions. Though not as advanced as other software packages, BeAn has the benefit of being more suitable for production work (DOD 2005). The software makes use of impulse response techniques of a linearized system (Rizos and Stehmeyer 2004). The mathematical background for BeAn is based on analytical models and solution techniques, first published by H.L. Fontijn (Fontijn 1988).

AQWA, a product offered by ANSYS®, a multinational simulation software company, was developed to model fluid-structure interaction. AQWA is a software suite that has extensible capabilities for most marine environment simulations; it has the ability to integrate with other

ANSYS multi-physics simulation software packages and work with structural mechanics finite element models (ANSYS 2012).

The Naval Facilities Engineering Command (NAVFAC) worked with the University of Alaska Fairbanks to calibrate analysis and design methods by using ANSYS AQWA for dynamic ferry berthing events (Seelig and Lang 2010). The U.S. Navy applied lessons learned in previous work to the specific Alaska modeling done for this study. The AQWA numerical model used in this study is built from ferry, float, and pile system components. Using these components, dynamic simulations of ferry berthing were conducted. Calculations were performed in the time domain to describe berthing events. Key parameters were systematically varied to obtain peak load predictions for each simulation. This research focused on berthing in the surge direction (end berthing), and therefore relates well to situations in Washington State. The Alaska ferry vessel-berthing events that were analyzed using AQWA showed little influence of added mass, and the energy required to dissipate was due to the vessel alone. Calculated added mass coefficients (C_m) in the end-berthing configuration from the AQWA analysis ranged from 1.038 to 1.121. Large under-keel clearance is one reason cited for minimal added mass effect in the end-berthing vessels. The study also determined that vessel size is not relevant for peak berthing loads in terms of kinetic energy. The recommendations are that simulations need to focus on the facility and that vessel size is not important as long as an adequate range of kinetic energies is considered (Seelig and Lang 2010).

Statistical Method

The berthing of a ship is a complex maneuver that is dependent on the pilot's level of experience as well as environmental and hydrodynamic effects. Each berthing event is a unique combination of these factors, and is a complex phenomenon to model analytically. Terminal design based upon the kinetic energy method requires the engineer to decipher uncertainties associated with approach velocity, the mass of the vessel, and the mechanics of energy dissipation within a fluid, berthing structure, and vessel.

The statistical method employs direct measurement of physical berthing parameters coupled with statistical techniques. Proper use of the statistical method provides a direct approach to the value of most interest in design, the berthing energy (Ueda et al. 2002). Various methodologies are used for measuring berthing parameters such as deflection and approach velocity. Using these measured parameters, berthing energies can be deduced and described statistically.

Relationships between berthing energy and frequency of occurrence can be developed using statistics and probability theory. This relationship can be used to extrapolate probabilities associated with design energy parameters having a likelihood of occurring or being exceeded. The designer selects a design energy value with an acceptably low probability of the value being exceeded within a given operational period. Uncertainties associated with approach velocity, mass, hydrodynamic effects, etc., are undefined, but are captured with the statistical sample, therefore releasing the engineer from the subjective judgments of berthing parameters (Ueda et al. 2001; Gaythwaite 2004).

The Washington State Ferries system has benefitted from direct measurements and statistical analysis since at least the early 1990s. Jahren and Margaroni (1993) used three different methods to track the approach path and velocity of ferry vessels operating between Edmonds and Kingston, Washington. By video recording vessel landings, video logging the vessel's radar

screen inside the pilothouse, and using the global positioning system (GPS), the study quantified approach velocity patterns as ships approached the ferry terminal. The authors recommend the use of GPS techniques for vessel velocity measurements due to improved accuracy and decreased labor requirements (Jahren and Margaroni 1993).

Jahren and Jones looked into design criteria for fenders at the Edmonds Terminal ferry landings just north of Seattle, Washington. Using video analysis techniques, a dataset of 568 berthing events at the Edmonds ferry terminal were analyzed to describe the distribution of approach velocities (both perpendicular and parallel to the wingwall) of vessels with published displacements between 2095 long tons and 3335 long tons. Utilizing closed-circuit video cameras aimed at each wingwall, approach velocity was estimated by scaling video images that contained calibration markings on the ferry deck to the timestamp of the recording. Multiple viewers were required for this estimation procedure, as observations contained significant variation; the reported accuracy of this study was ± 0.2 feet per second for vessel approach-velocity estimations. A similar video analysis technique was used to investigate berthing energy. During the study, the wingwall was deflected with a barge-mounted winch to calibrate movements in the video image of the wingwall timbers. Experienced observers then estimated the deflection of the wingwall from the video recording to estimate the amount of energy absorbed by the wingwall. From this information a berthing coefficient from 18 events was estimated at $C_b = 0.6$ (Jahren and Jones 1996).

A study concerned with sizing fenders given traditional ship berthing energy methods and applying statistical methods was done by Ueda et al. (2001). The authors focused on a probabilistic method that considers values of ship size, ship mass, approach velocity, virtual mass coefficient, eccentricity factor, and absorption energy of fenders as variables instead of deterministic values. These variables are then used to develop a probability of exceedance using a Monte Carlo simulation to investigate when berthing energy exceeds the energy absorption of the fender. The study, which focused on ships between 10,000 DWT and 35,000 DWT, concludes that many ships in this size range exceed the registered size, and this should be considered when determining berthing energy. Consideration of all aforementioned parameters with statistical characteristics was then used in a Monte Carlo simulation to calculate whether the probability of a ship's berthing energy would exceed the design energy absorption of the fender system (Ueda et al. 2001).

This research is continued in Ueda et al. (2002), where the authors present guidelines for the reliability design of fenders by presenting the statistical characteristics of design factors and safety factors. Given a sufficiently large number of observations, it was stated that all cumulative frequency distributions could be approximated by lognormal distributions. However, it should be noted that the authors did not directly assess berthing energy and observe it to be fitting a lognormal distribution. They calculated berthing energy using experimentally determined values of mass, approach velocity, and berthing coefficients. All berthing energy calculations were developed using random numbers that fit a lognormal distribution. Further treatment is given to the capacity side of the facility as described by Z, a "factor of energy absorption of fender"—the ratio of actual energy absorption to the manufacturer's published value of energy absorption of the fender (Figure 2.4).

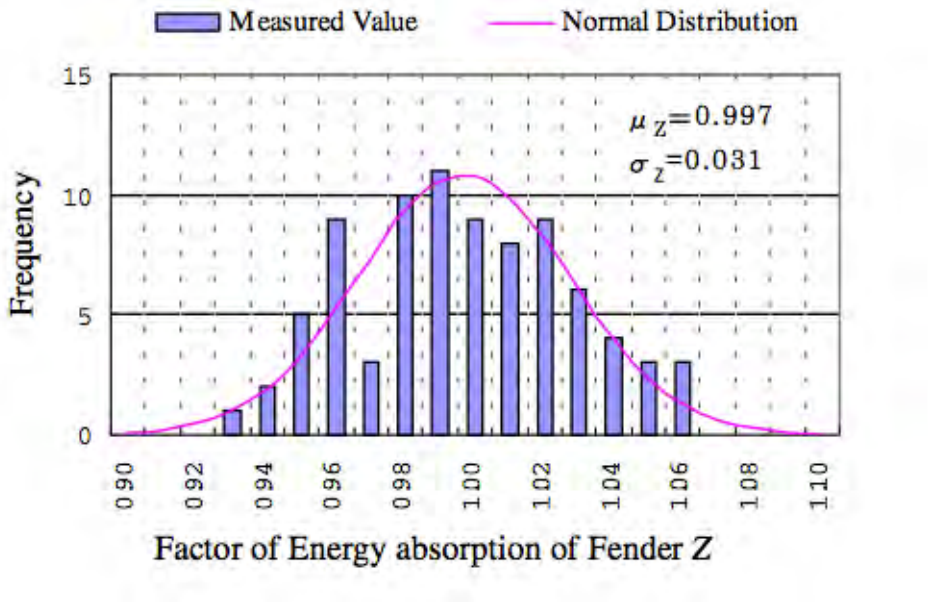

Figure 2.4: Factor of energy absorption (Ueda et al. 2002)

Dickenson (2007) discusses the current state of facility monitoring with regard to port facilities. He states the application of sensors and instrumentation systems at port facilities has lagged behind other sectors of civil infrastructure for multiple reasons including installation difficulties, longevity and maintenance concerns in the marine environment, and lack of funding sources. Unlike highway transportation systems, buildings, dams, and power facilities, ports have not typically been included in long-term instrumentation programs. Dickenson states that the use of instrumentation systems would help to validate the increasingly heavy reliance on numerical methods to simulate performance of waterfront structures. Most of these issues have been surmounted by other sectors of civil infrastructure, where application of instrumentation systems combined with data processing and analysis has provided direct benefits to engineering evaluation of system performance, maintenance, and life cycle cost evaluation (Dickenson 2007).

Though statistical methods are currently used, a consensus for measurement techniques and application of statistical techniques has not been reached. Unfortunately, due to cost and the individuality of berthing locations, there is little applicable berthing energy information to draw on in most cases. In situations where a facility operator has incentive to implement a direct measurement system, the information can be a benefit to long-term facility planning and life cycle costs.

Empirical Approach

Another method that takes advantage of measured data is the empirical approach. Relationships or formulas can be developed by some combination of measured data and experience. This methodology is suited to sites that have fairly constant vessel size, and to berthing frequency and berthing conditions (Gaythwaite 2004). Design energy has been proposed by Girgrah (1977) as based on vessel displacement and a constant that can be varied to a designer's experience:

$$E_f = \frac{\Delta}{120 + \sqrt{\Delta}}$$ Equation 2.8

where

Δ = Vessel displacement in long tons

E_f = Design fender energy in long-ton meters

Reliability Engineering

Traditionally, the approach to engineering marine structures has focused on embedding a high factor of safety into a design. In this deterministic method, a multiplier known as a factor of safety is applied to the expected load, or stress, a system would expect to experience in order to come up with a robust design. Utilizing the concept of reliability represents a shift in the way failures are treated. The reliability point of view treats system and component failures as random probabilistic occurrences. Given a large enough sample, this random failure process may be described by a probability distribution, and the systems' likelihood of failure (or non-failure) can be predicted statistically (Ebeling 1997).

Reliability is defined as the probability that a system or component will perform its intended function for a specified period of time under prescribed operating conditions (Ebeling 1997). Given that all failure modes cannot be eliminated for a given design, reliability engineering is also concerned with identifying the most likely failure modes and actively working toward mitigating the effects of those failures. The goal is to meet a specified probability of success at a given statistical confidence level. If a system does not perform its intended function, it is viewed as unreliable even if no failure has occurred (Ebeling 1997).

Determining reliability in an operational sense requires specific description of several factors. An unambiguous and observable description of failure must be explicitly defined. These failures need be defined relative to the function performed by the system or component in question. A specified interval must be chosen, such as a unit of time or number of cycles, and the system should be observable in its normal state, including design loads, environment, and other operational conditions. Reliability theory is also based on specified operating conditions, no system can be considered reliable given unlimited operational conditions (Ebeling 1997). As a system's reliability increases, initial costs associated with the system design also increase. The challenge is to select an appropriate reliability level that balances the initial costs and maintenance/failure costs over the life cycle of the system.

Strict application of reliability theory for complex systems such as wingwalls can be difficult to implement due to the challenges associated with combining the reliabilities of the various components in the overall structural assembly. This study will focus on the application of reliability concepts to the demand placed on the structure, not on the capacity of the individual components or composite structural assembly.

Load Resistance Factor Design

From a basis in reliability theory, load resistance factor design (LRFD) is rapidly becoming the standard methodology for designing buildings and bridges in the United States and abroad.

Load resistance factor design considers capacity (strength of materials or components in an assembly) to be a statistical quantity, which assumes that strength is merely a probability, not less than a specified value. Load resistance factor design treats demand the same way, as a probability that the load will not be greater than a specified value. Typically, materials have a coefficient that is less than one to factor the capacity downward to accommodate uncertainties associated with fabrication and materials. Demand placed on a structure uses factors greater than one in order to account for uncertainties in the load's application (Gaylord et al. 1992). The goal of applying LRFD is to ensure a safe and functioning structure by designing with a rational approach based on the quantified uncertainties of applied loads and material properties.

The LRFD methodology takes into account the following factors (Gaylord et al. 1992):

- Variability of a material's mechanical properties
- Uncertainty of loading conditions
- Possibility of deterioration of structural health over time
- Quality of fabrication
- Risks associated with structural failure with regard to injury, loss of life, and damages

Figure 2.5 displays graphically an application of the LRFD principles. The probability density for load is *q(S)* located on the left, and the probability density for resistance is located on the right *q(L).* A structure would then be designed for a load that is some factor greater than the mean load, and so that the capacity of the structure is designed for a factor well below the mean capacity. Following this procedure, a failure will only occur when an unusually high demand is placed on an unusually weak structure (Jahren and Jones 1993).

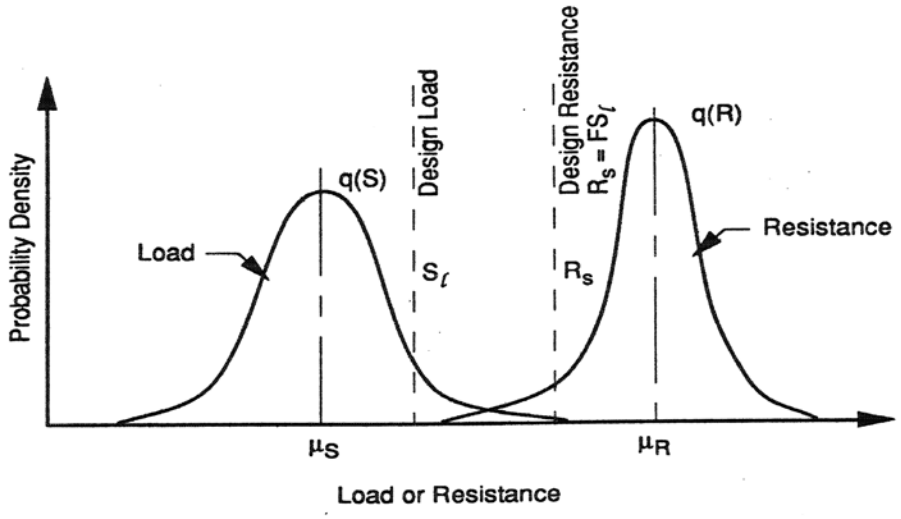

Figure 2.5: Load resistance factor design (Jahren and Jones 1993)

Chapter 3A – Means and Methods: Auke Bay

Overview

The load environment on ferry landings is not well quantified, and remains largely based on assumptions and historical knowledge developed over a number of operation/failure cycles. Previous literature has focused primarily on tanker-sized vessels and cargo ships of a magnitude much greater than the ferries used by the Alaska Marine Highway System (AMHS). The limited amount of information, specifically for Alaska, has led to the design of structures with an unknown reliability.

It is the intent of this study to improve upon our understanding of the load environment on ferry landing structures. This study will focus on the Auke Bay facility with the following goals:

- Formulating risk-based design criteria consistent with reliability engineering methods, using measurements from the Auke Bay landing.
- Providing a broad set of statistical design parameters that can be readily applied to current AMHS design methods.
- Assessing current design criteria

Findings are based on in situ monitoring of berthing events from four vessels at the Auke Bay ferry landing in Juneau, Alaska. Vessel displacements range from 5552 to 7683 long tons. Field testing was designed to measure berthing parameters simultaneously to develop a time history of the vessel-structure interaction before, during, and after vessel impact. Specifically, the following parameters were measured:

- Vessel position vs. time
- Fender displacements during impact
- Strains in piling
- Tide levels

Site Description

The Auke Bay ferry terminal is located in southeastern Alaska in Juneau, naturally protected by a series of islands and fjords. The landing features both side and stern berths and can accommodate three ferries at any time. The side-berthing portion of the landing consists of fourteen dolphins and two transfer bridges divided into the east and west berths (Figure 3.1). The stern berth is for a catamaran ferry and was not included in this study. This investigation focuses on side-berthing dolphins most affected by the vessels: the east berth dolphins, labeled W2, E1, E2, E3, and E4 in Figure 3.2.

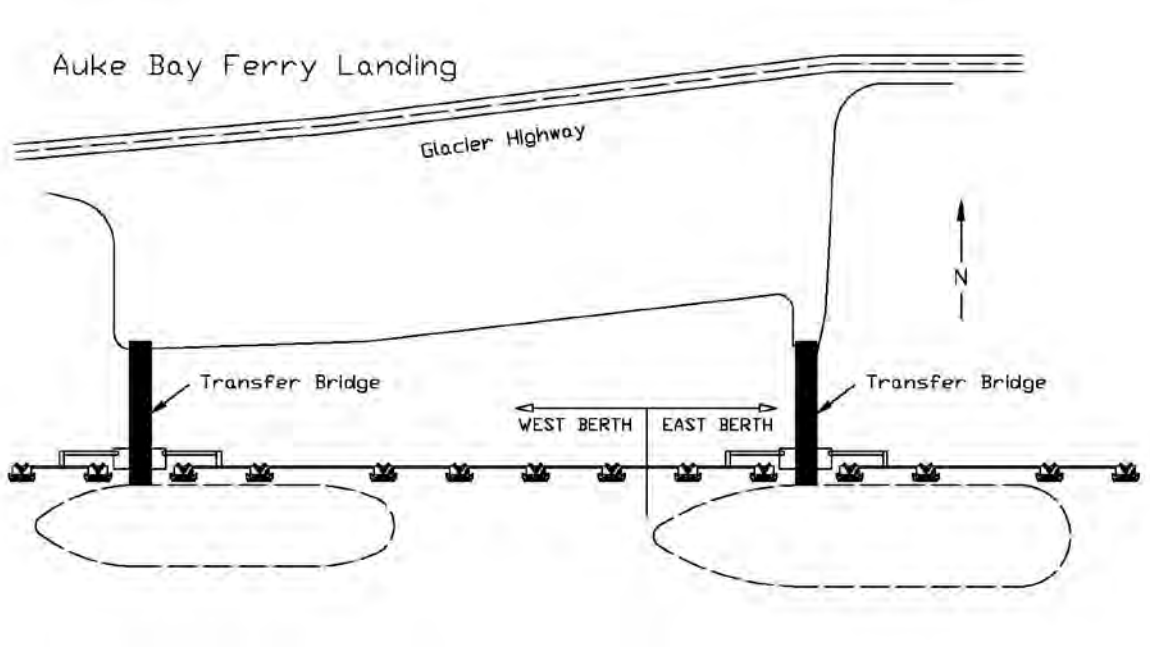

Figure 3.1: Auke Bay side berth

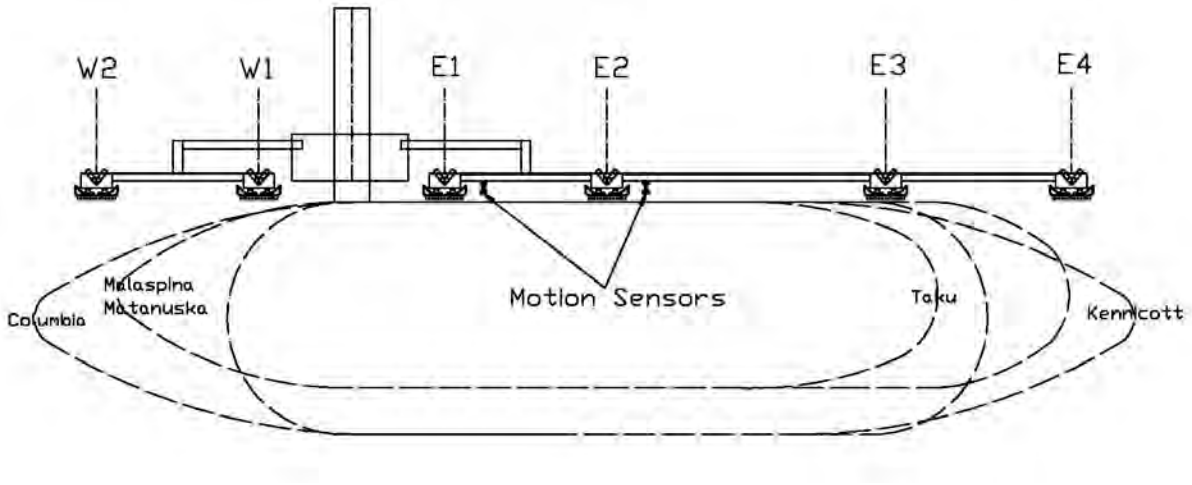

Figure 3.2: Auke Bay east side berth

Berthing Structure Description

Each mooring dolphin consists of two separate components: a fender system and a tripod system. The fender system consists of two 40-inch side-loaded cylindrical fenders, and four 18-inch-diameter vertical fender piles supporting a timber facing. The tripod system consists of three 18-inch-diameter steel piles; a single vertical pile and two piles battered at approximately 3:1 (see Figure 3.3 for details).

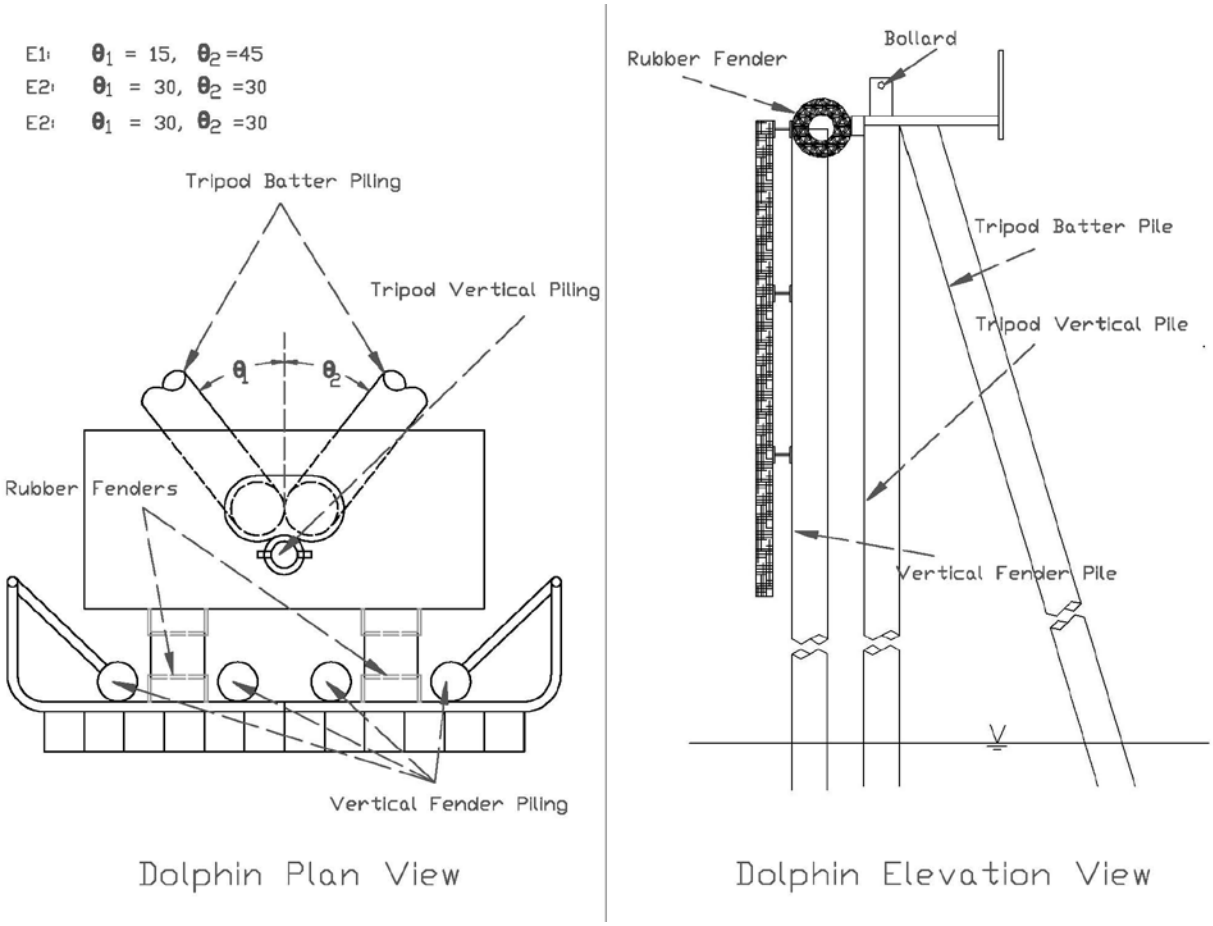

Figure 3.3: Typical Auke Bay berthing dolphin

Vessel Description

Berthing events from the four different vessels that land on the east berth were monitored. The vessels range from 5552 to 7683 displacement (long tons). Table 3.1 has general vessel information. Figure 3.4 shows the vessels.

Table 3.1: Vessel Specifications

Vessel Information				
Vessel Specs	Matanuska	Malaspina	Columbia	Kennicott
Length (ft)	408	408	418	382
Beam(ft)	74	74	85	85
Displacement (long tons)	5569	5552	7683	7503
Loaded Draft (ft-in)	16′ 11-5/8″	16′ 11-3/8″	17′ 6-1/8″	17′ 6″

Figure 3.4: Auke Bay study vessels
(clockwise from the top left: Columbia, Matanuska, Malaspina, and Kennicott)

Instrumentation Description

To measure the desired berthing parameters, an automated instrumentation system was designed and installed at the Auke Bay terminal along the east berth, labeled W2, E1, E2, E3, and E4 in Figure 3.2. During instrument deployment, it was observed that Dolphins E1, E2, and E3 were experiencing berthing action. Impacts were not observed at Dolphins E4 or W2 or W1, and were used exclusively for securing mooring lines. Dolphin E2 also experienced mooring loads in addition to berthing loads, serving as a springline support used to align the vessel's cargo door to the loading ramp of the landing. Dolphins E1 and E3 were thus instrumented to monitor impact effects only. Dolphin E2 was instrumented for both mooring and berthing effects.

The complete Auke Bay instrumentation system consisted of:

- Two Campbell Scientific CR5000 dataloggers
- Three Senix TSPC motion sensors
- Six linear motion transducers (LMTs or string pots)
- Twenty-six 90 degree chevron strain gauges (two ¼ bridges per gauge)
- One field computer running RTDAQ® (Real Time Data Acquisition) software developed by Campbell Scientific. Inc.

Additional hardware included environmental protection boxes for the dataloggers, Belden instrumentation wire, two Raven XT cellular digital modems, and two modem antennas.

The system was designed to monitor simultaneously all the instrumentation installed on dolphins W2, E1, E2, E3, and E4 during any given berthing event. The instrumentation components were hardwired into the two dataloggers, with W2 and E1 wired into Datalogger 1 and E2, E3, and E4 wired into Datalogger 2. The dataloggers operated and received instructions via an internal program written in *CRBasic* using RTDAQ. The system was set to read and collect at 5 Hz to adequately capture the events. Each berthing event was captured and recorded for 10 minutes in order to obtain a solid time history of each event both during impact and tie up.

The berthing aspect of the instrumentation system was designed to measure the approach distance versus time of an incoming vessel, fender displacement, axial force in the tripod piling, and tide level during the event. To accomplish this, the following hardware was installed (Figure 3A.8):

- Four ¼ bridge (2 chevron) strain gauges mounted 180 degrees apart around the surface of each tripod pile on Dolphins E1, E2, and E3.
- Two *Senix TSPC* motion sensors mounted on the catwalk (walkway between dolphins) 10′ from Dolphins E1 and E2.
- Two LMTs per dolphin mounted adjacent to each rubber cylindrical fender on E1, E2, and E3
- One Senix TSPC motion sensor mounted on E1 and oriented perpendicular to the water surface.

The strain gauges were used to obtain the response of the tripod-systems-to-vessel impact by measuring axial strain. The two rosette gauges were wired into a full bridge to measure axial strain only. The gauges, mounted on stainless steel shims, were welded to the surface of each pile and coated in a sensor-safe silicone sealant to protect them from the harsh environment (Figure 3.7).

Motion sensors mounted on the catwalk were used as data collection triggers. When the vessel was at a predefined distance from the motion sensors, the datalogger began saving data. The motion sensors were set to trigger the program “on” to begin recording at a vessel distance of 200 inches from the face of the sensor, and trigger “off” after 10 minutes. Data was collected at 5 Hz over the 10-minute period, resulting in a time history for each instrument of approximately 3000 records.

The LMTs were used to measure the linear displacement in the rubber cylindrical fenders (of known stiffness) on each dolphin during an event (Figure 3.6). The LMTs were mounted adjacent and parallel to each cylindrical fender. A motion sensor mounted on E1 was used as a tide gauge to monitor water elevation (Figure 3.6).

Figure 3.5: Position sensors

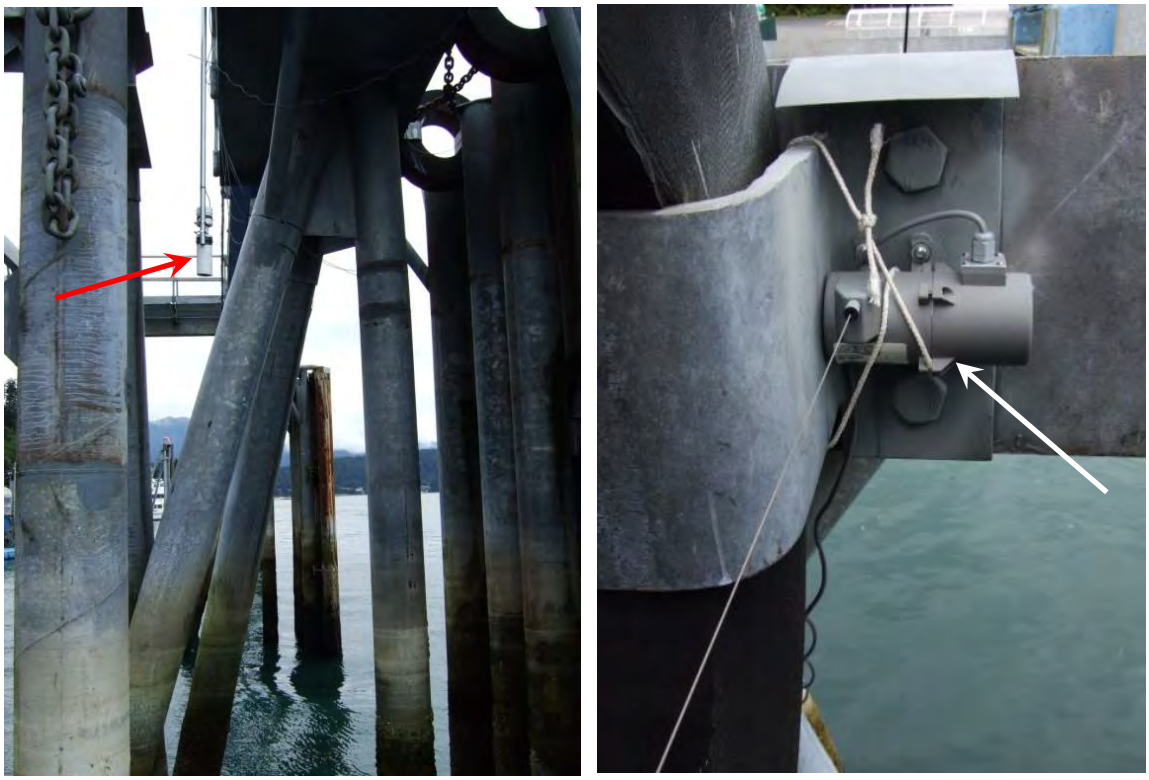

Figure 3.6: Tide gauge (left); LMT (right)

Figure 3.7: Strain gauges mounted on pile

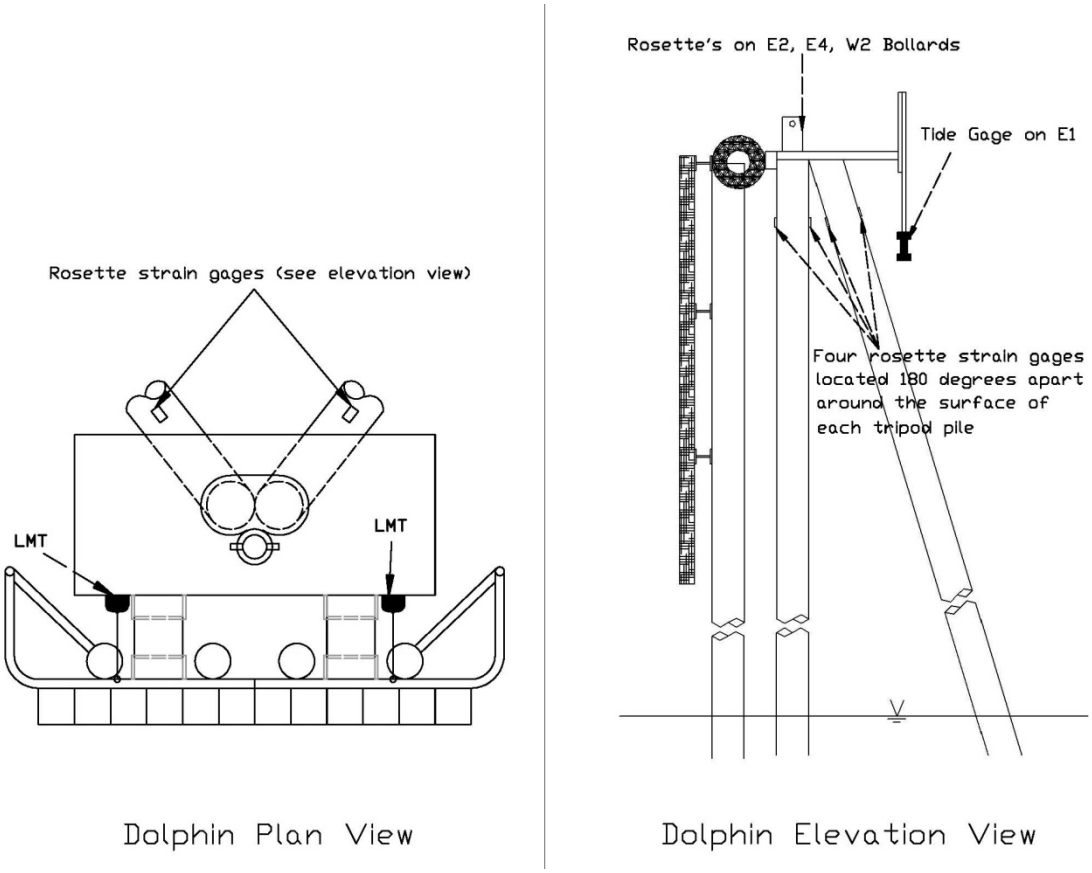

Figure 3.8: Instrumentation placement

Vessel Position Measurements

Time histories of measurements were used to estimate approach velocities just prior to impact on Dolphins E1 and E2. Fender displacement data, recorded simultaneously with vessel motion, were used to ascertain the time of impact. Approach velocities were determined from the vessel motion versus time graphs and averaged over approximately 1 second prior to impact.

Figures 3.9 through 3.16 show typical profiles for position versus time for all four vessels. Fender displacement and vessel position are together in Figure 3.17. The raw position versus

time graphs provide valuable insight into many aspects of a berthing maneuver, showing how the maneuver and approach can vary significantly depending on vessel and event. The sharp peaks in the graphs generally indicate the use of bow thrusters or mooring lines/winches used to move the vessel closer to the berthing structure. The sharp valleys in the graphs generally represent either impact or rebound off the fenders, or the use of bow thrusters, which reverse the vessel's direction normal to the fender face.

Impact events are easily determined when the position versus time and fender displacement versus time graphs are compared (Figure 3.17). Notice in Figure 3.17 that the four primary displacement maximums (valleys) in the fender displacement data align well with valleys in the vessel position versus time graph, indicating impact. The static offset from the zero position indicates the displacement of the fenders after the vessel has been tied up.

Berthing maneuvers vary per event, and a number of variables affect the transfer of kinetic energy to the dolphins. It is interesting to note that most berthing events do not consist of one single impact followed by mooring. The 10-minute time histories show that multiple impacts are frequent. In addition, the maximum approach velocity per berthing event is often not the result of initial approach and impact, but rather the result of maneuvers used to position the vessel after initial contact. It was observed that such maneuvers typically result from sources such as bow thrusters and mooring lines (in particular, the springline attached at Dolphin E2)/winching activity used to position the vessel.

Berthing Energy Measurements

Berthing energy is the most common parameter used by marine engineers for the design of berthing structures. When a vessel impacts a berthing structure, a portion of the kinetic energy of the vessel must be absorbed by the structure being impacted. Current fender design usually assumes that all berthing energy will be absorbed by the fender, with energy that is absorbed by the structure and the vessel hull neglected. This assumption is reasonable for very stiff structures. However, when the assumption of rigidity may not be reasonable, the elastic energy absorbed by the backup structure may be significant. A previous study has shown that energy absorbed by the supporting structure may be as much as 10–25% of the total berthing energy (Gaythwaite 2004).

Previous literature has also typically used only fender deflections as a basis for determining berthing energy. While this assumption is valid in many cases, elastic energy absorbed by the tripod structures at Auke Bay will be included in this study.

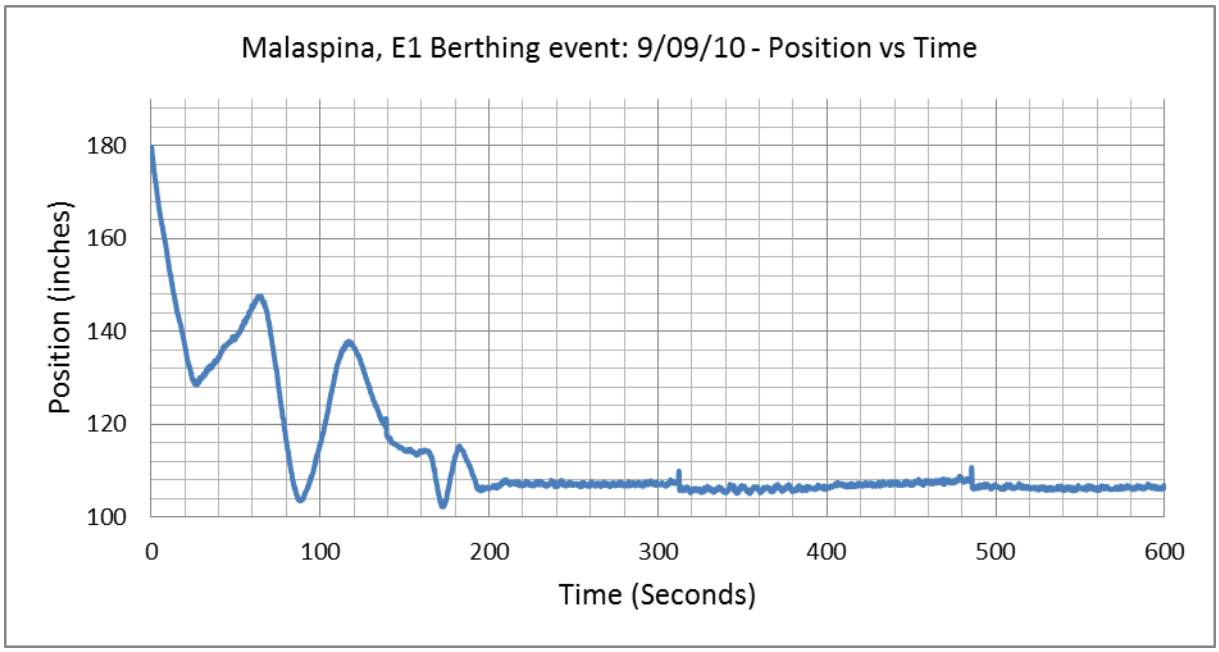

Figure 3.9: Position vs. time for the Malaspina, E2

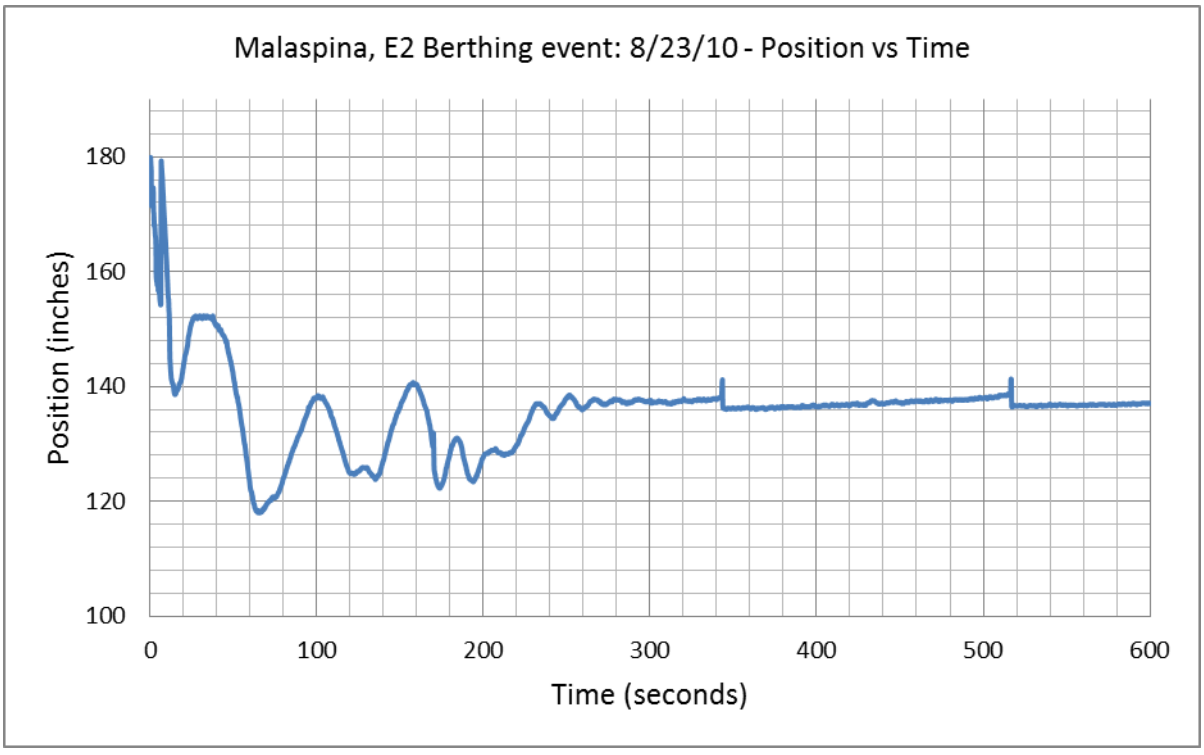

Figure 3.10: Position vs. time for the Malaspina, E1

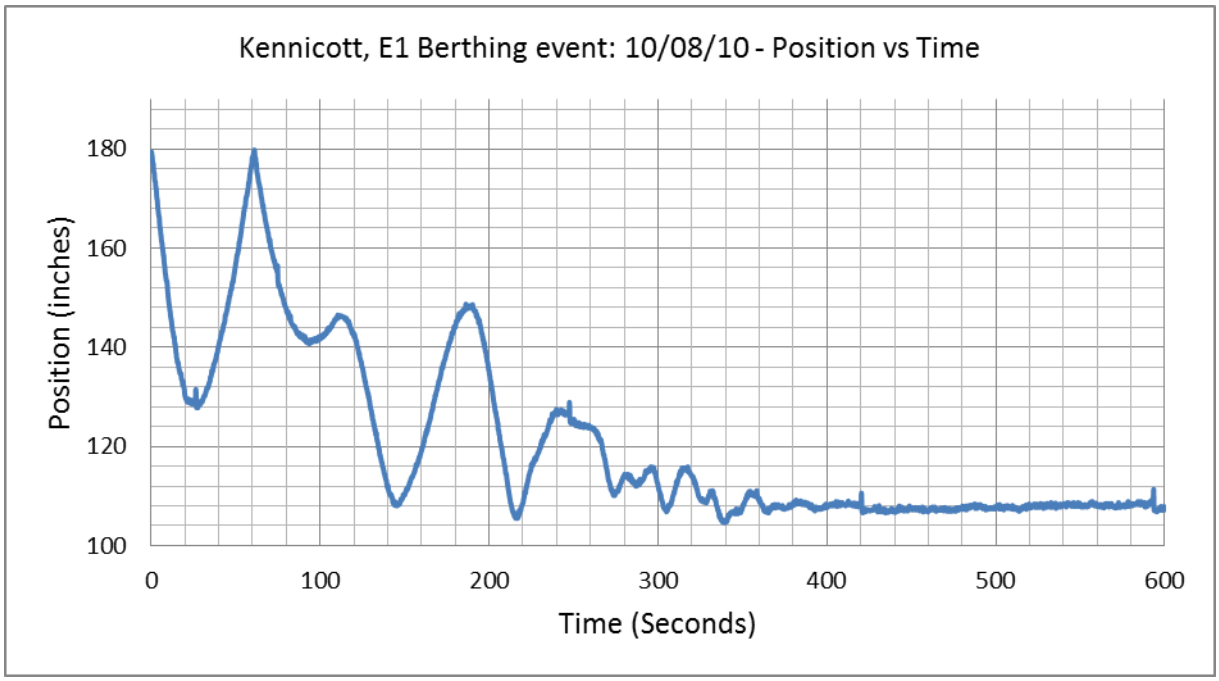

Figure 3.11: Position vs. time for the Kennicott, E1

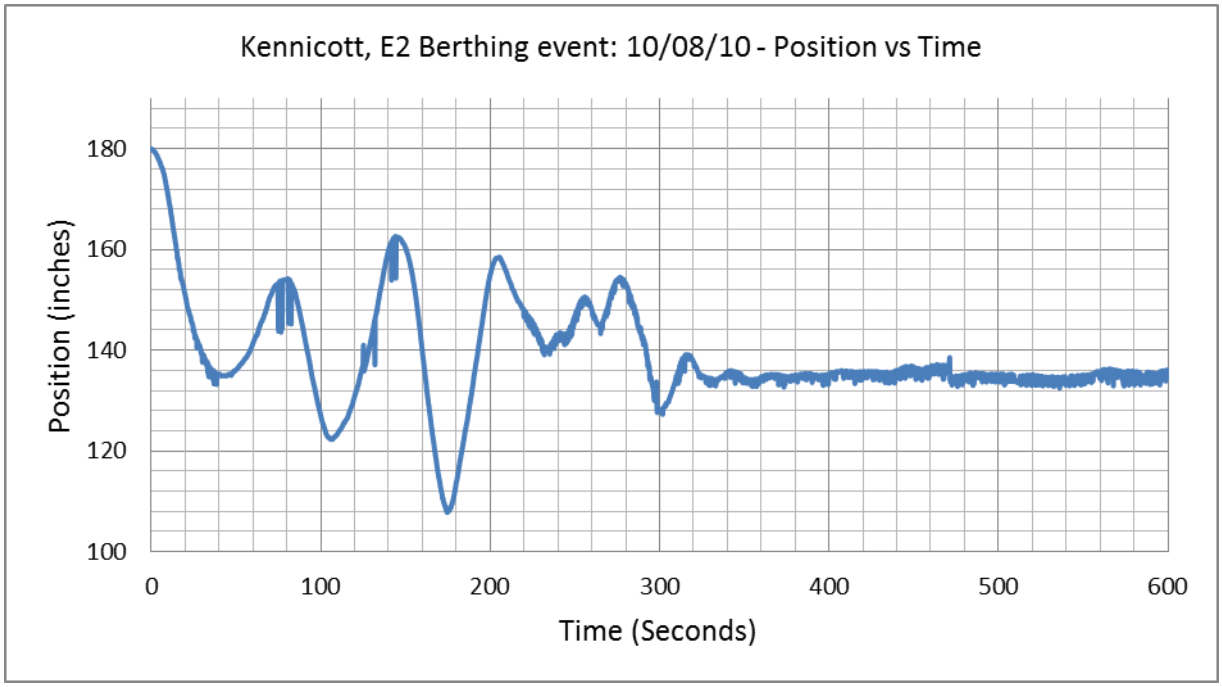

Figure 3.12: Position vs. time for the Kennicott, E2

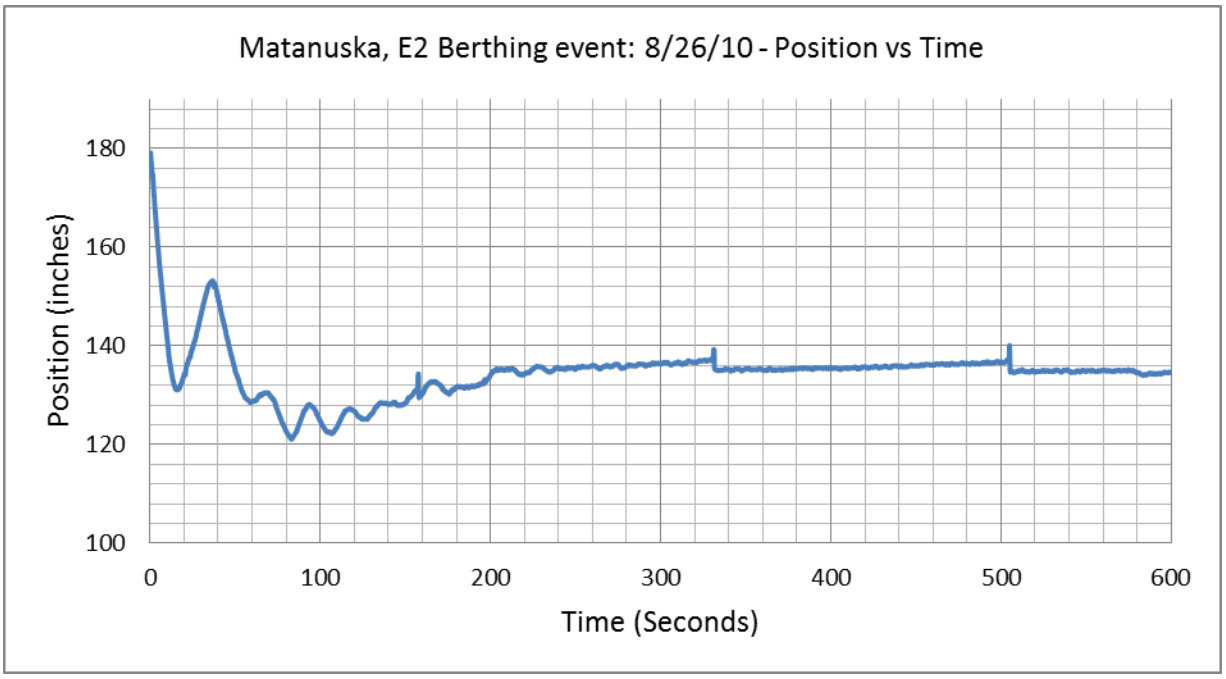

Figure 3.13: Position vs. time for the Matanuska, E2

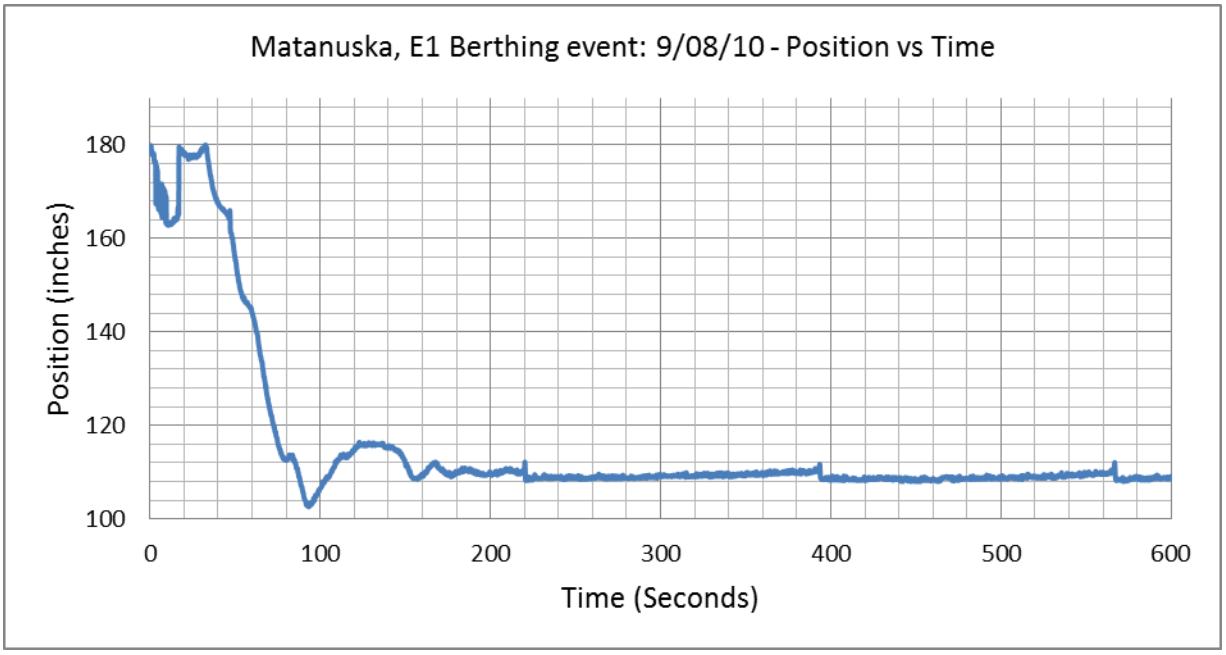

Figure 3.14: Position vs. time for the Matanuska, E1

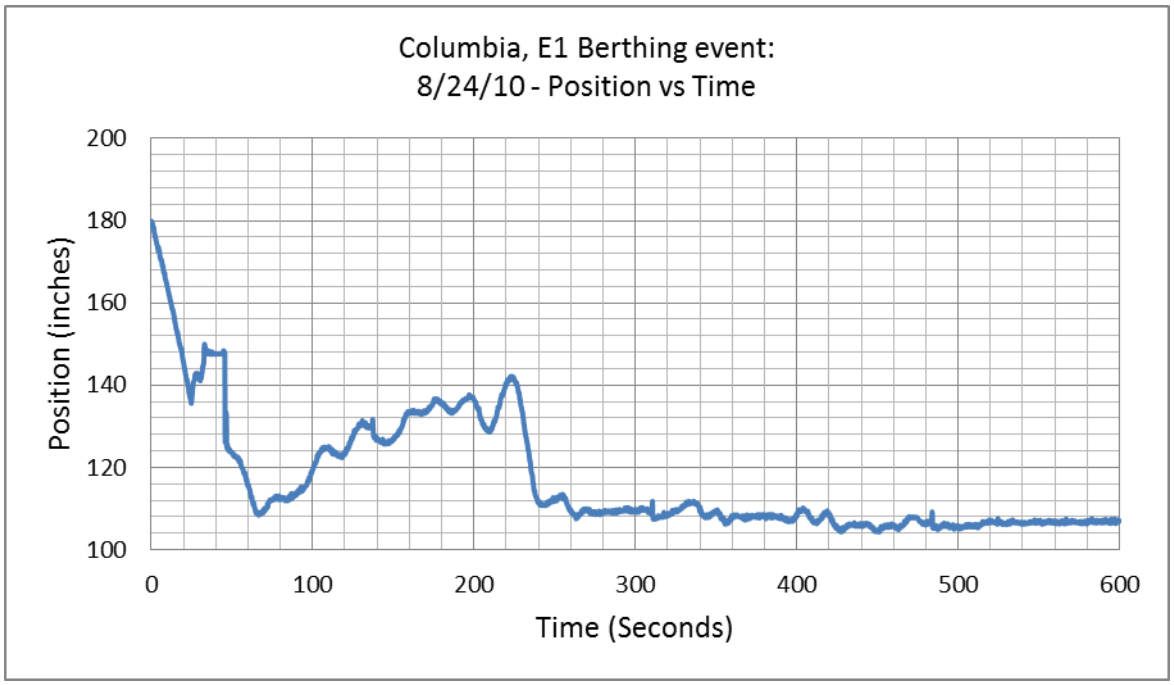

Figure 3.15: Position vs. time for the Columbia, E1

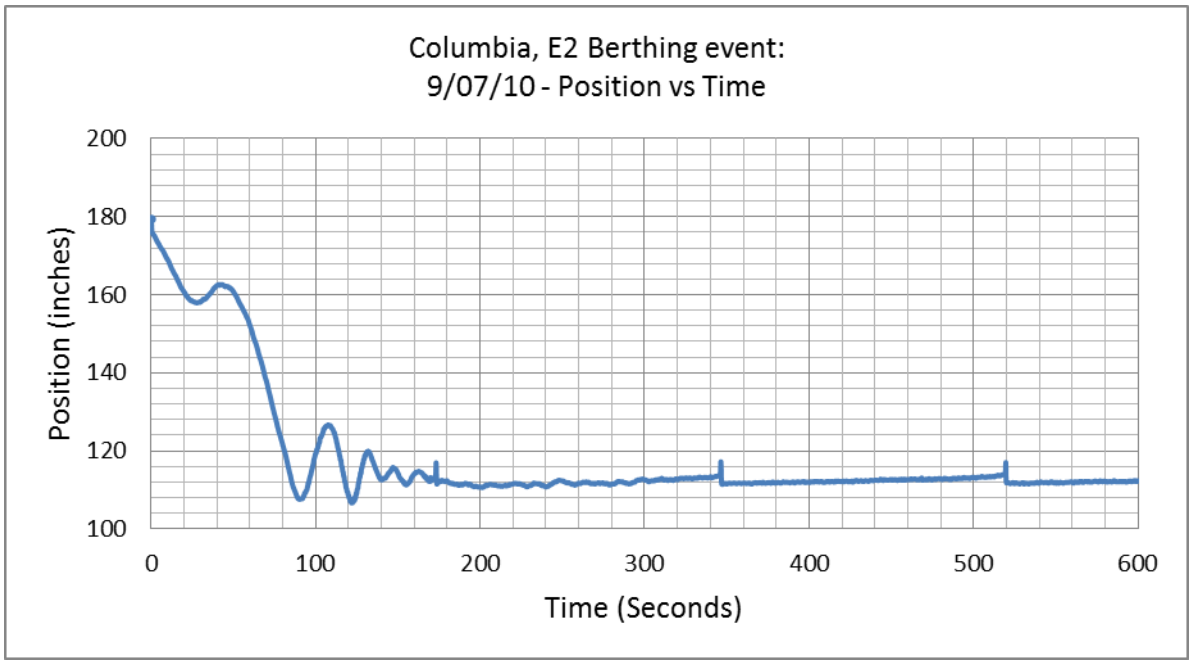

Figure 3.16: Position vs. time for the Columbia, E2

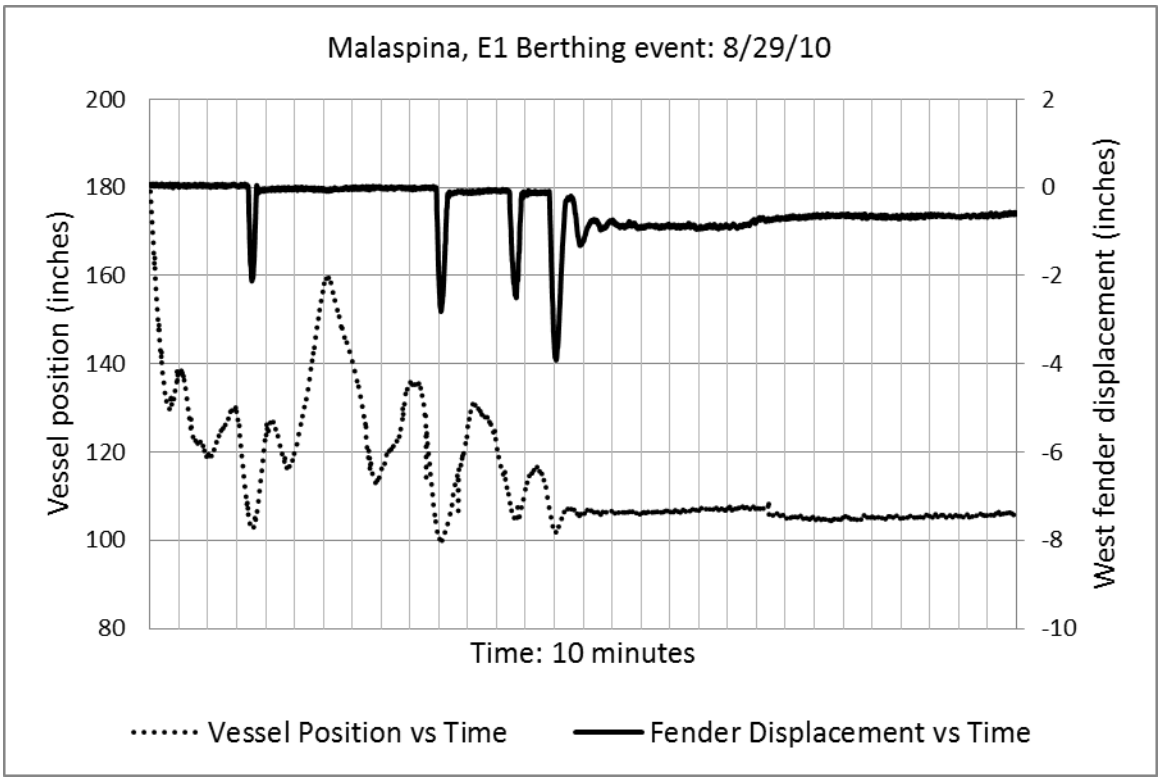

Figure 3.17: Vessel motion and fender displacement

The fender system on each dolphin consists of two side-loaded cylindrical fenders (40″ diameter) designed to deflect approximately 13.25 inches and resist a 15-kip load, and four vertical fender piles covered in a timber facing (Figure 3.3). The four piles are assumed to have no rotational stiffness at the bottom; they are "pinned" at the bottom, essentially. This assumption is based on pile driving logs provided by the ADOT&PF, which indicate the presence of extremely soft material with low lateral stiffness until the last couple of feet. All hydrodynamic, inertial, and damping effects on the outboard piling are considered insignificant.

To determine the overall energy absorbed by the dolphins during a berthing event, the total stiffness and deflection of both the fender system and the tripod for each dolphin needed to be quantified. The stiffness of each tripod system was estimated separately for Dolphins E1, E2, and E3, using structural-analysis software (SAP2000). With details from the working drawings, the geometry and mechanical behavior of each dolphin was modeled as accurately as possible. Pile driving logs were used to roughly estimate pile tip elevations for each vertical pile. The rubber cylindrical fenders were modeled as springs separating the fender face from the tripod. The stiffness of the tripods and the combined tripod and fender systems were determined by applying a unit load to the fender faces of each model, from which the deflection was recorded. Stiffness was obtained from the load/deflection results (Figure 3.18).

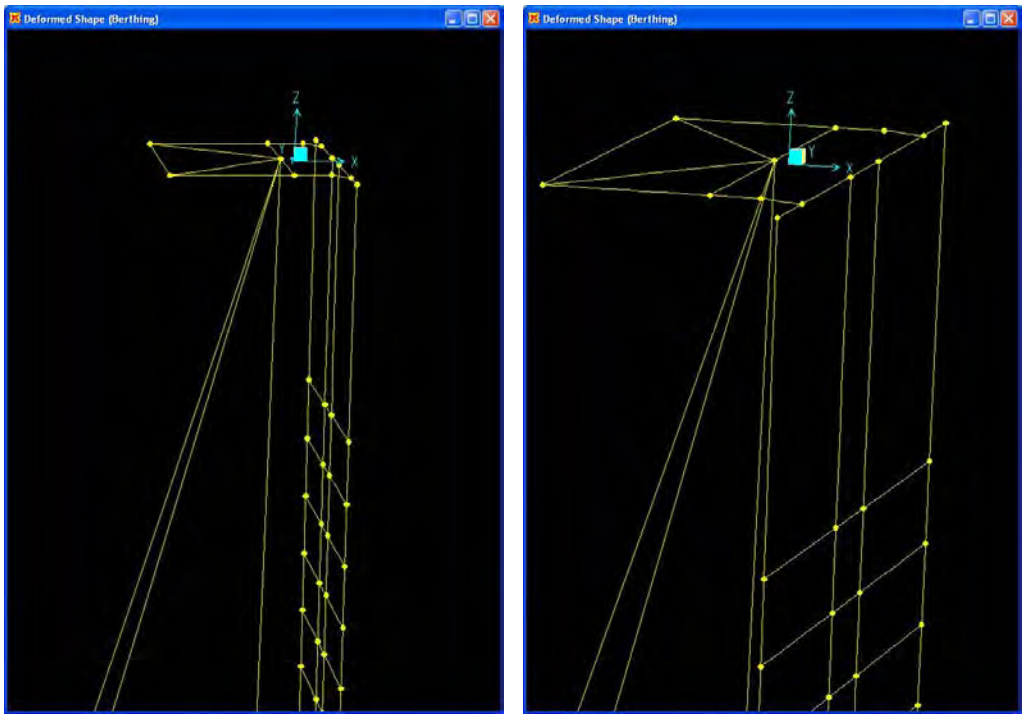

Figure 3.18: Sap 2000 structural model of Dolphin E2

Three dolphins (E1, E2, and E3) were instrumented with LMTs adjacent to each cylindrical fender to monitor the displacement of each fender during a berthing event. Using known stiffness for the cylindrical rubber fenders, the maximum displacements (measured by the two LMTs) from each event were then used to determine the energy absorbed by the fender system using basic spring mechanics, shown in Equation 3.1.

$$E_F = \frac{1}{2} K_f (x_{wf}^2) + \frac{1}{2} K_f (x_{ef}^2) \qquad \text{Equation 3.1}$$

where

$E_F = Energy absorbed by the fender system\ (Kip * ft)$

$K_f = stiffness of each\ rubber\ fender\ (\frac{Kips}{inch})$

$x_{wf} = Displacement of the\ west fender\ (inches)$

$x_{ef} = Displacement of the\ east fender\ (inches)$

K_f = 2.046 kips/inch per rubber fender, or 4.091 kips/inch total (two fenders per dolphin) for Dolphins E1, E2, and E3. Fender system stiffness was interpolated based on fender manufacturer specifications.

The equation for the total combined energy absorption of the fender and tripod system is described by Equation 3A.2, and schematized as a series of springs in Figure 3A.19.

$$E_T = \frac{1}{2}K_f(x_{wf}^2 + x_{ef}^2) + \frac{1}{2}K_t x_t^2$$ Equation 3.2

where $E_T = Total\ energy\ absorbed\ by\ the\ fender + tripodsystem\ (Kip - ft)$

$K_t = Stiffness\ of\ the\ tripod\ system\ (\frac{Kips}{inch})$

$x_t = Displacement\ of\ the\ tripod\ system\ (inches)$

$x_T = Total\ displacement\ of\ the\ dolphin\ (x_t + x_f)(inches)$

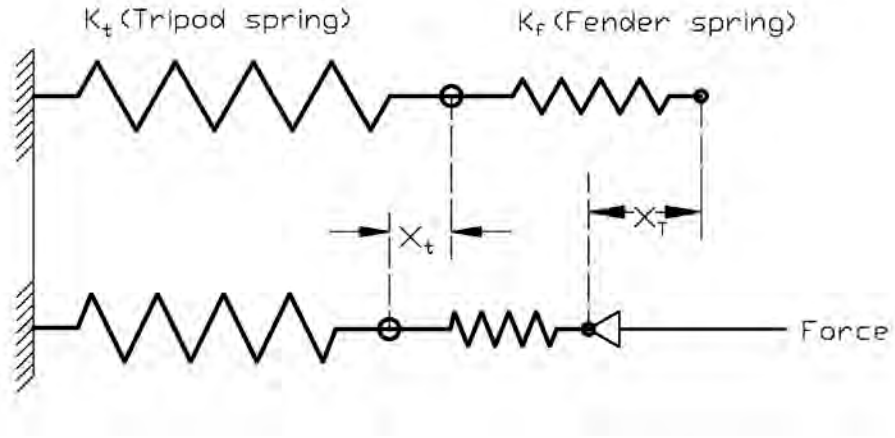

Figure 3.19: Dolphin spring schematic

Figures 3A.20 through 3A.22 show the force versus deflection (stiffness) curves for the tripod, fender, and combined system for each dolphin. Figures 3A.23 through 3A.25 show the energy contribution of each component as a function of fender displacement. Fender displacements versus time graphs are provided for some typical events in Figures 3A.26 through 3A.29 for all four vessels.

The stiffness of the tripods (K_t) on E1, E2, and E3 were found to be 27.661, 23.419, and 25.696 kips/inch, respectively, from the SAP models. The total potential energy of Dolphins E1, E2, and E3 (fender + tripod) were determined in terms of fender energy as follows:

$$E_T = 1.148E_F for E1$$ Equation 3.3

$$E_T = 1.151\ E_F for E2$$ Equation 3.4

$$E_T = 1.159\ E_F for E3$$ Equation 3.5

It is evident from the energy/deflection curves as well as Equations 3.3 through 3.5 that the fender backing structures (tripods) contribute a non-trivial portion to the total energy absorption capacity of each dolphin. The tripods on E1, E2, and E3 each contribute 12.9%, 13.1%, and 13.7%, respectively, to the total energy absorbed.

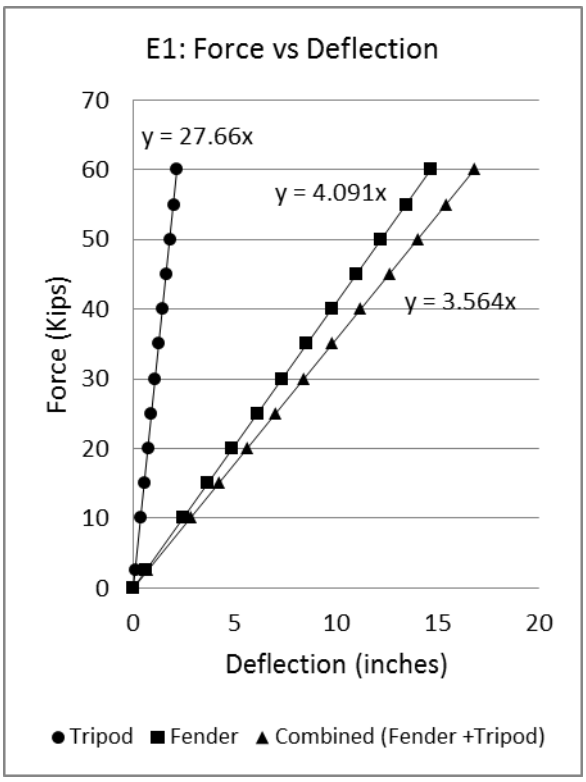

Figure 3.20: Dolphin E1 stiffness

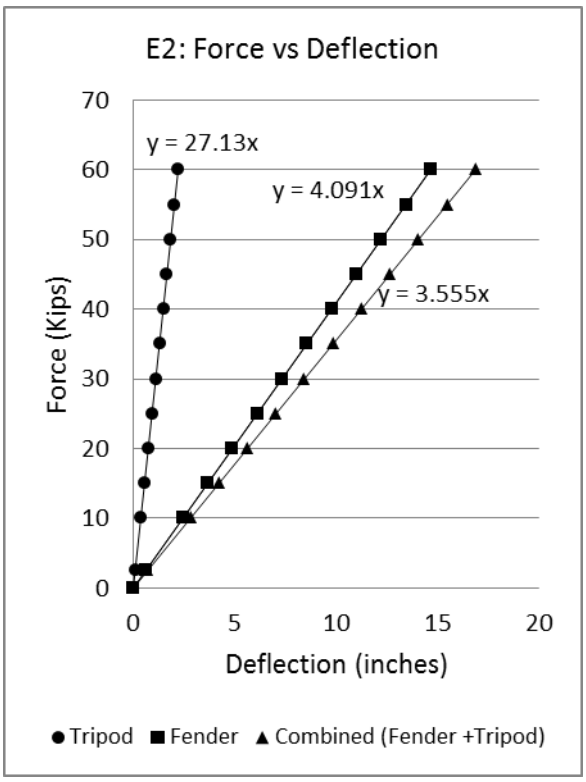

Figure 3.21: Dolphin E2 stiffness s

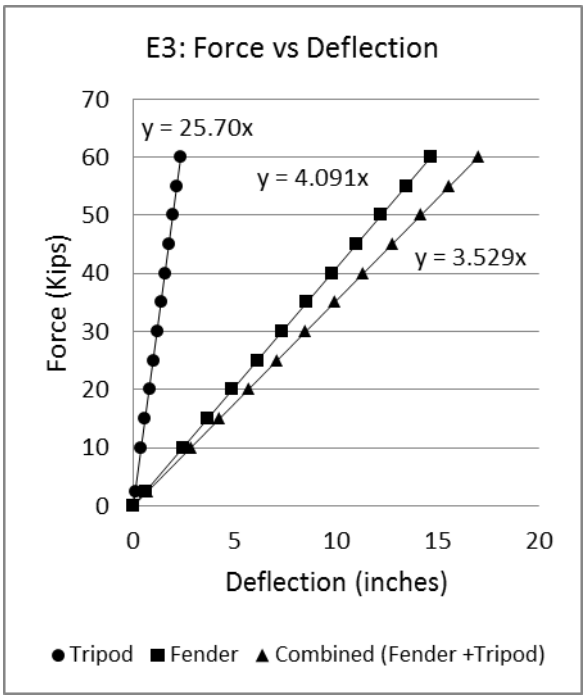

Figure 3.22: Dolphin E3 stiffness

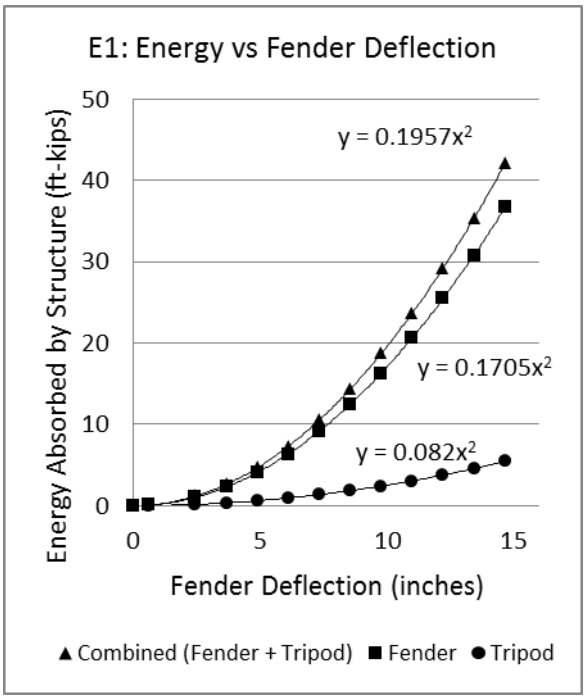

Figure 3.23: Dolphin E1 energy

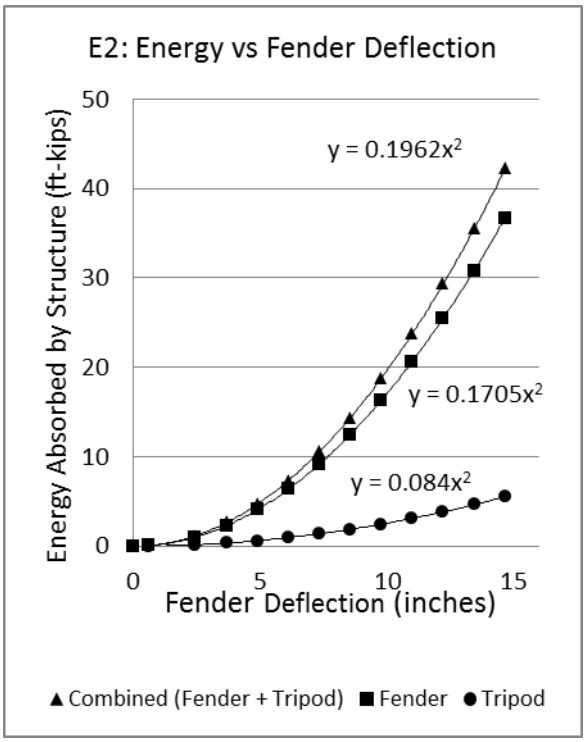

Figure 3.24: Dolphin E2 energy

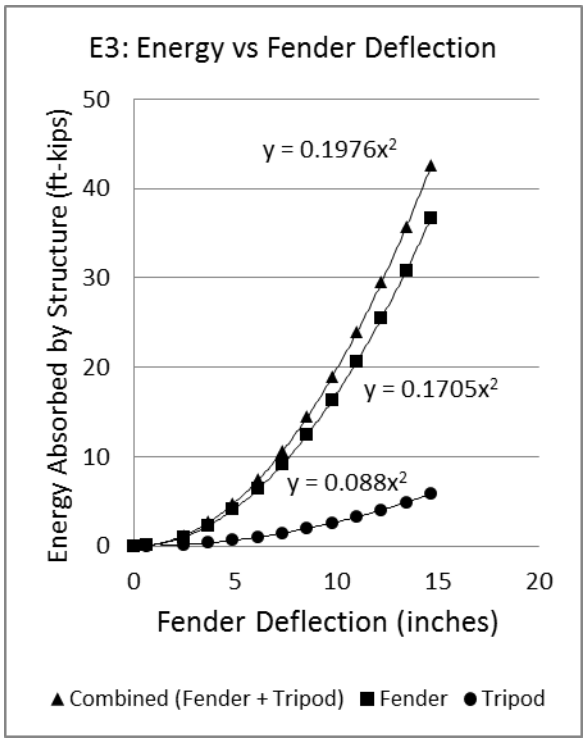

Figure 3.25: Dolphin E3 energy

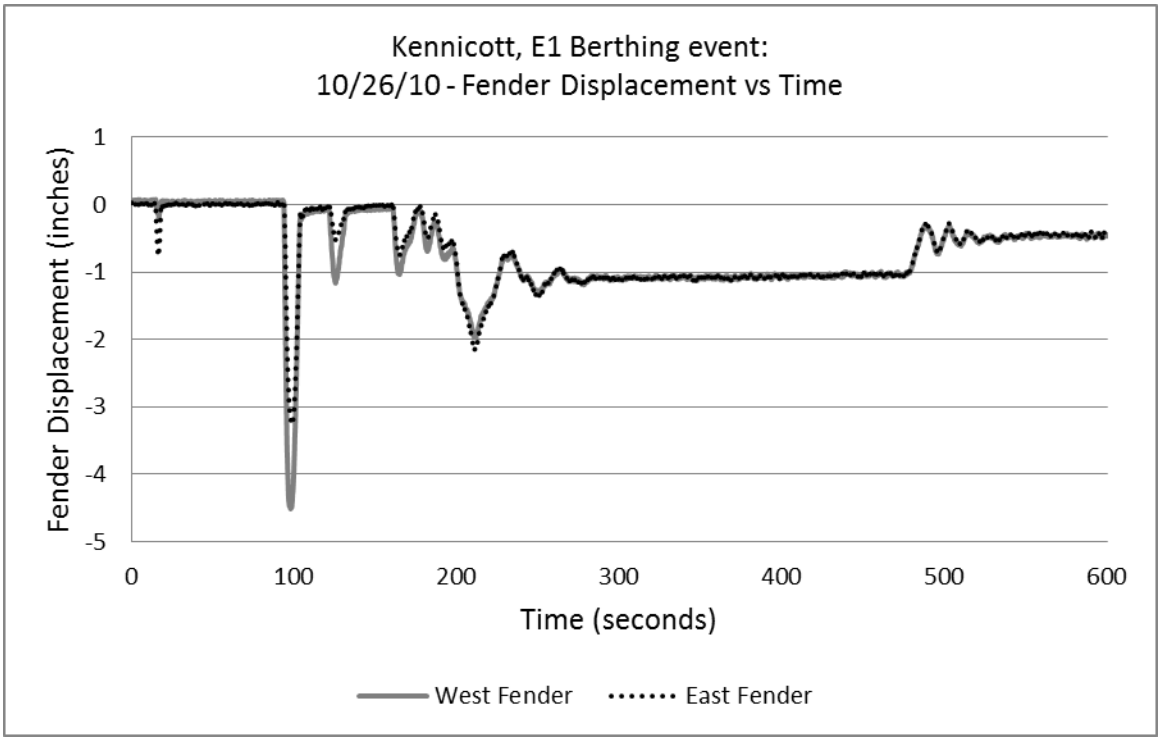

Figure 3.26: Fender deflections for the Kennicott on E1

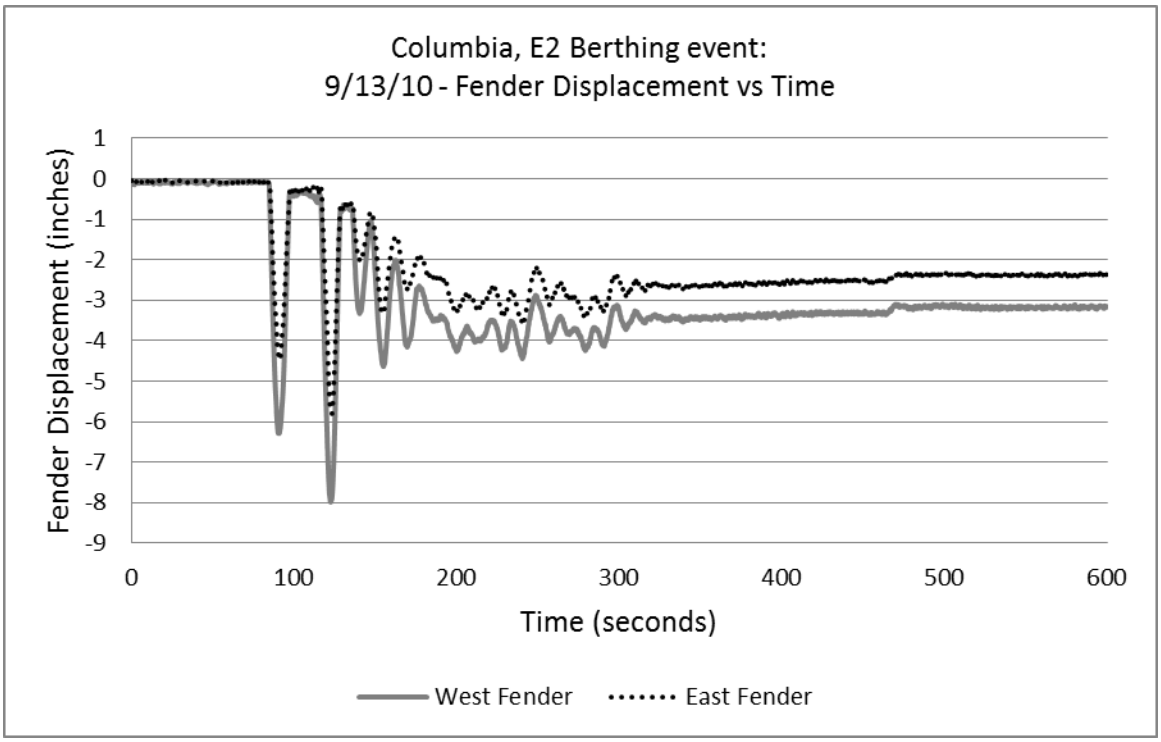

Figure 3.27: Fender deflections for the Columbia on E2

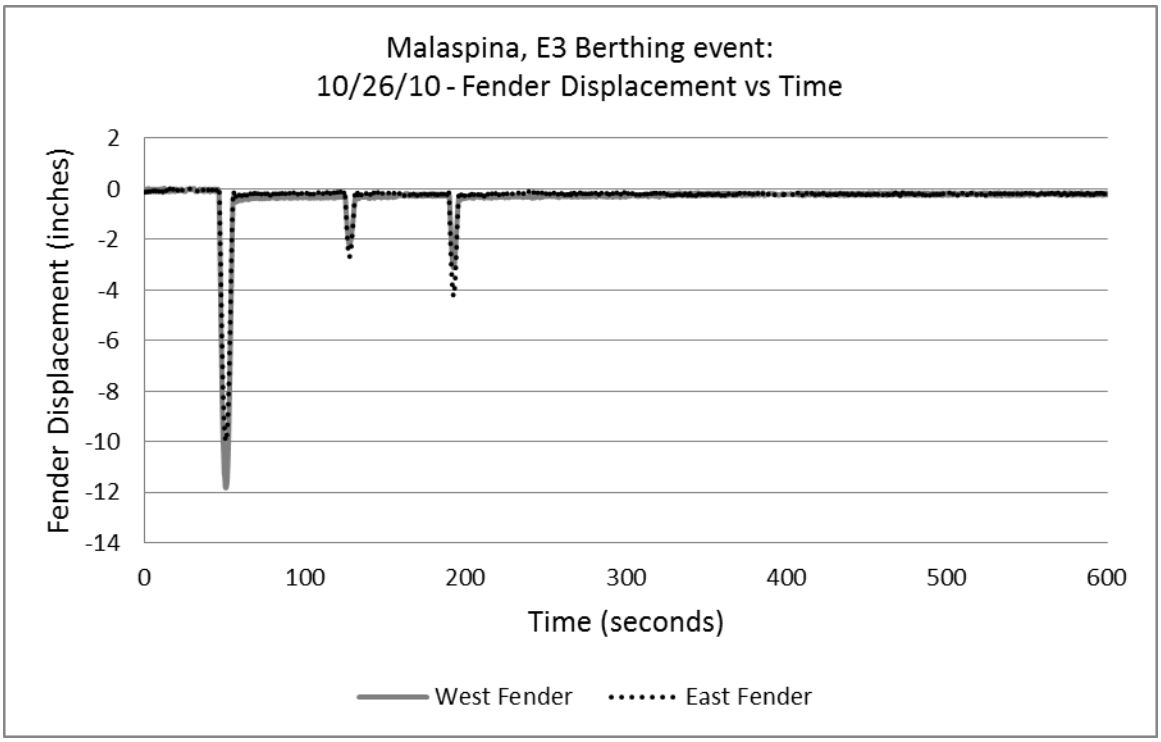

Figure 3.28: Fender deflections for the Malaspina on E3

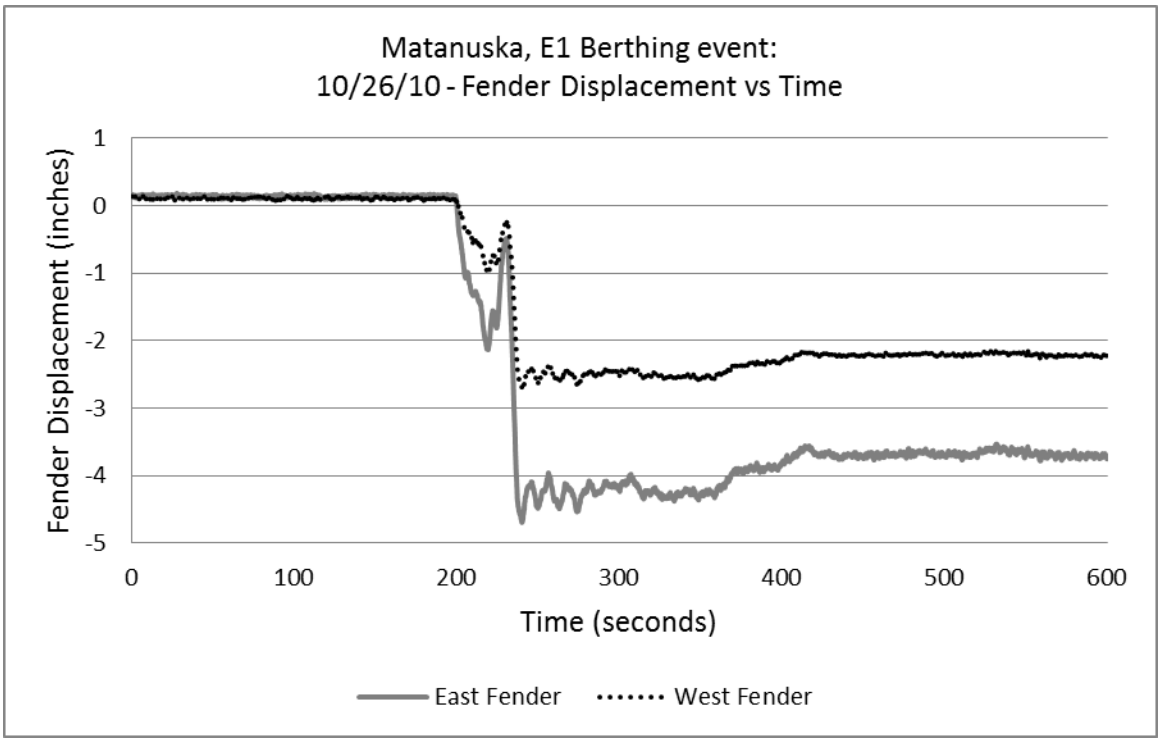

Figure 3.29: Fender deflections for the Matanuska on E1Berthing Coefficient and Berthing Factor

The energy transferred to a berthing structure is typically less than the total kinetic energy of the impacting vessel. Quantifying the amount of energy transferred is complex. Historically, estimating kinetic energy has been dependent on a series of berthing coefficients, according to the Kinetic Energy Method described in Chapter 2. These coefficients vary with vessel type and location, and are difficult to determine either analytically or empirically. In particular, determining the virtual mass of a vessel remains a challenge, and published values often vary substantially. What is clear from previous studies is that added mass is highly variable and has a considerable effect on the transfer of energy from a vessel to a berthing structure. Unfortunately, it is infeasible to separately measure added mass and other berthing coefficients at full scale.

To simplify the approach, the four primary berthing coefficients used by the Kinetic Energy Method (C_e, C_m, C_c, C_s) have been combined into a single berthing coefficient (C_B).

Equation 2.1 then turns into Equation 3.6:

$$E_f = \frac{W}{2g} V_n{}^2 C_B \qquad \text{Equation 3.6}$$

(C_B) is calculated semi-empirically for any berthing event by using a direct ratio between the vessel's kinetic energy and the total energy absorbed by the berthing structure (Equation 3.7).

$$C_B = (C_e X C_m X C_c X C_s) = \frac{E_T}{E_v} \qquad \text{Equation 3.7}$$

where $E_v = \frac{W}{2g} V_n^2 = Kinetic\ energy\ of\ the\ berthing\ vessel\ just\ before\ impact$

$E_T = The\ total\ energy\ absorbed\ by\ the\ berthing\ dolphin\ (fender + tripod)$

(E_T) is empirically determined as discussed earlier in this section. E_v is calculated using the measured approach velocity along with the published displacement weight for each vessel.

Design values for (C_B) as recommended by Costa (1964) commonly range from 0.4 to 0.7, where the total energy absorbed by the fender system is 40–70% of the total kinetic energy of the vessel (Gaythwaite). This range will vary on a vessel, site, and operator basis. In particular, this range will tend to vary more on side-berthing landings than on direct bow or stern berths due to the higher variability in approach and manner of impact. In a side-berthing event, first impact is often made near the bow or stern of the vessel, such that there is an eccentricity between the vessel's center of mass and the point of impact. Larger eccentricities reduce the contribution of a vessel's kinetic energy to the total energy transferred to the berthing structure. Vessels at Auke Bay were often observed to approach the dolphins at a very shallow angle with a large eccentricity at impact. In this instance, the berthing coefficient is expected to be low. For other scenarios in which the fender is impacted near the vessel's center of mass, the berthing coefficient is expected to be large. Other factors such as pitch, yaw, and roll also contribute to the value of the berthing coefficient; however, it is very difficult to quantify these effects empirically during a berthing event. By comparing the kinetic energy of a vessel prior to impact with the actual energy absorbed by the berthing structure, these complex effects can all be accounted for in a single factor, C_B. A strong statistical set of measurements makes differentiation between energy caused by pitch, yaw, and roll unnecessary.

As discussed earlier in this report, the maximum energy absorbed by a berthing structure is often not a function of the initial kinetic energy of the vessel alone, but rather a combination of energy contributed from bow thrusters, environmental effects, and mooring lines/winches after initial impact. For these cases, an accurate berthing coefficient cannot be determined from the ratio between absorbed energy and kinetic energy, as described in Equation 3.7. Berthing coefficient results (Chapter 4A) are thus based on events in which impact is primarily a function of the vessel's initial kinetic energy, with minimal effects occurring after initial impact. An example of this is shown via fender displacement data in Figure 3.28.

Another approach to the berthing coefficient concept is obtained by determining the energy-per-unit mass of each berthing event, obtained simply by dividing the elastic potential energy from each event by the mass of the berthing vessel. This term is referred to here as the *berthing factor* (f_b), shown in Equation 3.8.

$$f_b = \frac{E_T\, g}{W} = \frac{V_n^2 C_B}{2} \qquad \text{Equation 3A.8}$$

$$E_T = \frac{W}{g} f_b \qquad \text{Equation 3A.9}$$

The term (f_b) represents a single berthing factor that can be used to estimate design energy for vessel displacements not observed in this study. This estimation is accomplished by multiplying the berthing factor by the mass of the vessel under consideration in units of $(\text{kips} * \text{ft}/\text{s}^2)$. The vessel weight is in units of kips, and *g* is in units of (ft/s^2).The berthing

factor (f_b) is in units of (ft^2/s^2), and energy in this instance is in units of $(kip - ft)$ (see Example 2 in Chapter 6 for reference).

Force Measurements

Design considerations for force on a berthing structure are significantly different from design considerations for energy. When dealing with fender springs, force is directly proportional to the stiffness of the system under load. Consequently, stiff fenders will experience greater force than soft fenders under the same applied energy. For example, if a vessel berths with 30 kip feet of energy on two fenders with different a stiffness, say 4.092 kips/inch and 8.184 kips/inch, the amount of force each fender must resist is 31.3 kips and 62.68 kips, respectively. Force in relation to displacement and energy follows the following relationships:

$$E_f = \int_0^{x_f} F_f \, dx \qquad \text{Equation 3.10}$$

$$F_f = K_f x_f = \sqrt{2 K_f E_f} \qquad \text{Equation 3.11}$$

where

$$F_f = Force\ in\ the\ fender$$

From Equation 3.10, force can be determined by recording fender displacement for fenders of known stiffness. The force in a linear fender is simply the displacement (x_f) multiplied by the stiffness (K_f). For nonlinear fenders (such as the Auke Bay fenders at displacements greater than 20 inches), Equation 3.11 can be used.

Fender force is only a portion of the total berthing force. For fenders that are coupled with systems of piling, like in Auke Bay, a portion of the berthing force will be resisted by the reaction piling (bottom) against the soil.

The fender systems at Auke Bay consist of four fender piles connected to the tripod backing structure via two rubber cylindrical fenders. The four fender piles, ranging from 97 feet to 106 feet, are connected rigidly with wide flange steel beams and large timbers that serve as a wearing surface. The fender piling are driven anywhere from 27 feet to 34 feet into soft material consisting of sandy silts and clays. Per the pile driving logs, "No blow counts were counted for the first twenty to thirty feet, with stiff material only encountered in the last couple feet." Due to the presence of soft material, the bottom reaction in the fender piling is assumed pinned at the midpoint between the bottom of the fender piling and the top of the stiff material. Soil springs in the very soft region are assumed insignificant.

Berthing force, representing the force at the point of impact of a vessel's sponson on the fender face, can be determined by simplifying the fender system into a beam with two supports: one on either end (Figure 3.30). The top support represented by a spring corresponds to the fenders. The bottom support represented by a pin corresponds to the soil reaction on the fender piling. The berthing force, *P,* can be found if the reaction at the top support (fender) and the location of impact (*h*) are known using statics (Equation 3.12).

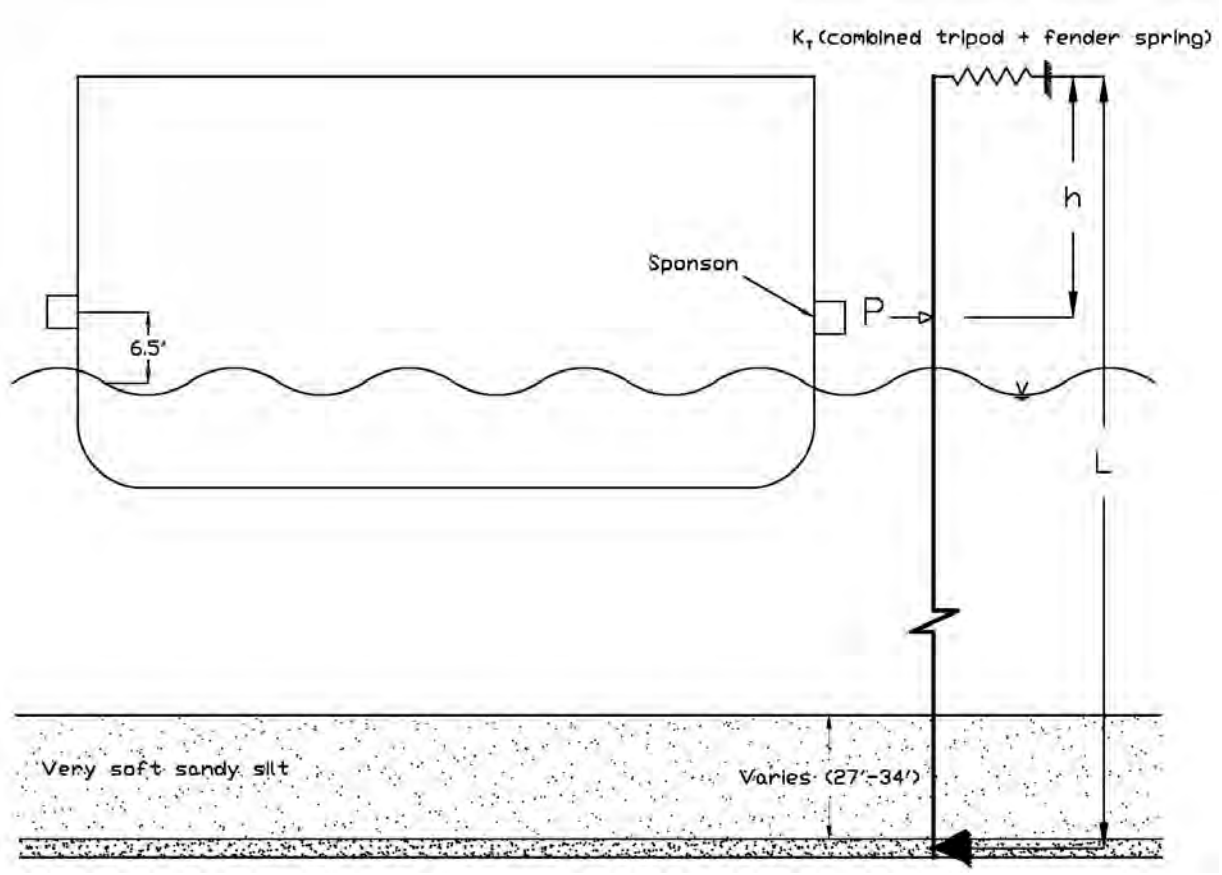

Figure 3A.30: Schematic of berthing force

$$\boldsymbol{P = \frac{F_f L}{L-h}}$$ Equation 3A.12

where $P = berthing\ force\ at\ the\ point\ of\ impact\ (kips)$

$F_f = force\ in\ the\ cylindrical\ fenders\ (kips) = K_f(x_{wf} + x_{ef})$

$L = beam\ span\ (average\ span\ of the\ four fender\ piling)(inches)$

$h = location\ of\ impact\ on\ beam\ measured\ from\ the\ top\ support\ (inches)$

The location of impact on the fender facing, *h,* varies with tide level and draft depth. Tide levels were monitored during each berthing event, and the sponson of each vessel was estimated at approximately 6.5 feet to midpoint above water level. Sponson height varies per event depending on passenger and cargo load; however, the variation is not significant. Knowing the elevation of the top support (fenders), the point of impact of the vessel on the fender face can be estimated.

Chapter 3B – Means and Methods: Seattle

Overview

The load environment of vessels with displacements between 1000 and 10,000 long tons is not well understood. Yet vessels of this size, which include passenger and vehicle ferries, place high demand on their berthing structures due to the high frequency of ladings (impacts) during regular service. Insufficient data on loading information for passenger ferries has led to the development of structures with known capacity, but no real corroborating evidence regarding demand. This situation has led to berthing structure designs that are based on empirical observations and experience that has developed over time. The designs of the structures are largely a result of improvements made over previous generations after a number of operational cycles and failures.

It is the intent of this study to improve the knowledge base regarding the load environment of the Washington State Ferries system. The goals of this study, which involves monitoring the Bremerton slip at the Seattle terminal over approximately one year, include the following:

- Present the operational characteristics of the Bremerton slip at the Seattle terminal
- Formulate probability-based design criteria consistent with reliability-based engineering methods
- Provide a number of design aids that can be used by Washington State Ferries engineers

Findings are based on over 6950 impact events observed, recorded, and analyzed at the Bremerton slip. The instrumentation was designed to provide a comprehensive time history of vessel-structure interaction before, during, and after impact. The following measurements were recorded with respect to time:

- Vessel position
- Fender displacements
- Strain in pilings
- Tide level

Site Description

The Seattle ferry terminal is located in Elliott Bay within Puget Sound, adjacent to downtown Seattle, Washington (Figure 3.31). The terminal features three end berths. Slip 1 services the community of Bremerton, located on the Olympic Peninsula, Slip 2 is used as an alternate berth, and Slip 3 services the ferry route to Bainbridge Island. The instrumentation was deployed on the Bremerton slip – Slip 1.

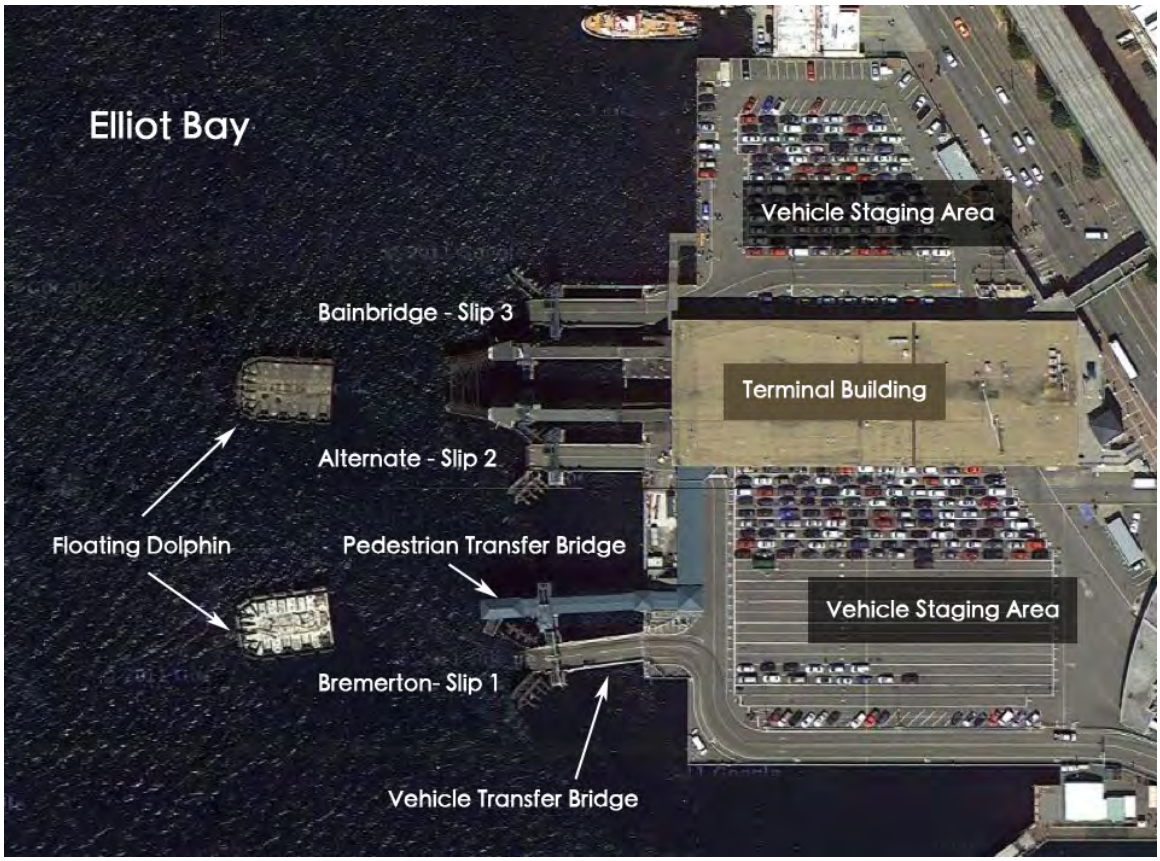

Figure 3.31: Seattle ferry terminal aerial view; courtesy Google Maps

Berthing Structure Description

The Bremerton slip (Figure 3.32) consists of two wingwalls and a vehicle transfer bridge connected to a pile-supported wharf that serves as the access point for ferries and includes a terminal building that consists of ticketing, concessions, and additional operational facilities. Each wingwall is oriented at 40 degrees relative to the vehicle transfer bridge, and consists of vertical and angled pipe piles, steel framing elements, an impact face, and marine fenders.

The most seaward pile line serves as a vessel impact structure, which consists of an impact/wearing face of timbers and replacement wide flange beams. These beams are attached to steel wide flange wales, which are welded to three 24-inch steel pipe piles. This outer pile line is embedded into the seafloor to a depth of 20 feet.

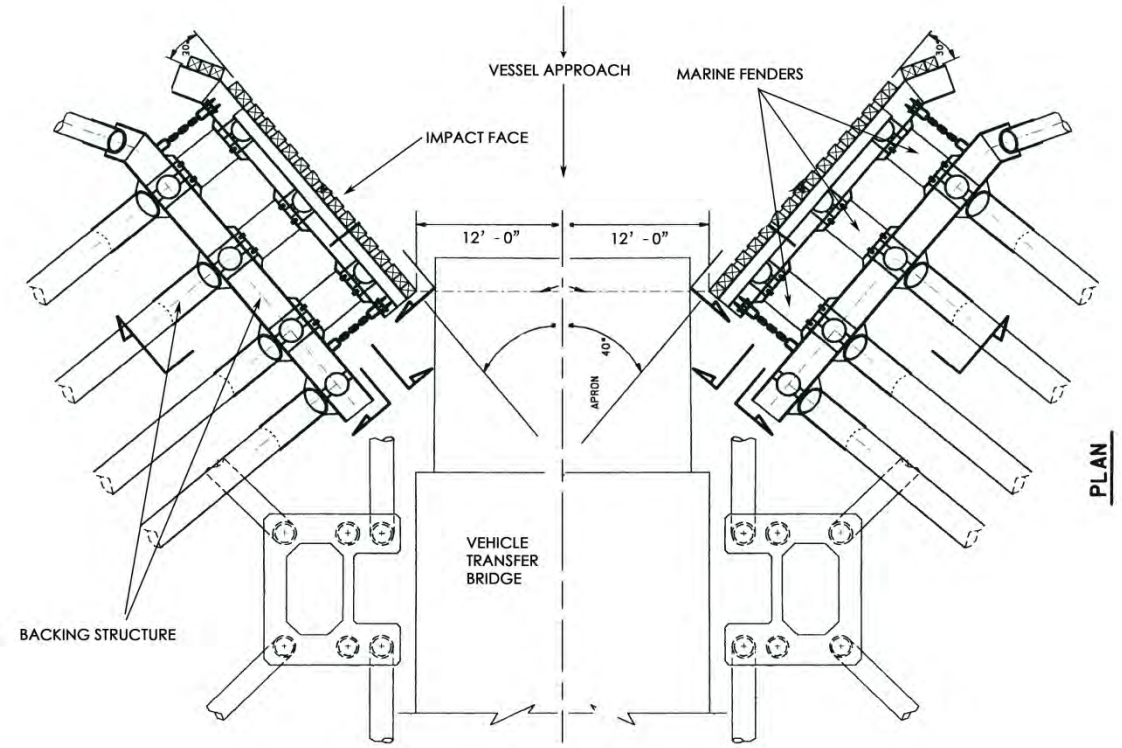

Figure 3.32: Bremerton slip as-built drawing plan view, courtesy WSF

The impact wall is connected to the backing structure by elastomeric buckling column fenders, which absorb the impact of the ferry, and with chains that provide lateral support to the wingwall. Three sets of fenders are located between the wearing fender and backing structure. The backing structure consists of a space frame that includes four 24-inch-diameter vertical steel piles filled with concrete, four 30-inch-diameter steel batter piles filled with concrete, and one 24-inch-steel "endo" pile filled with concrete. The structure contains considerable steel framing to connect the piles, and consists of wide flange beams and 16-inch steel piles (see Figures 3.33 and 3.34 for details).

Figure 3.33: Photos of wingwall structure

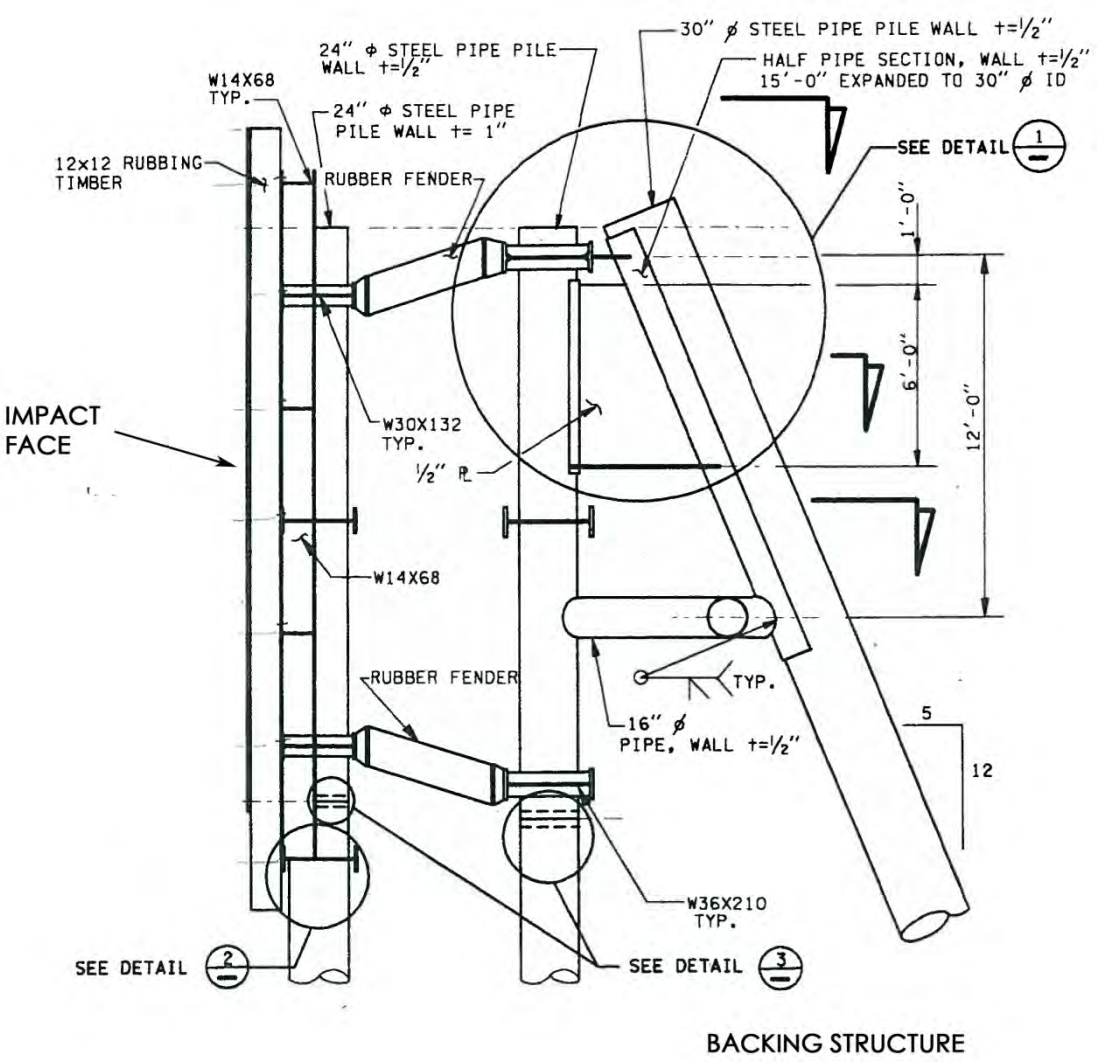

Figure 3.34: Wingwall as built, elevation view; courtesy WSF

Vessel Description

The Bremerton slip primarily services the M/V Kitsap and M/V Kaleetan, double-ender vehicle and passenger ferry vessels. The M/V Kitsap and the M/V Kaleetan have published displacement of 2475 and 2704 long tons, respectively. When these vessels are fully laden with passengers, vehicles, and fuel, displacement increases to 2947 and 3251 long tons. Table 3.2 contains additional information. A picture of the M/V Kitsap is shown in Figure 3.35.

Table 3.2: Vessel Information

Vessel	Gross Tonnage (long tons)	Length (ft)	Beam (ft)	Draft (ft)	Passengers	Vehicles	Horsepower
Kitsap	2475 published, 2947 operational	328′	78′ 8″	16′ 6″	1200	124	5250
Kaleetan	2704 published, 3251 operational	382′	73′ 2″	18′ 6″	2000	144	8000

Figure 3.35: M/V Kitsap

All vessels in the Washington State Ferries system have diesel electric propulsion on both ends. Illustrations of the vessels are represented in Figures 3.36 and 3.37.

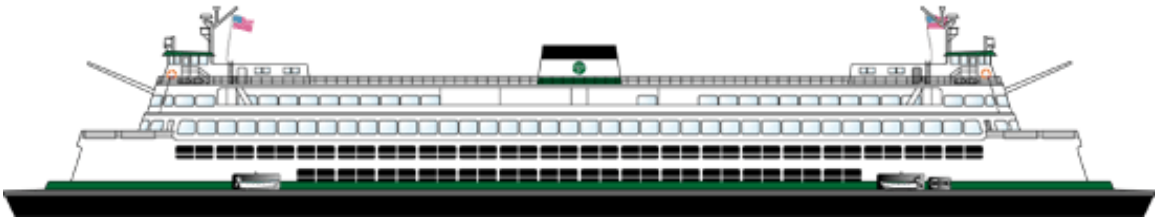

Figure 3.36: Illustration of the Kaleetan: vessel class, Super; courtesy WSF

Figure 3.37: Illustration of Kitsap: vessel class, Issaquah; courtesy WSF

General Berthing Procedure Description

The general ferry berthing procedure consists of decelerating from the crossing velocity and slowly maneuvering into the berth. The incoming ferry uses two wingwall structures oriented at approximately 40 degrees to the vehicle transfer bridge when berthing and unloading passengers and vehicles. The opposing wingwalls form a pocket-shaped berth that is used to attenuate the impact energy of berthing events (Playter 1994). Depending on weather conditions, the vessel may use one or both wingwalls to arrest its forward progress before coming to rest between both walls to proceed with the off-loading procedure. After coming to a stop, the vessel is tied off to the transfer bridge and remains under power using the wingwalls and a large floating dolphin on the north side of the vessel to maintain a stable position for loading/unloading.

Instrumentation Description

To measure the berthing parameters, an instrumentation system based on the principles used in the 2010–2011 Auke Bay Load Environment study was designed and implemented at the Bremerton slip at the downtown Seattle ferry terminal. To capture the complete berthing event, the instrumentation was installed on both the north and south wingwalls (see Figures 3.38 and 3.39 for further details regarding instrumentation layout).

The instrumentation scheme at the Bremerton slip of the Seattle ferry terminal consisted of:

- Two Campbell Scientific® CR5000 dataloggers housed in environmental protection boxes
- Three Senix TSPC ultrasonic distance sensors
- Six Celesco aluminum linear motion transducers
- Six Celesco stainless steel pressure-tested linear motion transducers
- Thirty-six 90 degree chevron strain gauges (two ¼ bridges per gauge)
- One Toughbook field laptop running Campbell Scientific's RTDAQ and LoggerNet software
- Two Sierra Wireless Airlink™ Raven XT cellular digital modems and associated hardware
- Belden 5 strand shielded instrumentation wire

The system was designed to monitor berthing parameters relevant to engineering design of berthing structures at the Bremerton slip subjected to vessel impacts. Each instrumentation system was wired into a datalogger, designated as North or South, corresponding to the wingwall position relative to the transfer bridge. The dataloggers were programmed with the CRBasic language, using the CRBasic Editor from Campbell Scientific®. CRBasic is a computer language

optimized to control Campbell Scientific dataloggers by offering functionality that supports and simplifies scientific measurements and data collection.

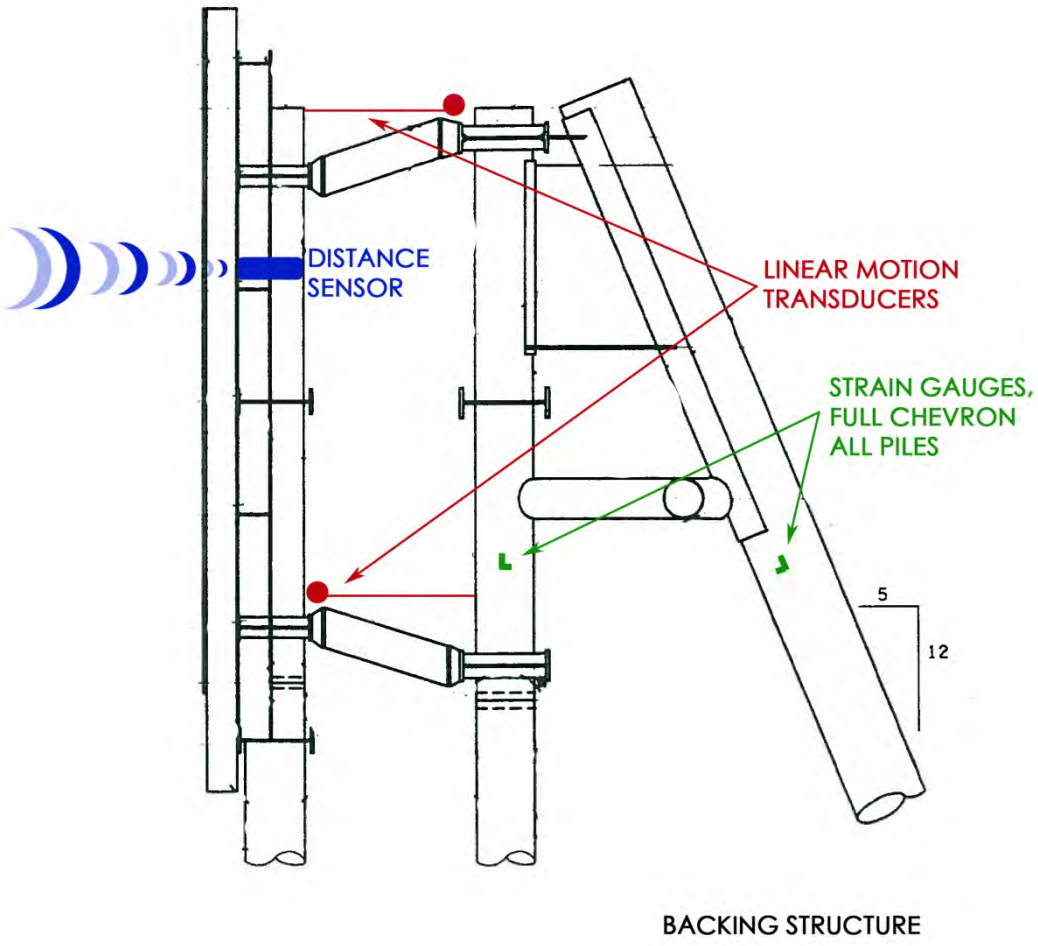

Figure 3.38: Instrumentation of wingwall, elevation

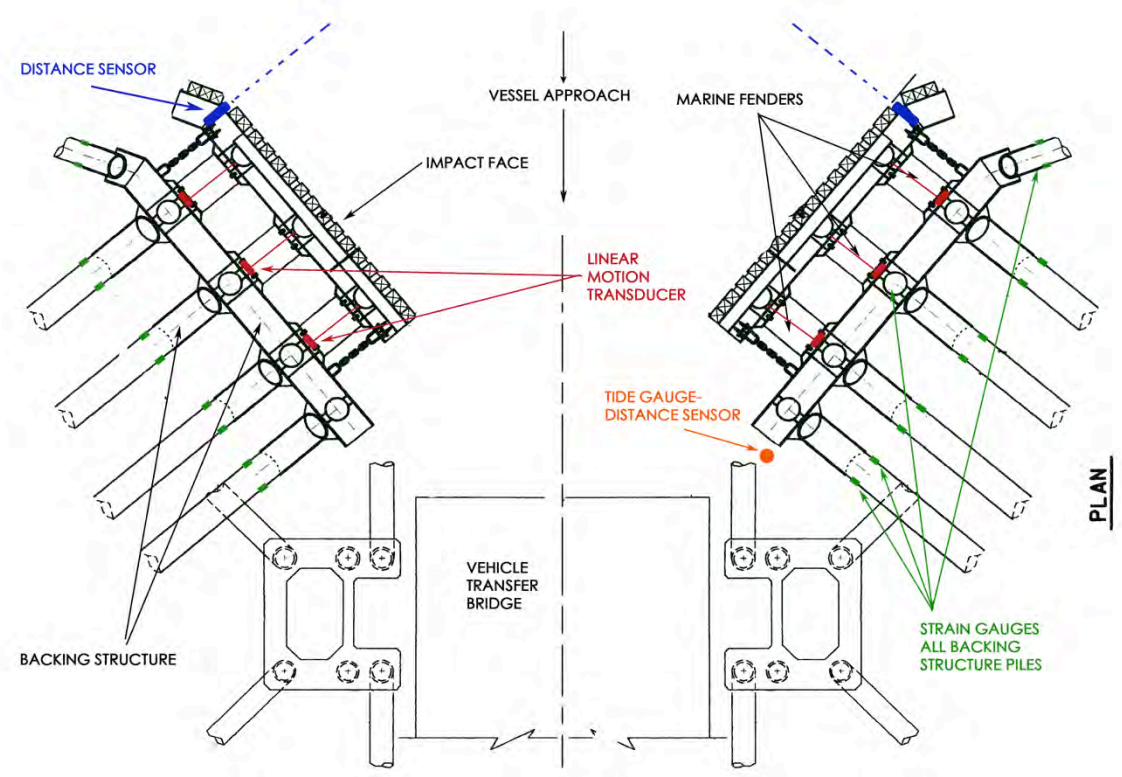

Figure 3.39: Instrumentation of wingwalls, plan view

To accurately capture the parameters of a berthing event, the system operated continuously at 5 Hz, taking measurements at a rate of five per second. When a ship crossed a threshold distance of 20 feet from the face of the wingwall, the dataloggers initiated a new event table and recorded the states of all system sensors. Once the vessel initiated the recording sequence, data were recorded for several minutes. After observing numerous landings, it was determined that a time of two minutes was adequate to capture the response of the wingwall prior to, during, and after berthing procedures. See Figures 3.40, 3.41, and 3.42 for photographs of the installed instrumentation.

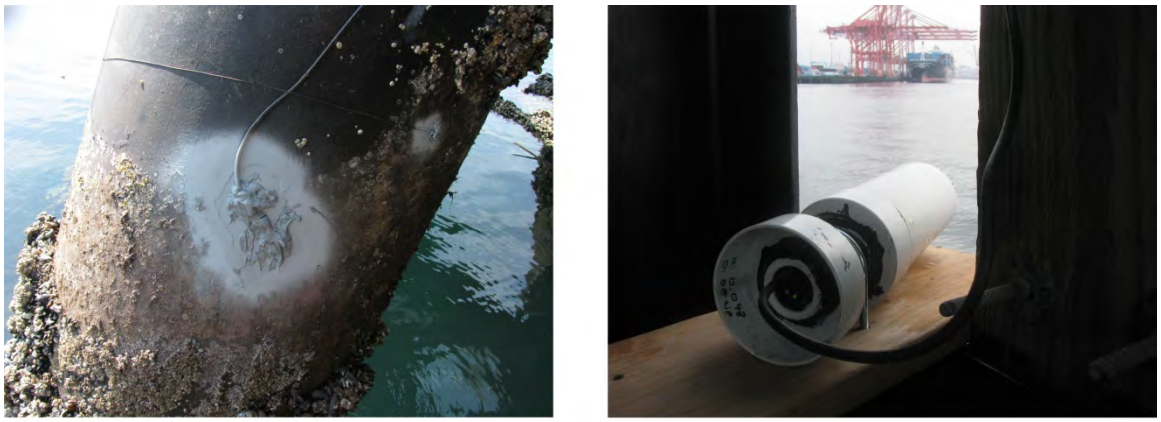

Figure 3.40: Installation of strain gauge (left) and distance sensor (right). Strain gauge covered in silicone and zinc-rich paint to protect against corrosive effects of saltwater. Distance sensor used to record vessel position measurements.

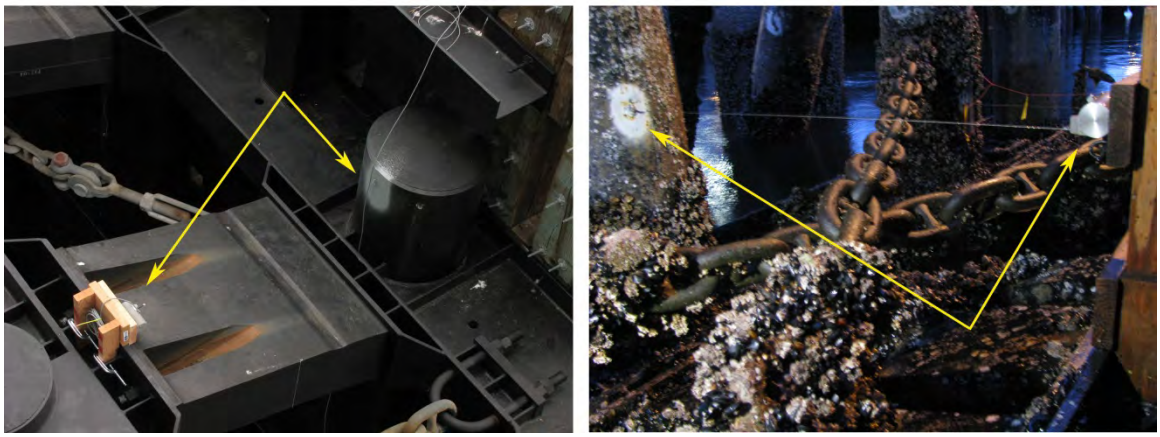

Figure 3.41: Linear motion transducer photos. Upper linear motion transducer (left) with cable affixed to vertical pile. Lower LMT (right) in the intertidal zone above the marine fender and above the chains.

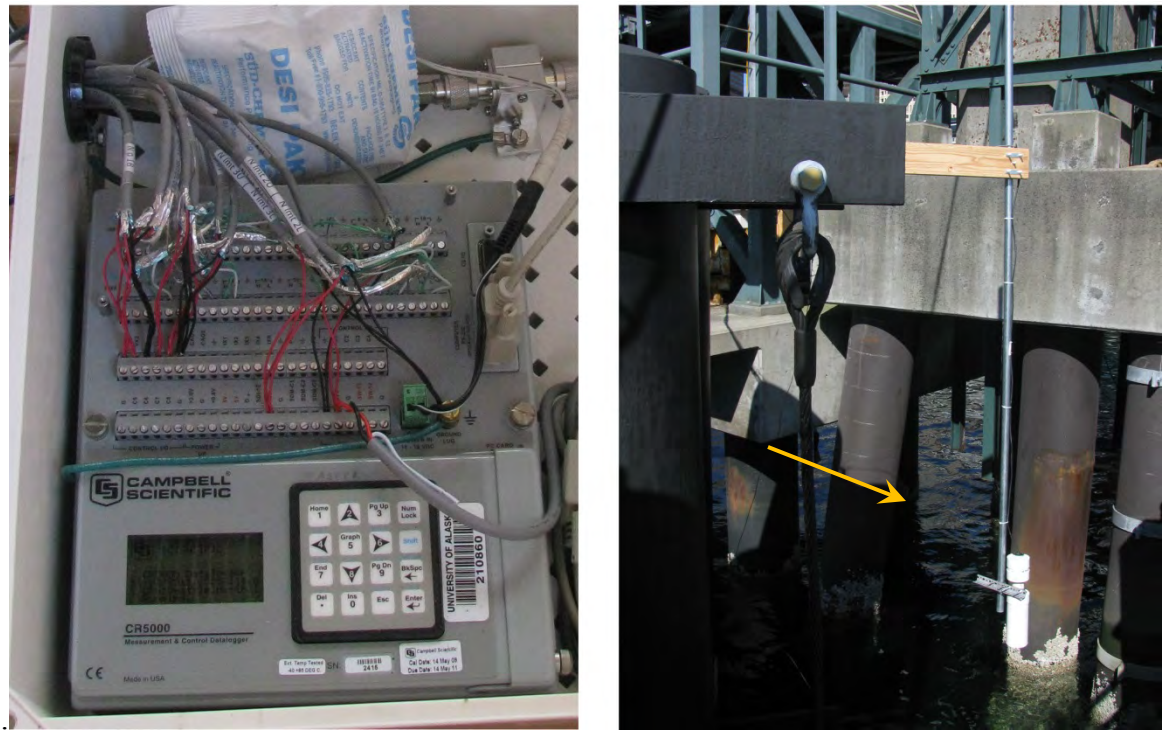

Figure 3.42: Datalogger and distance sensor photos. Datalogger (left) wired with wingwall instrumentation; distance sensor (right) measuring the tide elevation.

Vessel Position Measurements

Monitoring of the incoming vessel position was accomplished using SenixToughSonic® TSPC ultra-sonic distance sensors. Vessel position information represents one of the most important tasks of the instrumentation installation. This measurement was crucial for two reasons: knowledge of the vessel position was required to initiate recording of berthing event parameters, and this recorded position, with respect to time, is the basis for the vessel approach-velocity calculation. Approach velocity was calculated from vessel position measurements 1 second before impact. Fender displacements were recorded concurrently with vessel position. Together this information was used to determine the time of impact.

Figure 3.43 displays a typical berthing event at the south wingwall of the Bremerton slip. The sharp valleys in the graphs indicate impact with the wall and align with maximum displacements of the fender system. Though this is a typical berthing procedure, many variations were observed.

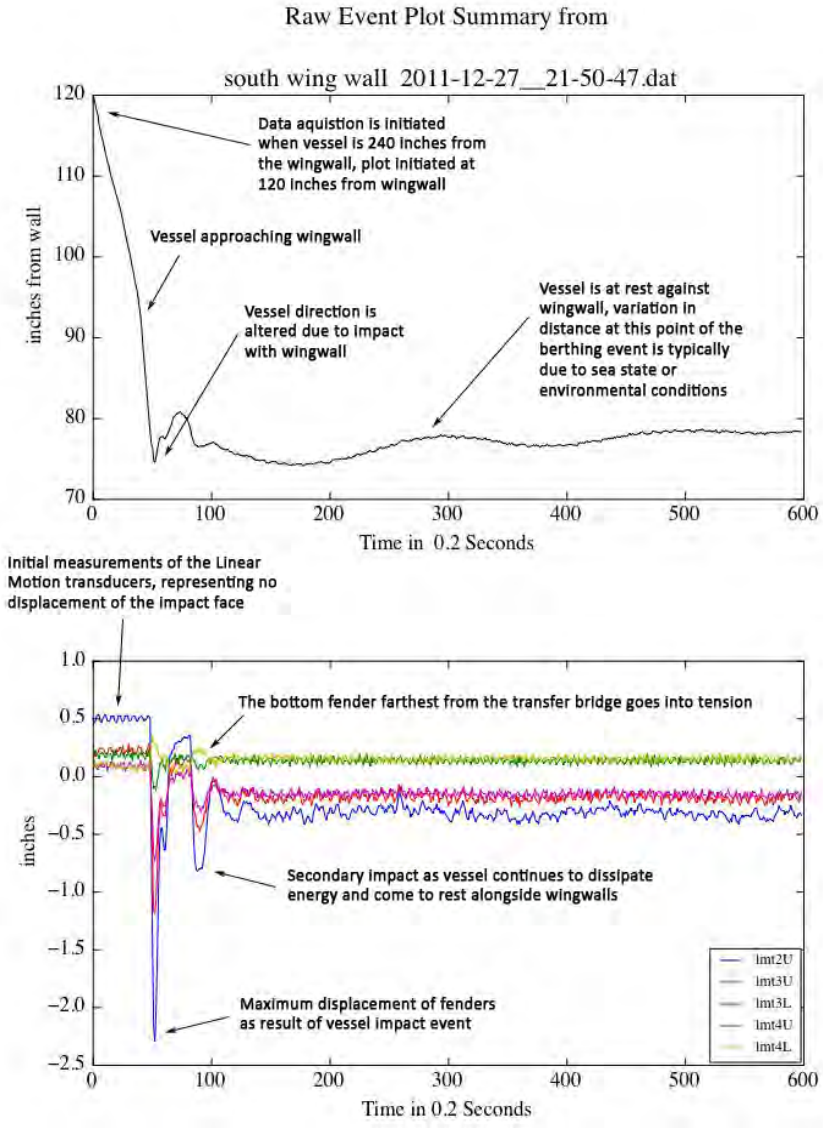

Figure 3.43: Vessel position and fender displacement plots with description.

Data Acquisition

Transferring raw data files from the datalogger in Seattle was accomplished by using a Sierra Wireless™ Airlink Raven XT cellular modem, controlled remotely by a laptop computer in Fairbanks. Two pieces of Campbell Scientific® software were employed to control the system remotely: LoggerNet and Real Time Data Acquisition (RTDAQ). LoggerNet was used as an automatic collection protocol, serving primarily to download data from the datalogger at a scheduled time every evening. RTDAQ was used for real-time system monitoring of berthing events to observe the functionality of the sensors. Both of these programs allowed for editing and uploading of user-developed code to run the instrumentation system. After the information was uploaded to the field laptop, it was backed up and transferred to the post-processing environment. Figure 3.44 illustrates the steps associated with the event capture procedure.

Software and Data Processing

To evaluate and process this large dataset, a suite of interactive software was developed to facilitate data processing and analysis. Software was developed using Python, an interpreted interactive, object-oriented, extensible programming language. Several programs were called upon to do the bulk of the event characterization; all were developed using Python, Version 2.7.4 (see Figure 3.45 for an overview of the program process flow).

The raw data table uploaded from the datalogger is a large file that requires refinement for efficient processing. A program named *batch_splitter.py* is used for this first data transformation. The primary purpose of this application is to open the large "raw" tables from the datalogger and filter them into discrete event files representing a single vessel-berthing event. These event files are then organized into batches, each batch containing one month of data at each wingwall.

Following the reorganization of raw files into discrete berthing events, the berthing events are characterized by identifying parameters that describe system response. These parameters are recorded and analyzed later in the process. The first step when characterizing an event is to understand if a berthing event file is valid (Figure 3.46). Oftentimes data are recorded without a vessel landing; for example, heavy weather (snow, rain) or birds may trigger the system to record. It is important to eliminate these "events" from the dataset.

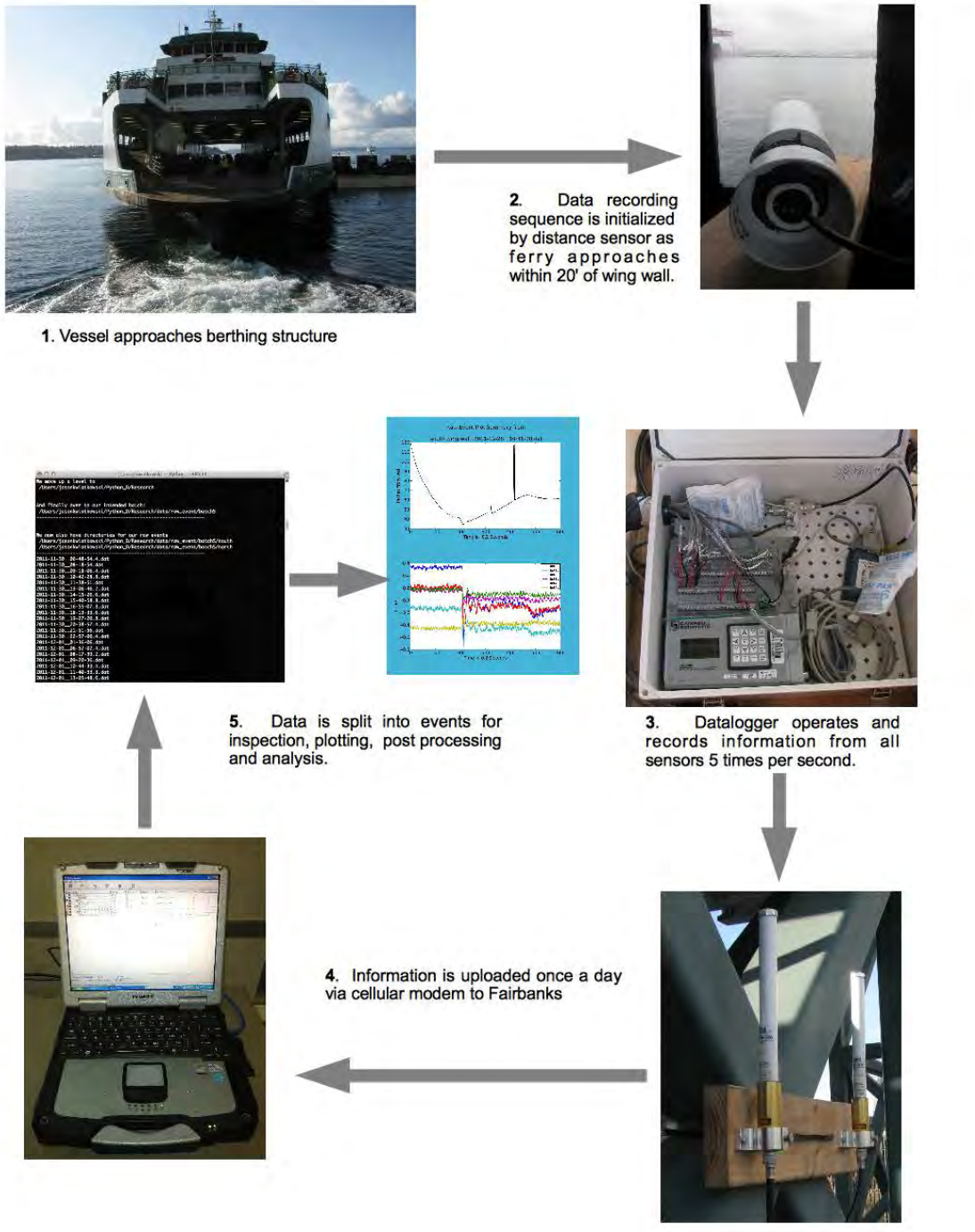

Figure 3.44: Event data acquisition sequence

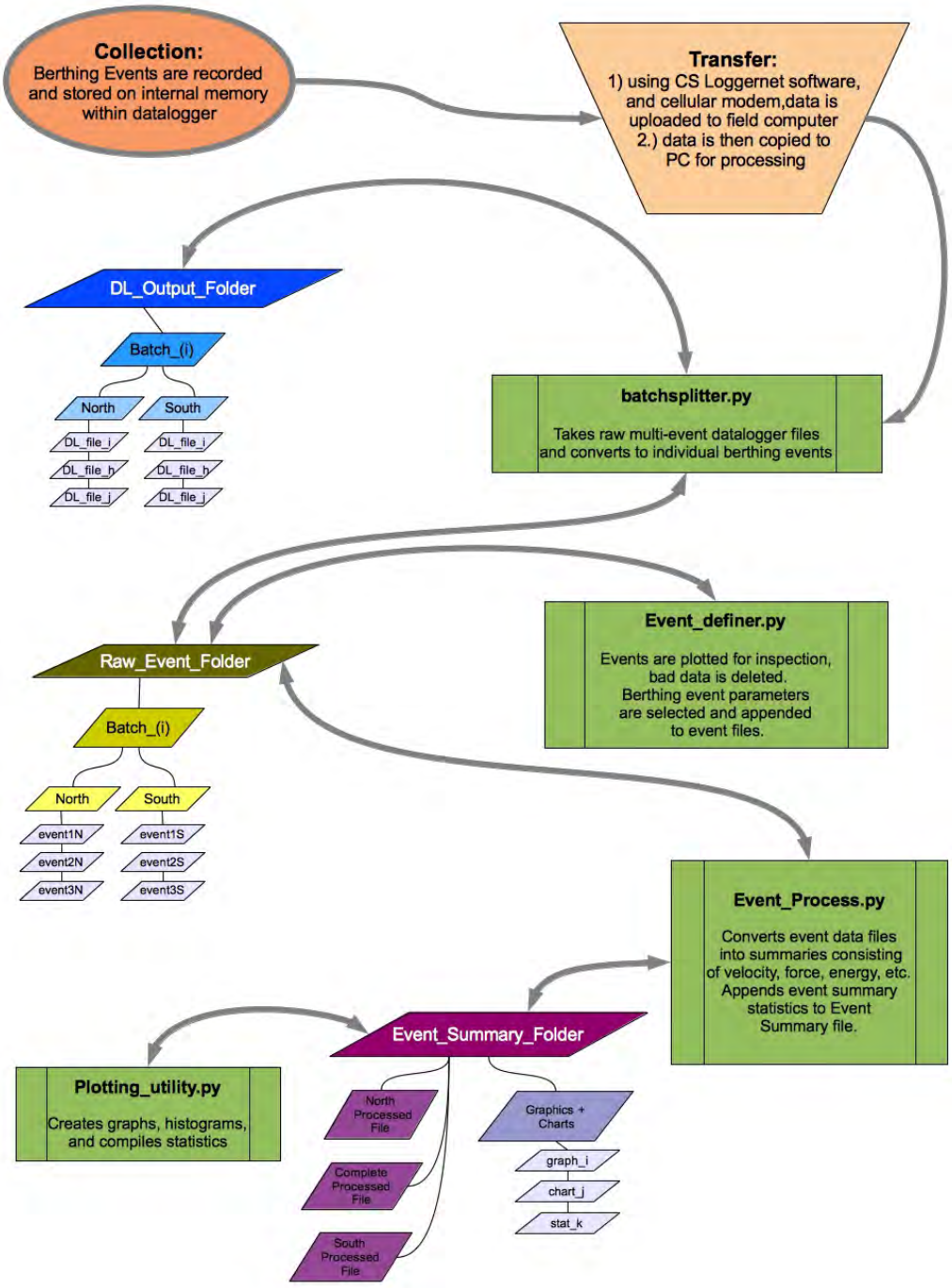

Figure 3.45: Software and data interaction diagram

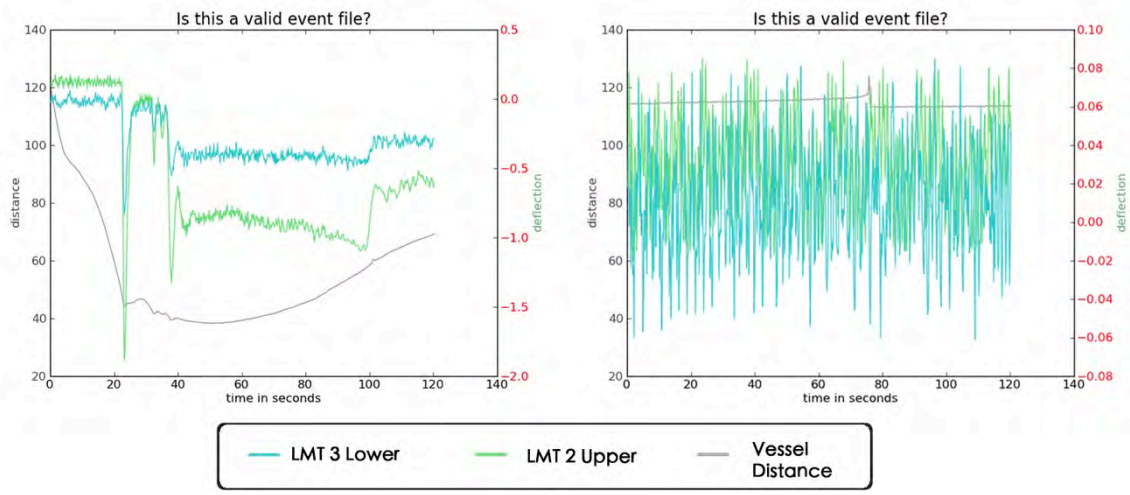

Figure 3.46: Event filtering decision graphic

Characterization of the berthing events is accomplished using the *event-definer.py* application. The goal of *event_definer.py* is to check and interpret an event dataset by visual inspection. This inspection serves to ensure that data recorded and eventually analyzed will in fact represent the system as it behaved and in the context of interest. The inspection is accomplished by using a graphical user interface (GUI) in conjunction with command line controls. After invoking the program, the user is asked which batch of event files to investigate. Next, an event is plotted to ensure it represents an actual berthing event and to select the key data points that characterize the berthing event. If an event does not represent a ferry landing, it is deleted.

Once an event is verified, the user is instructed to select (using a mouse or track pad) the point of maximum vessel impact from a plot of the berthing event data. The plot displays two of the linear motion transducer (LMT) displacement measurements, and the position of the ferry (normal to the wingwall) with respect to time. The maximum discrete impact point, as evidenced by displacement of the marine fenders, is selected either automatically or manually depending on characteristics of the berthing event (see Figure 3.46 for more details). For this study, the *impact point* was selected to be the maximum impact recorded by the LMTs (translating to maximum fender deflections). Maximum deflections associated with a vessel power-up against the impact face were not considered an impact event and were omitted in the event analysis.

The visual investigation of recorded data enables the filtering of events that do not meet criteria associated with an incoming vessel. Figure 3.46 presents a plot on the right consisting of electronic noise, and is devoid of relevant information portrayed by the actual vessel-berthing event on the left.

The *event_definer.py* application allows for manual selection of data points that characterize the berthing event. The point of maximum deflection and the point that represents the initial state of the system are shown in Figure 3.47. Once the maximum displacement is selected, the initial state of the system is identified and selected using the original graphical selection procedure. To verify that the characterization is accurate, the graph is again presented with highlighted points that characterize the berthing event. Should incorrect selection of points occur, the points could be erased and chosen again. Once accuracy is verified, the indexes (which represent positions

within the event file) of the maximum displacement, the initial conditions, and 1 second prior to the initial impact are appended to the event file as an immutable tuple (a list of data that cannot be altered).

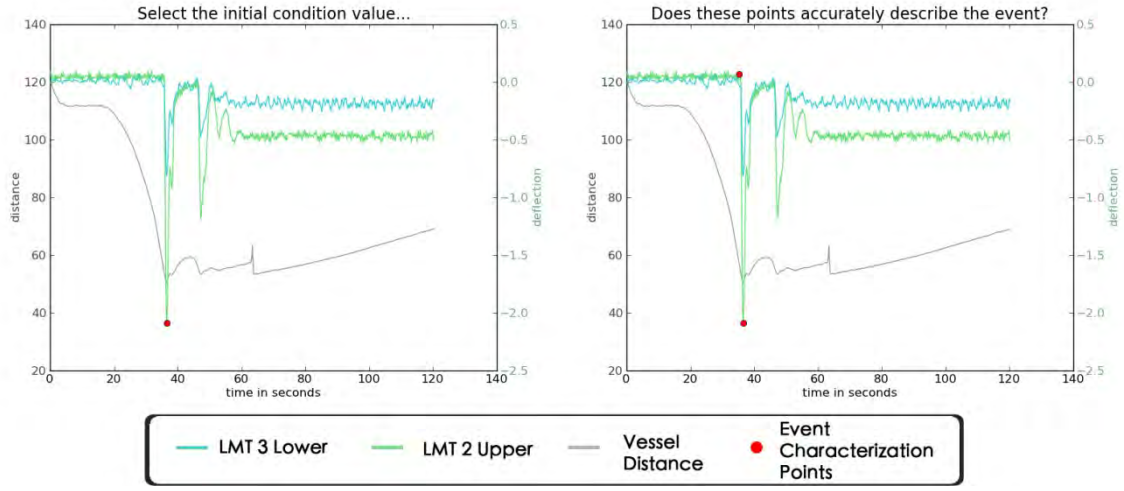

Figure 3.47: Event characterization graphic

After a batch of berthing events has been characterized, the next step is to process the parameters that describe the event (such as initial velocity, force, energy, etc.) and output the data to a summary file using the *event_process.py* application. This program requires a dataset to operate; however, after inputting which dataset to analyze, the processing is completely automated. Once a dataset is specified, the application opens each event file and uses the output tuple from the previously executed program (*event_definer.py)* as the basis for all calculations regarding berthing force, energy, and approach velocity. For example, the index values of maximum displacement for each transducer are subtracted from the initial state of the system (resulting in a measurement of fender deflection). These values are then inputted into polynomials that describe the fender reaction or energy. This step is completed for all sensors on the wingwall. After all calculations are made, the data are then appended to a summary file that consists of differing berthing events, the raw measurements that make up the event (vessel position, transducer deflection, tide, etc.), and the calculated data that describe the berthing parameters of each event, such as approach velocity, absorption energy per fender, and total absorption energy.

In addition to these primary programs, a number of utilities were employed using this framework to facilitate other aspects of the project, including plotting, assembling data from the north and south wingwalls, and checking for duplicate records.

Structural Model

A structural model was created using the software SAP 2000 V15 (produced by Computers & Structures, Inc.) to investigate the performance of the entire structural system (Figures 3.48 and 3.49). Constructing the model was facilitated by as-built plans and geotechnical information provided by Washington State Ferries personnel. Support characteristics were determined from soil *p-y* curves and idealized as soil springs in the model.

Figure 3.48: SAP model of wingwall

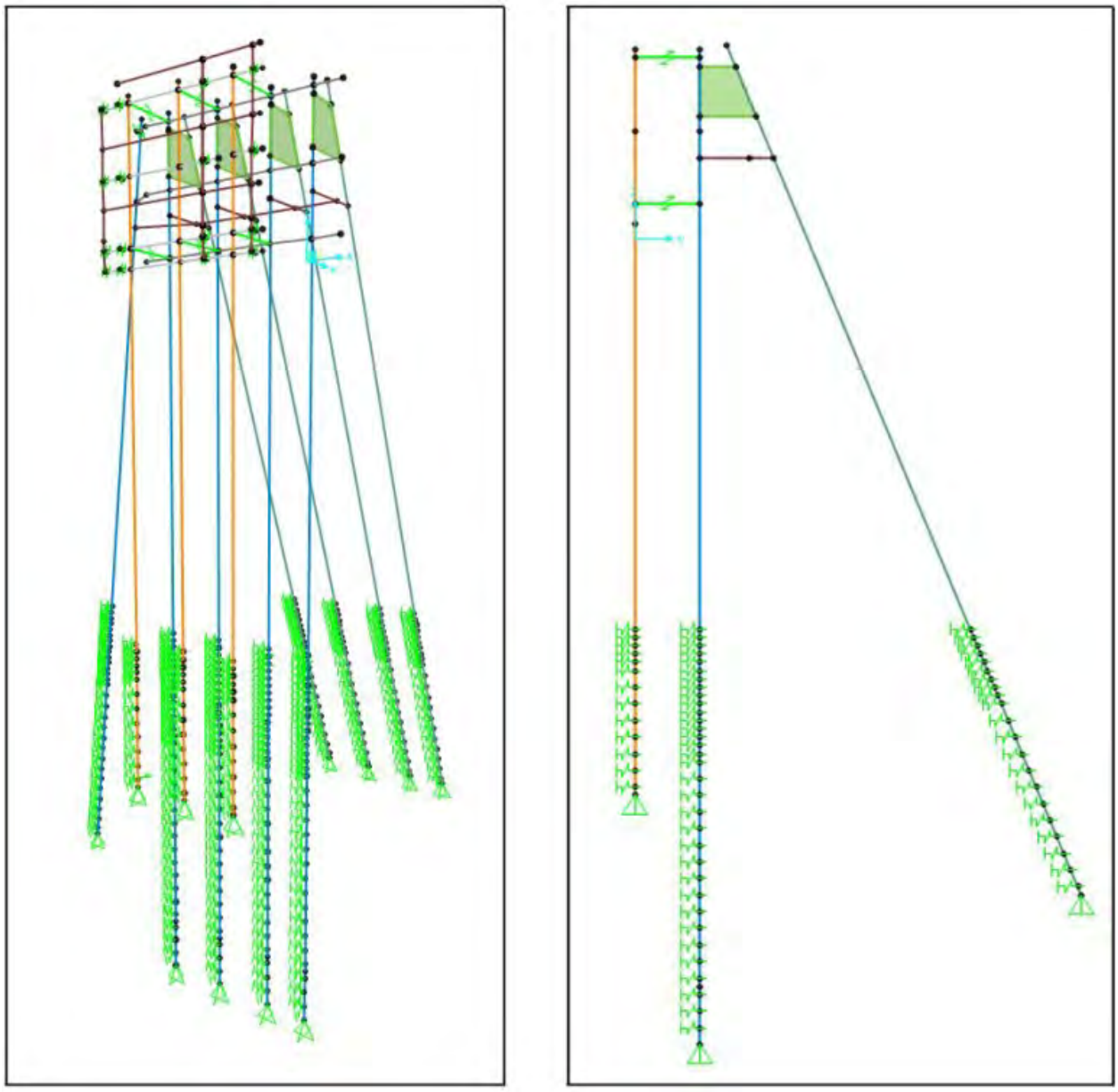

Figure 3.49: SAP wingwall model, isometric and elevation view

The wingwall system at the Bremerton slip consists of an impact face, marine fenders, and a backing structure. The impact face consists of timber, UHMW, and steel wales attached to three steel vertical pipe piles. As-built information indicates the fender piles were driven 20 feet below the mud line. The impact face and piles are connected by six rubber buckling-column marine fenders to a reaction frame backing structure comprised of vertical and battered concrete-filled pipe piles connected by steel wide flange and pipe framing elements. The four vertical piles were driven 50 feet below the mud line; the four batter piles penetrate 35 feet below the mud line, and the one "endo" pile (a batter pile driven to resist lateral movement of the wingwall) penetrates 45 feet below the mud line (Jahren and Jones 1996).

The primary function of the structural model was to determine the relative stiffness of the structural components. Unit loads were applied to the wingwall model at the experimentally determined center of force (more information regarding the point-of-impact calculation procedure will be presented later in this section). Deflections resulting from the applied loads were recorded vertically halfway between the fender lines to determine impact face and piling-stiffness values. The backing structure deflection was determined at the centroid of the four vertical backing structure piles in the plan, and at an elevation between the upper and lower fender mounts on the vertical backing structure piles. The generalized stiffness of the system for this analysis is the unit load divided by the deflection of the reaction frame backing structure. Information regarding system and component stiffness values are found in Table 3.3. The wingwall stiffness was calculated at between 53.95 and 49.47 kips per inch, depending on the amount of force applied. A model of the impact face and piles without a backing structure or fenders was used to determine stiffness characteristics of the impact face and pilings (see Figure 3.50).

Table 3.3: Generalized Structural Stiffness of Assembly and Components

Component	Stiffness	Deflection notes	Force Application Notes
Complete Wingwall System	53.95 to 49.47 kips/inch	Deflection measured at center of backing structure, dependent on amount of fender deflection.	Force applied at experimental force centroid
Reaction Frame Support Structure	307.9 kips/inch	Deflection measured at center of backing structure	Forces applied at fender mounts on backing structure
Impact Face and Piling Assembly	2.267 kips/inch	Deflection measured at center of impact face, halfway between upper and lower fender mounts.	Force applied at experimental force centroid
Single Vertical Piling of Impact Face (impact face consists of 3 pilings)	0.7554 kips/inch	Halfway between upper and lower fender mounts.	Force applied on pile, halfway between upper and lower fender mounts
Marine Fenders	18.89 to 5.1 kips/inch	Nonlinear stiffness dependent on amount of deflection	Manufacturer's published reactions

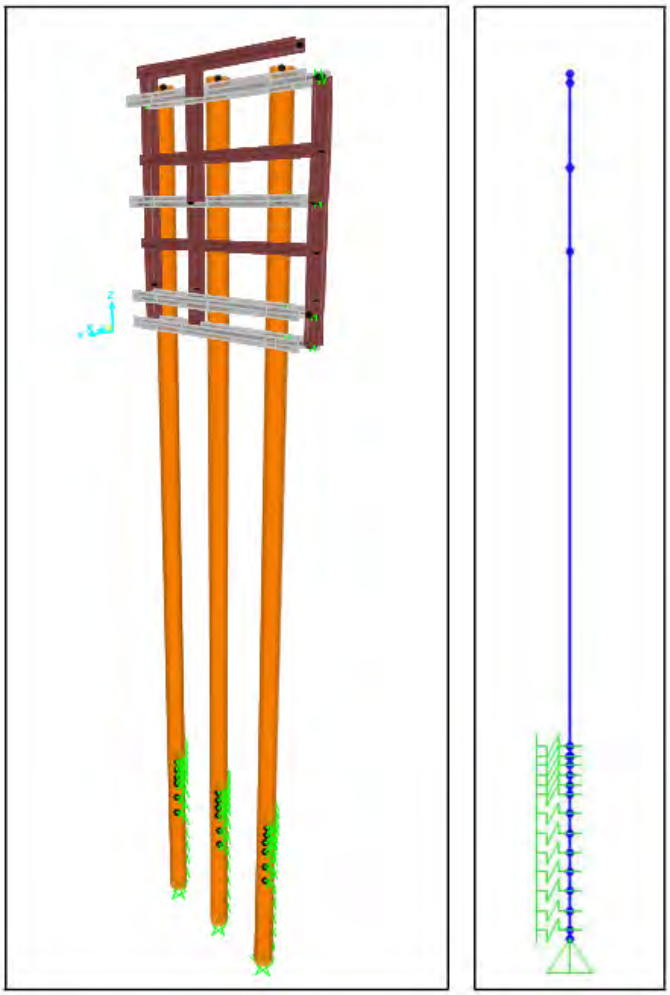

Figure 3.50: SAP impact face model (L); SAP single impact pile model (R)

The structural model was also used to develop relationships between fender deflection and displacement of the reaction frame support structure. Using the component stiffness values and the fender-reaction frame-deflection relationship, energy distribution throughout the wingwall assemblies could be determined. See Table 3.4 and Figure 3.51 for the relative amounts of elastic potential energy for the structural assemblies.

Table 3.4: Energy Absorption Characteristics of Structural Components

Force Applied to Structure (kips)	Total deflection of Fenders (inches)	Impact Pile Elastic Energy (kip-feet)	% of total energy	Fender (kip-feet)	% of total energy	Support Structure Elastic Energy (kip-feet)	% of total energy	Total Elastic Energy (kip-feet)
5	0.26	0.000	0.04	0.61	99.48	0.003	0.48	0.62
10	0.50	0.001	0.08	1.18	98.9	0.012	1	1.19
20	0.99	0.004	0.15	2.39	97.9	0.048	1.95	2.44
100	4.96	0.092	0.60	14.03	92.19	1.097	7.21	15.22
250	12.93	0.633	1.09	50.45	87.2	6.770	11.7	57.85
500	27.05	2.742	1.43	160.26	83.63	28.610	14.93	191.61

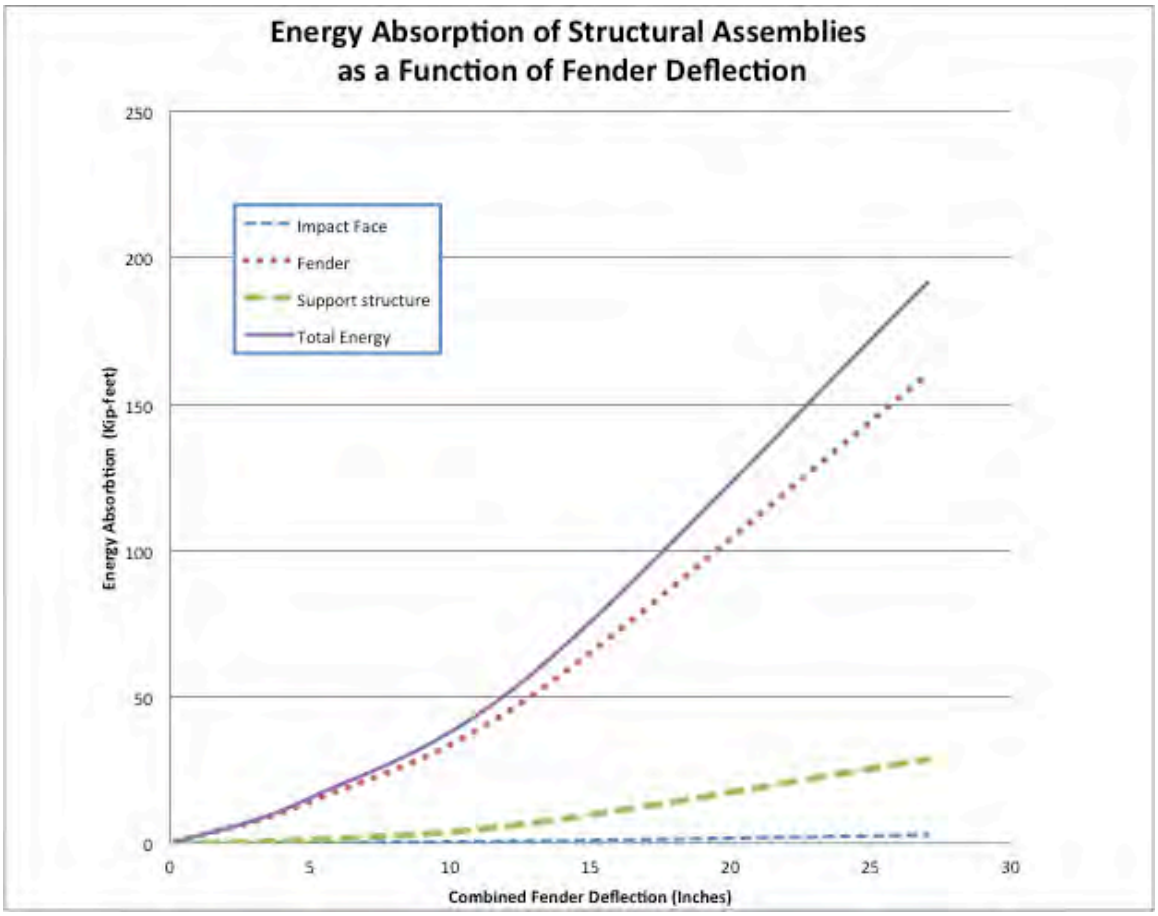

Figure 3.51: Energy absorption of structural assemblies

Berthing Energy Estimates

Marine structural engineers typically use berthing impact energy to design structures for vessel impacts. When a vessel impacts a berthing structure, most of the kinetic energy is transformed to elastic energy of the deformed structure. Marine structural design uses the conservative assumption that all berthing energy will be absorbed by the marine fender, and the amount of energy transmitted to the backing support structure and the vessel's hull is minimal (Gaythwaite 2004).

At the Bremerton slip, LMTs positioned to record the deflection characteristics of each marine fender with respect to time allowed for berthing energy information to be determined. As a vessel impacts the wingwall, the marine fenders compress as the impact face deflects towards the backing structure. Combining known displacements of the marine fenders and information regarding the energy-deflection characteristics of the marine fender supplied by the manufacturer (Figure 3.52, Table 3.5, Equation 3.13,), the energy absorbed by a fender can be estimated.

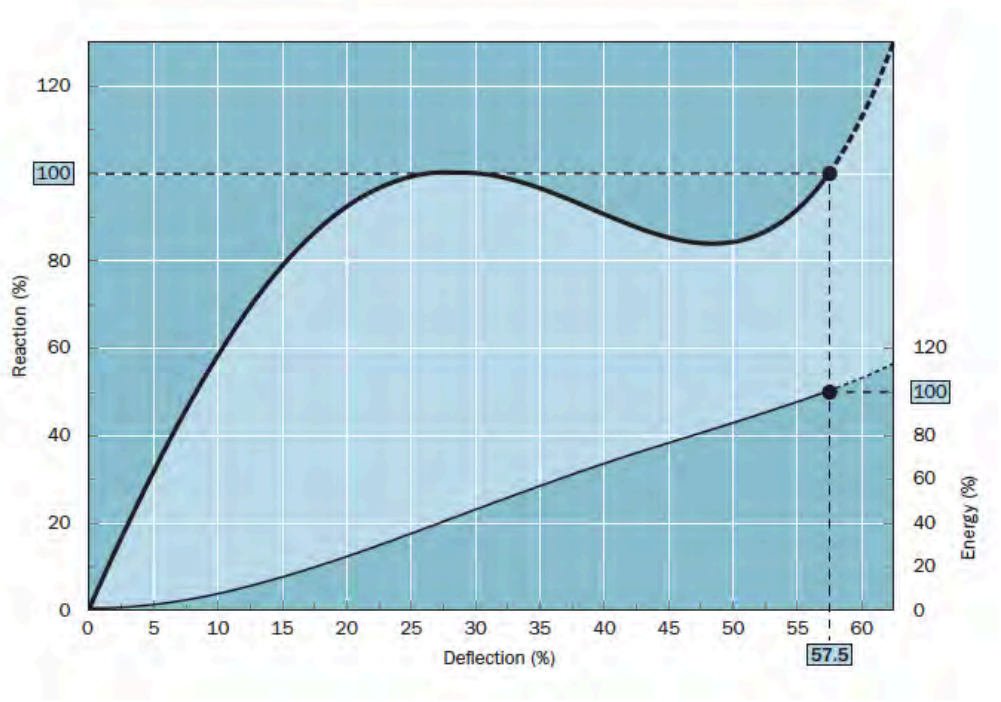

Figure 3.52: Energy absorption of marine fenders, courtesy Trelleborg

Table 3.5: Trelleborg Fender Characteristics

Trelleborg MV1250 x 1000A

Nominal Rattings

Energy 283 Kip Ft

Reaction 150 Kips

Deflection %	mm	inches	inches Squared	Energy %	Energy Kip-Ft	Reaction %	Reaction Kips
-5	-62.5	-2.4606		-2	5.66	-31	-46.5
0	0	0.0000	0.0000	0	0	0	0
5	62.5	2.4606	6.0547	2	5.66	31	46.5
10	125	4.9213	24.2188	7	19.81	58	87
15	187.5	7.3819	54.4923	14	39.62	78	117
20	250	9.8425	96.8752	24	67.92	92	138
28	350	13.7795	189.8754	41	116.03	100	150
35	437.5	17.2244	296.6803	56	158.48	96	144
40	500	19.6850	387.5008	66	186.78	90	135
45	562.5	22.1457	490.4307	76	215.08	85	127.5
50	625	24.6063	605.4700	85	240.55	84	126
57.5	718.75	28.2972	800.7340	100	283	100	150
62.5	781.25	30.7579	946.0468				
100	1250	49.2126					

$$E_{fender} = 0.00004x^5 - 0.0027x^4 + 0.04x^3 + 0.2856x^2 + 2.1748x$$ Equation 3.13

where

E_{fender} = Energy absorbed by marine fender

x = Displacement of fender

The fender system employed on each wingwall at the Bremerton slip in Seattle consists of six buckling column-type fenders, mounted in two rows that connect to the pile-supported impact face and the space frame backing structure. Each fender employed at the Bremerton slip is rated to absorb 283 kip feet of energy at maximum displacement.

The energy dissipated by the entire structural system consists of energy absorbed by the fenders, and a portion of the energy is dissipated by the deflection of the impact face and reaction frame backing structure. The energy absorption characteristics are represented as a kinematic model in Figure 3.53.

The equation for the total berthing energy associated with a ferry landing at the Bremerton slip is described by Equation 3.14:

$$E_{total} = \sum_{i=1}^{6} E_{fender} + \frac{1}{2} K_{frame} \Delta_{frame}^{\ 2} + \sum_{j=1}^{3} \left[\frac{1}{2} K_{impactpile j} \left(\frac{\Delta_{lmtjL} + \Delta_{lmtjU}}{2} \right)^2 \right]$$ Equatio

where

E_{total} = Total energy absorbed by the complete structural system

E_{fender} = Energy absorbed by marine fender

K_{frame} = Stiffness of reaction frame backing structure

Δ_{frame} = Displacement of backing structure

$K_{impact\ pile}$ = Stiffness of pile supporting the impact face

Δ_{lmtjL} = Displacement of fender *j*L (lower fender, at position *j*)

Δ_{lmtjU} = Displacement of fender *j*U (upper fender, at position j)

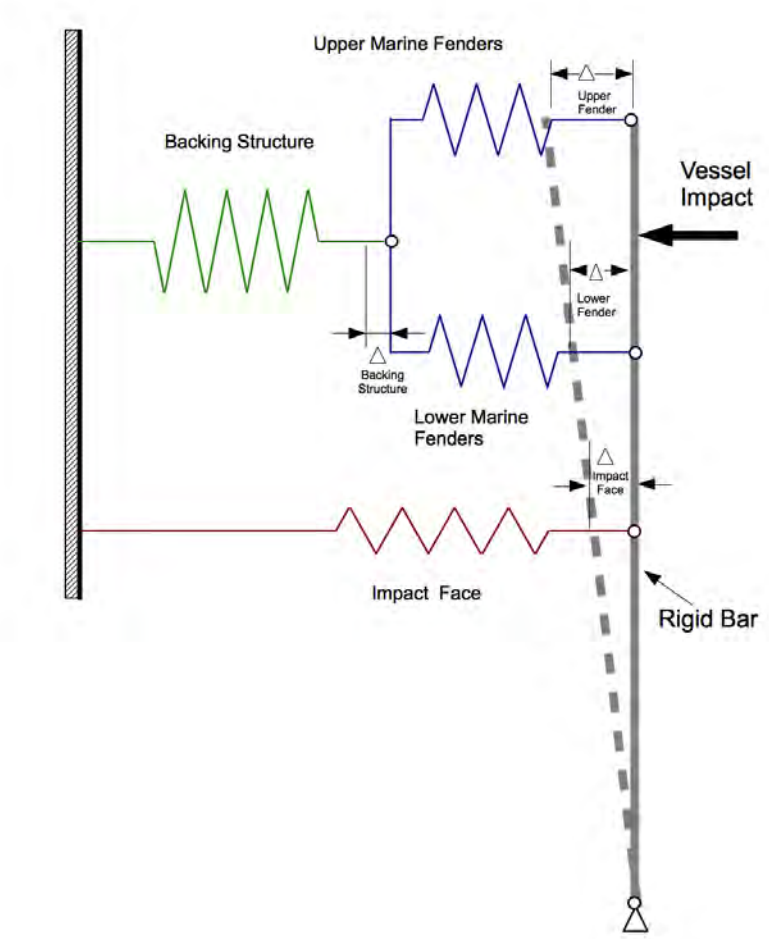

Figure 3.53: Kinematic model of wingwall

Chapter 4A – Results: Auke Bay

Overview

In this chapter, results are presented for six separate parameters: berthing energy, kinetic energy, berthing force, fender force, approach velocity, and berthing coefficient. Results are displayed in the form of histograms, probability distribution fits, probability curves, and regression fits. Results are also displayed as load (demand) values for various reliabilities over practical design lives (i.e., number of berthing events over the design service life of the structure).

The histograms provide a graphical representation of the frequency distribution of each load parameter observed over a range of measurements. The purpose of the histograms is to evaluate the relative frequencies of each parameter by displaying the number of times various measurements occurred over the total sample of berthing events. Probability density functions (pdfs) were fitted to their respective histograms; pdfs associate measurements or experimental results with their respective probabilities of occurrence. Probability curves were also constructed; they are particularly useful for analyzing the probability of non-exceedance at extreme values, and graphically depict the "goodness of fit" of the probability distribution to the empirical data. The degree of linearity is reflective of how well a distribution matches the empirical data.

Parameter values are provided for a wide range of percentiles (99.99%–99.9998%). This percentile range corresponds to typical reliability levels over various design lives (design berths). For reference, the 99.99^{th} and the 99.9998^{th} percentiles correspond to risk levels of 10% in 10 events and 2% in 10,500 events (approximately 30 years at Auke Bay), respectively.

The design charts and tables provide load values for five parameters as a function of reliability and number of berths. These charts can be used directly to select design values for a desired probability of non-exceedance.

Velocity Results

Approach velocity was determined from the position versus time data and is displayed in the form of histograms, statistical distribution fits, and probability curves.

While multiple approaches and impacts frequently occur during a vessel berth, these figures only reflect the approach velocity and impact corresponding to the largest fender deflection on each dolphin for each berthing event. Table 4.1 provides a summary of the velocity data.

Table 4.1: Summary of Approach Velocity

	Velocity		
	Max (ft/s)	Mean (ft/s)	# of Measurements
All Vessels	0.83	0.156	350
Columbia	0.5	0.136	39
Kennicott	0.5	0.165	52
Malaspina	0.83	0.162	178
Matanuska	0.46	0.099	82

Several probability distributions were fit to the velocity data. The probability distribution found to fit velocity histograms most accurately was the Lognormal distribution (Figure 4.1). A probability plot was created using the Lognormal distribution (Figure 4.2). These plots display the probability that a certain approach velocity will not be met or exceeded in any one berthing event. Table 4.2 provides a summary of the velocity for various probabilities of non-exceedance.

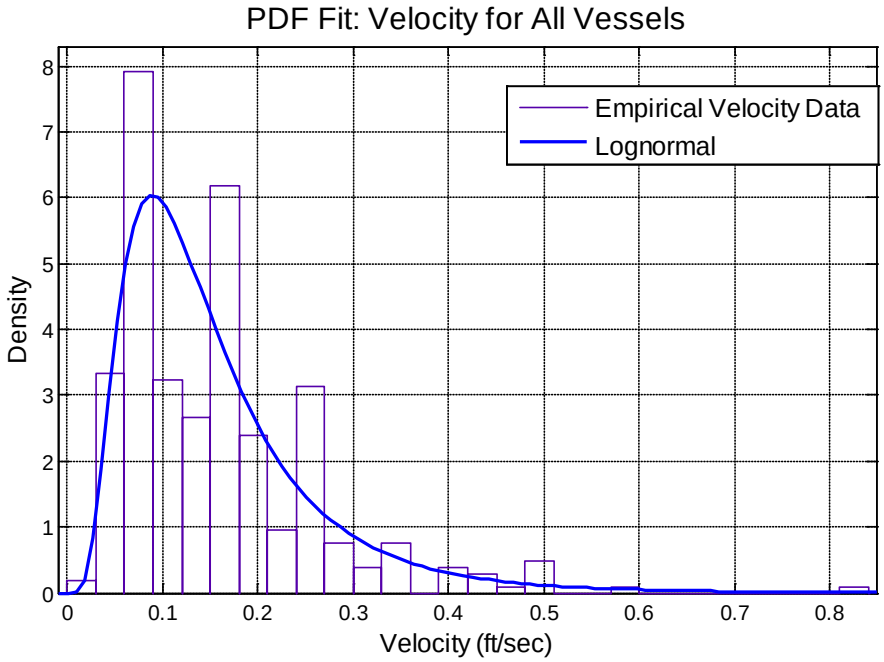

Figure 4.1: Velocity distribution fit for all vessels

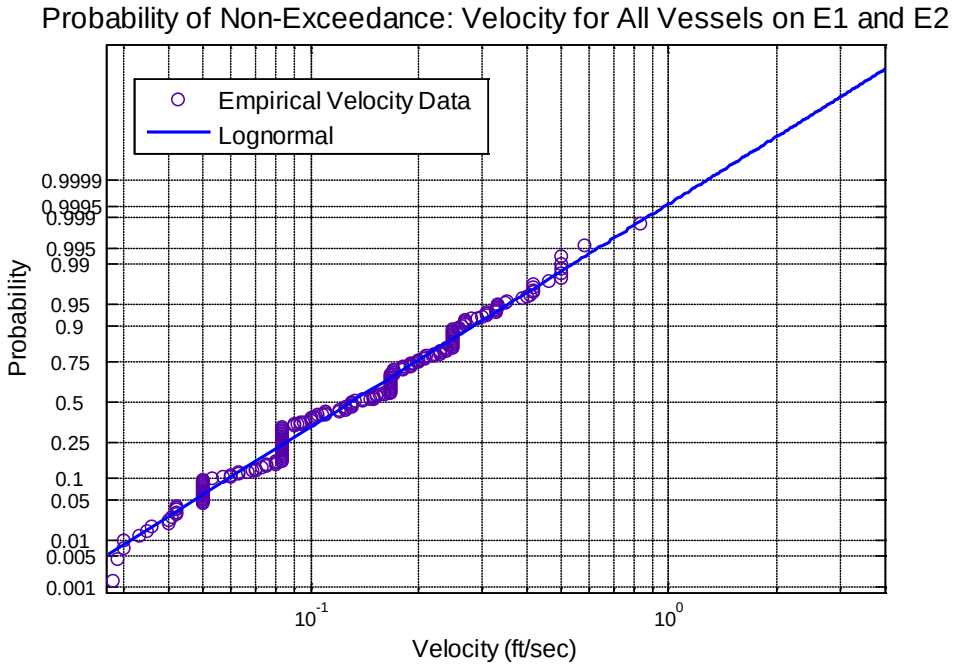

Figure 4.2: Velocity probability plot

Table 4.2: Probability of Non-exceedance: Velocity

Summary of Approach Velocity Data (ft/sec)					
	Columbia	Kennicott	Malaspina	Matanuska	All Vessels
(1-*p*)%					
90	*	*	0.30	0.23	0.29
95	*	*	0.38	0.28	0.36
98	*	*	0.49	0.36	0.46
99	*	*	0.58	0.42	0.54
99.9	*	*	0.92	0.65	0.87
99.99	*	*	1.34	0.94	1.27
99.995	*	*	1.49	1.03	1.42
99.999	*	*	1.87	1.28	1.78
99.9995	*	*	2.06	1.40	1.96
99.9999	*	*	2.52	1.70	2.41
# of events			178	81	350

* Lognormal distribution did not fit smaller dataset and therefore was not evaluated

Energy Results

Energy results are presented in the form of histograms, statistical distribution fits, and probability curves. Berthing energy is the total energy absorbed by the berthing structure, which takes into consideration the fender system as well as the backing structure (tripod). Table 4.3 is a summary of the energy data.

Table 4.3: Summary of Energy Data

Energy			
	Max (kip-ft)	Mean (kip-ft)	# of Measurements
All Vessels	47	3.9	486
Columbia	43	5.1	54
Kennicott	26.5	3.8	62
Malaspina	47	4.2	253
Matanuska	28.3	2.8	117

Several distributions were fit to the elastic potential energy data. The distribution found to fit the berthing energy histograms most accurately appeared to be the Weibull distribution, which is commonly used in lifetime modeling (Figure 4.3). The Weibull distribution was chosen particularly for its closeness of fit to the energy data, and its ability to predict extreme berthing energy values (Figure 4.4). Table 4.4 provides a summary of the absorbed energy for various probabilities of non-exceedance.

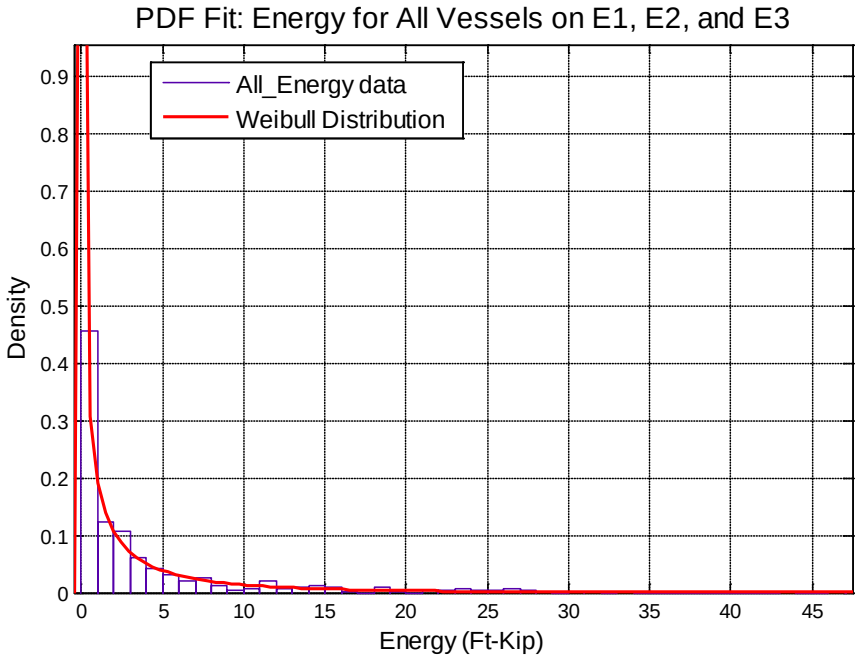

Figure 4.3: Energy distribution fit for all vessels

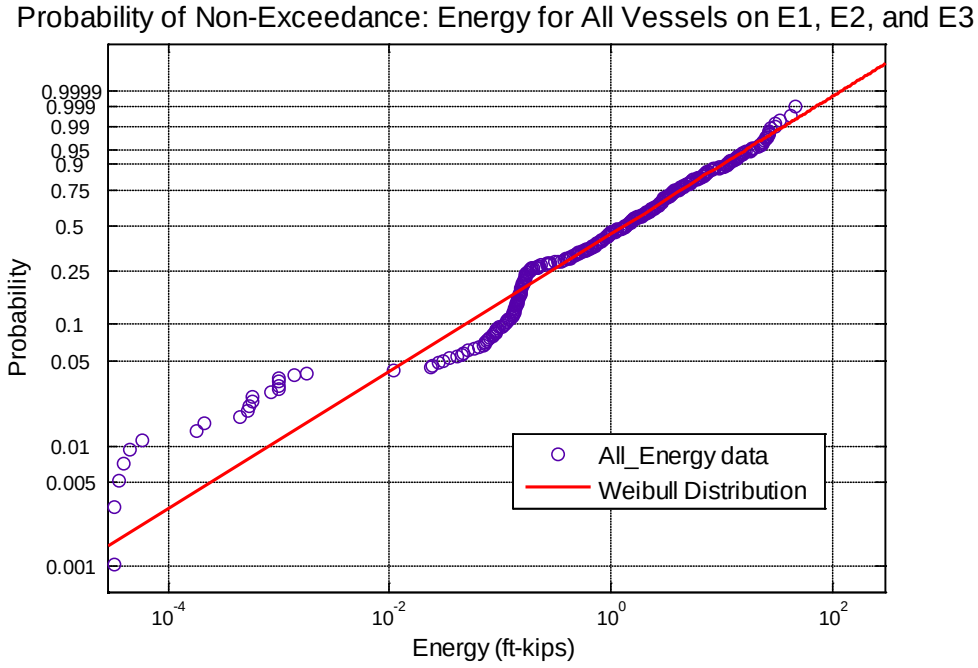

Figure 4.4: Energy probability plot for all vessels

Table 4.4: Probability of Non-exceedance: Energy

Summary of Berthing Energy data (ft-kips)					
	Columbia	Kennicott	Malaspina	Matanuska	All Vessels
(1-*p*)%					
90	13	11	11	7	11
95	21	18	18	11	17
98	33	30	29	18	27
99	43	40	38	23	35
99.9	86	83	78	45	72
99.99	139	139	130	73	118
99.995	157	158	147	82	134
99.999	203	207	192	106	175
99.9995	224	230	213	117	194
99.9999	276	288	265	143	240
# of events	54	62	253	117	486

Berthing Coefficient

Berthing coefficients (see Table 4.5) were determined in accordance with Equation 3.6 (Chapter 3A). For this study, berthing coefficients were calculated as the ratio of the elastic potential energy of the deformed structure to the apparent kinetic energy of the vessel.

Table 4.5: Berthing Coefficients

Berthing Coefficient (C_b)			
	Max	Mean	# of Measurements
All Vessels	1.22	0.32	293
Columbia	1.22	0.48	30
Kennicott	0.59	0.28	44
Malaspina	1.16	0.33	151
Matanuska	0.91	0.26	68

Berthing Factor Results

In this study, the berthing factor is defined as the energy-per-unit mass of the vessel; it may be used to estimate the berthing energy of other classes of vessels (having different displacements) not observed in this study. Obtaining the berthing factor is accomplished by dividing the elastic potential energy of the deformed structure by the mass of the vessel. The mass of the vessel was determined using the published vessel displacement (see Table 4.6).

Table 4.6: Berthing Factor Summary

Berthing Factor			
	Max	Mean	# of Measurements
All Vessels	0.1217	0.0093354	486
Columbia	0.0805	0.0096176	54
Kennicott	0.0508	0.0072696	62
Malaspina	0.1217	0.010792	253
Matanuska	0.0731	0.0071509	117

A variety of probability distributions were fit to the berthing factor results data (Table 4.7). The probability distribution found to fit berthing factor histograms most accurately was the Weibull distribution (Figure 4.5). A probability plot was created using the Weibull distribution (Figure 4.6). These plots display the probability that a certain berthing factor will not be met or exceeded in any one berthing event.

Table 4.7: Berthing Factor Probability of Non-exceedance Values

Probability of Non-exceedance: Berthing Factor (ft^2/s^2)					
	Columbia	Kennicott	Malaspina	Matanuska	All Vessels
(1-*p*)%					
90	0.03	0.02	0.03	0.02	0.03
95	0.04	0.04	0.05	0.03	0.04
98	0.06	0.06	0.07	0.05	0.06
99	0.08	0.08	0.10	0.06	0.08
99.9	0.16	0.16	0.20	0.12	0.17
99.99	0.26	0.27	0.34	0.19	0.28
99.995	0.29	0.30	0.38	0.21	0.32
99.999	0.38	0.40	0.50	0.27	0.42
99.9995	0.42	0.44	0.55	0.30	0.46
99.9999	0.52	0.55	0.69	0.37	0.57
# of events	54	62	253	117	486

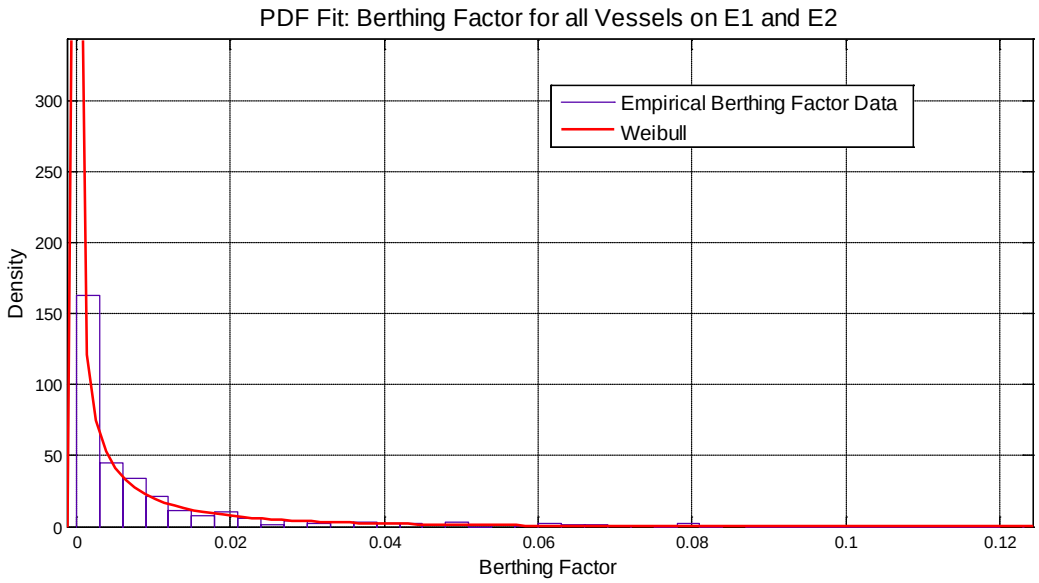

Figure 4.5: Berthing factor distribution fit for all vessels

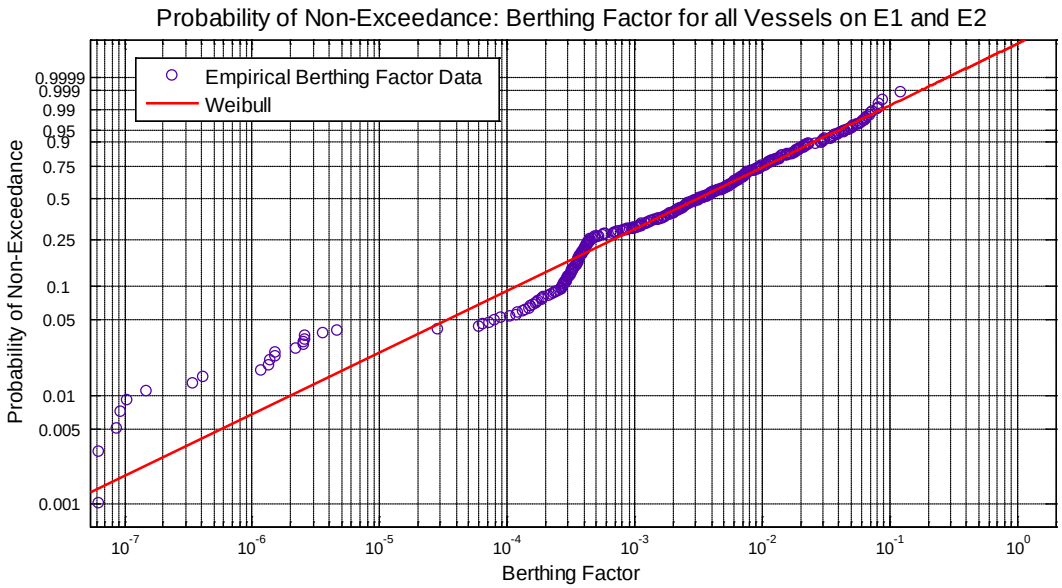

Figure 4.6: Berthing factor probability plot for all vessels

Berthing Force Results

Knowing the stiffness of the system and displacement, the force applied to the system can be determined. Equations for determining the force of impact at each site were formulated based on known force-displacement relationships of the fenders, stiffness of the support structure, and statics. While the energy values are generally applicable, impact force values presented here are only applicable to the Auke Bay site as it is presently constructed (see Tables 4.8 and 4.9).

For each event, values of force were determined using Equation 3.12 (Chapter 3A).

Table 4.8: Berthing Force Summary

Berthing Force			
	Max (kip)	Mean (kip)	# of Measurements
All Vessels	77.3	16.3	485
Columbia	77.3	19.0	54
Kennicott	26.5	15.3	62
Malaspina	64.6	16.9	253
Matanuska	65.1	14.2	116

Table 4.9: Probability of Non-exceedance: Berthing Force

Probability of Non-exceedance: Force (kips)					
	Columbia	Kennicott	Malaspina	Matanuska	All Vessels
(1-*p*)%					
90	41	34	37	30	35
95	51	44	46	38	45
98	64	57	58	47	56
99	73	67	67	54	65
99.9	103	99	96	76	93
99.99	131	130	124	97	120
99.995	139	139	132	103	128
99.999	158	161	150	117	146
99.9995	166	170	158	123	154
99.9999	184	191	176	137	171
# of events	54	62	253	116	485

Several probability distributions were fit to the force results. The probability distribution found to fit force histograms most accurately was the Weibull distribution (Figure 4.7). A probability plot was created using the Weibull distribution (Figure 4.8). This plot displays the probability that a certain impact force will not be met or exceeded in any one berthing event.

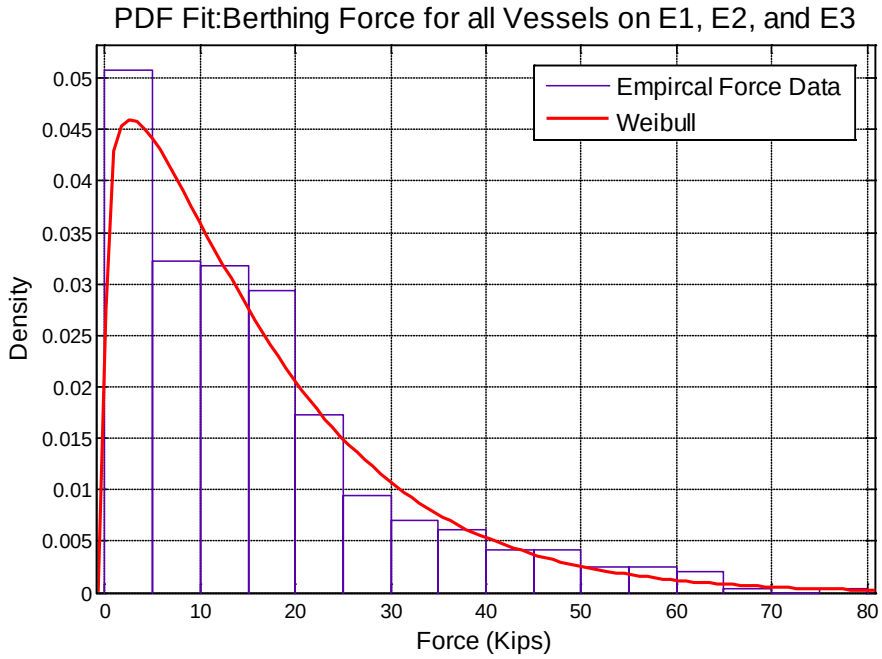

Figure 4.7: Berthing force distribution fit for all vessels

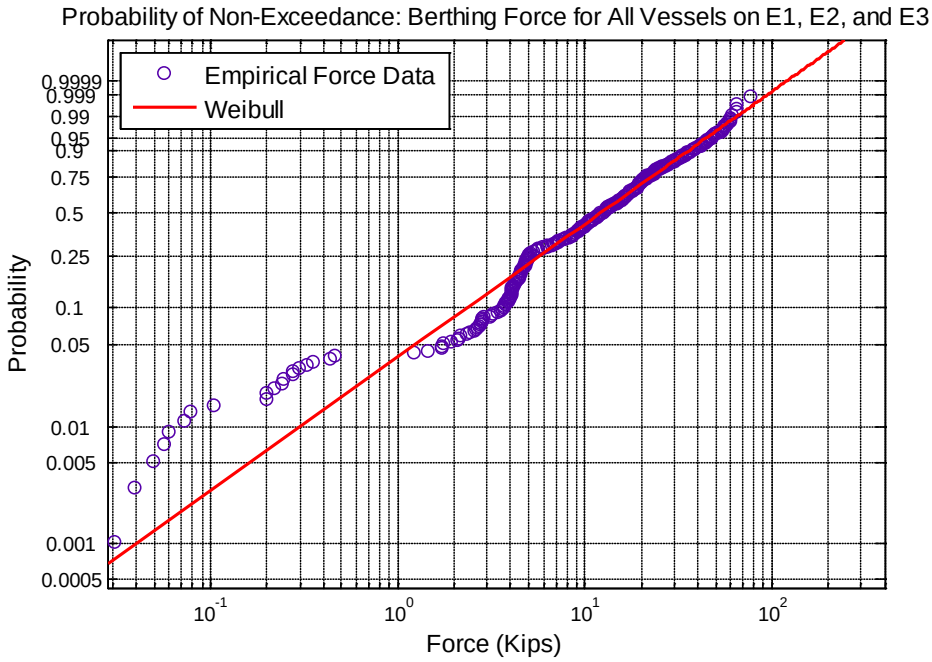

Figure 4.8: Berthing force probability plot for all vessels

Reliability Design Charts

The following design charts (Figures 4.9 through 4.12) are based on the distribution and probability plots shown in the previous sections Parameter values are displayed for three different probabilities of non-exceedance (reliabilities) commonly used in practice: 90%, 95%, and 98%. Reliabilities for 99%, 99.9%, and 99.99% have also been included and will provide insight on berthing demands for extreme events. The *x*-axis of the design charts represents the design number of berths or number of berthing events that a structure is expected to experience over its intended design life.

Table 4.10 provides a summary of design values for berthing parameters at various reliabilities and design lives, and Table 4.11 provides various load factors for berthing parameters.

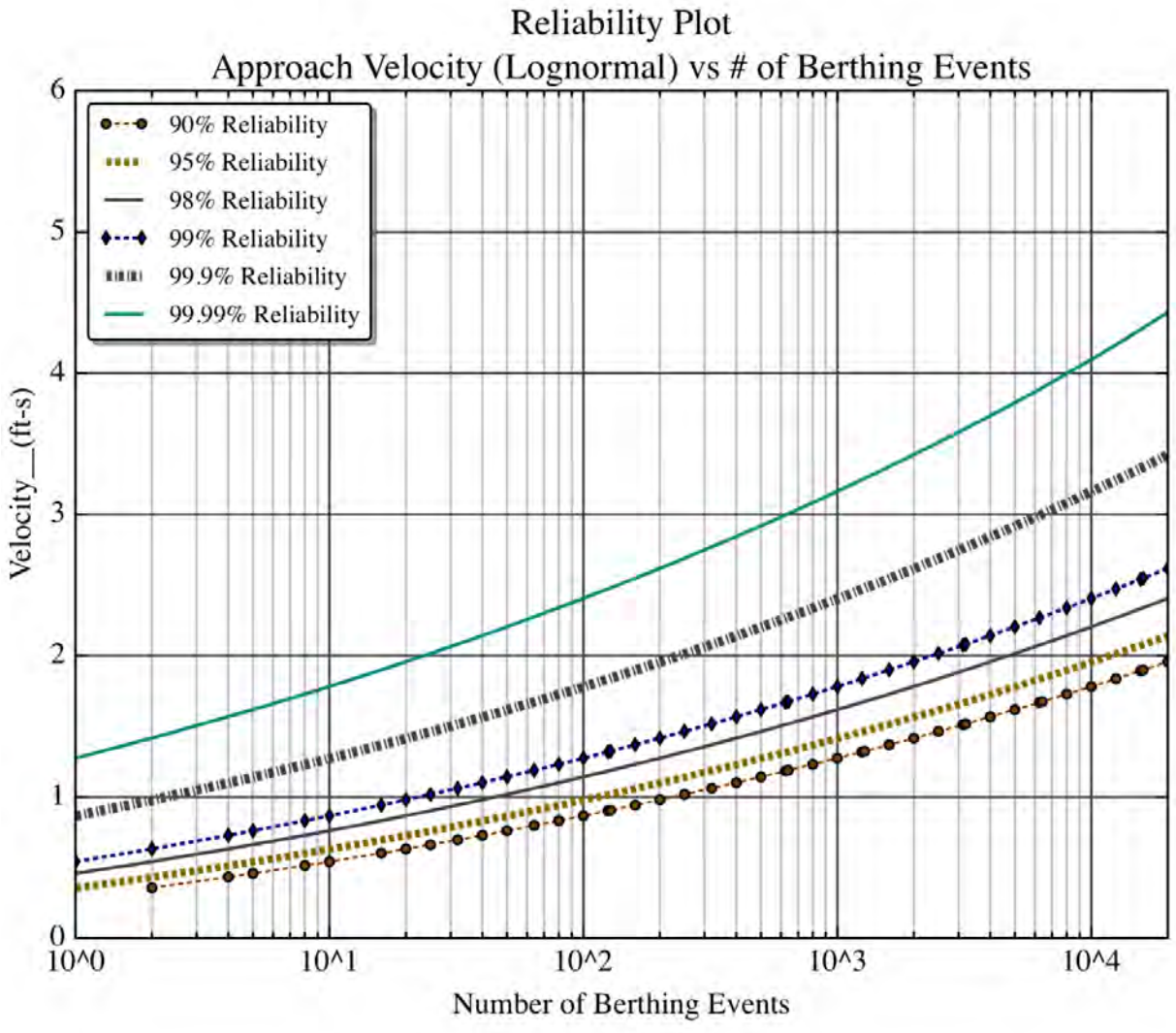

Figure 4.9: Velocity design chart

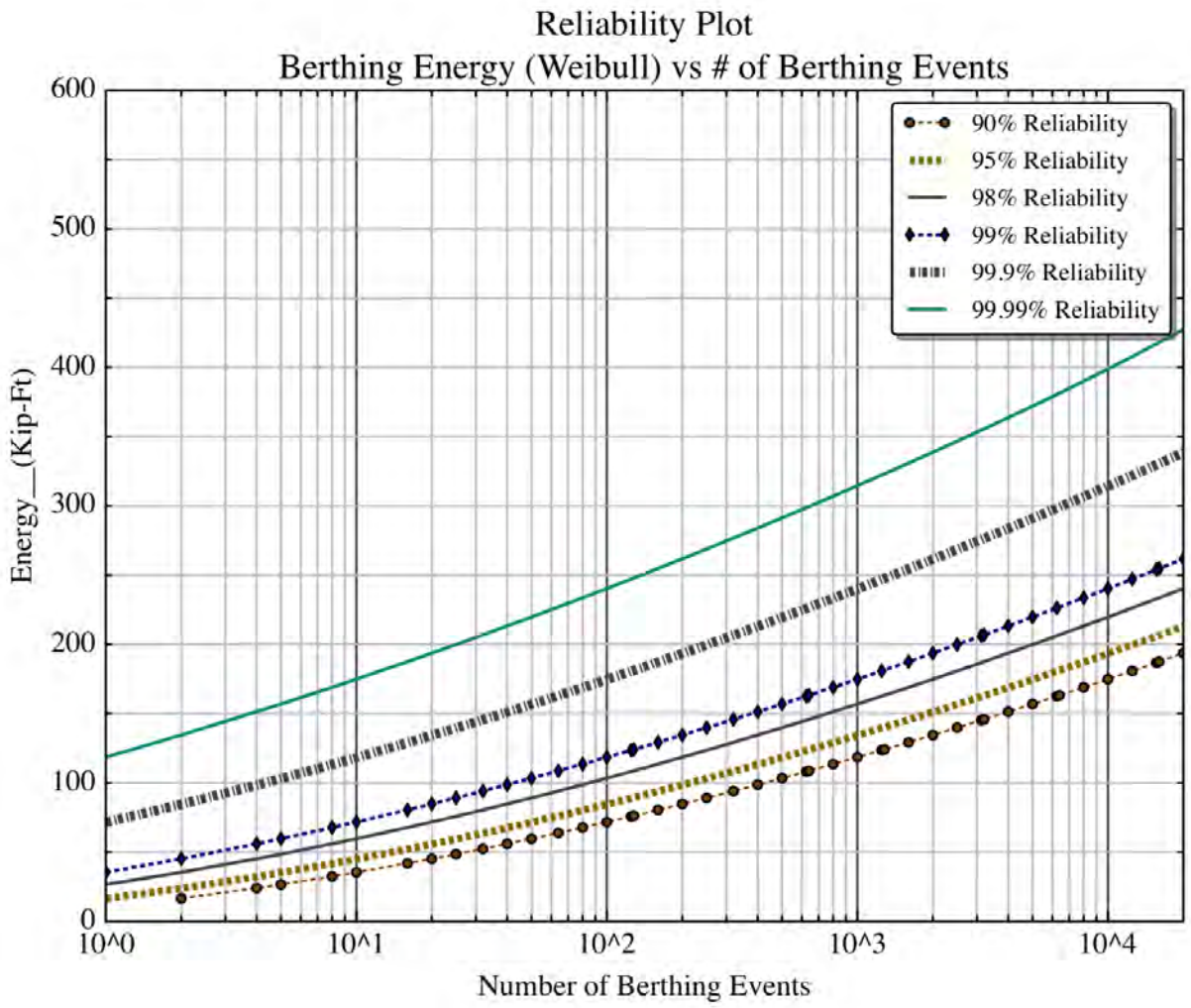

Figure 4.10: Energy design chart

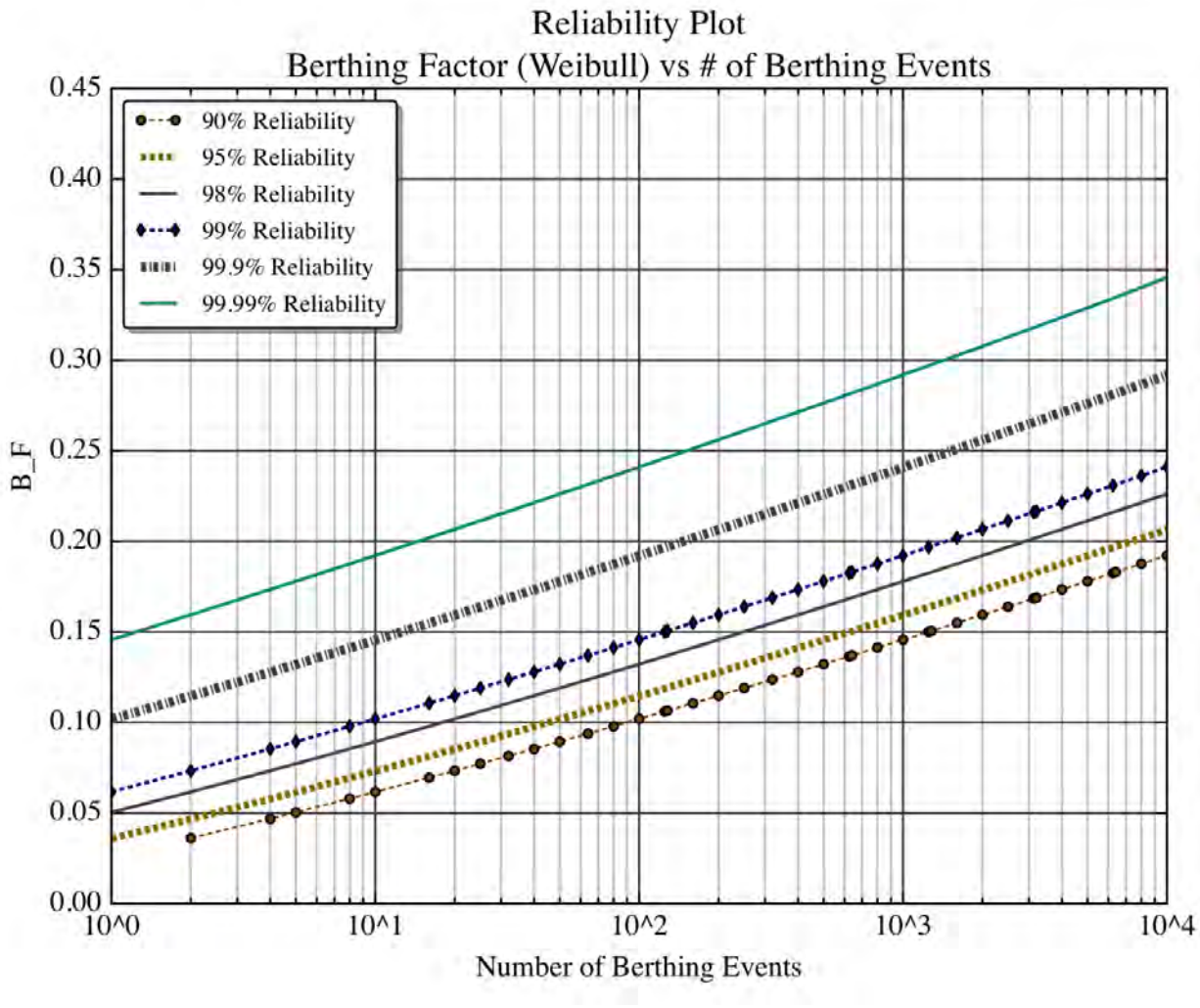

Figure 4.11: Berthing factor design chart

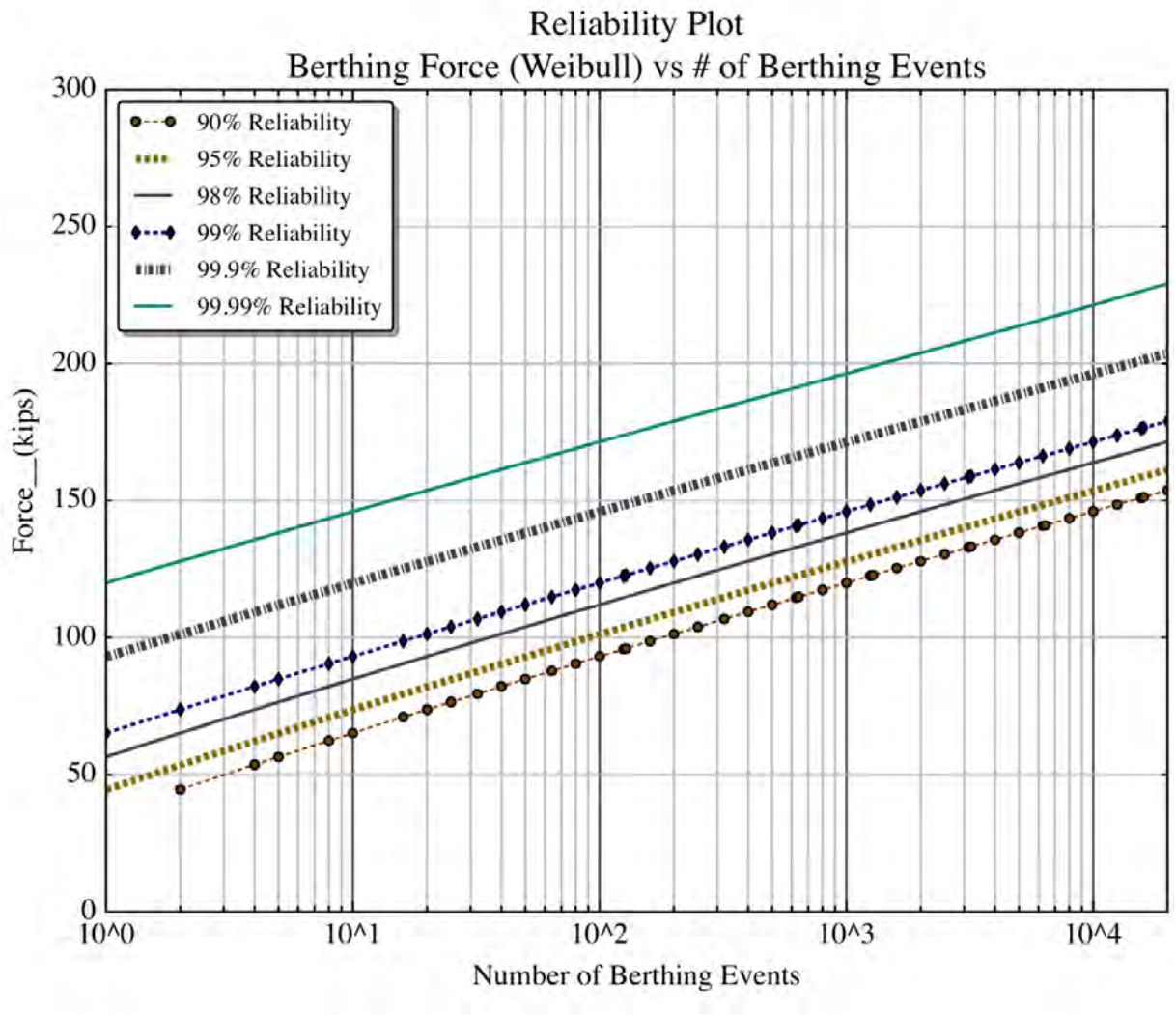

Figure 4.12: Berthing force design chart

Table 4.10: Summary of Design Values

Nominal/Service Loads, 90%, 30 events		
Berthing Energy	51	kip-ft
Berthing Force	78	kip
Approach Velocity	0.68	ft/sec
Berthing Factor	0.121	

Nominal is a 99.65 percentile per event, which is a 90% probability of non-exceedance in 30 events

Ultimate Loads, 90%, 3500 events		
Berthing Energy	147	kip-ft
Berthing Force	134	kip
Approach Velocity	1.53	ft/sec
Berthing Factor	0.354	

99.997% percentile per berthing event, a 90% probability of non-exceedance in 3500 events

Ultimate Loads, 98%, 10,500 events		
Berthing Energy	220	kip-ft
Berthing Force	164	kip
Approach Velocity	2.2	ft/sec
Berthing Factor	0.525	

99.9998% percentile per berthing event, a 98% probability of non-exceedance in 10,500 events

Table 4.11: Load/Parameter Factors

Loads	Nominal/Service Loads, 90%, 30 events	Ultimate Loads, 90%, 3500 events	Load Factor	Ultimate Loads, 98%, 10,500 events	Load Factor
Energy (kip-ft)	51	147	2.9	220	4.3
Force (kips)	78	134	1.7	164	2.1
Velocity (feet/second)	0.68	1.53	2.3	2.2	3.2
Berthing Factor ($feet^2/second^2$)	0.121	0.354	2.9	0.525	4.3

Mooring Line Forces

An additional component of the Auke Bay study was an attempt at measuring mooring line loads on the bollards located on the dolphins (see Figure 4.13). A technique for accomplishing this was developed and tested under laboratory conditions. The Appendix details the development and validation of the method. The technique developed for estimating bollard loads requires a known distance between the mooring line and strain gauges placed on the bollard. The technique requires that the mooring line be tight against the crossbar to establish the moment arm to the strain gauges. Figure 4.14 shows actual tie-up conditions in which the mooring line is somewhat below the crossbars. Actual conditions at the precluded successful measurement of mooring line forces with the technique developed that purpose. An alternative method implemented in the field did not provide measurements of any value. The attempt to measure mooring line forces was unsuccessful at Auke Bay. See the Appendix for additional information.

Figure 4.13: Typical bollard at Auke Bay ferry landing

Figure 4.14: Typical tie-up conditions at Auke Bay

Chapter 4B – Results: Seattle

Overview

All events were analyzed using the software package described earlier in this report. Following filtering and event characterization, the dataset for the north wingwall contained approximately 3448 impact events; the south wingwall dataset contained 3504 impact events, for a total of 6952 vessel impact events.

Results are presented for six parameters: approach velocity, berthing energy, berthing force, berthing factor, berthing coefficient, and vessel point of contact. These parameters are investigated as a collection of individual events at the wingwalls. Results concerning how a particular wingwall experiences berthing parameters are introduced through summary tables. Results are displayed through histograms, probability distribution fits, cumulative probability plots, and probability of non-exceedance plots.

Histograms provide a graphical representation of the frequency distribution of each parameter, such as approach velocity, berthing energy, and frequency of occurrence. The purpose of the histograms is to display the relative frequencies of each parameter by displaying the number of times that magnitudes within a certain range occur over the sample size.

Probability density functions (pdfs), fitted to the corresponding histograms, attempt to match a well-defined pdf to the empirical data. Using probability distributions that correlate with the experimental data, a probability of occurrence can be associated with the experimentally determined results.

Cumulative probability distributions are derived from the cumulative sum of pdf curves and associate measured parameters with the probability of not being exceeded or equaled, displayed in percentile form. The purpose of the cumulative probability graph is to display the relative fit between the selected probability distribution and the empirical data.

Percentile plots (or probability plots) are another method of visualizing the cumulative probability distributions. The vertical axis of these plots is a percentile value representing a probability that a given parameter value will not occur or be exceeded during a berthing event. This percentile value represents a parameter value for a given percentage of measurements that occurred or were below the parameter value. For example, a percentile value of 0.99 represents a parameter value of which 99% of recorded values were at or below that parameter value, and 1% of recorded values measured above that level. The benefit of the percentile plot is twofold; first, they are useful for analyzing the probability of occurrence at extreme values, and second, they graphically display the “goodness of fit” of the probability distribution to the experimentally obtained dataset. The angle and degree of linearity illustrate how well the distribution matches the empirical data. The probability distribution, which is represented as a line, displays the relationship between the parameter of interest and its probability of not being exceeded in any one berthing event. The distribution line allows for extreme values and corresponding probabilities of occurrence to be estimated, and presents the designer with a methodology for selecting design parameter values, that is, engineering design criteria.

Parameter values in each section are provided over a range of percentiles matched to the needs of Washington State Ferries (WSF) personnel and corresponding design lives of the wingwall structures. The wingwall structures have a design service life of 50 years, which,

depending on the terminal, ranges from approximately 200,000 to 730,000 berthing events at current sailing schedules. The Bremerton slip 50-year design life is approximately 237,750 berthing events. For instance, a parameter value corresponding to the 99.99^{th} percentile would correspond to a 43.75% probability of not being exceeded over the course of one year at the Bremerton slip, which receives approximately 5475 berthing events in a year. A parameter value corresponding to the 99.9999999^{th} percentile would have a 0.005% of not being exceeded in the course of ten years at the Bremerton slip, and a 0.02% probability of not being exceeded over the course of 50 years at the Bremerton slip. See Chapter 5B for more information concerning reliability and risk-level determination.

Velocity Results

Approach velocity was determined using the sonic distance sensor data with respect to time. The distance sensor recorded the position of the vessel normal to the wingwall and at the seaward side of the wingwall. See Figures 3.38 and 3.39 (Chapter 3B) for the placement of the distance sensor on the wingwalls. The position of the distance sensor may have a significant effect on the recorded approach velocity of the berthing vessel; this topic is discussed in Chapter 5B. See Table 4.12 for a summary of recorded velocity information. The velocity information in this section represents the combined dataset.

Table 4.12: Velocity Summary Table

Approach Velocity, feet/second				
Wall	Mean	Standard Deviation	Max	# of Events
North	0.324196	0.19329	1.6525	2672
South	0.322774	0.20073	1.6358	2455
Combined	0.323515	0.91689	1.6525	5127

Often, multiple impact events occur during a berthing event. The dataset analyzed for this study has been selected to represent the largest discrete impact event at the wingwall (as determined from the deflection of the marine fenders), which may or may not be the first impact event at the wingwall. Berthing events that contain instances of the vessel powering up against the wingwall in secondary berthing maneuvers are not considered discrete impacts, though they may represent the maximum deflection of the fenders; in these instances, the discrete vessel impact is used for parameter determination.

The dataset for velocity information is smaller than the dataset associated with the deflection parameters due to challenges associated with obtaining unambiguous velocity data. The end-berthing ferries observed in this study have the common characteristics of a large open bow that allows the transfer bridge to be loaded onto the deck of the ferry to facilitate vehicle loading. This large opening necessitated location of the distance sensors aft of the open bow, on the seaward side of the wingwalls (see Figure 4.15).

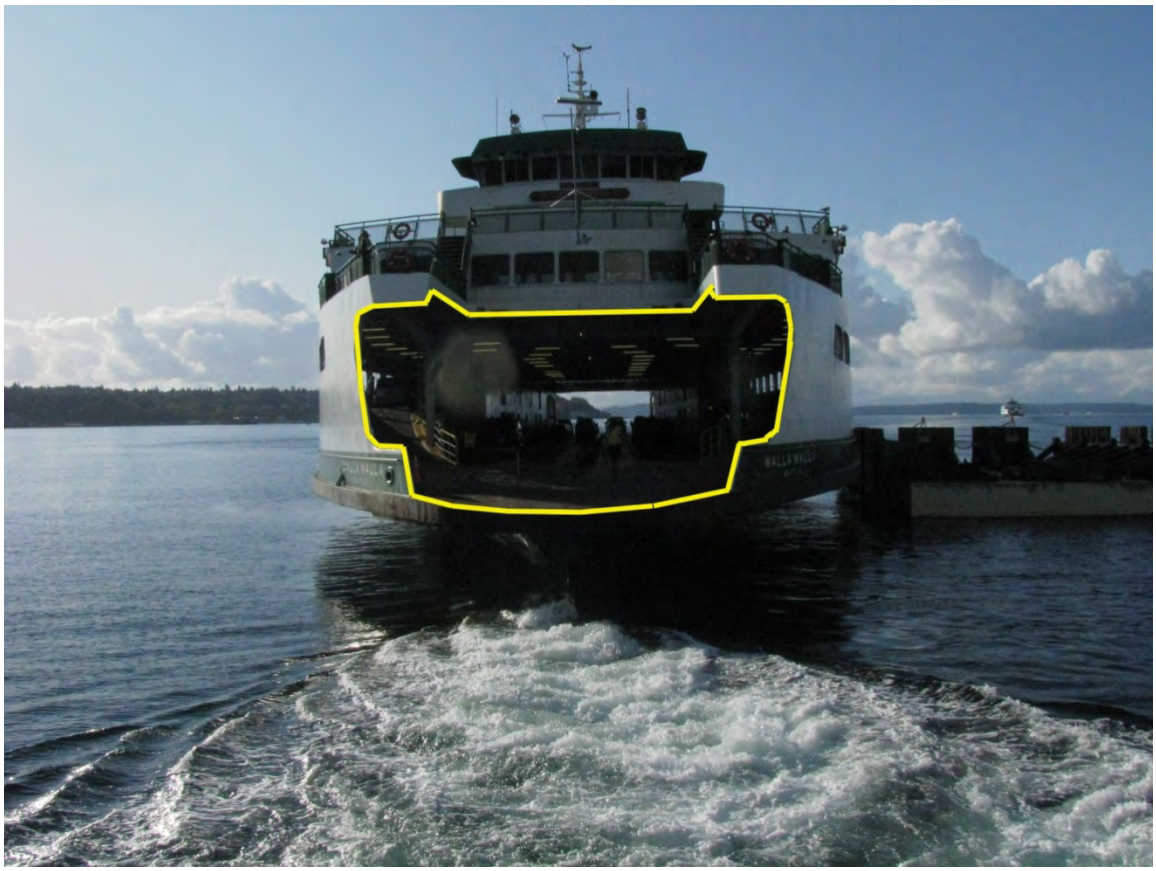

Figure 4.15: Typical ferry bow/stern; opening highlighted in yellow

The elevation of distance sensor placement was above the extreme high water of the terminal to keep the equipment from getting wet. This setup provided for generally good position versus time data; however, at certain tide levels the distance sensor received data that indicated a return signal that was reflecting off a curved surface, reflecting off the vessel's sponson intermittently, or perhaps occasionally passing through an opening in the hull of the vessel. During the event-characterization process, any velocity information that was deemed suspect at the time of interest was filtered out and removed from the velocity dataset (see Figure 4.16). The highest velocities that satisfied the initial characterization went through an additional inspection to further scrutinize the validity of the data. The second inspection consisted of re-plotting the vessel position with respect to time and visually inspecting the berthing event. Velocity information for these outlying events was omitted from the velocity dataset if there was ambiguity regarding the vessel's "actual" position with regard to what the plotted data represented.

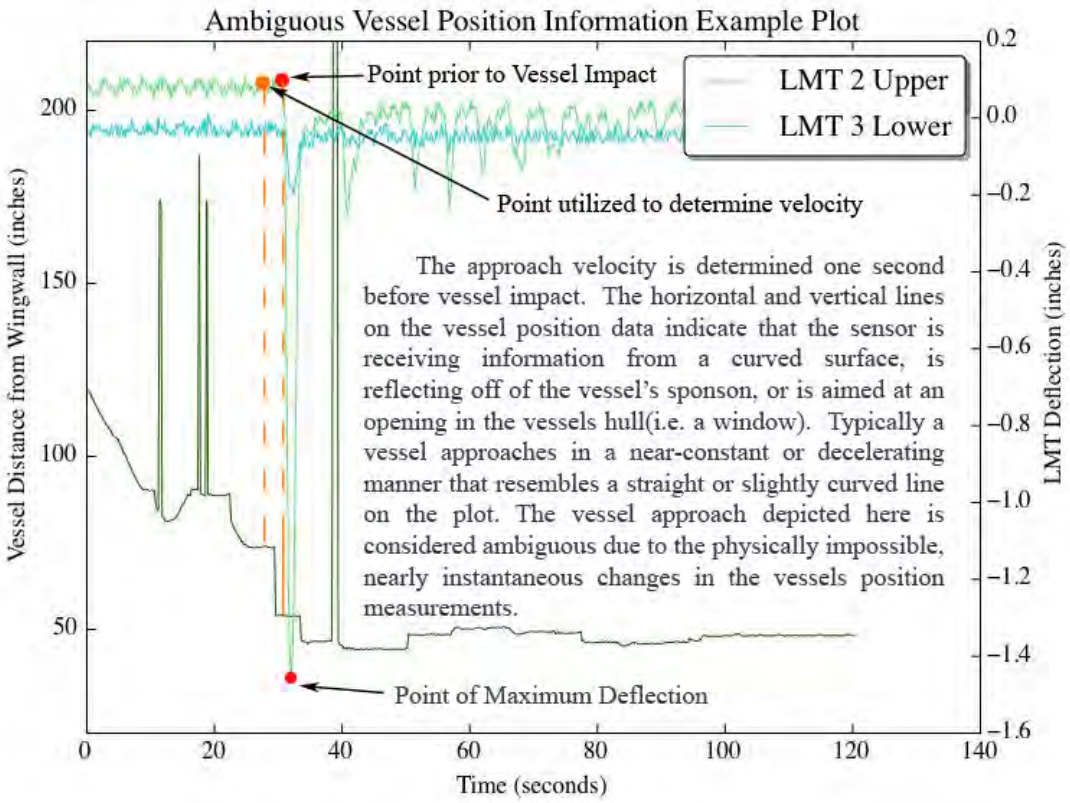

Figure 4.16: Ambiguous vessel position graphic

The velocity data were filtered again to remove any values that were less than 0.035 feet per second (0.42 inches per second). Following event characterization of the entire dataset, it was determined that below this rate of speed, the vessel approach velocity neared zero and did not properly correlate to deflection of the LMTs. Further discussion regarding the characterization of vessel approach velocity is found in Chapter 5B.

After experimenting with several probability distributions, the Weibull distribution exhibited the closest correlation to the velocity dataset. The Weibull distribution was then applied to the density histogram (Figure 4.17), the cumulative probability (Figure 4.18), and the probability of non-exceedance plots, that is, probability plots (Figure 4.19). Matching the empirical data to a probability distribution such as the Weibull allows the ability to estimate extreme approach velocity values. Using the percentile plots illustrates the probability relationship between a given approach velocity and its likelihood of not being exceeded in any one berthing event. The Weibull distribution relates a velocity value to a corresponding probability to predict a velocity value that has a given probability (such as 99.999% or 99.9999999%) of not being exceeded in any one berthing event (see Table 4.13).

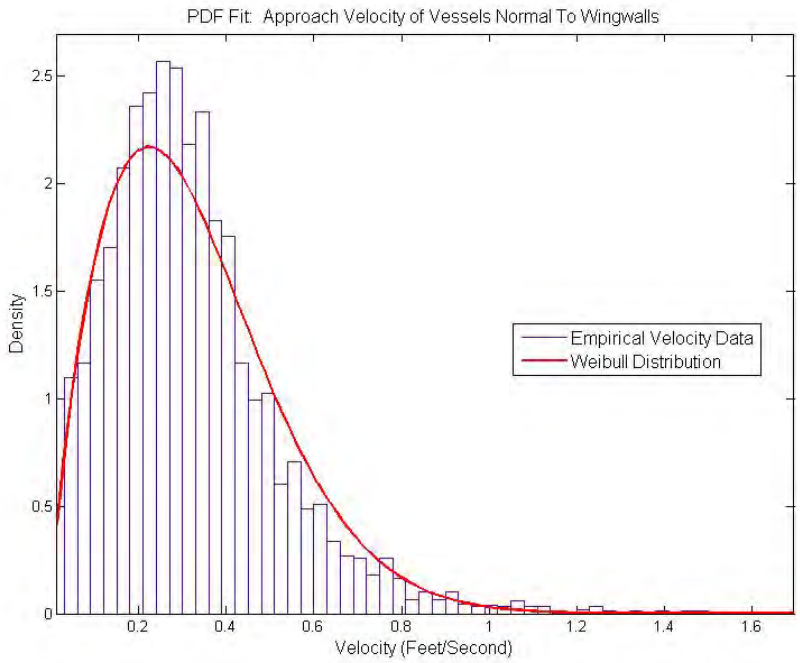

Figure 4.17: Weibull probability distribution fit to approach velocity data

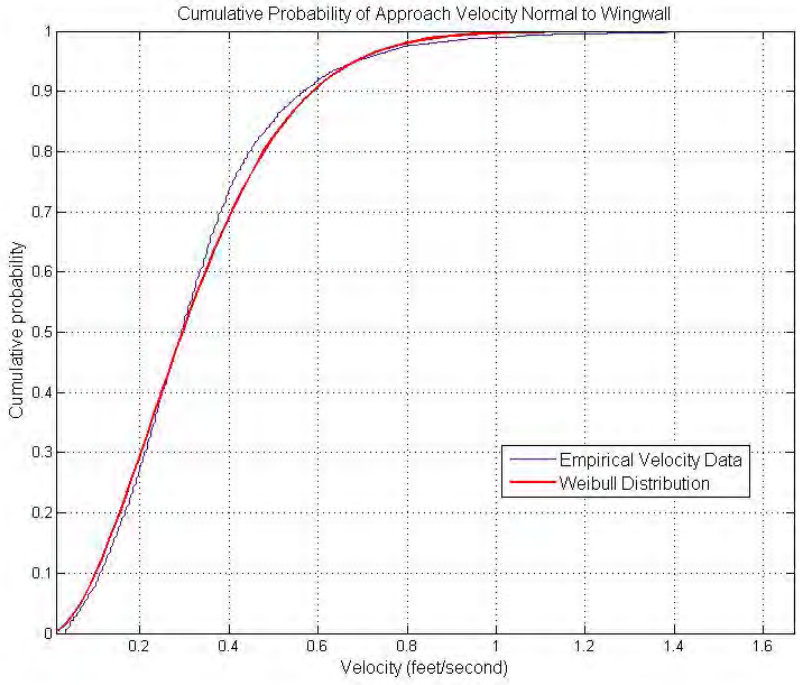

Figure 4.18: Cumulative probability of approach velocity normal to wingwall

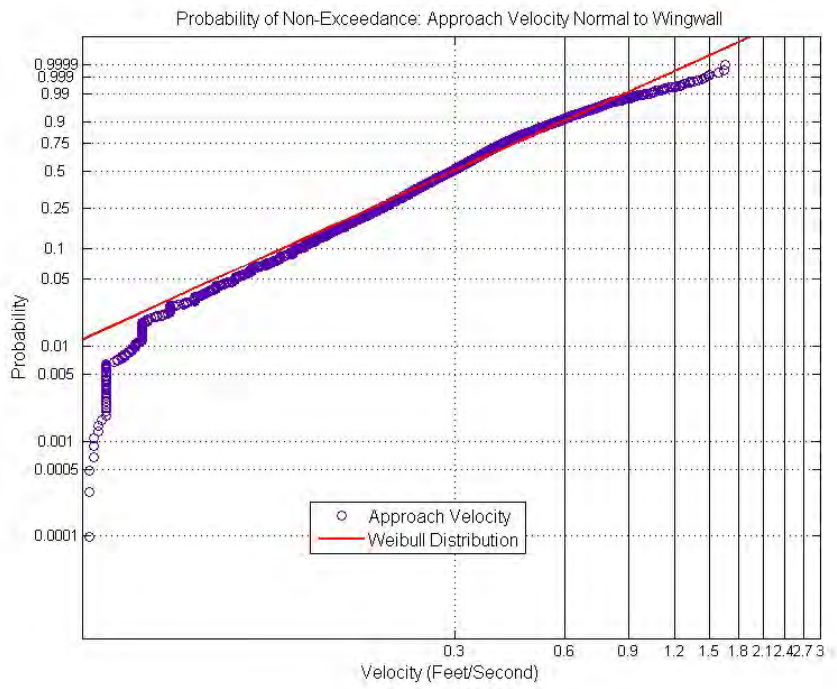

Figure 4.19: Probability of non-exceedance: Approach velocity normal to wingwall

Table 4.13: Approach Velocity Probability of Non-exceedance in any one event

Approach Velocity at Wingwalls			
One Event	Complete Set	North Wingwall	South Wingwall
Probability of Non-exceedance, %	feet/second	feet/second	feet/second
98	0.79728	0.78845	0.80652
99	0.87558	0.86443	0.88728
99.9	1.1051	1.0866	1.1248
99.99	1.3037	1.278	1.3309
99.999	1.4819	1.4494	1.5165
99.9995	1.5325	1.498	1.5693
99.9999	1.6455	1.6064	1.6872
99.99995	1.6924	1.6513	1.7362
99.99999	1.7978	1.7523	1.8464
99.999999	1.9411	1.8894	1.9965
99.9999999	2.0769	2.0192	2.1389

Energy Results

Energy results are presented as histograms, probability distribution fits, cumulative distribution fits, and probability curves.

Berthing energy is presented for the complete dataset of all berthing events, with each berthing event defined as a vessel that impacts either the north or south wingwall. Berthing energy for these results is the total energy absorbed by the wingwall. Table 4.14 presents a summary of wingwall energy absorption.

Table 4.14: Summary of Wingwall Energy Absorption

Energy Absorbed by Wingwalls, kip feet				
Wall	Mean	Standard Deviation	Max	# of Events
North	12.74	9.095	146.17	3448
South	11.946	8.287	80.476	3484
Combined	12.341	8.707	146.17	6932

Several distributions were fit to the berthing energy data, and the lognormal distribution was deemed a reasonable fit for the data (Figures 4.20 and 4.21). Matching the empirical data to the lognormal distribution allows the ability to estimate extreme energy values that the wingwall structure would need to endure. Using the percentile plots, the relationship between a given amount of kinetic energy absorbed and its likelihood of not being exceeded in any one berthing event is developed (Figure 4.22). The lognormal distribution is also used to assign an amount of strain energy to a corresponding probability to predict an energy value that has a given probability (such as 99.999% or 99.9999999%) of not being exceeded in any one berthing event (see Table 4.15).

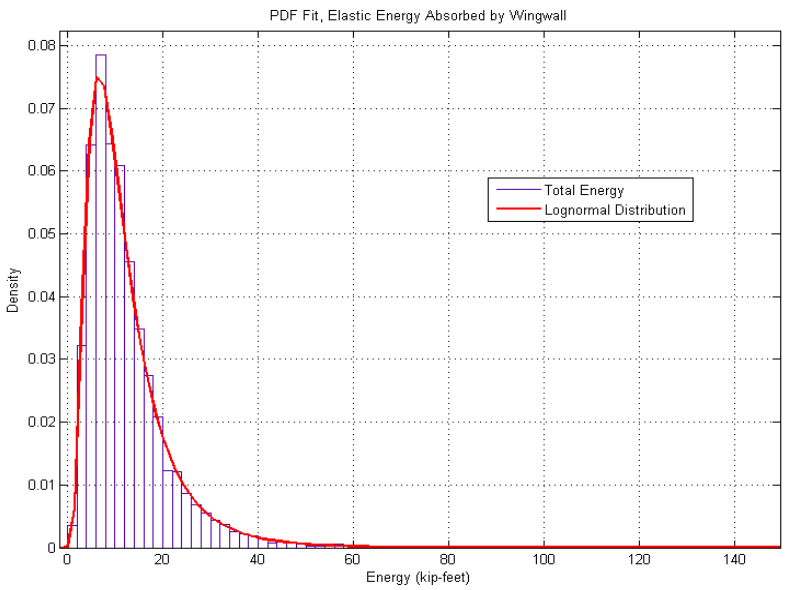

Figure 4.20: PDF fit: Lognormal distribution and energy absorbed by the wingwall

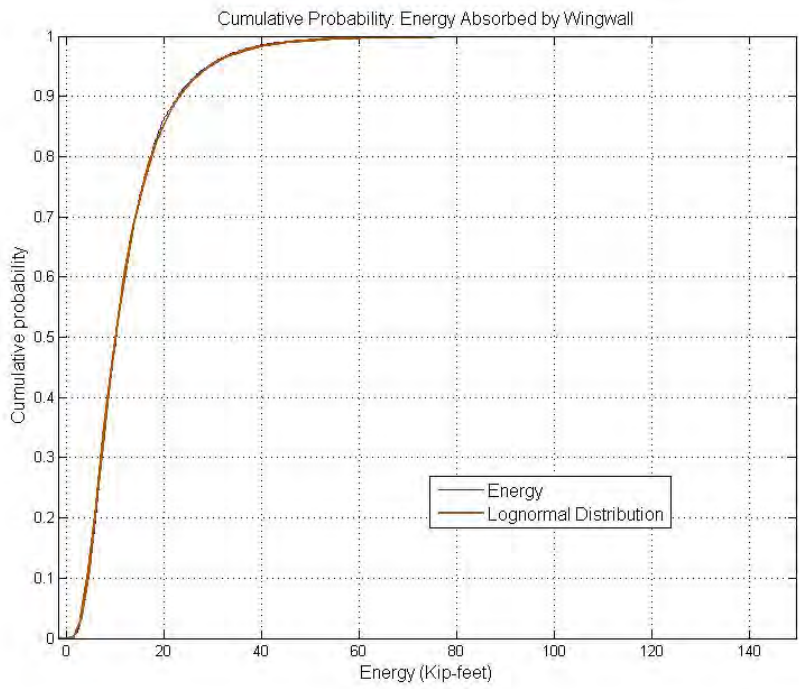

Figure 4.21: Cumulative probability of energy absorbed by the wingwall

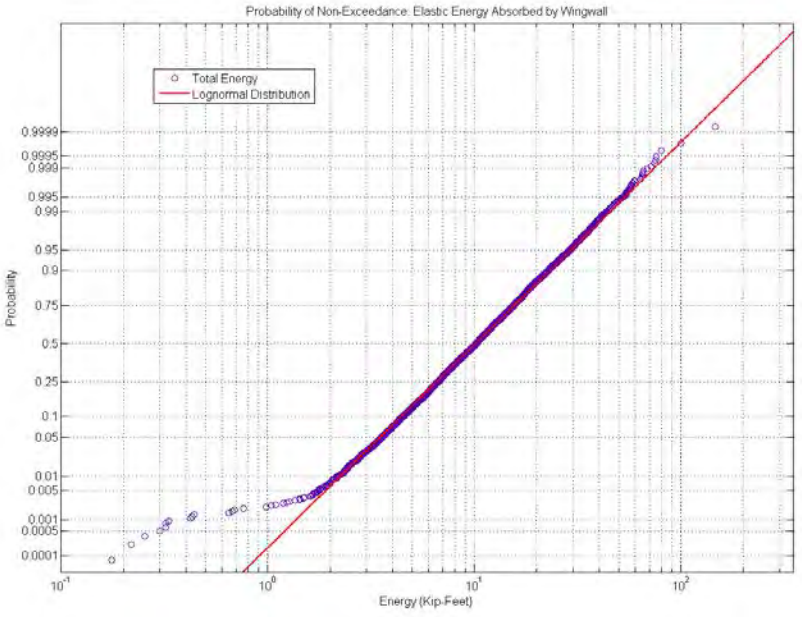

Figure 4.22: Probability of non-exceedance: Elastic energy absorbed by the wingwall

Table 4.15: Kinetic Energy Probability of Non-exceedance

Elastic Energy Absorbed by Wingwalls			
One Event	Complete Set	North Wingwall	South Wingwall
Probability of Non-exceedance, %	kip-ft	kip-ft	kip-ft
98	38.03	38.34	37.57
99	45.37	45.58	44.96
99.9	74.38	73.99	74.32
99.99	111.74	110.24	112.41
99.999	159.09	155.85	161.00
99.9995	175.57	171.65	177.98
99.9999	218.26	212.46	222.06
99.99995	238.68	231.92	243.20
99.99999	291.28	281.89	297.79
99.999999	380.45	366.22	390.71
99.9999999	488.36	467.75	503.65

Berthing Force

Although designers are most interested in energy imparted to the berthing structure, there are times when utilizing force calculations can be helpful. Designing for force considerations is significantly different from designing for energy, since force is proportional to the stiffness of a system. A stiffer system responds with more force than a soft system if the energy applied to both systems is the same.

Simple spring mechanics describe the force in a spring as displacement multiplied by stiffness of the spring (Equation 4.1). The fender units installed throughout the WSF systems are buckling column fenders, and the stiffness decreases nonlinearly as the fender is compressed. The manufacturer has provided tools that allow for the development of equations that describe the reaction and energy absorption characteristics of the fender units (Equation 4.2). When a vessel impacts a wingwall, the berthing force is resisted by a combination of the fenders, fender piles, and soil supporting the piling.

$$F_f = K_f(x_f)x_f \qquad \text{Equation 4.1}$$

$$F_f = -0.00005x^5 + 0.002x^4 - 0.0621x^3 - 0.1006x^2 + 19.257x \qquad \text{Equation 4.2}$$

where

F_f = Force of fender

x_f = Displacement of fender

$K_f(x_f)$ = Stiffness of fender at displacement x_f

Upon berthing, the ferry applies force to the wingwall through the vessel's sponson, a projection from the vessel's hull that is designed for impact forces. To estimate force applied to the wingwall, the measured reaction of the two marine fenders and the calculated stiffness of the impact face and piles are combined to describe the reaction of the system. The force applied to the wingwall is represented in Equation 4.3:

$$F_{total} = \sum_{i=1}^{6} F_{fender} + \sum_{j=1}^{3} \left[K_{impactpilej} \left(\frac{\Delta_{lmtjL} + \Delta_{lmtjU}}{2} \right) \right] \quad \text{Equation 4.3}$$

where

F_{total} = Total force on the wingwall

F_{fender} = Reaction force of marine fender

$K_{impact\ pile}$ = Stiffness of pile supporting the impact face

Δ_{lmtjL} = Displacement of fender jL (lower fender, at position j)

Δ_{lmtjU} = Displacement of fender jU (upper fender, at position j)

Results concerning the force applied by the vessel are displayed in Table 4.16 and Figures 4.23 through 4.28 in the form of histograms, distribution fits, and probability plots. Berthing force is presented for the complete dataset of all berthing events in this section. Berthing force represented here is the combination of the force applied by displacing the marine fender and by displacing the impact face.

Several distributions were fit to the berthing energy data. The lognormal distribution and the gamma distribution were found to be the closest matches to our dataset. The lognormal distribution in this instance is quite conservative at the extreme levels, and the gamma distribution may be more realistic at extreme values. Both are presented to illustrate their respective differences. Matching the empirical data to the lognormal and gamma distributions allows the ability to predict extreme berthing forces applied to the wingwall structure. Using the percentile plots illustrates the probability relationship between a given amount of kinetic energy that needed to be absorbed and its likelihood of not being exceeded in any one berthing event. The lognormal and gamma distributions are also used to assign an amount of berthing to a corresponding probability to predict an energy value that has a given probability (such as 99.999% or 99.9999999%) of not being exceeded in any one berthing event, see Table 4.17 for the gamma distribution results and Table 4.18 for the lognormal distribution results.

Table 4.16: Berthing Force Summary

Berthing Force at Wingwalls, kips				
Wall	Mean	Standard Deviation	Max	# of Events
North	74.272	41.7	413.139	3448
South	75.725	40.302	307.286	3484
Combined	75.002	41.01	413.139	6932

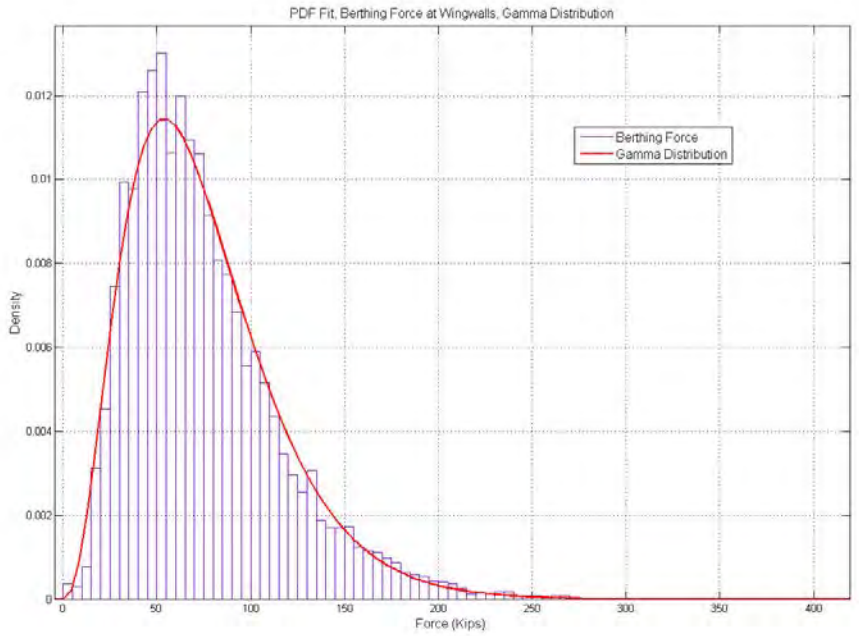

Figure 4.23: PDF fit: Berthing force at wingwall, gamma distribution

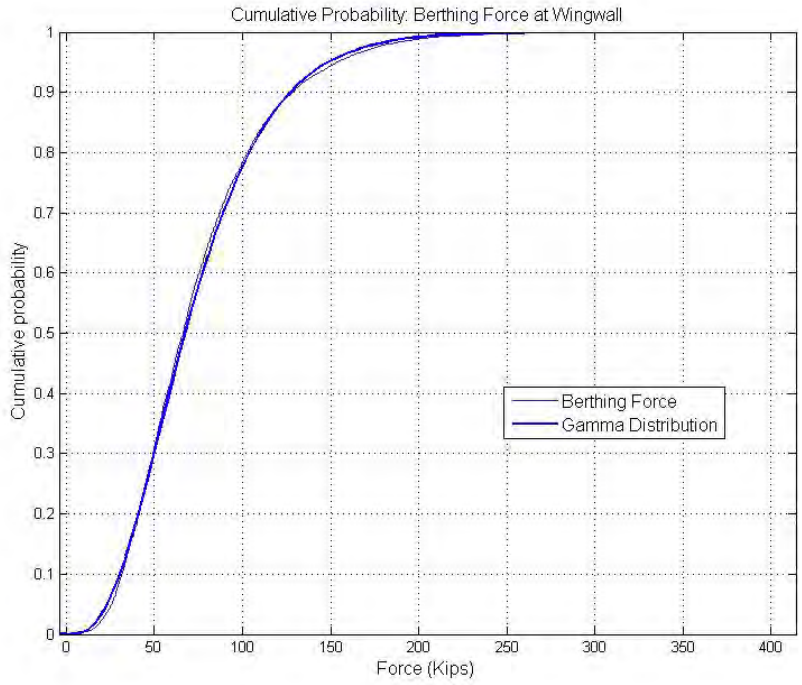

Figure 4.24: Cumulative probability: Berthing force, gamma distribution

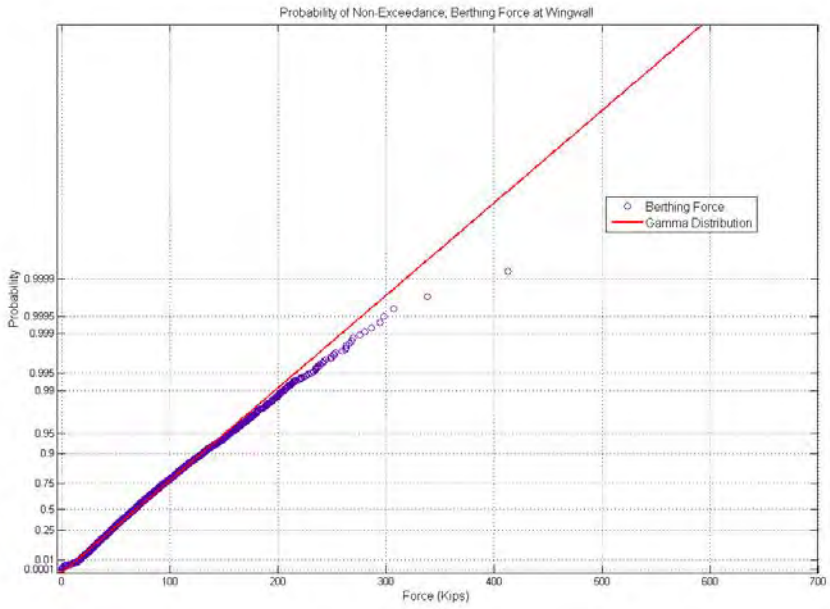

Figure 4.25: Probability of non-exceedance: Berthing force, gamma distribution

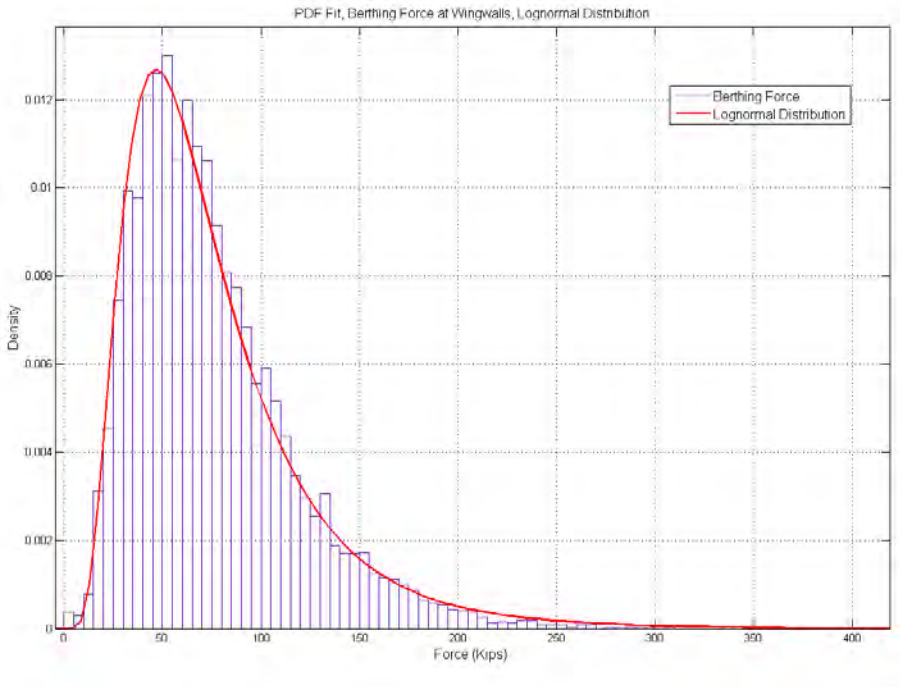

Figure 4.26: PDF fit: Lognormal distribution and berthing force (lognormal)

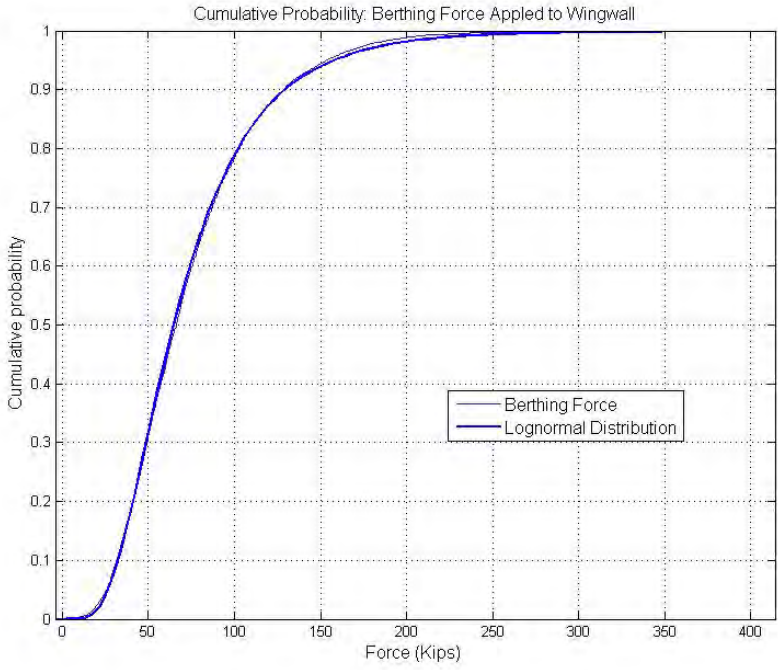

Figure 4.27: Cumulative probability of berthing force (lognormal)

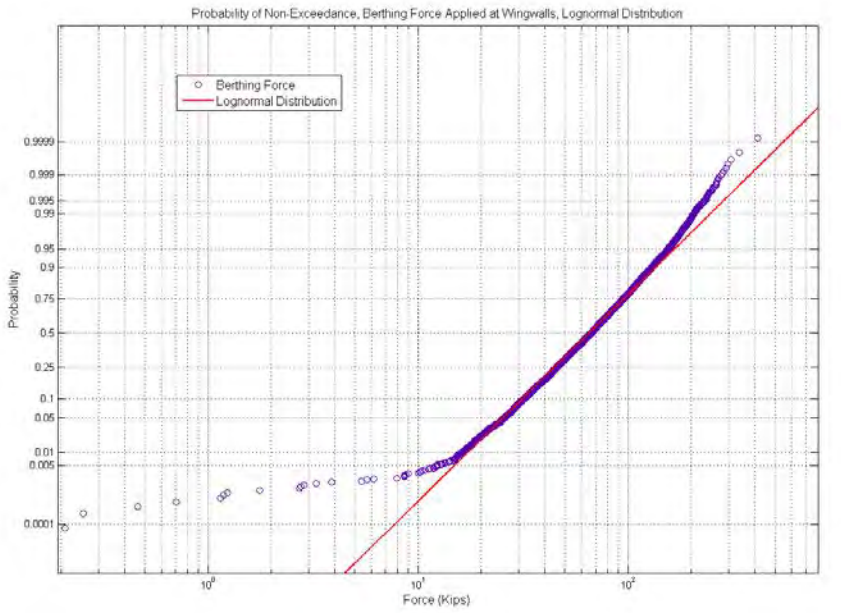

Figure 4.28: Probability of non-exceedance: Berthing force (lognormal)

Table 4.17: Berthing Force Probability of Non-exceedance, Gamma Distribution

Berthing Force Applied to Wingwalls (Gamma)			
One Event	Complete Set	North Wingwall	South Wingwall
Probability of Non-exceedance, %	kips	kips	kips
98	177.25	176.44	177.98
99	196.90	196.12	197.59
99.9	258.86	258.21	259.39
99.99	317.71	317.22	318.04
99.999	374.69	374.37	374.80
99.9995	391.58	391.31	391.62
99.9999	430.41	430.27	430.29
99.99995	446.99	446.91	446.80
99.99999	485.21	485.27	484.85
99.999999	539.31	539.58	538.71
99.9999999	592.87	593.34	592.01

Table 4.18: Berthing Force Probability of Non-exceedance, Lognormal Distribution

Berthing Force Applied to Wingwalls (Lognormal)			
One Event	Complete Set	North Wingwall	South Wingwall
Probability of Non-exceedance, %	kips	kips	kips
98	209.48	202.66	216.31
99	244.82	236.19	253.47
99.9	378.95	362.75	395.26
99.99	542.94	516.41	569.80
99.999	741.87	701.71	782.73
99.9995	809.38	764.37	855.22
99.9999	980.99	923.27	1039.96
99.99995	1061.68	997.81	1127.01
99.99999	1265.95	1186.06	1347.89
99.999999	1602.92	1495.45	1713.55
99.9999999	1998.64	1857.32	2144.63

Berthing Coefficient

Describing the amount of energy absorbed by a berthing structure because of vessel impact is complex and often ascertained by estimating a number of coefficients that relate to the interaction of ship and structure. A berthing vessel imparts an amount of energy to the berthing structure that ranges from 40% to over 100% of the vessel's incoming kinetic energy. This energy is due to a number of factors, discussed in Chapter 2, that describe aspects of the ship, the berthing facility, and berthing maneuvers. Individual evaluation of berthing coefficients is not realistic, as they are acting simultaneously when a ship comes to rest. Together, a product of these effects can be described as a berthing coefficient, C_b (Equation 4.5).

Using direct measurements of berthing events allows the amount of berthing energy to be quantified and provides an opportunity to combine the berthing factors (C_m, C_g, C_d, C_c, C_e) into a single berthing coefficient, C_b. Equation 2.1 then becomes simplified to the format presented in Equation 4.4. The berthing coefficient (Equation 4.5) can be explained as a semi-empirical ratio of energy absorbed by the berthing structure and the vessel's apparent kinetic energy (which is defined as the kinetic energy based upon the recorded approach velocity, with no berthing coefficients applied).

$$E_T = \frac{W}{2g} v^2 C_b \qquad \text{Equation 4.4}$$

$$C_b = C_m C_g C_d C_c C_s = \frac{E_T}{E_v}$$ Equation 4.5

where

E_T = Total energy absorbed by wingwall, including fender and impact face

$E_v = \frac{W}{2g} v^2 =$ Energy of vessel just prior to impact

where W = weight, g = gravity, v = approach velocity

C_b = Berthing coefficient, consisting of individual coefficients describe in Chapter 2

The total energy in the above equation, E_T, is the energy determined according to procedures described in Chapter 3B. The vessel energy term, E_v, is measured using the approach velocity recorded for each berthing event and the published displacement weight for each vessel. Typical values for C_b range from 0.4 to 0.7; however, direct end berthing can have a coefficient up to 1.0, and in certain situations with low under-keel clearance, the berthing coefficient can exceed 1.0 (Gaythwaite 2004).

Berthing coefficient results are displayed in Figures 4.29 through 4.31 in the form of histograms, distribution fits, and probability plots. There are two vessel classes landing with nearly equal frequency at the Bremerton slip with loaded displacements between 2947 and 3251 long tons. For simplicity, the berthing coefficient calculation used the weighted average of these two displacement figures, as the M/V Kaleetan has one more scheduled departure from the Bremerton slip than the M/V Kitsap does. A summary of berthing coefficient results is found in Table 4.19.

Several distributions were fit to the berthing coefficient data. The lognormal distribution, which is a commonly used distribution for lifetime modeling, was found to be the closest match to our dataset. Matching the empirical data to the lognormal distribution allows the ability to predict extreme values of the berthing coefficient. Using the percentile plots illustrates the probability relationship between a given berthing coefficient and its likelihood of not being met or exceeded in any one berthing event. The lognormal distribution is also used to assign a berthing coefficient value to a corresponding probability to predict a value that has a given probability (such as 99.999% or 99.9999999%) of not being exceeded in any one berthing event, see Table 4.20.

The results are not in line with what would be traditionally expected of a berthing coefficient, as the mean values exceed the limits of approximately 1.1 proposed for end-berthing vessels (Gaythwaite 2004). The mean value of the berthing coefficient represents the wingwall absorbing 3.3 times the energy predicted by a simple application of the Kinetic Energy Method without any berthing coefficients. A discussion of these atypical results is in Chapter 5B. To summarize the forthcoming discussion, a relatively large number of the recorded events had a somewhat low velocity at the time of impact. During the berthing maneuvers, vessel controls are used to slow down, steer, and power up the vessel to obtain a stable berthing position for offloading passengers and vehicles. It is believed that the source of additional energy, represented by the empirical berthing coefficient estimations is a result of vessel control usage during docking. Subsequent sections will elaborate on this notion.

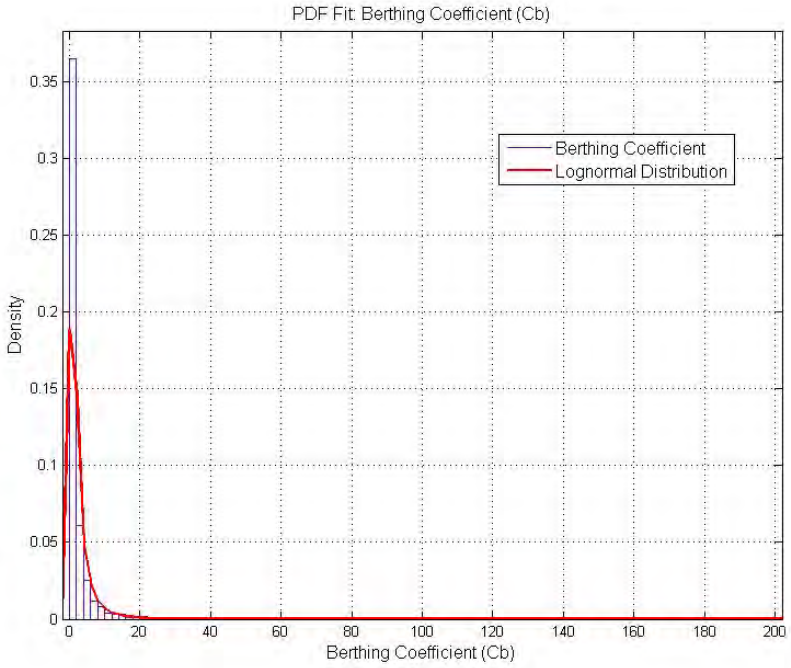

Figure 4.29: PDF fit: Berthing coefficient results and lognormal distribution

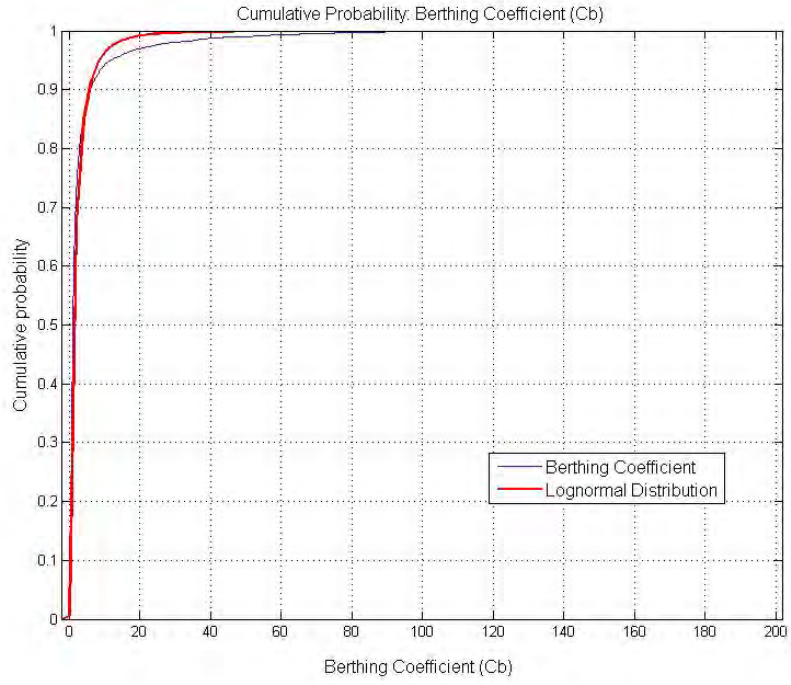

Figure 4.30: Cumulative probability of berthing coefficient results

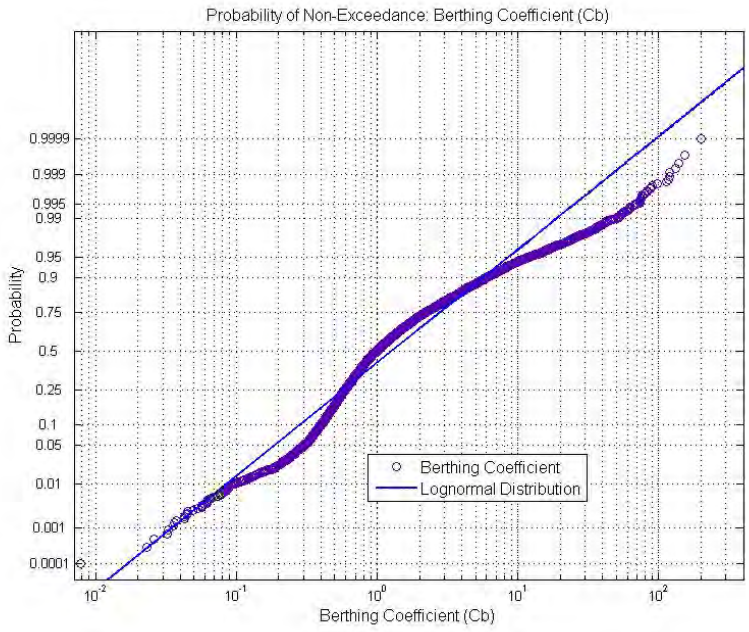

Figure 4.31: Probability of non-exceedance: Berthing coefficient

Table 4.19: Berthing Coefficient Results Summary

Berthing Coefficient (C_b)				
Wall	Mean	Standard Deviation	Max	# of Events
North	3.24	8.948	151.09	2648
South	3.309	9.78	198.68	2417
Combined	3.272	9.36	198.68	5065

Table 4.20: Berthing Coefficient Probability of Non-exceedance

Berthing Coefficient (C_b)			
One Event	Complete Set	North Wingwall	South Wingwall
Probability of Non-exceedance, %			
90	5.5445	5.4213	5.6704
95	8.4527	8.1541	8.768
98	13.587	12.909	14.32
99	18.643	17.535	19.86
99.9	45.246	41.366	49.656
99.99	93.872	83.839	105.58
99.999	176.89	154.81	203.23
99.9999	311.86	268.03	365.2
99.99999	523.28	442.34	623.53
99.999999	844.78	703.26	1023

Berthing Factor

Extending the concept of a berthing coefficient to a scalable tool, the berthing factor, f_b, is introduced. The berthing factor is the energy-per-unit mass of the vessel. The berthing factor extends the application of the empirically determined berthing energy information to a greater range of vessel displacements. Obtaining the berthing factor is accomplished by dividing the elastic energy of the deformed structure by the mass of the vessel (Equation 4.6). Once the berthing factor has been developed from a sample of berthing events, it can be multiplied by the vessel mass to estimate the amount of energy absorbed by the wingwall (Equation 4.7).

$$f_b = \frac{E_t g}{W} \qquad \text{Equation 4.6}$$

$$E_T = \frac{W}{g} f_b \qquad \text{Equation 4.7}$$

where

$f_b =$ Berthing factor

$E_T =$ Total energy absorbed by wingwall, fender, and impact face

$W =$ Vessel weight

$g =$ Acceleration of gravity

This methodology is further explained in Chapter 6. The primary assumption is that berthing factor values are directly proportional to vessel displacements.

Berthing factor results are displayed in the form of histograms, distribution fits, and probability curves. As before, the berthing factor calculation uses the weighted average of the two vessel displacements. The procedure used to estimate the berthing factor is detailed in Chapter 3B. A summary of berthing factor results is found in Table 4.21.

Several distributions were fit to the berthing factor data (Figures 4.32 through 4.34). The lognormal distribution, which is a commonly used distribution for lifetime modeling, was deemed a reasonable fit. Matching the empirical data to the lognormal is a basis for estimating extreme values of the berthing factor. Using the percentile plots illustrates the probability relationship between a given berthing factor and its likelihood of not being met or exceeded in any one berthing event. The lognormal distribution is also used to assign a berthing factor to a corresponding probability to predict a value that has a given probability (such as 99.999% or 99.9999999%) of not being exceeded in any one berthing event (see Table 4.22).

Table 4.21: Berthing Factor Results Summary

Berthing Factor, f_b				
Wall	Mean	Standard Deviation	Max	# of Events
North	0.586	0.0429	0.675	2648
South	0.548	0.0377	0.372	2417
Combined	0.568	0.0405	0.675	5065

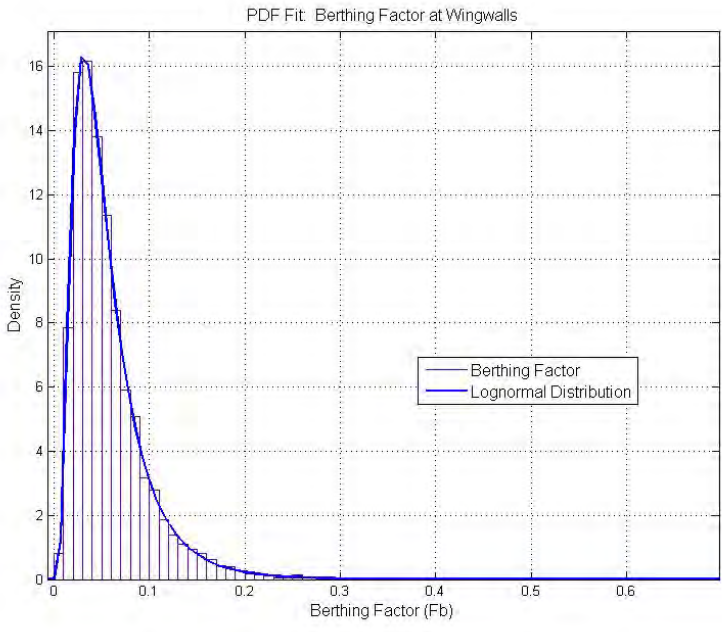

Figure 4.32: PDF fit: Berthing factor and lognormal distribution

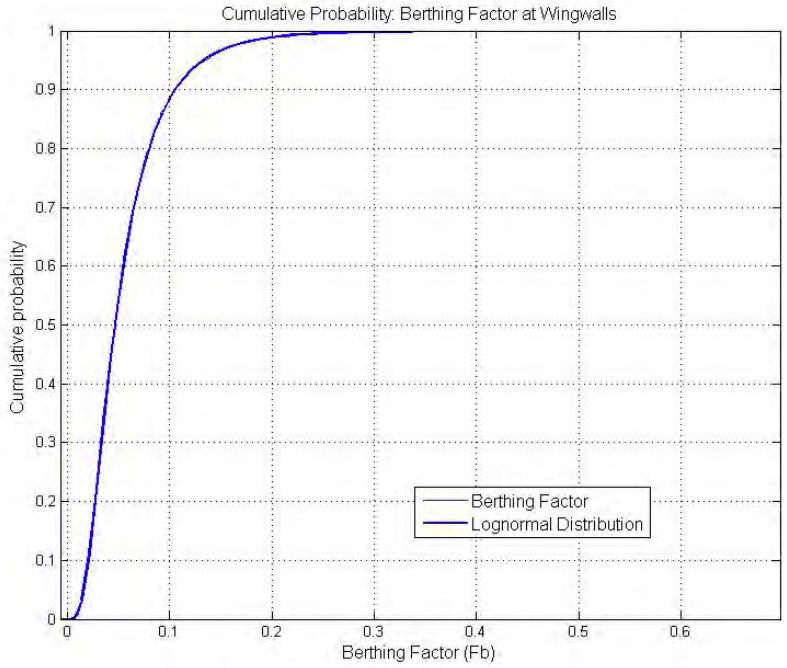

Figure 4.33: Cumulative probability: Berthing factor and lognormal distribution

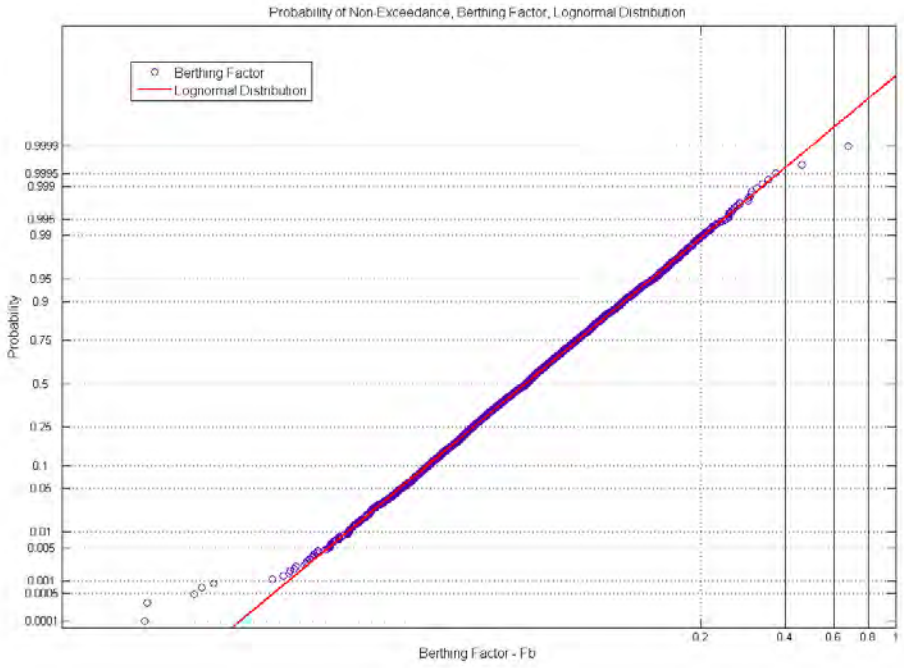

Figure 4.34: Probability of non-exceedance: Berthing factorTable 4.22: Berthing Factor Probability of Non-exceedance

Berthing Factor, f_b

One Event	Complete Set	North Wingwall	South Wingwall
Probability of Non-exceedance, %	ft^2/sec^2	ft^2/sec^2	ft^2/sec^2
95	0.1319	0.1352	0.1282
98	0.1711	0.1750	0.1664
99	0.2035	0.2079	0.1981
99.9	0.3307	0.3370	0.3225
99.99	0.4933	0.5014	0.4819
99.999	0.6980	0.7079	0.6827
99.9999	0.9522	0.9640	0.9326
99.99995	1.0397	1.0520	1.0186
99.99999	1.2643	1.2779	1.2397
99.999999	1.6436	1.6586	1.6134
99.9999999	2.1006	2.1167	2.0640

Reliability Design Charts

Reliability design charts present the relationship between a given number of berthing events and a parameter (such as approach velocity or energy) at varying levels of reliability. Figures 4.35 through 4.39 are design charts for five different design parameters presented with reliability levels of 90%, 95%, 98%, 99%, 99.9%, and 99.99%. The horizontal axis of the design charts corresponds to a design life of a berthing structure. The design life of a Washington State Ferries terminal ranges from 200,000 to approximately 730,000 berths at current scheduling levels. Using the plots is accomplished by selecting a design number of berthing events and a given reliability level. The projection onto the vertical axis is defined as a value of the parameter of interest that will not be met or exceeded at the given reliability level and the given number of berthing events.

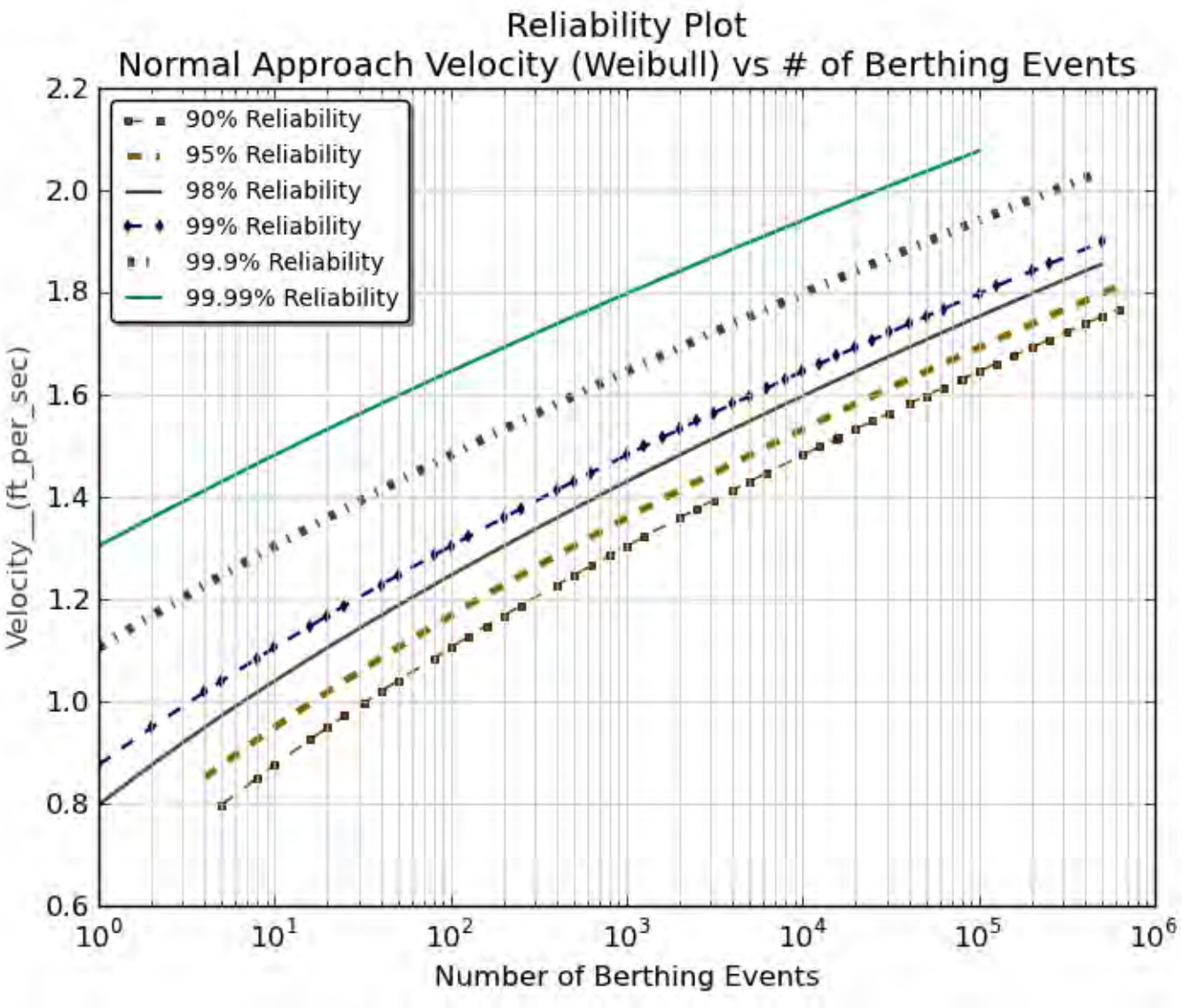

Figure 4.35: Berthing event reliability plot, approach velocity (Weibull)

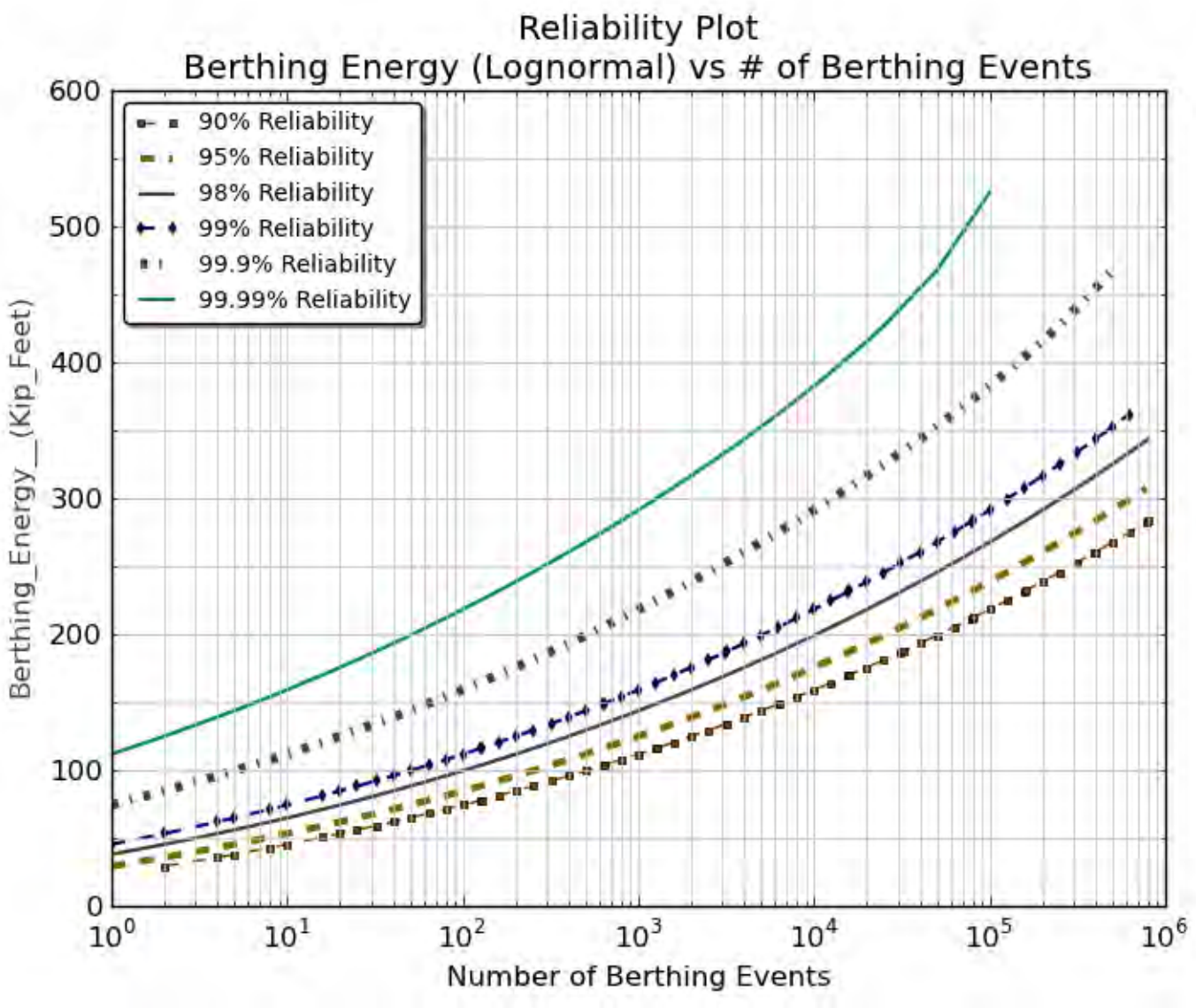

Figure 4.36: Berthing event reliability plot, kinetic energy (lognormal)

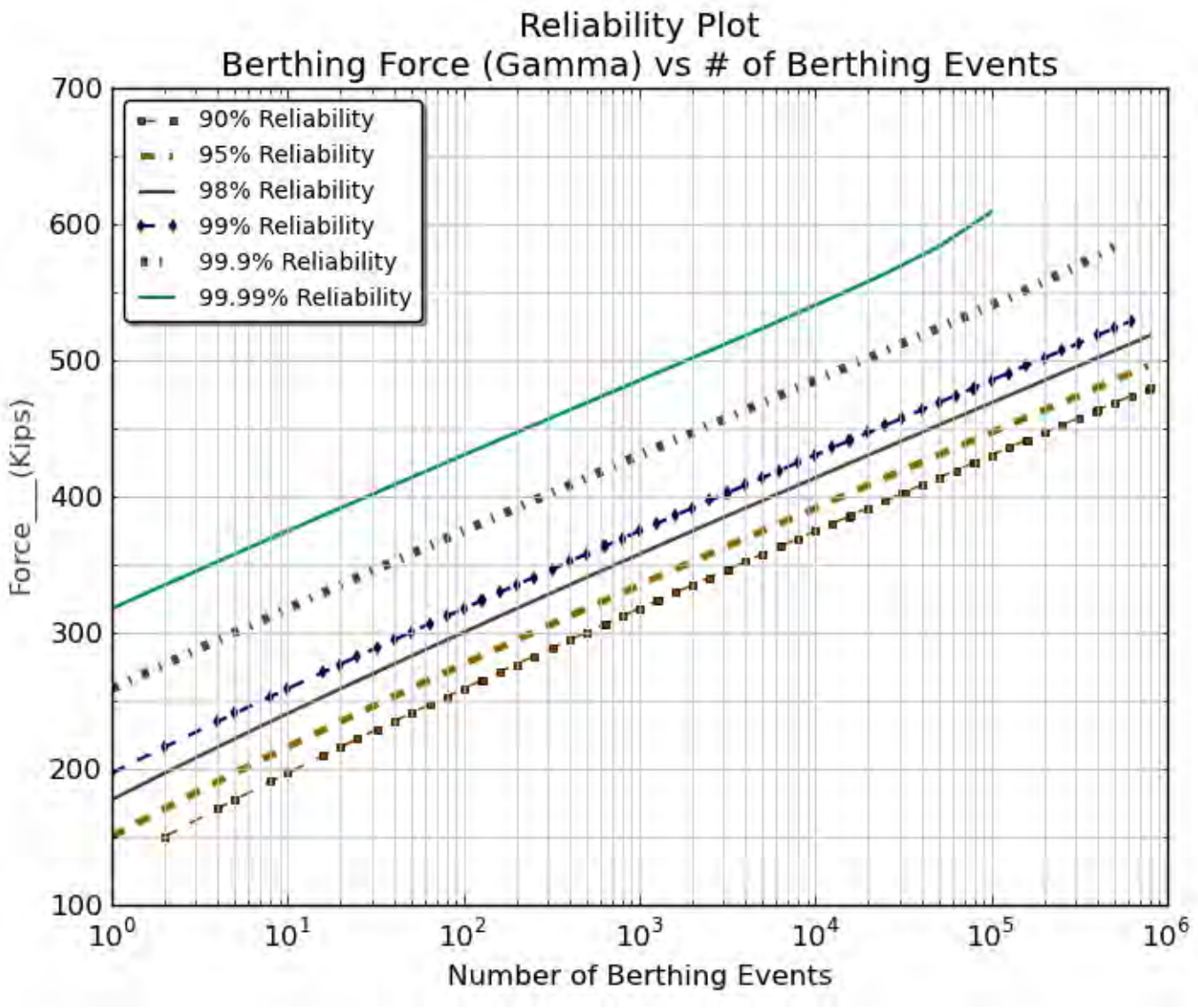

Figure 4.37: Berthing event reliability plot, berthing force (gamma)

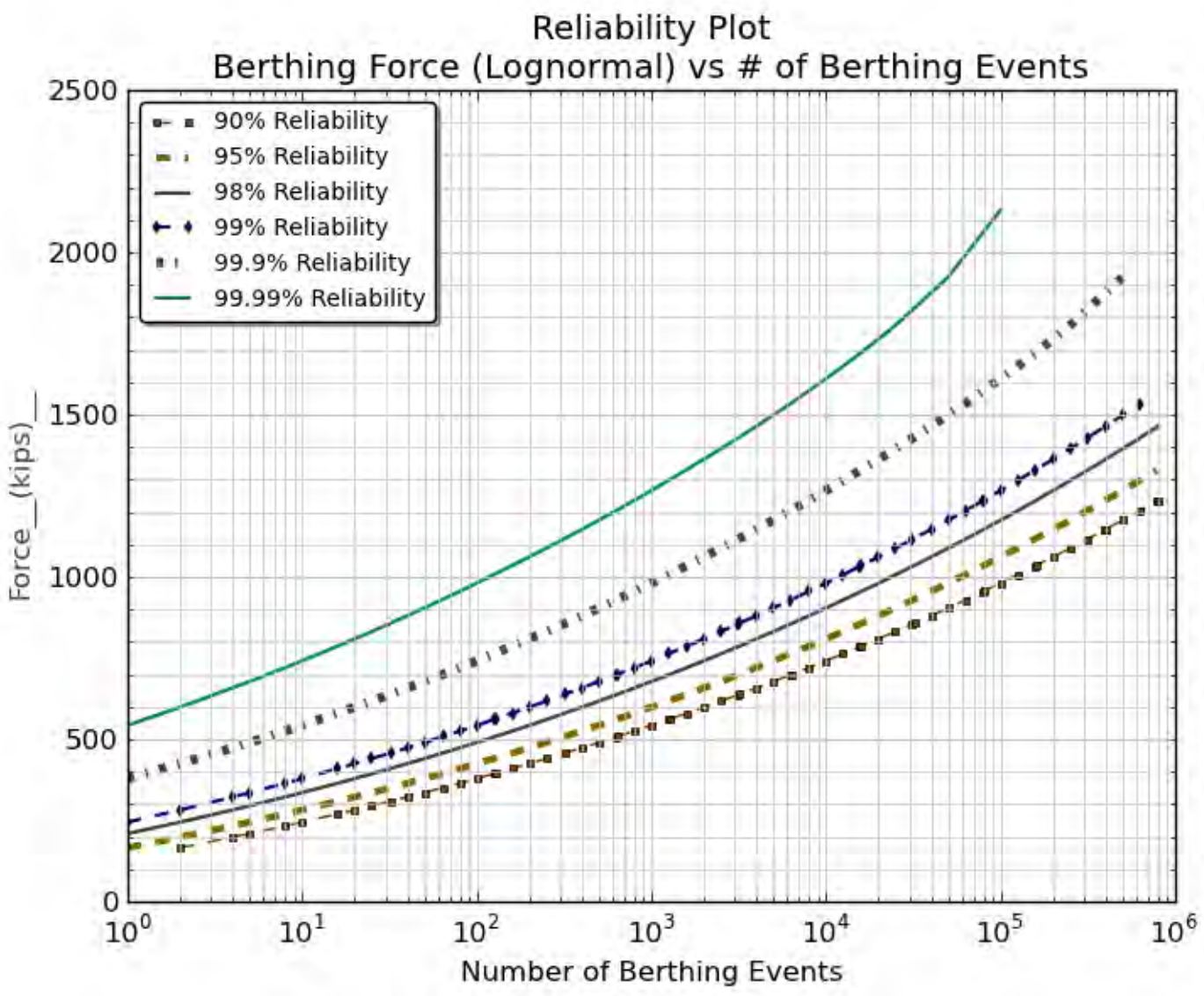

Figure 4.38: Berthing event reliability plot, berthing force (lognormal)

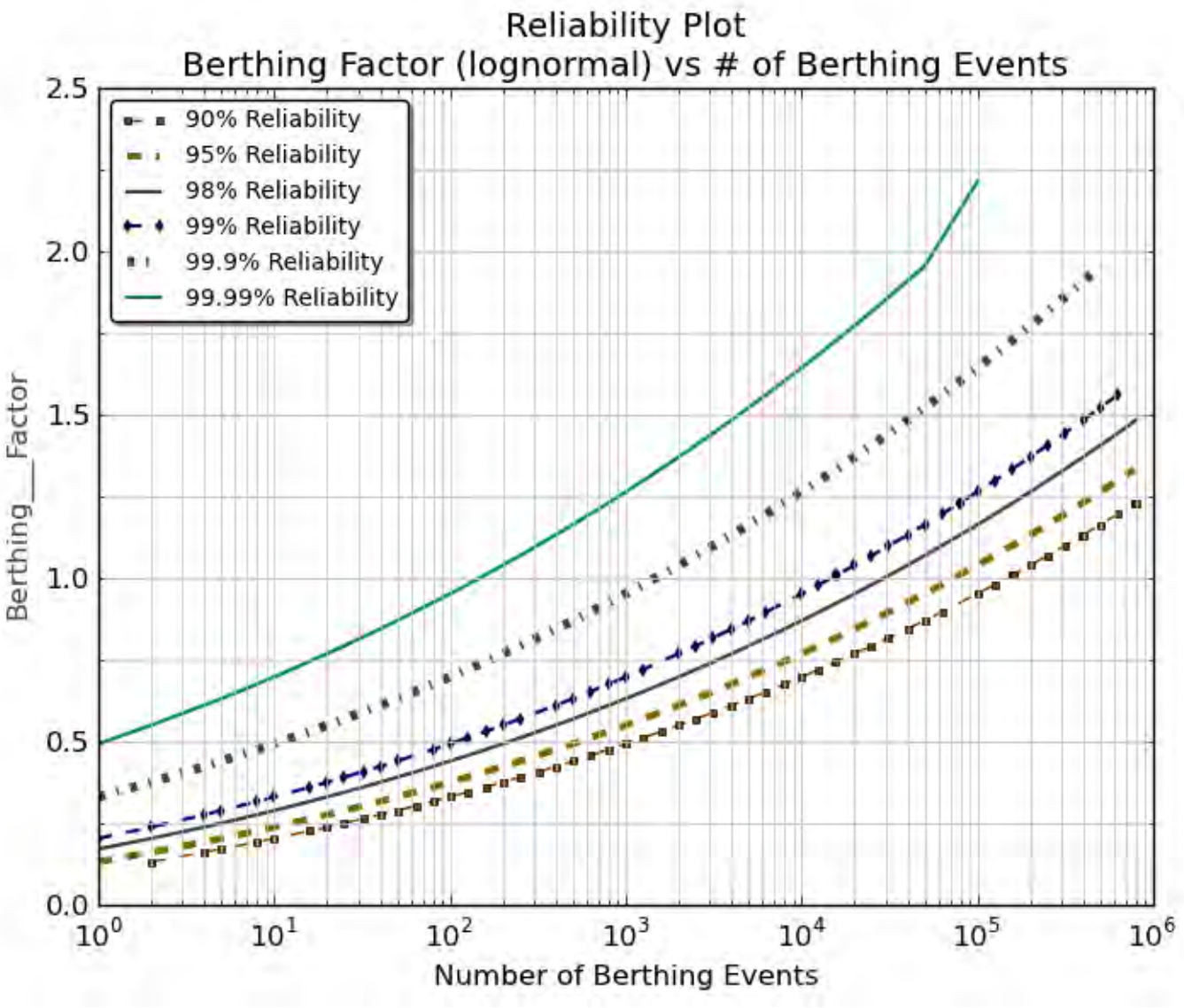

Figure 4.39: Berthing event reliability plot, berthing factor (lognormal)

Pagination error: After page 148, page numbering jumps to 191, but NO CONTENT IS MISSING.

Point of Impact Results

The instrumentation of all wingwall fenders allows a fairly precise determination of where the vessel is contacting the impact face. Using the deflection characteristics of each fender in a given event allows estimation of the vessel contact point with the impact face for each event using Equations 4.8 and 4.9. Fender deflection is nonlinear; therefore, the force absorbed by each fender is used in order to determine the point of contact.

$$\bar{x} = \frac{\sum_1^6 F_i * x_i}{\sum_1^6 F_i} \qquad \text{Equation 4.8}$$

$$\bar{y} = \frac{\sum_1^6 F_i * y_i}{\sum_1^6 F_i} \qquad \text{Equation 4.9}$$

where

$\bar{x}$ = Horizontal location of vessel impact with respect to impact face

$\bar{y}$ = Vertical location (elevation) of vessel impact with respect to impact face

F_i = Force absorbed by fender *i*

x_i = Horizontal distance to fender *i*

y_i = Vertical distance to fender *i*

Point-of-impact results are displayed in Figure 4.40 in the form of scatter plots and histograms presented at scale overlaid on the wingwalls. The results are segregated into north and south wingwalls. A large floating dolphin is located adjacent to the north wingwall (see Figure 3.31, Chapter 3B). The graphic of Figure 4.40 is a representation of the wingwalls as viewed from the water, looking toward the shore. A point of impact summary is given in Table 4.23.

Table 4.23: Point of Impact Summary

Mean Point of Impact Summary		
	North	**South**
Lateral distance from "throat" of wingwall (feet)	5.84	8.61
Elevation with respect to bottom edge of wingwall (feet)	16.18	14.54

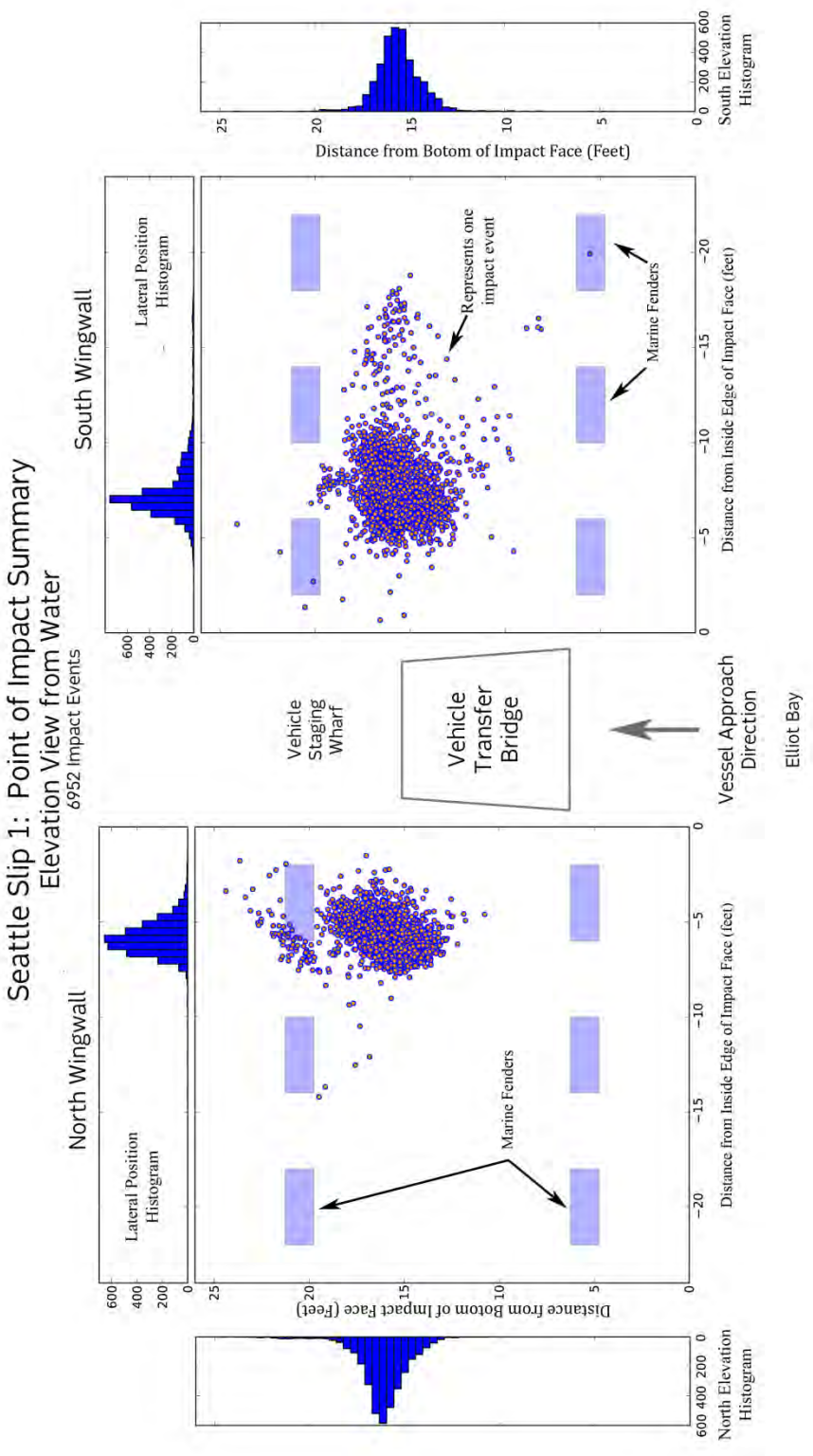

Figure 4.40: Point of impact summary graphic

Chapter 5A – Discussion and Recommendations: Auke Bay

Measurements from 486 impact events were collected over approximately 11½ months. No exceptional or extreme events were observed, and all empirical load values are assumed typical for berths at Auke Bay. The results in Chapter 4A are assumed to reflect the load environment form a "typical" year of service at Auke Bay.

Probability and Design Charts

In general, results for each parameter are formatted for use with reliability engineering principles. The probability plots represent the probability that a parameter value will not occur or be exceeded in any one berthing event, denoted by (1-*p*). This value is often referred to as the *percentile,* or the value below which a certain percentage of measurements occurred. For example, a 98th percentile velocity represents the velocity at which 98% of the measured approach velocities are lower, and 2% meet or exceed it.

The purpose of the distribution fits and the probability plots is to estimate the probabilities at which extreme (i.e., ultimate) design values occur, and how far they deviate from service loads. While an efficiently designed structure cannot be designed to resist every possible load, quantifying the occurrence probabilities of extreme loads allows the designer to rationally select design loads based on risk level. Ultimately, risk level should be determined over an interval such as design life or total number of berths. For example, a berthing structure that is expected to last for 30,000 total berths should not be designed (to limit state) for a load that is expected to occur every 3000 berths.

The design charts in Chapter 4A can be used to determine design loads for common reliabilities over a design number of berths. Results are based on the probability plots in Chapter 4A.

Note that these values represent *ultimate* values and are appropriate for a limit-state design methodology, such as load resistance factor design (LRFD).

Determining Risk Level

If the probability of occurrence for a parameter value is known, the probability of that parameter being exceeded over a number of events or the design life can be determined. From basic probability and statistics, the probability that a certain parameter value will be exceeded at least once out of *n* trials is determined from Equation 5.1.

$$p_n = 1 - (1 - p)^n \qquad \text{Equation 5.1}$$

where

p_n = probability that a parameter of specified magnitude with be exceeded in *n* berthing events

p = probability of a parameter being exceeded in any one berthing event

Equation 5.1 can be rearranged as follows:

$$(1 - p) = (1 - p_n)^{(1/n)} \qquad \text{Equation 5.2}$$

Notice that in Equations 5.1 and 5.2, the term (1-*p*) represents the percentile per berthing event, or the probability that a parameter of specified magnitude will *not* be exceeded per berthing event. This term is provided in the "probability of non-exceedance" charts (probability plots). The term p_n is the risk level, and $(1 - p_n)$ represents the target reliability for *n* events.

The parameter values in the tables in Chapter 4A are provided for a wide range of percentiles (1-*p*) that reflect meaningful risk levels. Table 5.1 gives a comparison of risk level versus number of berthing events for various percentiles (for any one berthing event). For reference, a 99.9 percentile (in any one berthing event) load value has a 29.54% chance of occurring or being exceeded in 350 events (1 year) or a 97% chance of being exceeded in 3500 events (10 years).

Table 5.1: Risk levels

Risk Level vs. Number of Berthing Events					
Percentile per Berth (1-p) (%)		99.9	99.99	99.999	99.9999
Approximate Time (*Auke Bay)	# of Berths	Risk Level (probability of design load being exceeded) Risk Level=(1-Reliability)			
1 day	1	0.10%	0.01%	0.00%	0.00%
1 month	30	2.96%	0.30%	0.03%	0.00%
1 year	350	29.54%	3.44%	0.35%	0.03%
5 years	1750	82.64%	16.06%	1.73%	0.17%
10 years	3500	96.99%	29.53%	3.44%	0.35%
20 years	7000	99.91%	50.34%	6.76%	0.70%
30 years	10500	100.00%	65.01%	9.97%	1.04%
40 years	14000	100.00%	75.34%	13.06%	1.39%
50 years	17500	100.00%	82.62%	16.05%	1.73%

* The Auke Bay east berth lands approximately 350 vessels per year

Using Equation 5.1, the design engineer can specify design reliability, or design value, for which the probability of exceedance over *n* number of berths is acceptably low. Selection of a suitable reliability takes into consideration a number of factors ranging from cost/strength tradeoffs to consequence of failure. Typical reliabilities range from 90% to 99%; however, it is beyond the scope of this report to make recommendations on target reliabilities for berthing structures of this nature.

Table 4.10 (Chapter 4A) contains design values of each parameter studied at Auke Bay for common target reliabilities of various numbers of berths (*n*). Depending on the load parameter under consideration, a lower or higher target reliability may be desired. It is left to the designer's discretion to decide what level of reliability $(1-p)$ is acceptable.

The design charts in Chapter 4A are provided for common reliabilities and number of berths from which design values can be chosen. Design values for other reliabilities between 90% and 98% can be interpolated from the charts. Alternatively, design values can be determined for any reliability using the following method:

- Determine the design number of berths (n) and desired risk (p_n) and put into Equation 5.2 to calculate the required probability of non- exceedance, or percentile (1-p) per berthing event.
- Look up the percentile (1-p) value for the desired parameters: energy, force, berthing factor, and velocity from the "probability of non-exceedance" plots

Using this method, a design value can be determined for any combination of design number of berthing events and target reliability $(1-p_n)$.

Load Factors

Allowable stress design (ASD) methods apply factors of safety to the working stress limits of a structure or component subject to nominal or service loads. Factors of safety are applied to the structures to allow exceedance of working stresses due to exceptional events. Factors of safety applied in this manner result in structures with unknown reliability. Existing Alaska Marine Highway (AMH) structures have not performed poorly using this design approach; however, it is the purpose of this study to provide a probability-based option, where factors of safety in load demand are rationally quantified based on risk level.

The basic LRFD design philosophy applies factors to both the load and material to compensate for uncertainties in loads and material strengths. Equation 5.3 is the basic LRFD design equation, in which the sum of all factored loads must be less than or equal to the factored strength of the member or component under consideration.

$$\varphi R_n \geq \sum_i^n Q_i \gamma_i \qquad \text{Equation 5.3}$$

where

$\varphi = Resistance\ factor\ (typically\ ranges\ from\ 0.75\ to\ 0.9)$

$R_n = nominal\ resistance\ (strength)\ of\ the\ component\ being\ considered$

$Q_i = nominal\ load\ effect\ or\ parameter\ such\ as\ a\ force\ or\ energy$

$\gamma_i = Load\ factor$

Load factors are chosen to reflect the predictability of a given load, and they amplify the load effect Q_i to compensate for uncertainties and variability in load. The term φR_n is equal to the design strength, while the sum of $Q_i \gamma_i$ is equal to the design load (the "factored load").

While a more complete variety of loads on ferry structures is needed before the LRFD method can be fully employed, the load factor approach can be used to develop a relationship between nominal berthing loads and maximum extreme loads.

The maximum extreme load divided by the nominal load equates to the load factor (γ_i). The load factor is a similar concept to the factor of safety employed by the ASD method. The load

factor rationally amplifies nominal or service loads to compensate for variability in loads due to exceptional events. Variability in material strength (φ) is contained in material standards of practice, for example, ACI 318 for reinforced concrete structures. Table 4.11 (Chapter 4A) provides load factors for parameters considered in this study. It is recommended that the results of this study be calibrated with the reliability of material code standards. The result will be an accurate LRFD presentation of load demands on ferry landings in the context of this study.

Recommendations

A range of recommended design parameters is provided in Tables 4.10 and 4.11. The preceding discussion should provide the reader with the background to determine design values for conditions not covered here. The design charts in Chapter 4A may also be used for this purpose.

Berthing Coefficient

Berthing coefficients were calculated as the ratio of the elastic potential energy of the deformed structure to the apparent kinetic energy of the vessel. In both the Auke Bay study and the Washington State study, it was found that the berthing coefficient for low vessel-impact velocities can be erroneously large. This is explained by the vessel controls (power and steerage) being actively involved in the berthing maneuver, which adds energy to the vessel motion. In contrast, the Kinetic Energy Method assumes that the vessel impacts the berthing structure at a dead drift. *Use of berthing factors derived in this study is not recommended*.

Velocity

Tables 4.10 and 4.11 provide a range of nominal and ultimate values for vessel impact velocity. The tables provide a nominal design velocity of 0.68 ft/s and a range of ultimate values of 1.53 ft/s (for a design life of 3500 berthing events) and 2.2 ft/s (for a design life of 10,500 berthing events). For determination of parameters outside these values, the reader should refer to the design charts.

The velocity data separated by vessel is intended to allow differentiation between approach speeds for each individual vessel. However, no definitive relationship between vessel size and velocity can be deduced from the results. More data are needed, particularly for the two largest vessels—the Kennicott and the Columbia—before any definitive conclusions can be drawn.

The velocity data in Chapter 4A can be used to implement the Kinetic Energy Method; however, the method itself must be used with discretion. The Kinetic Energy Method considers only a vessel's energy before impact with the fender, while ignoring any effects that may occur during and after impact. For this reason, in cases where energy is supplied during and after initial impact, the maximum energy transferred to the dolphin is not a simple function of the vessel's approach velocity. A common occurrence is a scenario where a vessel approaches with a certain velocity and impacts a fender, displacing it X number of inches; the fender is then displaced an additional Y inches during and after the initial impact as a result of either bow thrusters, rudder action, or reaction from the springline. The final fender displacement in this instance ($X + Y$) is not caused by the initial kinetic energy of the vessel alone, but by a combination of actions and factors.

This type of scenario can potentially cause the maximum energy from a berthing event to exceed the maximum kinetic energy of the vessel, implying a berthing coefficient value larger than 1.0.

Figure 5.1 is an example of such a scenario. Notice in Figure 5.1 the five extreme fender displacement values (valleys). Commonly, a vessel impacts a fender with a certain velocity and then rebounds, allowing the fender to fully decompress to a displacement of zero. However, oftentimes the vessel rebounds only partially off the fender before recompressing the fender an even greater amount than resulted from the initial impact. At the third valley at $t = 180$ seconds (Figure 5.1), the fender is initially compressed 8.5 inches. The vessel then bounces off the fender, allowing the fender to decompress approximately 6 inches. Before the fender is fully decompressed, it becomes compressed further to ~12.5 inches. Further compression occurs again at $t = 245$ seconds, where the maximum fender displacement for the event was recorded at 13.05 inches. The maximum displacement in this instance was due to incremental sources of energy (and force from reaction of the springline) that were supplied during and after initial impact, in addition to the vessel's initial kinetic energy.

This occurrence demonstrates the difficulty in rationally quantifying design energies for fender and berthing structures. Since the maximum energy from a berthing event often exceeds the maximum kinetic energy of the vessel, designers should exercise caution when designing berthing structures based on approach velocity. Statistical samples of berthing energy are often preferred over velocity measurements because they take all uncertainties associated with a berthing vessel into consideration, including effects such as human influence and environmental conditions at the time of berth.

Energy

Overall, the berthing energy recommendations in this chapter are in close agreement with published values for tanker vessels, as shown in Chapter 2. (Dent and Saurin 1969) recommend a berthing energy of 16.8 ft-kips per 1000 long tons displacement at yield state in the fender and structure. This measurement equates to an ultimate design energy range of 93.5 to 128.5 ft-kips for the vessel displacements considered in this study. These values could be taken as consistent with the results of this study, depending on the desired level of probability of non-exceedance and number of events.

In general, the berthing structures have performed adequately, but it is interesting to note that there is evidence that the capacity of the fenders on Dolphins E1, E2, and E3 (37.5–38 ft-kips) has been exceeded in nearly thirty years of operation. Exceedance of allowable fender displacement is visibly evident in the form of gouges in the seaward toe-kick plate, located on the south side of the platforms, as well as bent pile caps on each dolphin (Figure 5.2). This minor damage occurred when an extreme event caused the fenders to displace beyond their free range of movement.

Note that the fenders themselves are fully capable of absorbing extreme events in excess of 100 ft-kips at their maximum allowable deflection of 24 inches. However, the fenders are physically limited to a maximum allowable deflection of 14 inches and are not detailed to operate within their full range. Due to the limitation, berthing energies in excess of the limited range (37.5–38 ft-kips) are absorbed by the tripod backing structure.

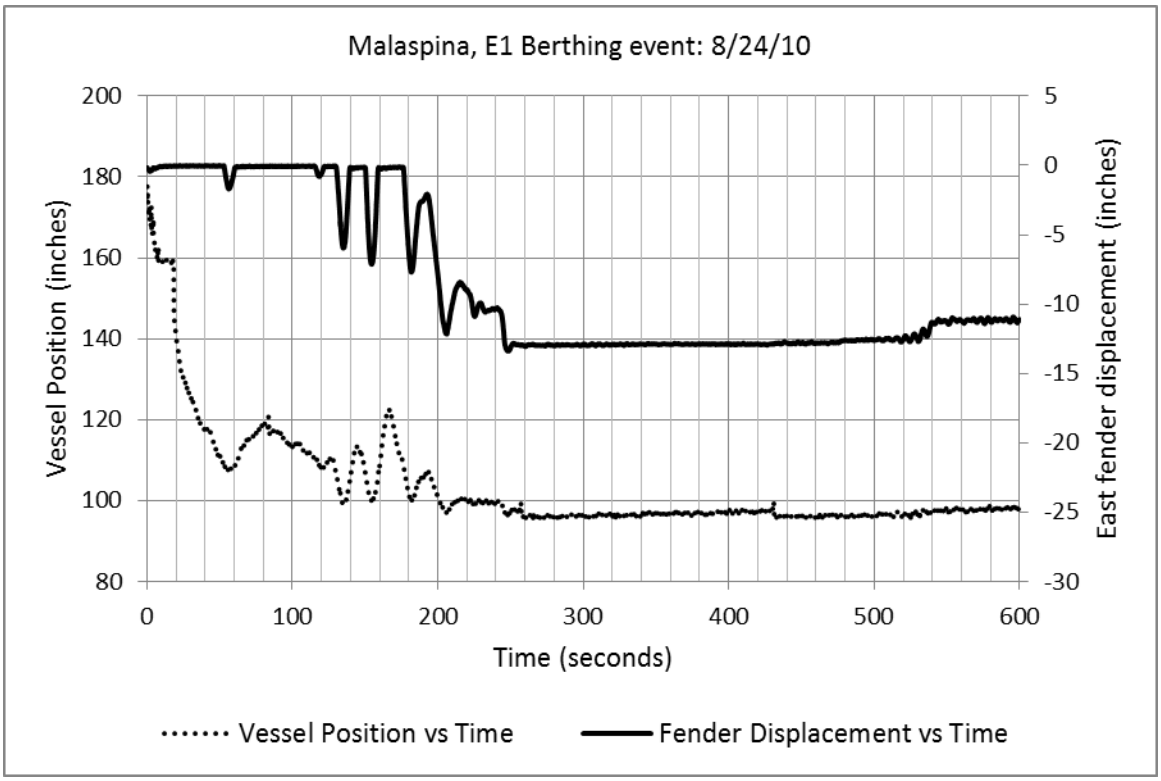

Figure 5.1: Malaspina position versus time and fender displacement

Figure 5.2: Evidence of extreme events

Energy data, separated by vessel, provide the information needed to compare the berthing energy of each of the four vessels. The comparison shows the relationship between vessel displacement and energy. Three of the four vessels in this study vary in size. The vessels berth in different ways depending on conditions at the time of arrival and at different frequencies, making it difficult to develop a relationship between displacements and berthing energy. In addition, berthing energy is often affected by the source of energy supplied by bow thrusters and mooring lines/winches during and after initial impact. In such a case, the maximum berthing energy is no longer a simple function of vessel displacement. The maximum berthing energy recorded—47

kip-ft—was the result of such an event. In general, results indicate that berthing energy is more a function of a number of variables that are difficult to characterize individually.

Out of the small sample of berthing events captured from the Columbia, results indicate consistently higher berthing energies than the other three vessels, as expected. More berthing samples are needed from the two largest vessels, particularly the Columbia, before any definitive conclusions can be drawn. The maximum berthing energy recorded was from the Malaspina.

The energy data separated by vessel and dolphin show the difference in berthing energy and frequency experienced by each dolphin. The variation in impact frequency per dolphin has an effect on the energy that each dolphin is expected to experience. Extreme impact events have a certain probability of occurring, and are directly related to the number of impacts felt by each dolphin. From the perspective of probability theory, a dolphin impacted 100 times per year is likely to experience lower maximum impact energy than a dolphin impacted 1000 times per year.

Results indicate that Dolphin E3, on average is subject to larger loads than Dolphins E1 and E2, with Dolphin E2 generally experiencing the smallest loads. However, Dolphin E3 is impacted only half as frequently as Dolphins E1 and E2. For most of the vessels, not enough energy data per dolphin are available to develop any definitive conclusions.

Out of a sample of 51 berthing events for the Malaspina (not the entire sample for the Malaspina), Dolphins E1, E2, and E3 were impacted 96%, 96%, and 60% of the time, respectively.[2] Dolphins E1, E2, and E3 were impacted 81%, 96%, and 67% of the time, respectively, by the Matanuska. Dolphins E1, E2, and E3 were impacted 100%, 44%, and 19% of the time, respectively, by the Kennicott. For the Columbia, Dolphins E1, E2, and E3 were impacted 71%, 71%, and 14% of the time, respectively. Overall, Dolphins E1, E2 and E3 were each impacted 92%, 82% and 49% of the time, respectively.[3]

Berthing Factor

The mean berthing factor out of 486 total measurements is ~0.0093, with a maximum measured value of 0.12. The service level design recommendation, 0.08, produces a design energy range of 46.7 ft-kips to 64.7 ft-kips for the span of vessel displacements at Auke Bay (5552 to 7683 long tons), which is in agreement with the service load recommendation for energy (51 ft-kips).

The ultimate design recommendations, 0.354 to 0.525, produce a design energy range of 137 to 189 ft-kips for the lower-bound berthing factor value, and 203 to 281 ft-kips for the upper-bound berthing factor value. The ultimate energy recommendations of Table 4.10 (Chapter 4A) fall within these ranges.

Berthing Force

In general, the design fender-force recommendations correlate well with the energy recommendations. Fender force ranges from 134 to 164 kips. Force recommendations are unique to Auke Bay because force is a function of fender stiffness; however, the values can be applied to designs of a similar nature.

---

[2]Note that one or all of the dolphins may be contacted during a berthing maneuver.

[3] This was for a sample consisting of the first 129 measurements collected during the field campaign.

Berthing force in this report represents the force at the point of impact of the vessel's sponson on the face of the fender. The actual forces felt by various components of the berthing structure can be determined from the berthing force, and will vary based on the elevation of impact.

The maximum measured berthing force by the Columbia was 77.3 kips. This berthing force corresponds to a total force of ~58 kips at the fenders. However, depending on tide level, the force felt by the fenders from this force could vary above or below this number.

The fenders at their full 24 inches of allowable deflection can easily resist forces in excess of 150 kips. However, the fenders are physically limited to a maximum displacement of 14 inches, allowing a maximum force of approximately 57.3 kips, or 28.6 kips in each cylinder. In cases where berthing energies exceed the allowable range of the fenders, the remainder of the energy and force must be absorbed by the tripod backing structure.

Berthing force data provided separately for the each vessel can potentially be used to determine design force values per vessel. However, more berthing data are needed for a wider range of vessel displacements before a relationship can be made between vessel displacements and berthing force.

Ultimate force values recommended in Chapter 4A assume a linear fender stiffness of 4.092 kips/inch (combined) over the entire displacement range (24 inches). In reality, the fenders are linear for 20 inches of displacement, and become progressively stiffer until reaching a maximum displacement of 24 inches at an average stiffness of 20 kips/inch. In addition, the fenders are physically limited to a maximum deflection of 14 inches, severely limiting the effectiveness of the fenders. Extreme events that exceed the 14-inch limited fender range must be absorbed by the tripod backing structure (see Figure 5.3), which was not taken into consideration in the *ultimate* fender and berthing force recommendations.

This assumption only applies to *ultimate* fender and berthing force recommendations. Since no recorded berthing events were large enough to displace the fenders more than 14 inches, all measured and nominal values are independent of this assumption.

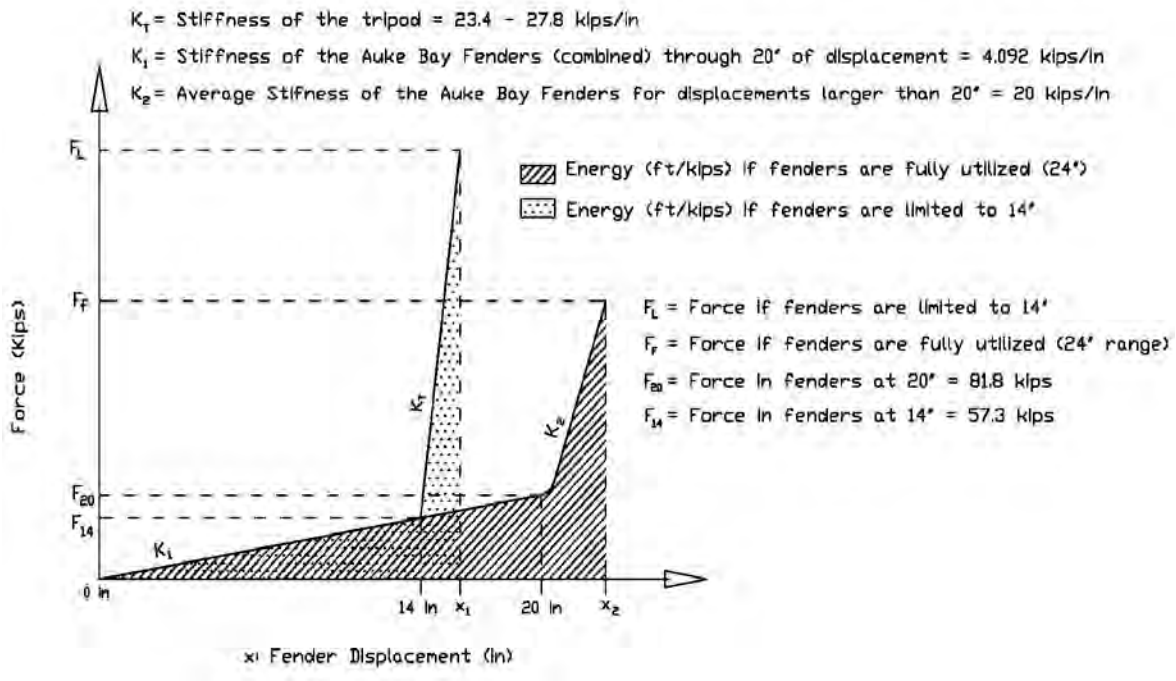

Figure 5.3: Force comparison chart

Chapter 5B – Discussion and Recommendations: Seattle

Overview

The instrumentation and monitoring program at the Bremerton slip was operational between August 2011 and July 2012, during which approximately 4875 vessel-berthing events occurred. Each vessel berthing can be characterized by an impact event at both the north and south wingwalls. Out of a possible 9750 impact events, more than 6950 wingwall impact events were recorded, characterized, and analyzed in this study. The sample collected at the site is assumed representative of Issaquah- and Super-class vessels landing at the Bremerton slip. This chapter discusses recommendations with regard to the results generated by this study and further details procedures used to obtain results and research products.

Reliability Design Charts

The application of reliability engineering methods to the berthing load environment is a major component of the research performed at the Bremerton slip. Estimation of extreme values is the primary objective of fitting probability distributions to the empirical data. The percentile plots and associated tables presented in Chapter 4B use probability density functions (pdfs) to predict the magnitude and occurrence of design parameters, and allow determination of *service* and *ultimate* values. Designers may apply the plots by first establishing reliability levels at which the service and ultimate loads are defined, and then matching the desired reliability level with the design parameter of interest. These empirically and statistically determined values provide a rational foundation upon which the designer may begin the process of designing an efficient structure that is both reliable and economical.

The design charts and tables presented in Chapter 4B are to be used for selecting design loads corresponding to both design life and reliability level. Selection of design values is dependent on the number of vessel-berthing occurrences a structure is expected to experience over a given life cycle. For example, if a wingwall design is to have a 50-year service life (design life), the appropriate design parameter value is determined by selection of a target reliability level that satisfies the number of berthing events a structure will experience over its design life. Figures 4.35 through 4.39 illustrate the relationship of design parameter, number of berthing-events, and reliability level. Design values corresponding to a structural life cycle of berthing occurrences at high reliability are considered “ultimate.”

Determination of Exceedance and Reliability Probability Levels

After establishing a dataset of empirically determined parameters and overlaying a pdf that appears to fit the data reasonably well, a probability associated with a given parameter value occurring or not occurring can be established. Knowledge of this determined reliability level also defines the probability of the value being exceeded. Equation 5.4 illustrates the relationship between reliability (also known as “probability of non-exceedance,” the probability of a parameter value not being exceeded in any one impact event) and the probability of exceedance (the probability that a parameter value will be exceeded in any one impact event). Extending these concepts to probability levels for a specific number of events is easily accomplished using probability theory in Equations 5.5 and 5.6.

$$R = 1 - p_{exceedance}$$ Equation 5.4

$$R_n = R^n = (1 - p_{exceedance})^n$$ Equation 5.5

$$R = R_n^{(1/n)}$$ Equation 5.6

where

$R =$ Reliability level or non-exceedance level; the probability that a parameter value will be at or below a specified magnitude in any one berthing event

$p_{exceedance} =$ Probability of exceedance; probability that a parameter of specified magnitude will be exceeded in any one berthing event

$n =$ Number of berthing events

$R_n =$ Reliability level, probability of non-exceedance in *n* events; the probability that a parameter will not be exceeded in *n* impact events

The parameter values presented in Chapter 4B are provided for a range of reliability levels (probability of non-exceedance levels) that a designer can employ. Table 5.2 further illustrates the relationship between reliability levels, number of berthing events, and design parameter exceedance probabilities.

The determination of reliability levels requires a multifaceted approach that is dependent on the goals of the designer and supporting organization. Considerations that need to be addressed include (1) the effects on the system of exceeding a design parameter; (2) the amount of redundancy built into the system to handle exceedance of a berthing parameter; and (3) the life cycle cost considerations associated with achieving reliability levels.

The design tables presented in Chapter 4B contain a large variety of reliabilities (probability of non-exceedance) for a designer to work with. Chapter 4B contains tables that summarize parameter design values corresponding to reliability levels over a range of design lives, on term of number of berthing events. These tables provide a range of options to better inform the structural design. If an engineer desires a design value that has not been illustrated in the charts, parameter values for any reliability may be accomplished by (1) using a design number of berthing events (n) and the corresponding reliability at that number of events (R_n) in Equations 5.5 and 5.6 to calculate the desired reliability in any one impact event (R), and (2) refer to the percentile for the desired parameter in Chapter 4B, using the calculated reliability (R) to determine the parameter value. Interpolation on the design charts may also be used for this purpose.

Table 5.2: Design Parameter Exceedance Chart, as a Function of Reliability and Number of Berthing Events

Reliability percentile, (Probability of Non-Exceedance of a selected berthing parameter for oneimpact event), %	90	95	99	99.99	99.9999	99.9999999
Number of Berthings, *n*	**Probability of design parameter being exceeded in *n* berths (1- Reliability), %**					
1	10.00	5.00	1.00	0.01	0.0001	0.000001
15	79.411	53.67	13.99416	0.1499	0.0015	0.000015
450	100	100	98.91398	4.4005	0.0450	0.000450
5475	100	100	100	42.1622	0.5460	0.005475
27375	100	100	100	93.5277	2.7004	0.027371
54750	100	100	100	99.5811	5.3278	0.054735
109500	100	100	100	99.9982	10.3718	0.109440
164250	100	100	100	100	15.1470	0.164115
273750	100	100	100	100	23.9478	0.273376
410625	100	100	100	100	33.6765	0.409783
547500	100	100	100	100	42.1606	0.546004
821250	100	100	100	100	56.0119	0.817887

Parameter Recommendations

Berthing design parameters for service loads and ultimate loads based on the results of the research accomplished at the Bremerton slip of the Seattle ferry terminal are presented in Table 5.3. The recommendations discussed in this section are specific to the site conditions and vessel classes landing at the Bremerton slip.

Service loads/parameters (also referred to as nominal loads/parameters) refer to the upper bound of typical loading conditions that the wingwall structure will need to endure on a regular basis. In this report, *service demand* is defined as a parameter that has a 10% probability of occurring or being exceeded in 450 berthing events per wingwall (this represents a month of berthing events at the Bremerton slip). This probability corresponds to a reliability level of 99.977% for any one berthing event, a 90% reliability level in a month of berthing events, and a 72.25% probability of occurrence in one year at the Bremerton slip (5475 berthing events per wingwall).

Ultimate loads/parameters in this report represent theoretical maximum parameters that could be expected during the design life of the berthing structure, at a particular reliability level. Ultimate loads represent events that may require the berthing structure to be taken out of service due to partial or total structural failure if exceeded. Two levels of ultimate parameter values are presented to provide a range that is dependent on the expected service life of a facility. The "lower" values for *ultimate demand* are defined here as a 2% probability that the berthing parameter will be exceeded in 273,750 berthing events (representing a 50-year life cycle at the Bremerton slip). This probability corresponds to 99.999993% reliability that the parameter will not be exceeded in any one berthing event and a reliability level of 98% over 50 years at the Bremerton slip. The lower ultimate values are greater than any parameter recorded in this study. The "higher" values for ultimate demand are defined here as a 2% probability that the berthing parameter will be exceeded in 750,000 berthing events (representing a 50-year life cycle at the highest frequency terminals in the WSF inventory). This probability corresponds to

99.9999973% reliability that the parameter will not be exceeded in any one berthing event, and a 98% reliability level over a 750,000-event service life.

Table 5.3: Empirically Determined Service and Ultimate Values

Loads	Service 10% 450 events	Ultimate 2% 273,750 events	Ultimate 2% 750,000 events
Energy – (kip-ft)	97	302	340
Force – Gamma (kips)	296	492	516
Force – Lognormal (kips)	479	1307	1451
Parameters			
Velocity (feet/second)	1.24	1.82	1.88
Berthing Factor (feet^2/second^2)	0.43	1.31	1.47

Load Factors

The load resistance factor design (LRFD) methodology is a standard design approach used by both the building and bridge industries in the United States and internationally. Structural design that uses the LRFD approach is a combination of applying resistance factors to the structural capacity, and multiplying loading conditions by a load factor. A design is considered safe and reliable when the factored capacity is greater than the factored demand. Resistance factors applied to the structural capacity have values that are less than 1.0, and loading conditions multiplied by load factors employ values that are usually greater than 1.0. Both the resistance and load factors are based on probability distributions that describe the limit states of the structural component and the likelihood of extreme loading condition occurring (see Equation 5.7 (Ellingwood et al. 1980).

$$\phi R_n \geq \sum_{i=1}^{n} \gamma_i Q_i \qquad \text{Equation 5.7}$$

where

ϕ = Resistance factor, less than 1.0, accounts for uncertainty in determining component resistance

R_n = Nominal Resistance corresponding to a limit state of a component being designed

γ_i = Load factor, typically greater than 1.0, though in load combinations can be less than 1.0 at times, accounts for uncertainty in determination of forces

Q_i = Nominal "load effect" such as force or energy

The combination of scaling down the capacity and scaling up the load is intended to compensate for the uncertainty and variability of materials and the loading conditions they must endure to remain functional. The commonly employed load factor criteria that control the design load are normally a combination of two or more loading conditions, such as dead, live, seismic,

etc., multiplied by their corresponding load factors. Since the maximums of two loading conditions occurring simultaneously are highly unlikely, the greatest combination of loads (multiplied by their load factors) is considered the design load. This report details the load environment associated with vessel berthing structures, which may be a starting point for incorporating the LRFD methodology into the marine infrastructure industry. Further research is required to define and quantify the additional pertinent loads that a wingwall (or other) structure must have to resist forces such as wind and wave loading.

The load factors developed here (see Table 5.4) are the result of dividing the ultimate load quantities by the corresponding service loads, as developed previously in this section. These load factors correspond to a 2% probability that the particular parameter will be exceeded in 273,750 or 750,000 berthing events, which is the approximate service life range of structures in the WSF inventory (98% reliability over 50 years).

Table 5.4: Load Factor Development for Berthing Parameters

Load Factor Development for Berthing Parameters					
Load Parameter:	Service/ Nominal Load (Q)	Ultimate Load ($Q\gamma$)	Load Factor (γ)	Ultimate Load ($Q\gamma$)	Load Factor (γ)
	10% exceedance	2% exceedance		2% exceedance	
	450 events	**273,750 events**		**750,000 events**	
Berthing Energy (kip-ft)	97	302	3.11	340	3.51
Berthing Force – Gamma (kips)	296	492	1.66	516	1.74
Berthing Force – Lognormal (kips)	479	1307	2.73	1451	3.03
Velocity (feet/second)	1.24	1.82	1.47	1.88	1.52
Berthing Factor ($feet^2/second^2$)	0.43	1.31	3.05	1.47	3.42

Normal Approach Velocity

Traditionally, approach velocity is the starting point for determining the impact energy associated with a berthing vessel when employing the Kinetic Energy Method. A suitable approach velocity is selected by either referring to previously published information or by direct determination. The velocity term is squared when determining a vessel's kinetic energy and therefore has significant influence on the calculated kinetic energy amount. The application of

various berthing coefficients then attempts to refine the calculated kinetic energy value of the vessel to better reflect the specific berthing situation.

Approach velocity is one of the foremost concerns using traditional design methodologies. Characterizing the ferry berthing maneuvers is the starting point in designing the wingwall structures. Several observations are presented here with the intent of assisting the design engineer in making appropriate use of the empirical dataset. The current practice used by the WSF personnel is to assume that the vessel either contacts both wingwalls simultaneously, or impacts one wall and continues to slide forward toward the centerline of the slip, loading both walls relatively equally (see Figure 5.4). Each wingwall is designed for one-half of the total calculated design berthing energy (WSF 2012).

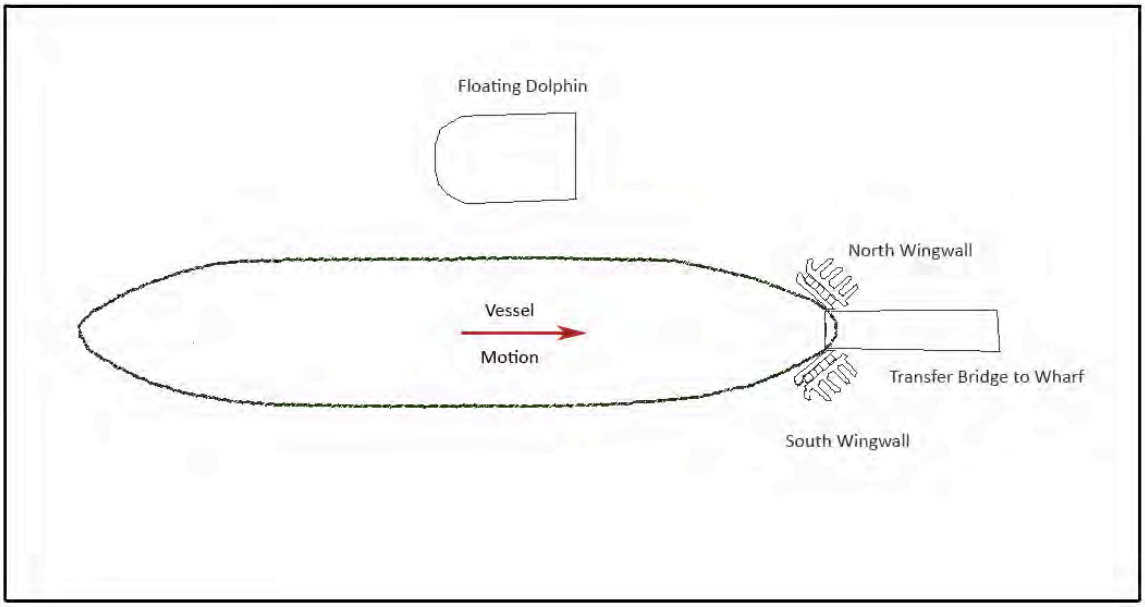

Figure 5.4: Idealized berthing overview, plan view

This approach has resulted in robust wingwall designs that have functioned well, with the backing structures even surviving two "runaway" vessel impacts over the past 19 years. However, the review of thousands of berthing events allows for further characterization of the actual manner in which the vessel interacts with the berthing structures. Primarily, the idea that the vessel contacts both wingwalls simultaneously and loads both wingwalls with approximately the same energy could benefit from some refinement. After visually observing dozens of landings at the Bremerton slip, and analyzing thousands more in the recorded data, it was determined that very few events involved the simultaneous impact of both wingwalls. The prominent condition involves ferry impacts at each wingwall that are independent, and the initial impact may, or may not, be the most significant impact of the event. The events analyzed at the Bremerton slip most frequently exhibit behavior that resembles a slow-motion "pinball": the vessel tends to alternate impacts with each wingwall before coming to rest in the pocket-shaped berth. Each wingwall is subject to multiple significant impacts in this typical vessel-approach scenario (see Figure 5.5 for an annotated plot that displays this behavior). With regard to approach velocity, this observation is significant because it differs from the methodology currently in use. The Kinetic Energy Method assumes a "dead float" into the structure. The dead-

float berthing scenario results in approach velocity measurements that would be nearly equal at either end of the wingwall structure (see Figure 5.6). Vessel berthing events observed and analyzed in this report depict a contrasting scenario. In reality, thrust and maneuvering influence the vessel motion up to, during, and following the initial vessel impact. The implementation of this approach velocity dataset may require adjustments to the design procedures to achieve desired wingwall capacity.

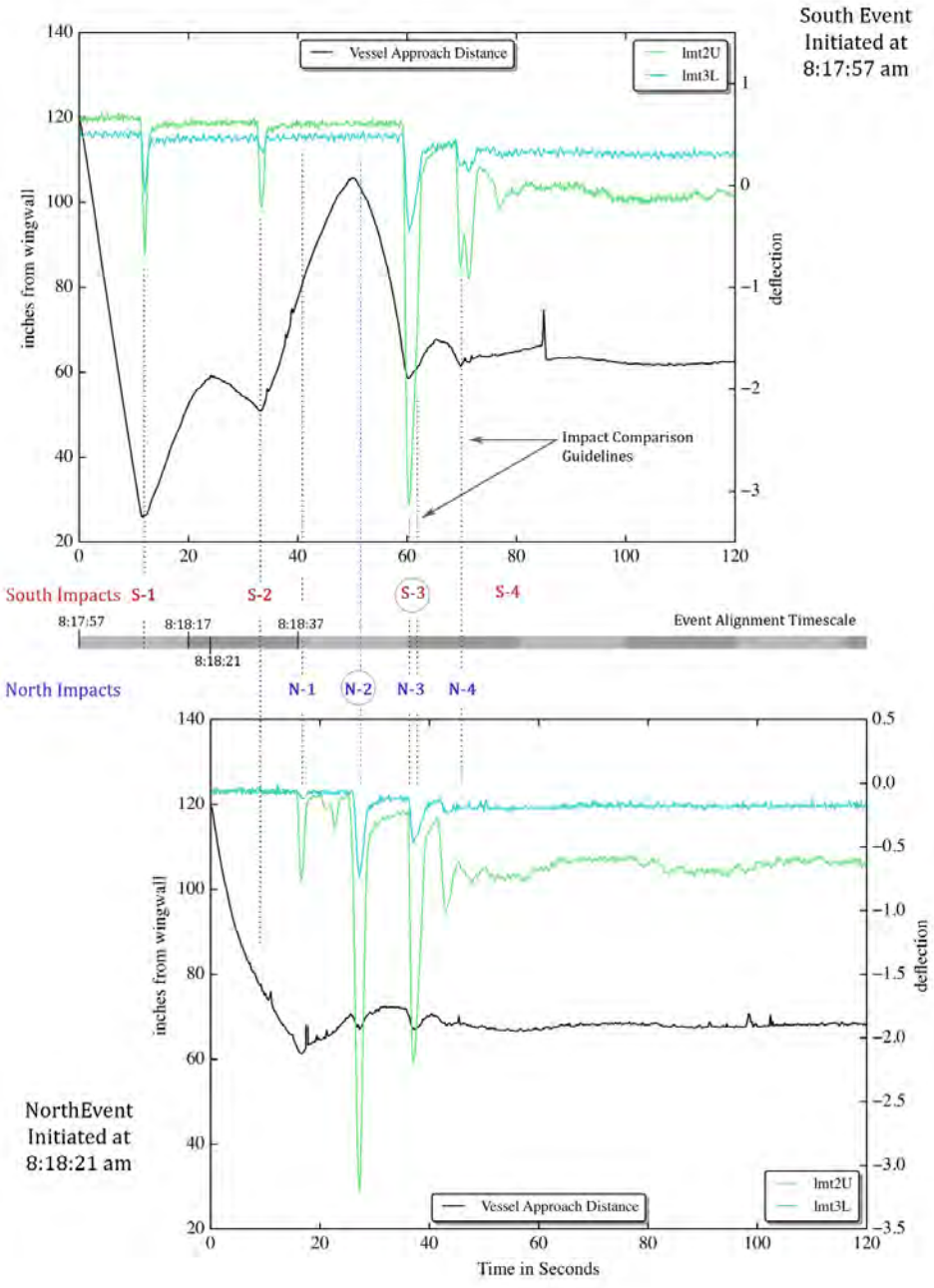

Figure 5.5: Illustration of complete berthing event with asynchronous impacts

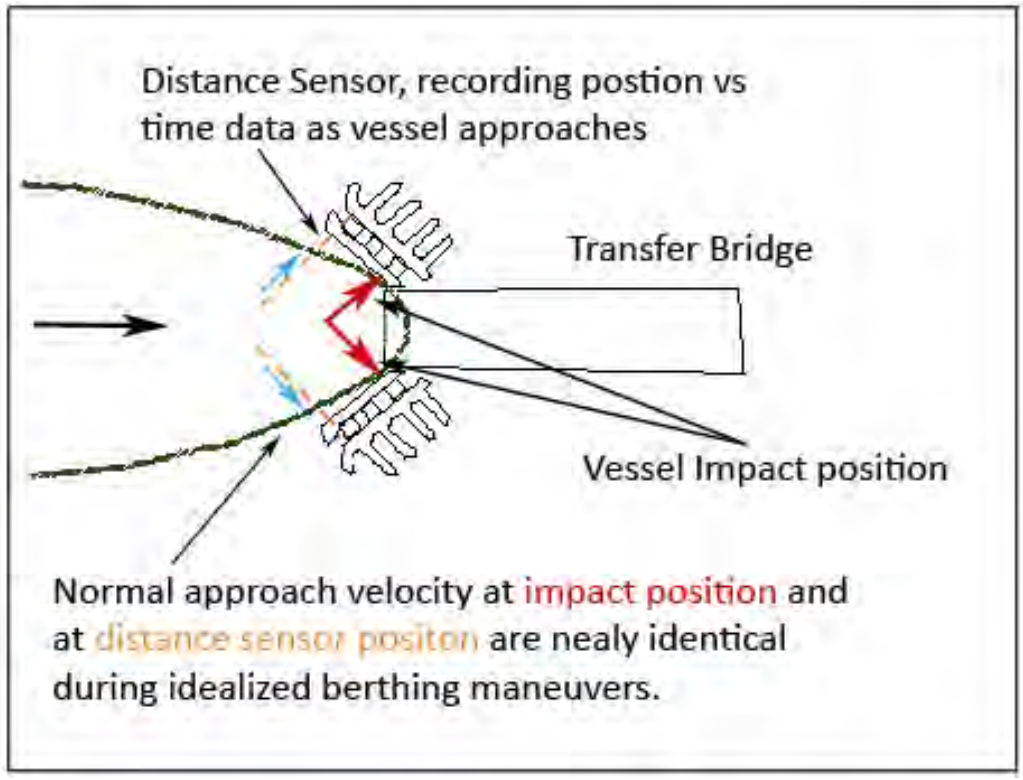

Figure 5.6: Close-up of idealized berthing

However, small (less than 0.1 feet/second) or negative approach velocities were frequently recorded just prior to the deflection of the impact face. A common scenario observed at the site that may explain these measurements involves the vessel approaching the slip at a slight angle (see Figure 5.7). Immediately prior to or upon contact with the wingwalls, motion in the yaw direction (likely due to steerage and/or environmental factors) was observed. Laying the vessel against the breasting dolphin was a frequently used maneuver that requires motion in the yaw direction. This maneuver was likely done to provide stability for off-loading/on-loading procedures. The result of these maneuvers is that the vessel has both a surge and a yaw component to its motion when berthing. This condition has significance for the amount of energy imparted to the berthing structure, and is not easily quantified by velocity measurements taken during the field campaign.

The concept of a rotational-velocity component also demonstrates that the initial velocity figure of interest is most meaningful at the point of impact, which varies for each event, thus making an accurate estimate of initial velocity elusive. Any amount of rotation about the vessel's vertical axis diminishes the applicability of the empirically recorded normal approach velocity at the edge of the wingwall, and contributes to the impact energy of the vessel's bow (see Figure 5.8).

For example, the normal approach velocity determined from the vessel position information may be determined to be 0.02 feet per second (0.25 inches per second), but the amount of energy absorbed by the wingwall can suggest that the impact velocity at the point of impact was likely greater than the recorded velocity at the outside edge of the structure. Figure 5.9 illustrates this concept using plots of two different events.

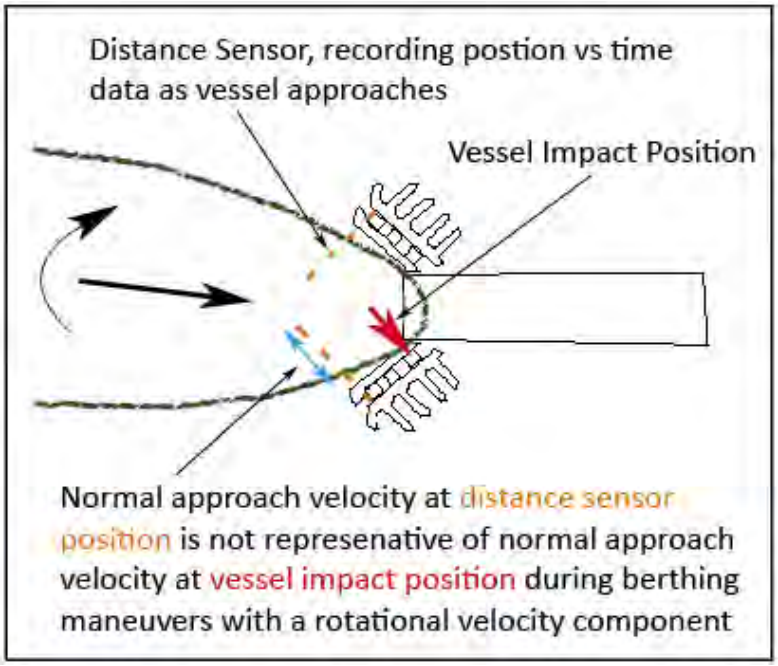

Figure 5.7: Close-up of berthing maneuver with yaw component

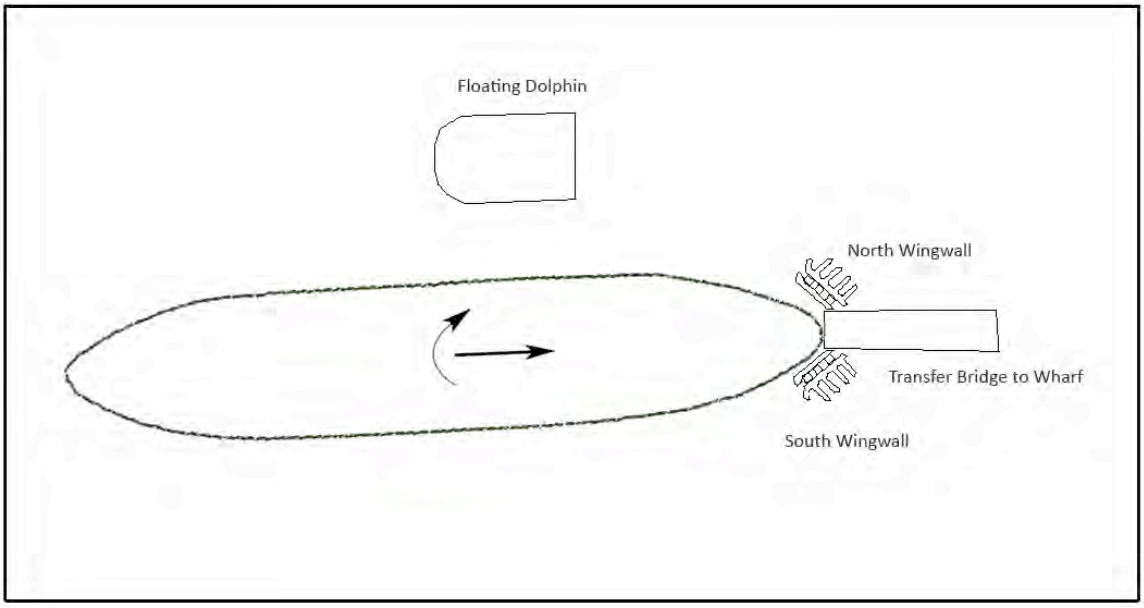

Figure 5.8: Berthing maneuver with rotational velocity component

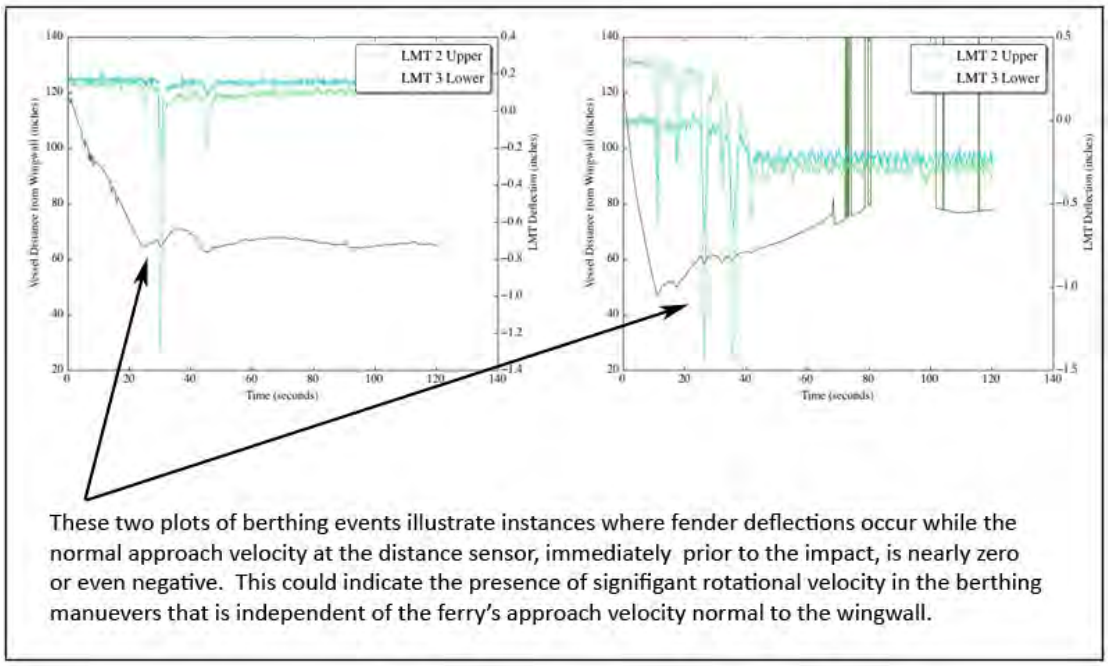

Figure 5.9: Evidence of rotational velocity component during vessel berthing impact

The velocity data presented in Chapter 4B is accurate at the outside edge of the wingwall and, for reasons discussed earlier in this section, should be used with some discretion when applied to the Kinetic Energy Method. Energy associated with the berthing event often surpassed the amount of kinetic energy (based on the recorded approach velocity) associated with the vessel, and therefore designers should use caution when attempting to design berthing structures based on normal-approach velocity distributions and berthing coefficients.

Berthing Energy

Empirically determined berthing energy information is a more direct and less ambiguous approach to designing berthing structures than employing the Kinetic Energy Method and empirically determined approach velocities. All factors affecting the berthing structure are included in the experimental sample of berthing energy, and the designer can employ the energy information with far fewer challenges.

The berthing energy results displayed in Chapter 4B represent the total energy absorbed by the impact face and fender. Challenges of operating instrumentation in the intertidal zone resulted in seven linear motion transducer (LMT) failures over the course of this study. Logistical challenges associated with replacement of the devices resulted in intervals of up to three weeks, during which a LMT was not recording information. The data obtained during these periods were adjusted to counteract the effects of the failed sensor. This adjustment was accomplished by first calculating the ratio of deflection experienced by each fender pair (upper and lower fender at the same piling) of the wingwall, when all sensors were operational over the period of the study. Next, the deflection ratio was applied to the fender pairing in an effort to approximate the amount of deflection that would likely be experienced by the out-of-service fender. For example, if the north side lower LMT, closest to the transfer bridge, was out of service for two weeks before being replaced, all data from that time period would under-

represent the total energy absorbed by the wingwall, since one of the six instruments was not functioning. The ratio of upper to lower deflection at that position is approximately 1.59 to 1.0. During a berthing event, the upper fender deflection was measured at 3.0 inches, and the corresponding measurement at the out-of-service LMT was 0.0 inches. Utilizing the deflection ratio, the lower fender displacement is approximated to be 1.887 inches, allowing for a more accurate estimation of vessel berthing energy.

The capacity of each marine fender at maximum displacement is approximately 283 kip-ft, which is greater than any event estimated over the duration of the study (147.6 kip-ft was the maximum estimated energy absorbed by the wingwall). This capacity suggests that the wingwalls employed at the Bremerton slip are designed with significant excess capacity. The north wingwall has a slightly higher mean energy absorption value than the south wingwall, and it recorded a maximum berthing event that was 1.8 times the maximum event that occurred on the south wingwall.

In quantifying the amount of energy absorbed by wingwalls, a typical landing by WSF personnel is considered a Type I berthing event, a landing that causes no damage. A starting point for WSF wingwall design is the "standard wingwall design energy" spreadsheet that incorporates berthing coefficients and variables for all vessels in order to establish a baseline design number. The Type I design energy absorbed by the wingwall is 343 kip-ft for the M/V Kitsap and 379 kip-ft for the M/V Kaleetan. These design values correlate to a 99.7% reliability level for a 50-year design life. The design of wingwalls for the WSF is complicated by the desire to protect shoreside infrastructure, such as the towers and transfer bridge, in the event of an extreme Type III berthing event. Type III berthing events, which include the failure of some part of the wingwall, are meant to account for a condition in which the vessel loses control of the propulsion system. The newest generation of wingwalls is softer and undergoes a partial analysis of a Type III berthing event to understand the amount the wingwalls will deflect during a Type III event that occurs directly at the throat of the structure. The purpose of this analysis is to quantify approximately how far the vessel can progress toward the shore, and to design the structure to fail in a controlled manner. The Type III design energy for the Kitsap and Kaleetan is 3160 and 3486 kip-ft.

Berthing Force

The berthing force recommendations are specific to the Bremerton wingwalls, as berthing force is dependent on system stiffness. The berthing force discussed in Chapter 4B represents the sum of the reaction forces at all six marine fenders and the force associated with displacing the impact face of the wingwall. The forces applied to various components of the wingwall can be determined from the berthing force data and structural analysis.

The maximum amount of force applied to the wingwall was approximately 408.5 kips, and each marine fender has a maximum rated reaction force of 150 kips. The stiffness of the wingwall system is directly related to the reaction force exerted by the wingwall, which makes it difficult to employ berthing force data to systems with different stiffness characteristics.

Berthing force results have been provided for both the gamma and lognormal probability distributions. Both distributions have qualities that may be of interest to the designer and are presented to provide additional context for the designer.

Berthing Coefficient

The berthing coefficient results of Chapter 4B display high variability and exceed ranges suggested in the literature (Costa 1964; Gaythwaite 2004). The challenges of measuring the approach velocity, as discussed in this section, help to illuminate the discrepancy between berthing coefficients that are empirically determined and those that are recommended in the literature.

The results associated with the berthing coefficient values suggest caution when applying the traditional kinetic energy approach, which uses a berthing coefficient and approach velocity to determining the vessel's impact energy. Most notably, approach velocity data that corresponds to very low approach speeds tend to have high berthing coefficients—high enough that when filtered out, the mean berthing coefficient drops significantly into a range more in line with the literature (see Figures 5.10 through 5.13 for filtered berthing coefficient histograms). However, the velocity dataset has previously been filtered and is considered representative of vessel behavior at the point of measurement; therefore, the justification required to manipulate the velocity dataset is absent. Further examination of the results reveals that as the calculated berthing coefficient (C_b) increases above 1.1 (the upper bound of published values), the mean velocity ($v_{approach}$) associated with the kinetic energy of the vessel prior to impact decreases.

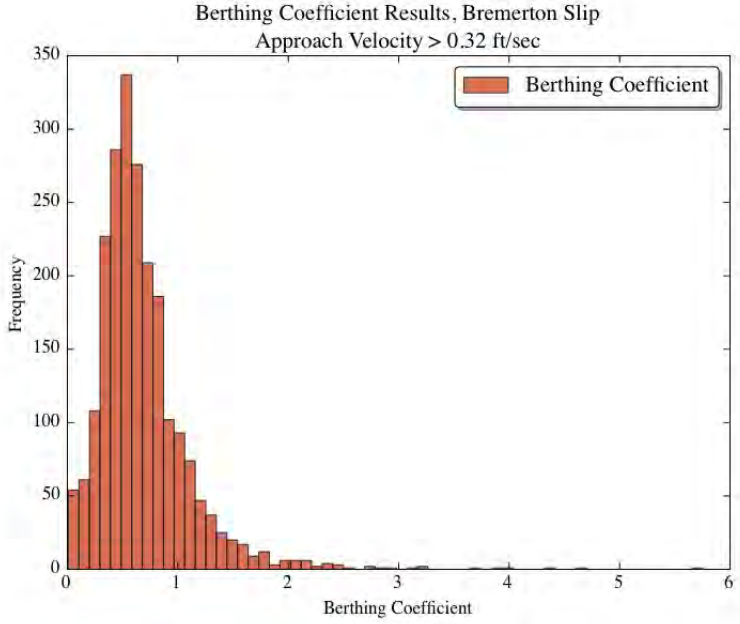

Figure 5.10: Berthing coefficient results, approach velocity > 0.32 ft/sec

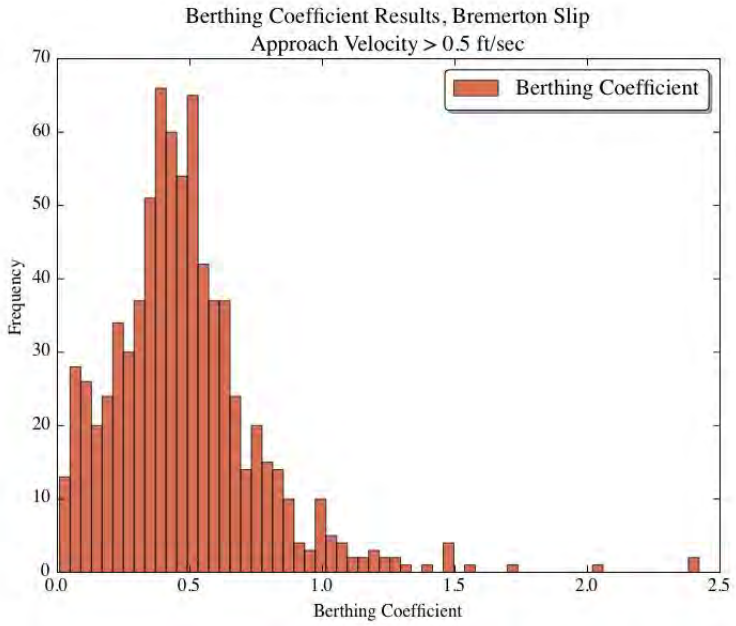

Figure 5.11: Berthing coefficient results, approach velocity > 0.5 ft/sec

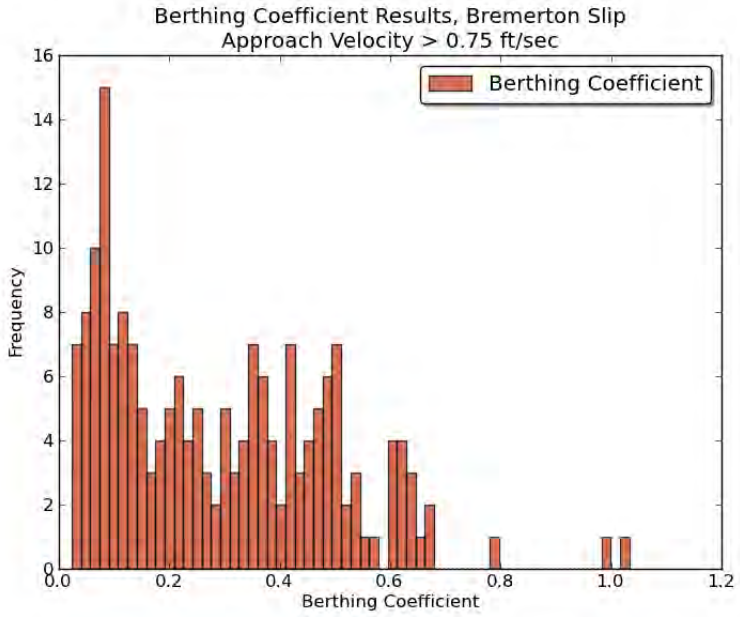

Figure 5.12: Berthing coefficient results, approach velocity > 0.75 ft/sec

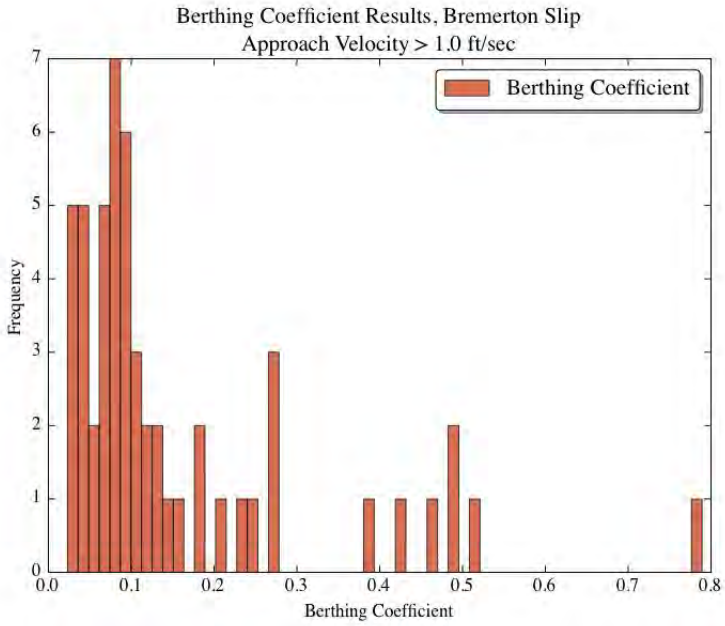

Figure 5.13: Berthing coefficient results, approach velocity > 1.0 ft/sec

The experimentally determined berthing coefficient results suggest that energy is being added to the berthing event that is not accounted for in a simple vessel kinetic energy calculation. Also, as discussed earlier, the presence of a yaw component to the vessel motion influences the approach velocity at the point of impact. The Kinetic Energy Method attempts to account for rotational velocity with the eccentricity coefficient. However, the application of values found in the literature (0.5 to 0.8) may not be representative of the berthing scenario at the Bremerton slip. Sources of additional energy not associated with a dead-drift approach velocity could be the use of the vessel's propulsion system or environmental conditions affecting the berthing procedures. Neither of these aforementioned factors are accounted for when developing a berthing coefficient, and given the high values associated with the empirically determined berthing coefficient, some components clearly cannot be overlooked. As discussed in this section, the rotational or yaw component of the incoming ferry motion provides insight into why vessel approaches with "slow" recorded approach velocities may apply larger than anticipated amounts of energy to the berthing structure.

The berthing coefficient results were further investigated to ascertain the influence of the approach velocity. Table 5.5 displays berthing coefficient information after filtering the lower bound of the approach velocity to illustrate its effect on the berthing coefficient estimates. By filtering out the lowest approach velocity measurements, the mean berthing coefficient drops significantly and does not converge to a value. This illustrates a challenge associated with utilizing the berthing coefficient approach; the berthing coefficient exhibits variation with respect to normal approach velocity.

Table 5.5: Berthing Coefficient Results with Lower-bound Approach Velocity Filtered

Berthing Coefficient (C_b)				
Approach Velocity Lower-Bound ft/sec	Mean	Standard Deviation	Max	# of Events
0.04	3.299	9.457	199.842	5065
0.32	0.683	0.436	5.76	2224
0.50	0.477	0.28	2.42	769
0.75	0.2896	0.202	1.03	186
1.00	0.1567	0.155	0.789	54

Despite the challenges associated with the experimental justification of a berthing coefficient, the kinetic energy approach is still considered the standard method for solving the berthing energy problem. The Alaska and the Washington State Departments of Transportation have successfully used this method by applying decades of experience in working with the berthing coefficients and approach velocities specific to their sites. The proper application of the Kinetic Energy Method is dependent on proper selection and *balance* of approach velocity and berthing coefficients. For example, multiple combinations of berthing coefficients could provide accurate berthing energy estimates based on erroneous approach velocity estimates. The challenge facing designers is how to proceed with using berthing coefficients that have been refined over time when presented with empirical velocity data that conflict with historically employed standards.

Attempting to derive a reasonable estimate for design energy using the estimated berthing coefficients (Chapter 4B) and approach velocities (also Chapter 4B) is not possible. Another method is proposed here to provide designers with a procedure that bridges the traditional kinetic energy methodology with the empirically determined estimates of berthing energy. Using empirically determined approach velocities and estimated berthing energies and their associated distributions, a reasonable estimate for berthing coefficients at varying reliability levels can be obtained. The kinetic energy equation for a berthing vessel is reprinted here as Equation 5.8.

$$E_w = \frac{W}{2g} v^2 C_b \qquad \text{Equation 5.8}$$

where

E_w = Berthing energy to be absorbed by wingwall

W = Vessel mass

v = Approach velocity

C_b = Berthing coefficient

Using Equation 5.9, the probability-based estimates of berthing energy and approach velocity, and solving for C_b, a range of berthing coefficient values can be obtained that corresponds to the empirical parameters (see Table 5.6).

$$E_{R\,\%} = \frac{W}{2g} v_{R\%}^2 C_{b-R\%}$$ Equation 5.9

where

$E_{R\,\%}$ = Berthing energy at a given reliability level

W = Vessel mass

$v_{R\,\%}$ = Approach velocity at a given reliability level

$C_{b-R\%}$ = Berthing coefficient at a given reliability level

Table 5.6: Berthing Coefficient Estimates

Berthing Coefficient Estimates		
Probability of Non-exceedance, %	Velocity, feet/second	C_b, estimated
98	0.797	0.555
99	0.876	0.549
99.9	1.105	0.565
99.99	1.304	0.609
99.999	1.482	0.672
99.9995	1.533	0.693
99.9999	1.646	0.747
99.99995	1.692	0.772
99.99999	1.798	0.835
99.999999	1.941	0.936
99.9999999	2.077	1.049

By utilizing the berthing coefficient estimations and velocity figures presented in Table 5.6, the design berthing energies can be calculated that are calibrated at the given reliability levels. The use of the data in this way is presented for illustration purposes; the use of the design berthing energy information represents a more direct application of the study.

Berthing Factor

The berthing factor results provide a methodology for scaling the empirically determined design berthing energy to vessel classes not represented in this study (vessels with different displacement values). After adjusting for proper units, the berthing factor may be multiplied by the vessel mass of interest to obtain a design berthing energy that is founded upon the empirical

data obtained in this study. Please refer to the Example 2 in Chapter 6 for details regarding this procedure.

The mean berthing factor observed in the study period at the Bremerton slip was 0.057, and the maximum recorded berthing factor was 0.684. The service value for berthing factors obtained in this study by methods detailed in Section 5B is 0.43, which corresponds to a service energy level of between 89.3 and 98.3 kip-ft when applied to the vessel displacements that service the Bremerton slip and compares favorably with the service level berthing energy recommendation for the slip of 97 kip-ft. The *ultimate* berthing factor value recommended by this study is 1.33, corresponding to 98% reliability over the course of 50 years. For ferries landing at the Bremerton slip, this value corresponds to ultimate values for the Issaquah-class vessels of 272.9 kip-ft, and ultimate values for the Super-class vessels of 301.0 kip-ft. These ultimate values correspond favorably with the ultimate berthing energy recommendations of 304.7 kip-ft suggested for the Bremerton slip.

Applying the berthing factor to vessel displacements, the design energy for service and ultimate loads can be extrapolated for a range of vessels (exhibited in Figure 5.14). Note that scaling parameters have limitations that may not be anticipated from the outset of design using scaled values. Design errors attributable to the effects of scaling up successful designs have been persistent throughout history (Petroski 2000), and every effort must be made to comprehend the potentially unique failure mechanisms and operational differences associated with larger (or smaller) systems.

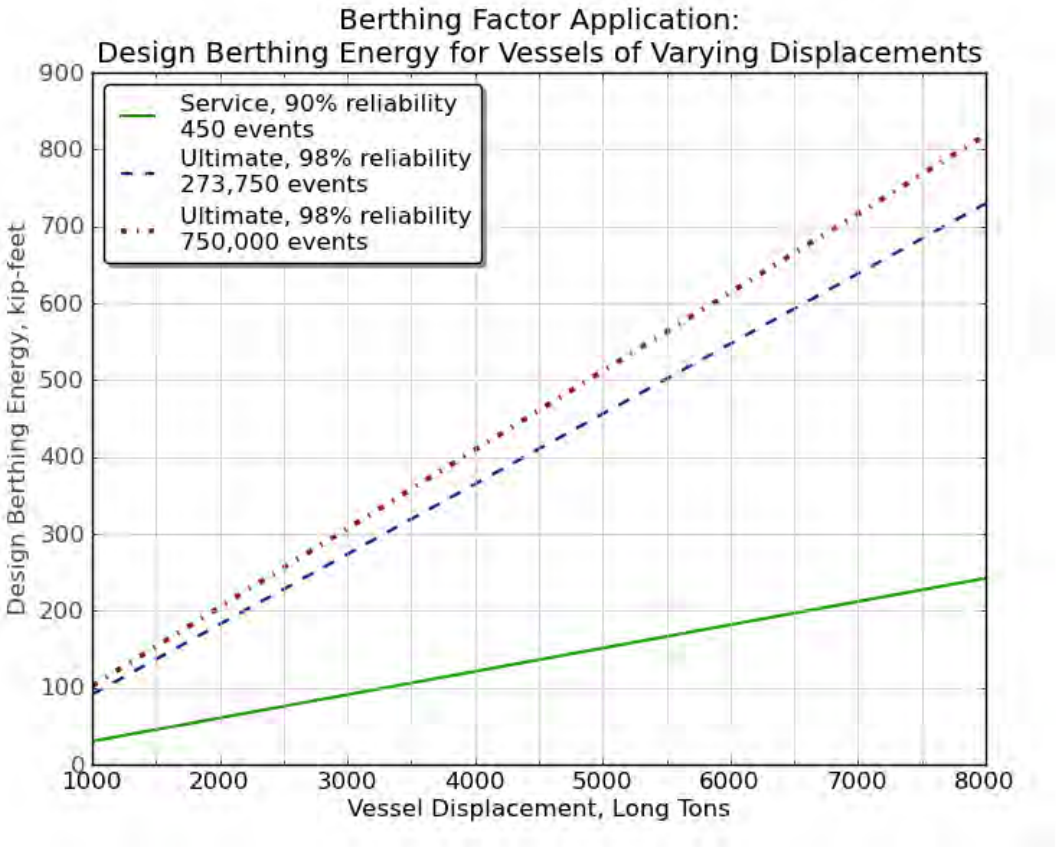

Figure 5.14: Application of berthing factor to a range of vessel displacements

Vessel Point of Impact Results

The point of impact results are intended to provide insight into where and with what frequency a vessel is contacting the impact face. The visual representation provided by the figures in Chapter 4B and the fender impact synopsis of Table 5.7 attempt to quantify the vessel landing location.

This analysis provides some interesting observations that may be useful to designers:

- The lower marine fender furthest from the "throat" typically goes into tension.
- There is less dispersion in the points of impact on the north wingwall than on the south wingwall. This difference may be attributed to the presence of the breasting dolphin along the north side of the approach. The mean impact elevation is located closer to the upper fender than the lower fender, and generally occurs between pile lines 2 and 3.

Table 5.7: Fender Impact Synopsis

North				
	Average Deflection (in.)	Average Force (kips)	Average Energy (kip-ft)	Average Energy Absorbed per Fender, %
LMT2 Lower	1.01	19.25	2.70	22.97
LMT2 Upper	1.69	31.61	5.00	42.51
LMT 3 Lower	0.40	7.74	0.95	8.10
LMT 3 Upper	0.87	16.52	2.22	18.86
LMT 4 Lower	-0.26	-5.05	0.55	4.66
LMT 4 Upper	0.14	2.74	0.34	2.91
South				
LMT2 Lower	0.90	17.07	2.35	21.37
LMT2 Upper	1.51	28.32	4.36	39.70
LMT 3 Lower	0.47	9.01	1.14	10.40
LMT 3 Upper	0.83	15.85	2.12	19.30
LMT 4 Lower	-0.07	-1.30	0.34	3.12
LMT 4 Upper	0.28	5.29	0.67	6.11

Chapter 6 – Implementation and Design Considerations

Overview

The use of a probability-based design approach is a rational way to characterize uncertainty associated with demands placed on a structure (see Figure 6.1). Although a structure cannot be efficiently designed to resist every possible loading condition, the use of reliability-based criteria allows for a design that is based on the likelihood of loads occurring over the service life of the project.

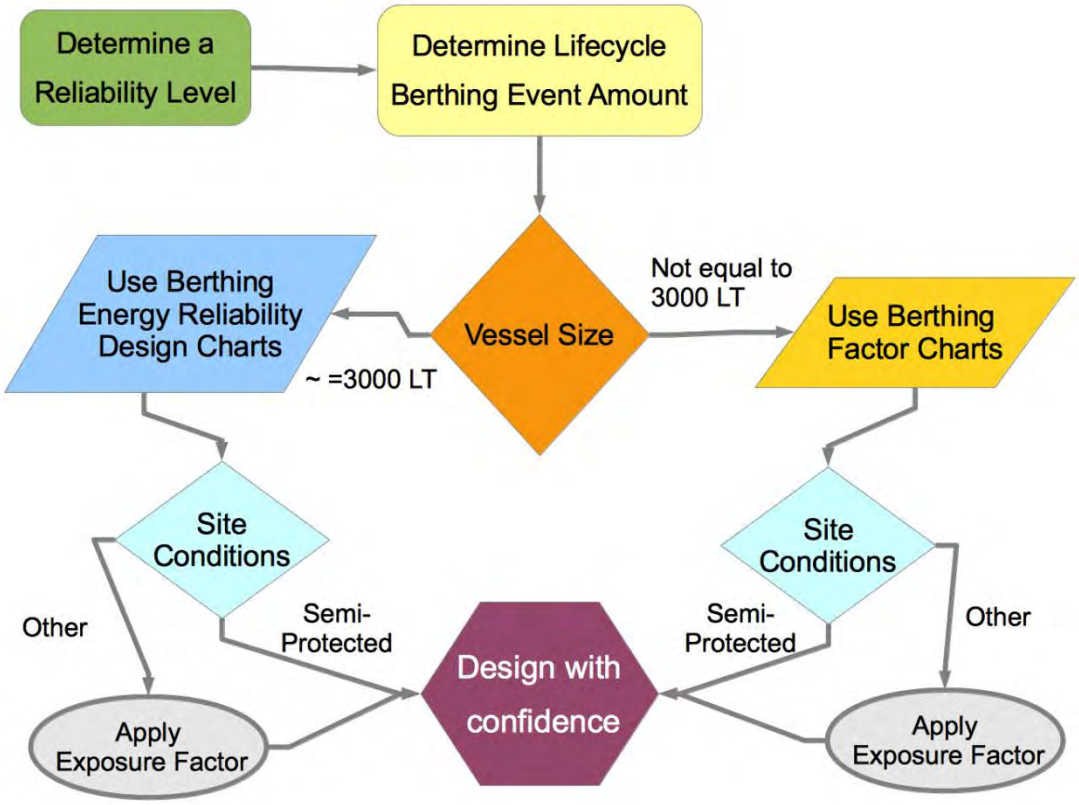

Figure 6.1: Implementation graphic

The transition to a reliability-based design approach requires an adaptation of the traditional design methodologies used when establishing design berthing energy. When employing a reliability-based approach, subjectively determined safety factors are replaced by rationally determined load factors, and the engineer is empowered with information that assigns a probability of demands being exceeded or not. Before the selection of a desired reliability level can proceed, the consequence of an associated failure must be clearly considered. The working definition of *failure* in this document is that the design parameter value is exceeded. All discussion of *reliability* levels relates to the idea that a design parameter is not being exceeded, and the *probabilities of exceedance* relate to design values being surpassed. It is important to note that if a design parameter is exceeded, structural failure is not implied by this definition.

Another factor that must be defined to properly employ reliability techniques is the interval of concern. For a ferry landing structure, the interval of concern is most easily described as the estimated number of berthing events expected during its service life.

When selecting a desired reliability level, potential failure mechanisms that could result if the design parameter is exceeded must be explored and analyzed with regard to repair/replacement costs, maintenance costs, and life cycle costs. Reliability levels of different structural elements may vary depending on the function of the element and the amount of redundancy. The cost/benefit analysis of the various reliability levels may be based on the historical performance of structures and the associated maintenance costs.

Examples

The use of berthing energy recommendations in Chapters 4A and 4B is the most direct application of this research. For locations that have analogous site conditions and receive vessels of similar size, the procedure is elementary. Following the selection of a desired reliability level and the number of berthing events that a structure is intended to receive, a design berthing energy may be selected from the reliability plots in Chapters 4A or 4B, as presented in Example 1. If the designer chooses to use a reliability level not represented in the plots in Chapters 4A or 4B, the procedure is outlined in Chapters 5 and further expanded in Example 2.

Application of the berthing energy recommendations to sites with conditions that vary from the Seattle terminal may be accounted for using an exposure factor, *k*, developed by Toppler and Weersma (1973) for tanker vessels with displacements between 300,000 and 500,000 long tons. The user may benefit from refinement of the factors for site-specific conditions.

Equation 6.1 is applicable to the Alaska Marine Highway and Washington State Ferries facilities:

$$E_{exposure-design} = k * E_{design} \qquad \text{Equation 6.1}$$

where

k = Exposure factor for location
= 1.10 for very exposed locations
= 1.0 for locations of normal exposure, Seattle terminal
= 0.85 for very sheltered locations

$E_{exposure-design}$ = Design berthing energy, adjusted for exposure

E_{design} = Design berthing energy

Example 1 – Using Berthing Energy Design Charts

Determine a design berthing energy for a berthing structure that will need to handle approximately 750,000 berthing events over the course of its design life. Assume that site conditions are similar to the conditions of this study and that the facility services Issaquah- and Super-class vessels.

(a) For a desired reliability level of 98% and a 500,000 event design life:

Using Figure 4.36 (Chapter 4B), the design berthing energy at the intersection of the 98% reliability curve and 500,000 berthing events is approximately 320 kip-ft.

$$E_{design} = 320 \text{ kip-ft}$$

(b) For a desired reliability level of 98% and a 900,000 event design life:

The 900,000 berthing event design life is not represented on Figure 4.36; therefore, an alternate method is required: (1) Determine the reliability level for one berthing event that corresponds to a 98% reliability level at 900,000 events by using Equation 5.6.

$$R = R_n^{(1/n)} \quad \text{->} R = 0.98_{900,000}^{(1/900,000)} = 0.999999975 \approx 0.99999999$$

Look up the appropriate value of *R* in Table 4.15 (Chapter 4B), remembering to convert to a percentage, and associate with the corresponding design berthing energy level.

$$E_{design} = 380.5 \text{ kip-ft}$$

Example 2 – Using the Berthing Factor

The berthing factor approach extends the use of the empirical data to a range of vessel displacements. Using the berthing factor results of Chapters 4A and 4B allows the design berthing energy to be defined as a function of vessel displacement and ultimate limit state, providing a means to estimate design berthing energy for vessels with displacements outside the field of study.

Example: Determine the ultimate design berthing energy of a vessel with an operational displacement of 6600 long tons at a 96% reliability level for a design life of 700,000 berthing events.

Solution: Determine the reliability level for one berthing event that corresponds to a 96% reliability level at 700,000 events by using Equation 5.6 of Chapter 5B.

$$R = R_n^{(1/n)} \text{->} R = 0.96_{700,000}^{(1/700,000)} = 0.99999994 \approx 0.9999999$$

Look up the appropriate value of *R* (Table 4.7 in Chapter 4A or Table 4.22 in Chapter 4B), remembering to convert to a percentage, 99.99999%, and find the corresponding berthing factor in the table.

At $R = 99.99999$; $f_b = 1.2643$ feet^2/seconds^2

Apply the berthing factor to the vessel displacement to obtain the design berthing energy.

$$E_{design} = f_b * \frac{W}{g} \qquad \text{Equation 6.2}$$

where

W = Vessel displacement, 6600 long tons * 2240 lb/ton

g = Gravity acceleration = 32.174 feet/second

f_b = Berthing factor = 1.28

Solving for E_{design}, and converting to kips; E_{design} = 588 kip feet

Note that the results of this study can be used in various ways not covered in the previous examples.

Chapter 7A – Conclusions: Auke Bay

General

Understanding vessel impact loads is crucial to the design of cost-effective and reliable berthing structures. When a berthing structure is designed, a certain level of uncertainty exists that is typically accounted for by using a simple factor of safety. Even with a factor of safety applied, there will always exist the potential for design energy, force, or velocity to be exceeded. Engineers have developed their own design guidelines through trial and adjustment over many operation/failure cycles, and have developed factors of safety that compensate for assumptions in load. However, precisely quantifying berthing loads remains a challenge, with limited information often leading to the design of structures rooted in assumptions and discretion.

A number of statistical studies were conducted in the late 1960s and early 1970s giving valuable design energy recommendations based on vessel displacement and berthing frequency. The studies were limited to tanker-type vessels, however, which vary significantly in size and geometry from ferry vessels. Additionally, published load values such as energy and approach velocity are site specific, and cannot always be interchangeably used with confidence.

The use of analytical models and computer software are valuable in handling the complex ship-fluid interactions of a berthing vessel, particularly when information is limited for the particular vessel type, size, and location. However, even the most advanced models cannot fully account for all aspects associated with a berthing vessel, including factors such as vessel maneuverability and vessel approach variations due to environmental and human influence. For this reason, non-empirical design values are often confirmed or used in conjunction with full-scale measurements, which inherently consider all variables.

Findings

A particular challenge associated with berthing structures is the large variation in load. Extreme events must be considered in addition to typical service loads. It is understood that certain extreme events can never be fully accounted for and to attempt to do so would result in an overly conservative design. Most extreme events have a quantifiable probability of occurring, so can be reasonably accounted for. Reliability engineering is a powerful tool when dealing with highly variable loads, because it allows engineers to develop rational designs based on anticipated extreme events and the associated risk levels.

This study analyzed the berthing events of four different vessels at the Auke Bay ferry landing in Juneau, Alaska. The results from this study will provide the ADOT&PF Marine Highway Department with a broad set of parameters for its information base, while also providing a probability-based design option for the design of future landings.

Results were compared with current design values for the berthing structures at Auke Bay. In general, the dolphins at Auke Bay have performed adequately for their intended purpose. Conversely, out of all the berthing events recorded at the site, loads in excess of the design values[4] (although rare) were observed; thus, recommendations on nominal and service load values have been provided.

[4] Per design documents provided by ADOT&PF.

Nominal load recommendations were selected to nearly reflect the maximum values measured at Auke Bay. Nominal loads represent the maximum service loads that the berthing structures are subject to on a regular basis. These values are similar to *design* values used by the ADOT&PF Marine Highway Department for berthing structures at Auke Bay. Alaska Marine Highway System (AMHS) engineers applied factors of safety to the structures in anticipation of working stresses being exceeded due to extreme events. While this design approach has proven adequate, this study provides an alternative design option, whereby factors of safety in load demand are rationally quantified based on risk level.

Ultimate load recommendations represent extreme event loads that the berthing structure must be expected to resist at limit state over a specified design life or number of berths. The decision as to what level of risk is acceptable is left to the designer.

Regarding the fenders currently used at Auke Bay, the fenders themselves are potentially adequate for resisting nominal loads in their linear range as well as ultimate loads in their nonlinear range, but the fenders are physically limited to a maximum displacement of 14 inches, which limits the allowable absorption capacity of the fenders. Loads in excess of the *limited* fender‘s capacity are absorbed by the backing structure, putting a high amount of stress on the piles.

Overall, the complex and variable load environment on berthing structures implies the advantages of a reliability approach, in which fenders and backing structures can be rationally designed for exceptional events.

Summary

The following is a summary of recommendations and comments:

- Fenders should be designed to resist ultimate loads from extreme events that are expected to occur over their design life or design number of berths. An overload allowance (load factor) of about three times the largest service energy is recommended.
- A vessel‘s initial kinetic energy does not always reflect the maximum energy per berthing event. Care must be taken when using the kinetic energy approach.
- Design velocity recommendations (service level and ultimate) apply to all four vessels. No definitive distinction between vessel displacement and approach speed was observed.
- Use Design Example 1 for landings that are similar to Auke Bay, in terms of vessel displacement and environmental/approach conditions.
- Use Design Example 2 when considering vessels with displacement other than those studied at Auke Bay.
- Berthing and fender force values are a function of fender stiffness and thus are unique to Auke Bay. Use design energy values to derive the required force.

Areas for Further Study

The primary limitation associated with the statistical approach to determining berthing energy is obtaining a sufficient number of measurements relevant to the desired berthing situation. This report focuses primarily on design parameters anticipated at Auke Bay for a combination of berths from all four vessels, but measurements for each separate vessel were

limited. The number of berthing measurements for the two largest vessels—the Kennicott and the Columbia—were insufficient to formulate any definitive relationships between vessel displacement and load. A future study would focus on obtaining a stronger set of measurements for a wider array of vessels to compare vessel displacement to various load parameters. The same study could also be conducted for the stern berth portion of Auke Bay.

Calibration of the results of this study with the ACI, AISC, and NDS timber codes would yield an accurate load and resistance factor design (LRFD) methodology. In this case, the LRFD method could be readily applied to future designs. To accomplish this methodology, the reliabilities of the demands must be calibrated with the reliabilities used to formulate the LRFD standards of practice.

Chapter 7B – Conclusions: Seattle

General

Selection of an appropriate design berthing energy is reliant on subjective decisions made by engineers with years of experience in marine structural design. Structures that prove to be resilient over their lifespan provide little information regarding the actual amount of energy they absorb. Without evidence regarding the loading conditions experienced by the structure, design is based on trial and adjustment. Uncertainties related to vessel-structure interaction and loading conditions are applied as berthing coefficients based on assumptions. Providing engineers with information regarding the actual demands placed on the structure allows for less reliance on subjectivity and results in more reliable and efficient designs.

Substantial research is available to assist facility designers in the shipping industry. This information corresponds to vessels with displacements of approximately 20 to 100 times the vessel displacements of the Washington State Ferries (WSF) fleet. Although these studies may expand analytical techniques and provide increased understanding of the berthing process, they are of limited applicability for engineers studying high-frequency ferry landings.

Advanced mathematical techniques and the use of software to analyze vessel-fluid-structure interactions allow the consideration of a range of options for varying berthing situations. The use of these techniques, however, requires highly trained individuals, is expensive, and has practical limitations for design professionals. The berthing maneuver of a ship represents a very complicated system that is dependent on many systems that are difficult to model, such as vessel piloting, the environment, and hydrodynamic effects.

Measurements of the berthing process capture all aspects of the berthing ship and provide the designer with a representation of the actual energy absorbed by the structure, which ultimately is the metric of concern to the design engineer. Compiling information for a sample of statistical relevance then allows for a more complete picture of the berthing demand placed on the structure. In the presence of a statistically significant sample of berthing events, the traditionally employed Kinetic Energy Method is obsolete. Empirical and statistical techniques provide a comprehensive understanding of the load environment, and provide a rational basis by which an engineer can implement a reliable and efficient design.

Findings

This study investigated and characterized thousands of ferry berthing events at the Bremerton slip of the Seattle ferry terminal. The findings of this research further the understanding of vessel-structure interaction and the load environment at the Bremerton slip. Due to the challenges of obtaining pertinent berthing demand data for ferries, the information from this study will serve to bridge the gap between design assumptions and operational realities. Another component of the analysis is to present design utilities based on statistical techniques and reliability engineering principles. Application of probability distributions to a large empirical sample allows extreme event parameters to be estimated by a probability of occurrence. The development of reliability-based tools is intended to quantify the likelihood of extreme events and provide designers a methodology to rationally determine service and ultimate berthing load parameters.

The wingwall structures at the Bremerton slip, which have significant excess capacity, have handled berthing demands without issue over the past 20 years. The maximum berthing energy recorded was less than 40% of the current design criteria.

This report focuses on the development of probability-based occurrences of berthing load demand, and facilitates a transition to a LRFD-based design methodology. The major assumptions associated with this approach are (1) that the extreme values are, in fact, approximated reasonably well by the selected probability density function; and (2) that the empirical data represent a stationary random process; that is, the year the facility was monitored is considered a typical year, and the associated statistical properties do not vary over time. The service and ultimate loads presented are based on probabilities associated with design values occurring or being exceeded. Service loads represent the maximum loads that the wingwalls experience on a regular basis. Ultimate loads represent the maximum loads the wingwalls are expected to experience over their service life. Both service and ultimate loads represented in this study are based on reliability levels arbitrarily chosen by the authors, and may not reflect the desired reliability level of the WSF.

Dissipation of kinetic energy associated with a berthing vessel is a complex process in which significant uncertainty is associated with the load environment. Quantifying this load environment with the characterization of nearly 7000 impact events provides information that can be confidently used by a design engineer to refine future structural designs.

Summary

The following is a compilation of findings, comments, and recommendations from the project:

- The WSF terminals are often characterized as end-berthing facilities as opposed to side-berthing facilities. The WSF terminal berths are shaped more like pockets, with the wingwalls oriented at 40 degrees to the berthing vessel. This arrangement allows vessel landings that share characteristics of side-berthing and end-berthing maneuvers, or something completely different from these two berthing maneuvers.
- The current WSF design assumption is based on the premise that the vessel contacts both wingwalls simultaneously and loads both wingwalls with approximately the same energy. After characterizing events over the past year, we have observed that each wingwall is subject to independent impacts and that the impact energy associated with the north and south wingwalls is rarely equal.
- Analysis of berthing events reveals that a vessel impacts each wingwall multiple times per berthing event, and the initial impact may, or may not, be the most significant.
- Approach velocity is a challenging quantity to measure accurately. It is most relevant at the point of impact and may be misleading when measured at even small distances from the impact location. Rotational velocity effects are present and may have significant effects on the kinetic energy of the berthing vessel. Eccentricity coefficients from the literature may not be appropriate for the berthing scenario common at the Bremerton slip.
- Kinetic energy estimates based on small approach velocities tend to substantially underestimate the amount of kinetic energy the structure absorbs, suggesting that the combination of ship propulsion and environmental and rotational velocity components may contribute significant amounts of energy to the berthing process.

- The wingwall system installed at the Bremerton slip contains substantial excess capacity based on the observation of this study.
- The transfer of energy to the wingwalls varies with each berthing event because of the effects of the propeller and rudder, and the effects of weather.
- The empirically determined kinetic energy data used in conjunction with the reliability-based approach represent a logical paradigm for developing design energies.
- Reliability design charts and tables offer a concise method of approximating design berthing energy demands over a given service life.
- Berthing factor results allow the empirical energy data to be used for vessels of different classes (displacements) than were recorded at the Bremerton slip.
- The berthing coefficient recommendations are general in nature, because the maximum energy absorbed by the berthing structure often includes additional effects unrelated to the initial kinetic energy of the vessel. In this study, a few examples of effects that were impossible to isolate were the use of the ship's controls (rudder[s]), the propulsion system, and wind, wave, and tidal effects. Therefore, it is recommended that the berthing coefficient results be used for preliminary inquiries only.
- Point-of-impact results provide information that could be used to refine the geometry and placement of the wingwall impact face.
- The existence of a statistically significant sample of energy absorbed by the structure renders the Kinetic Energy Method obsolete

Areas for Further Study

Future research concerning the load environment of ferry terminals could focus on similar instrumentation schemes for the current generation of reaction frame wingwall systems used by the WSF. Another area of study could focus on instrumentation of a terminal that services a larger class of vessel. By focusing on a terminal that handles the largest vessels, Jumbo Mark II class, the berthing factor approach could be validated and provide a design berthing energy chart that reduces uncertainties associated with the berthing events of larger vessels. Continuation of this research could liberate terminal design engineers from subjective evaluation of berthing parameters, and future ferry landing design could be more efficient and have a quantifiable degree of reliability. If the Kinetic Energy Method is still a priority for designers in the WSF staff, more study could be directed at investigating the rotational velocity (and associated rotational kinetic energy) component that is associated with berthing maneuvers.

Calibration of the results of this study with the ACI, AISC, and NDS timber codes would yield an accurate load and resistance factor design (LRFD) methodology. In this case, the LRFD method could be readily applied to future designs. To accomplish this methodology, the reliabilities of the demands must be calibrated with the reliabilities used to formulate the LRFD standards of practice.

References

ANSYS (2012). ANSYS Aqwa. from http://www.ansys.com/Products/Other+Products/ANSYS+Aqwa.

Beckett-Rankine (2010). Berthing Velocities and Brolsma's Curves. London, Beckett Rankine Marine Consulting Engineers.

Brolsma, J. U. (1977). On Fender Design and Berthing Velocities. PIANC 24th International Naval Congress, Leningrad, U.S.S.R.

BSI (1994). British Standard: Maritime Structures. Part 4: Code of practice for design of fendering and mooring systems. England, British Standard Institute.

Costa, F. V. (1964). The Berthing Ship: The Effect of Impact on the Design of Fenders and Other Structures. The Dock & Harbour Authority.

Cummins, W. E. (1962). The Impulse Response Function and Ship Motions, Department of the Navy.

Dent, G.E. and Saurin, B.F. (1969, Nov.). "Tanker Terminals Berthing Structures". In *Conference on Tanker and Bulk Carrier Terminals*, Institute of Civil Engineers.

Dickenson, S. E. (2007). Instrumentation and Monitoring of Port Facilities: Planning, Funding, Field Applications, and Long Term Benefits. ASCE Ports 2007: 30 Years of Sharing Ideas…1977-2007. San Diego, California, ASCE-TCLEE Ports Lifelines Committee.

DOD, U. (2005). Unified Facilities Criteria. Design: Piers and Wharves, U.S. Department of Defense.

Ebeling, C. E. (1997). *An Introduction to Reliability and Maintainability Engineering*. United States: McGraw-Hill Companies, Inc.

Ellingwood, B., et al. (1980). Development of Probability Based Load Criteria for American National Standard A58. Washington, D.C., U.S. Department of Commerce, National Bureau of Standards.

Fontijn, H. L. (1980). The Berthing of a Ship to a Jetty. *Journal of the Waterway, Port, Coastal, and Ocean Division*, WW2 (15407): 239-259.

Fontijn, H. L. (1988). On the prediction of fender forces at berthing structures Part II:Ship berthing related to fender structure. NATO Advanced Study Institute of Advances in Berthing and Mooring of Ships and Offshore Structures, Trondheim, Norway, Kluwer Academic Publishers.

Gaylord, E. H., et al. (1992). Design of Steel Structures. United States, McGraw Hill, Inc.

Gaythwaite, J. W. (2004). *Design of Marine Facilities for the Berthing, Mooring and Repair of Vessels.* Reston, Virginia, ASCE.

Girgrah, M. (1977). *Practical Aspects of Dock Fender Design.* PIANC 24th International Navigation Congress, Leningrad, PIANC.

Hutchinson, J. (2011). Characterizing the berthing load demand at Alaska DOT&PF ferry landings. Thesis. May 2011. University of Alaska Fairbanks. Fairbanks, Alaska

Jahren, C. T. and R. Jones (1993). Ferry Landing Design. Phase 1, Washington State Transportation Center, Washington State Department of Transportation, U.S. Department of Transportation, Federal Highway Administration.

Jahren, C. T. and R. Jones (1996). Design Criteria for Ferry Landings. *Journal of the Waterway, Port, Coastal, and Ocean Engineering* (July/August 1996): 187-195.

Jahren, C. T. and S. J. Margaroni (1993). Vessel Tracking Methods for Ferry Landing Design. Seattle, Washington, Washington State Transportation Center (TRAC), Washington State Department of Transportation.

Kwiatkowski, J. (2012). Characterizing the berthing load environment of the Seattle Ferry Terminal, Bremerton Slip. Thesis. December 2012. University of Alaska Fairbanks. Fairbanks, Alaska

MARIN, M. R. I. N. (2012). MARIN website. from http://www.marin.nl/web/Facilities-Tools/Software/Offshore-Multibody-Software.htm.

Petroski, H. (2000). *Design Paradigms: Case Histories of Error and Judgement in Engineering.* United States, Cambridge University Press.

PIANC (2002). Guidelines for the Design of Fender Systems:2002. Brussels, Belgium.

Playter, D. (1994). The End Berthing Simulation Model. *Civil Engineering*. Seattle, Washington, University of Washington. M.S.: 136.

Rizos, D. C. and E. H. Stehmeyer, Jr. (2004). Software Development for Berthing Analysis and Structural Loading on Waterfront Facilities. *Ports 2004: Port Development in the Changing World*, ASCE, American Society of Civil Engineers**:** 1-10.

Seelig, W. N. and G. Lang (2010). Dynamic Modeling of Ferry Berthing. *Technical Memorandum.* Port Hueneme, California, Naval Facilities Engineering Command.

Toppler, J. F. and J. Weersma (1973). Planning and Design of Fixed Berth Structures for 300,000 to 500,00 DWT Tankers. *Journal of Petroleum Technology* (July 1973): 764-774.

Transportation, W. S. D. o. (2012). from http://www.wsdot.wa.gov/ferries/.

Tsinker, G. (2004). *Port Engineering; Planning, Construction, Maintenance, and Security.* Hoboken, New Jersey, John Wiley & Sons, Inc.

Ueda, S., et al. (2002). *Reliability Design Method of Fender for Berthing Ship.* PIANC 2002, 30th International Navigation Congress, Sydney, Australia.

Ueda, S., et al. (2001). *Statistical Design of Fenders for Berthing Ship*. 11th International Offshore and Polar Engineering Conference, Norway, International Society of Offshore and Polar Engineers.

WSF (2012). Terminal Design Manual, Washington State Department of Transportation. **1**.

Appendix

Estimating Mooring Line Loads from Strain Measurements of a Steel Pipe Bollard: Feasibility Study

Andrew T. Metzger, Ph.D., P.E.
Assistant Professor
Department of Civil Engineering
University of Alaska Fairbanks
Fairbanks, AK 99775

Jonathan Hutchinson, BSCE, EIT
Alaska Department of Transportation and Public Facilities
Fairbanks, AK 99709

Abstract

Estimation of mooring line loads with direct measurements is a sparse area of study. However, this prospect is very attractive from the perspective of validation of current analysis methodology used in estimating mooring line forces for vessels secured to berthing structures, i.e., piers, docks, etc. Proprietary mooring hardware that includes hardware and software platforms for measuring mooring line forces is available but is costly and must be built-in to a facility. These devices are often not feasible for existing structures. The purpose of this technical note is to present results of a study of the feasibility of instrumenting an existing steel pipe bollard in such a fashion as to estimate the force and orientation of a mooring line slung around it. The technique described here uses elementary Solid Mechanics theory and strain gauges. The strain gauges used in this study are the weld-able-type designed for extended use in an outdoor environment. The feasibility study was conducted in a laboratory environment by applying a known force vector to a pipe bollard mock-up with a rope. Various magnitudes and orientation of the force were applied to the mock-bollard. Strain measurements were used to estimate the force. The calculated force was compared to the actual and results are shown graphically and in tabular form. In general, the method described herein provided results that agreed reasonably well with actual force values for cases where the vertical angle of the mooring line, with respect to the horizontal plane, was relatively small.

Introduction

Estimation of mooring line loads with direct measurements is a sparse area of study. However, this prospect is very attractive from the perspective of validation of current analysis methodology used in estimating mooring line forces for vessels secured to berthing structures, i.e., piers, docks, etc. Proprietary mooring hardware that includes hardware and software platforms for measuring mooring line forces is available. However, it is costly and must be built into the dock structure. There do not appear to be any such products for existing mooring hardware, not already designed for making measurements.

The purpose of this technical note is to present results of a study of the feasibility of instrumenting a steel pipe bollard in such a fashion as to estimate the force and orientation of a mooring line slung around it. The technique described here uses elementary Solid Mechanics

theory and strain gauges. The strain gauges used in this study are the weld-able-type designed for extended use in an outdoor environment. The feasibility study was conducted in a laboratory environment by applying a known force vector to a pipe bollard mock-up with a rope. Various magnitudes and orientation of the force were applied to the mock-bollard. Strain measurements were used to estimate the force. The calculated force was compared to the actual and results are shown graphically and in tabular form.

In general, the method described herein provided results that agreed reasonably well with actual force values for cases where the vertical angle of the mooring line, with respect to the horizontal plane, was relatively small.

This work represents a first-step in the development of a simplistic, readily implemented, means of estimating mooring line forces at an existing marine vessel berthing facility.

Literature Review

The estimation of mooring line loads on port facilities has not been studied extensively. The current design process generally involves obtaining an estimate of environmental conditions for a particular site. Loads are calculated based on these anticipated environmental demands (UFC 2005).Load demands are usually based on mathematical models or results from scaled laboratory testing.

There is a perceived need among engineers that design berthing structures to verify forces from mooring lines. This is true not only for environmental demands but during tie-up procedures. While complete vessel breakouts are not a common occurrence, small-scale mooring accidents (i.e. partial breakouts) are more frequent and repairs can be expensive if a pier or vessel is damaged.

Because of the complexities of calculating environmental loads that cause mooring line forces, mathematical and physical scale models are often used in their estimation (Gaythwaite 2004). Environmental conditions causing mooring line forces include: wind, waves, currents and other passing vessels. Other causes include winching of lines during vessel tie-up and tidal changes. For any of these, the character of the mooring line forces can be site specific.

Very little empirical data is available to validate the mathematical and/ or scale physical model estimates of mooring line forces. A study conducted by the Hydraulic Research Center of the Canadian Coast Guard (Eryuzlu, N.E. and Boivin, R. 1978) compared the results from scaled model tests to an analytical model purchased from a private consultant. It was concluded that analytical models should be used with extreme caution, preferably as a backup method for design. Furthermore, it was recommended that in the presence of severe conditions, full scale mooring line data become increasingly necessary.

Recognizing the current shortage in analytical mooring load prediction methods and available empirical data, particularly in extreme environmental conditions, the development and implementation of Mooring Load Monitoring Systems (MLMS) has rapidly grown in popularity over the last few decades (Barr, et al. 1979). A number of proprietary MLMS products exist, each with its own hardware and software platforms for determining mooring line forces. The products tend to be costly and must be built into the structure. In general, MLMS products are intended to be used for in-service operational and safety monitoring.

The literature is virtually devoid of studies that validate mathematical or scale model results for determining mooring line loads. However, breakouts do occur. There is a perceived need to verify mooring line design load criteria. However, it would be cost-prohibitive to re-fit mooring hardware with MLMS, in many cases. A means to estimate mooring line forces using existing mooring hardware is attractive and would have great utility in verifying design methodology like that published in (UFC 2005).

Theory

If a thin circular ring is subjected to pure bending, as shown in Figure 1, the normal stresses in the ring may be determined with the Flexure Formula.

$$\sigma_y = -\frac{M_{X'} z'}{I} \tag{1}$$

Where y is positive out of the page and z' may be expressed with:

$$z' = r\sin\left(\frac{\pi}{2} + (\alpha - \theta)\right) = r\cos(\alpha - \theta) \tag{2}$$

For the normal stress at the outer perimeter of the ring:

$$z_o' = r_o \cos(\alpha - \theta) \tag{3}$$

Where: r_o is the outer-radius of the ring.

Substituting Equation 3 into Equation 1 results in Equation 4:

$$\sigma_y = -\frac{M_{X'}}{S}\cos(\alpha - \theta) \tag{4}$$

Where: $S = \frac{I}{r_o}$; i.e., the section modulus of the ring

It can be seen from Equation 2 that the stress distribution is sinusoidal around the ring. This is illustrated in Figure 2.

If an axial force coincident with the 'Y' axis, in the positive direction, at a distance from the cross-section sufficient to result in uniform normal tensile stresses, is applied simultaneous with the bending moment, the stress at the perimeter of the ring may be expressed by Equation 5.

$$\sigma_y = \sigma_t - \sigma_A \cos(\alpha - \theta) \tag{5}$$

Where: $\sigma_t = \frac{T}{A}$; normal tensile stress

T is the axial force

A is the cross-sectional area of the ring

$$\sigma_A = \frac{M_{X'}}{S}$$

Hypothesis:

If stresses σ_1, σ_2 & σ_3 *at locations* $\theta_1 = -\frac{\pi}{2}$, $\theta_2 = \frac{\pi}{2}$ & $\theta_3 = 0$, *(respectively; as shown in Figure 2) are known, the following equations may be used to determine the loads applied to the thin-ring system:*

$$\sigma_t = \frac{\sigma_1 + \sigma_2}{2} \tag{6}$$

$$\alpha = \tan^{-1}\left[\frac{\sigma_1 - \sigma_2}{\sigma_1 + \sigma_2 - 2\sigma_3}\right] \tag{7}$$

$$\sigma_A = \frac{\sigma_1 + \sigma_2 - 2\sigma_3}{2\cos(\alpha)} = \frac{\sigma_1 - \sigma_2}{2\sin(\alpha)} \tag{8}$$

(see derivation at the end of this appendix)

Application of the Theory

We will now apply the theory to a circular pipe bollard supporting a vessel mooring line. This condition is illustrated in Figures 3 and 4.

The line-of-action of the vector of the mooring line force is assumed to intersect the centerline of the bollard at a distance h from the point of strain measurement (pipe cross-section at which σ_1, σ_2 & σ_3 are known). The mooring line force, P, has an angle of inclination, β, and angle, α, with respect to the normal of the dock-face. α also corresponds to a plane normal to the moment vector intersecting the center of the ring in Figure 1.

It is assumed the vertical component of P will induce a tensile stress on the bollard. Relating this to σ_t of Equation 5:

$$P\sin(\beta) = \sigma_t A \tag{9}$$

The moment in the bollard caused by the horizontal component of the mooring line force is:

$$M_{X'} = \left(P\cos(\beta)\right)h \tag{10}$$

Substituting (10) into the σ_A equation of Equation 5:

$$\left(P\cos\left(\beta\right)\right)h = \sigma_A S \tag{11}$$

Rearranging then dividing (9) by (11):

$$\frac{P\sin\left(\beta\right)}{P\cos\left(\beta\right)} = \frac{\sigma_t A}{\frac{\sigma_A S}{h}} \rightarrow \tan\left(\beta\right) = \frac{hA}{S}\cdot\frac{\sigma_t}{\sigma_A} \tag{12}$$

Substituting (6) and (8), then solving for β:

$$\beta = \tan^{-1}\left[\frac{hA}{S}\cdot\frac{\left(\sigma_1+\sigma_2\right)\cos\left(\alpha\right)}{\sigma_1+\sigma_2-2\sigma_3}\right] = \tan^{-1}\left[\frac{hA}{S}\cdot\frac{\left(\sigma_1+\sigma_2\right)\sin\left(\alpha\right)}{\sigma_1-\sigma_2}\right] \tag{13}$$

Solving (11) for P results in an expression for the magnitude of the mooring line force:

$$P = \frac{S}{h\cos(\beta)}\cdot\sigma_A = \frac{S}{h\cos(\beta)}\cdot\frac{\sigma_1+\sigma_2-2\sigma_3}{2\cos\left(\alpha\right)} = \frac{S}{h\cos(\beta)}\cdot\frac{\sigma_1-\sigma_2}{2\sin\left(\alpha\right)} \tag{14}$$

For a small β, the magnitude of the mooring line force may be approximated with:

$$P \approx \frac{S}{h}\cdot\frac{\sigma_1+\sigma_2-2\sigma_3}{2\cos\left(\alpha\right)} = \frac{S}{h}\cdot\frac{\sigma_1-\sigma_2}{2\sin\left(\alpha\right)} \tag{15}$$

In reality, the above implementation of the theory is idealized. The manner in which the mooring line *drapes* around the bollard and crossbar could induce stresses beyond what is accounted for in the discussion. Accounting for other actions aside from tension and pure bending would require a more sophisticated analysis; beyond what will be presented here.

The instrumentation and equipment used for filed implementation has limitations with respect to the theory. As an example, the derivation above use stress determined at a point. The types of strain gages used for field implementation have “foot print” so large as to preclude this, precisely.

In this study, we assessed the degree to which other (undefined) actions may (or may not) influence the validity of the hypothesis. This was accomplished experimentally by applying a known load vector, intended to simulate a load from a mooring line, to a bollard model in laboratory environment. The experimental campaign is presented in the next section.

Experimental Campaign

From the Theory of Elasticity, the axial stress in the pipe bollard may be found with Hooke's Law for tri-axial stress in an isotropic medium:

$$\sigma_y = \frac{E}{(\nu+1)(2\nu-1)}\left[(\nu-1)\varepsilon_y - \nu(\varepsilon_r + \varepsilon_\theta)\right] \tag{16}$$

Where: ε_y = axialstrain

ε_r = radialstrain

ε_θ = tangentialstrain

In this instance of a thin-walled tube, we will neglect the radial strain yielding:

$$\sigma_y = \frac{E}{(\nu+1)(2\nu-1)}\left[(\nu-1)\varepsilon_y - \nu\varepsilon_\theta\right] \tag{17}$$

Therefore, knowing the axial and tangential strains, as well as the material properties, will allow estimation of the longitudinal normal stress, σ_y.

Experimental Approach

The approach taken herein was to build a model of a pipe bollard in a laboratory setting and apply a known load vector with a rope. The load-frame fabricated for this study is shown in Figure 7.The frame is a steel space-truss consisting of a vertical post and horizontal track. The post has nine bolt holes spaced 10" apart vertically along its length. The track has a series of bolt holes designed to accommodate a bollard in eight possible locations transversely along its length. The test frame allows a 0 to 360 degree loading angle variation on the bollard in the horizontal plane (α angle in Figure 3), and a zero to 35 degree variation in the vertical plane (β in Figure 4).

The bollard model is shown in Figure 8 and is intended to be a scaled-down version of an actual bollard (Figure 9) at the Alaska Marine Highway facility at Auke Bay, Juneau, Alaska.

The model consists of a 4" diameter Schedule 40 steel pipewith two ¾" diameter steel tubes welded on the sides that represent the bollard crossbar.

A known load is applied to the model using a rope-puller and measured with a homemade load-cell (Figures 10 &11).The load cell was constructed to measure only tensile force and provides the magnitude of the applied force while the attachment points on the frame define the sense of the force vector.

Ultimately, this methodology will be applied in a field setting to monitor in-service mooring line loads. This will require the use of weld-able strain gages suitable for prolonged outdoor use. Thus, weld-able strain gages were used on the bollard model. The gages used were

manufactured by HITEC Products, Inc. Figures 4, 5 and 6 show schematics of the strain gage locations for field implementation. Figure 12 shows the test apparatus with weld-able strain gages attached. The gages are design to measure strain in the direction of their long dimension.

Each strain gage represents a "quarter bridge" of a Wheatstone Bridge, commonly used in strain measurements. Completion bridges were built (Figure 13) so that each gage was one leg of a Wheatstone Bridge. The bridges were driven by a Campbell Scientific CR5000 datalogger. Measurements were monitored real-time with the Campbell Scientific RTDAQ software and a laptop computer. Figure 14 shows the entire test apparatus.

The datalogger recorded data from the load cell and strain gages simultaneously as the rope was tensioned with the rope-puller. The data was downloaded and the theoretical stresses, calculated with the load-cell force and Equation 5, were compared to stresses calculated with strain measurements and Equation 17.

Experimental Results

Figures 15 through 18 are examples of test data compared with theoretical stresses. This sample of results illustrates significant observations from the experimental campaign. The following is a summary of the results for each plot.

Figure 15: $\alpha = 0^{\circ}; \beta = 0^{\circ}$

The two σ_3 stresses agree well. σ_1 and σ_2 stresses deviate from the theoretical value of 0. The deviation is attributed to shear strains. For this loading condition, the largest shear strains will occur at $\theta = \pm\frac{\pi}{2}$ (Inferred from the *shear formula*; See (Gere and Goodno 2013)). The strain gage weld-tab is subjected to this strain and this is likely the cause of the deviation from 0. The deviation between σ_1 and σ_2 is attributed to tolerances when installing the gages. I.e., the strain gages may not be precisely π radians apart.

Figure 16: $\alpha = 30^{\circ}; \beta = 0^{\circ}$

There was good agreement between theoretical and empirical stresses with this loading condition. Deviations between theoretical and empirically derived stress was only a few percent.

Figure 17: $\alpha = 45^{\circ}; \beta = 20^{\circ}$

In this loading condition, the empirical values tend to agree with the theoretical values. The deviation is notably more than the previous case. Generally, several percent difference (less than 10%).

Figure 18: $\alpha = 30^{\circ}; \beta = 30^{\circ}$

In this case, the deviation noted in Figure 17 tended to increase. Based on the results shown in Figure 16, this breakdown in agreement is attributed to the increasing angle β.

Table 1 is a summary of the range of tests conducted in the experimental campaign.

Results

For the purposes of this study, "reasonable" or "good" agreement will be taken to be ≤ 10% difference between the actual and calculated force or direction. Inspection of Table 1 reveals that in most cases there is good agreement between values of magnitude of the force, P, and the angle in the horizontal plane, α. However, this is not true for an α angle of 0. The error of the latter case is attributed to the small axial strains at locations θ_1 and θ_2 coupled with proximity to maximum shear stress. A general trend was observed that the error in P and α tended to increase as β increased.

In most cases there was not good agreement for the angle with respect to the horizontal plane, β. An exception where agreement was observed was in the special case of $\alpha = 45^\circ$.

Conclusions

The method developed in this feasibility study provides reasonable results for estimating mooring line magnitude and orientation in the horizontal plane. The procedure does not appear to be appropriate for estimating the angle with respect to the horizontal plane, β.

While more refined techniques for strain measurement could be employed, the purpose of the strain measurement scheme is to be durable and readily deployed. More sophisticated means of strain measurement including rosettes, which could yield shear strain information, may not survive a marine environment or the rigors encountered by an in-service mooring bollard.

Appendix Figures and Table

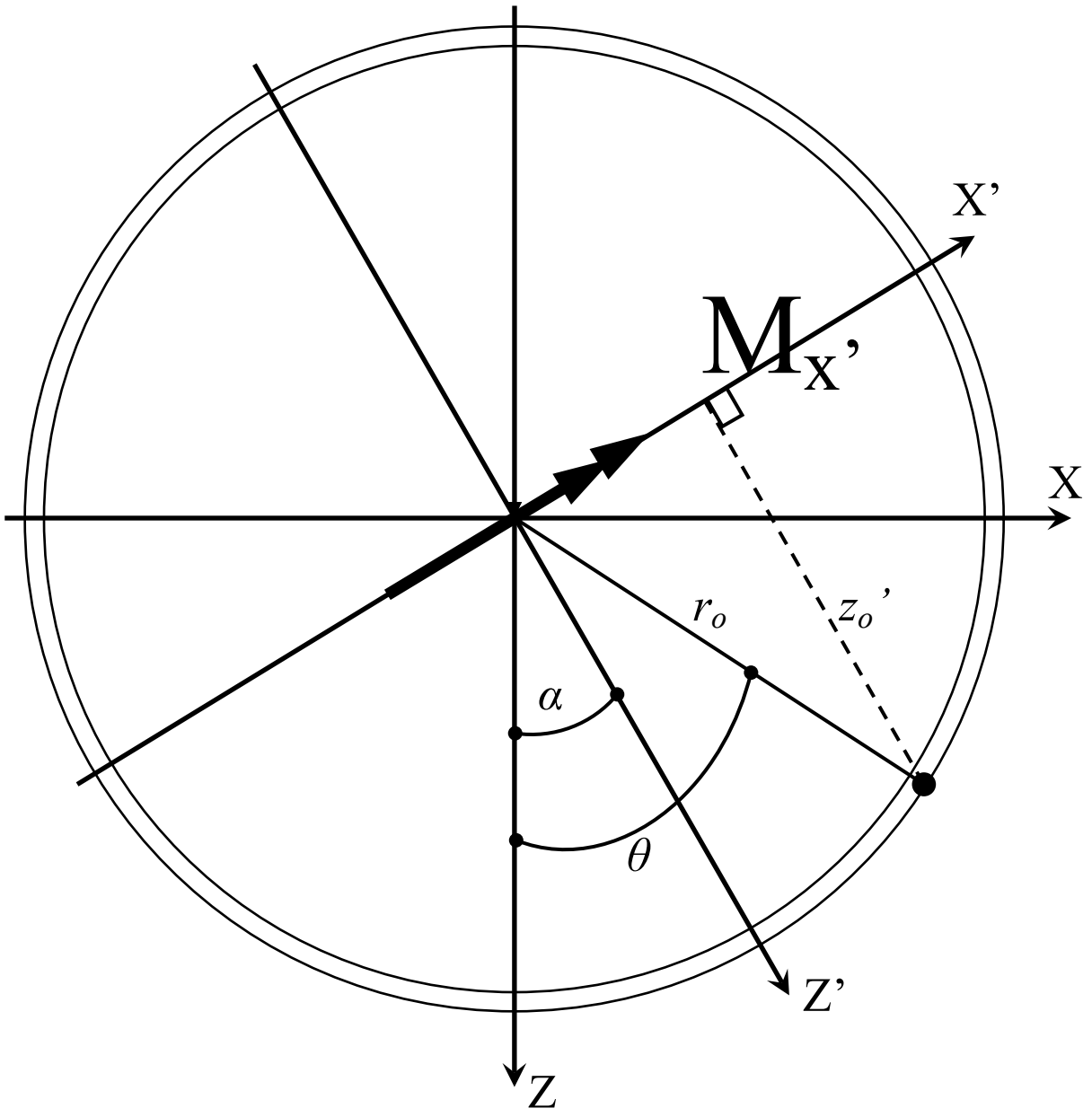

Figure 1: Cross-section of thin ring with applied moment; X' and Z' are orthogonal

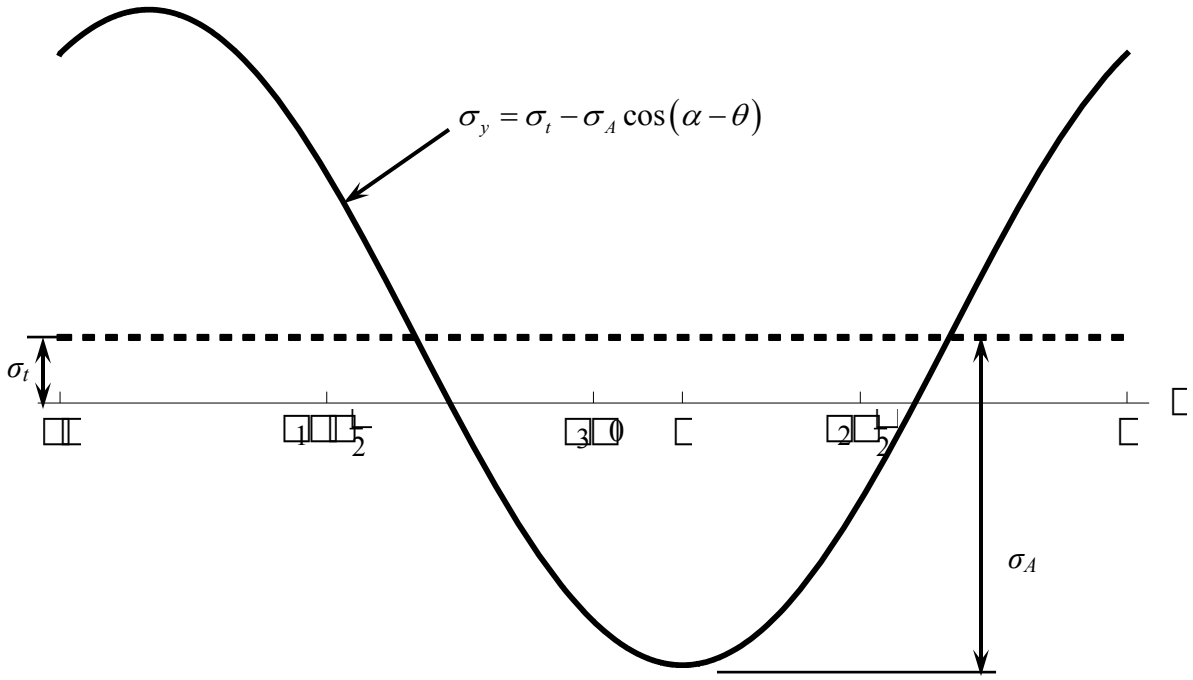

Figure 2: Plot of stress distribution around ring

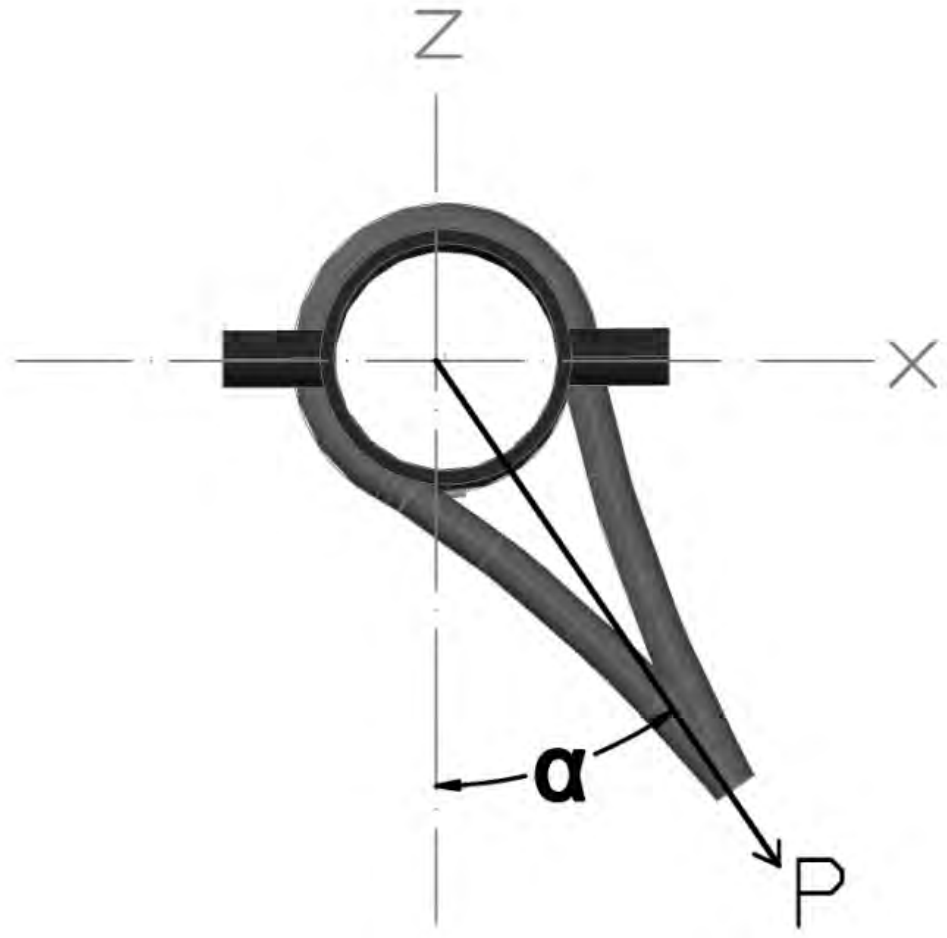

Figure 3: Plan-view of a Pipe Mooring Bollard

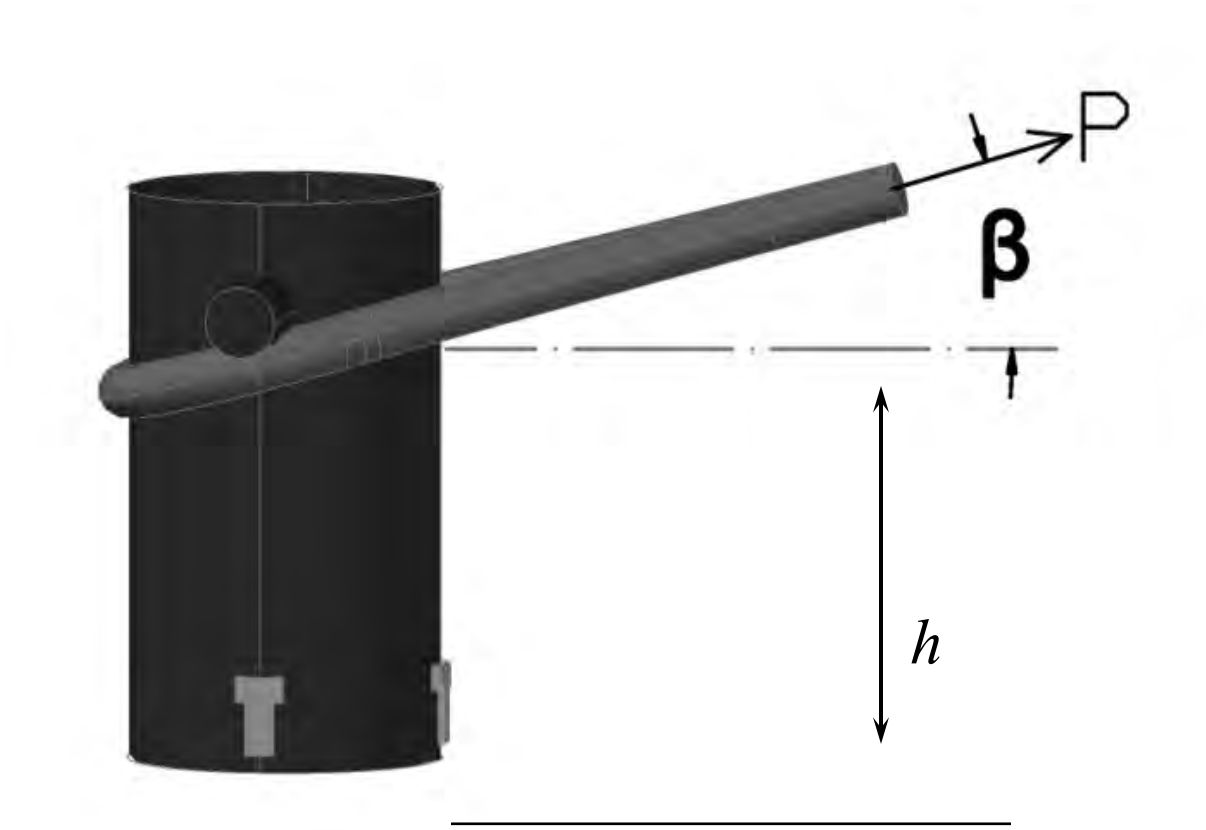

Figure 4: Profile-view of a Pipe Mooring Bollard

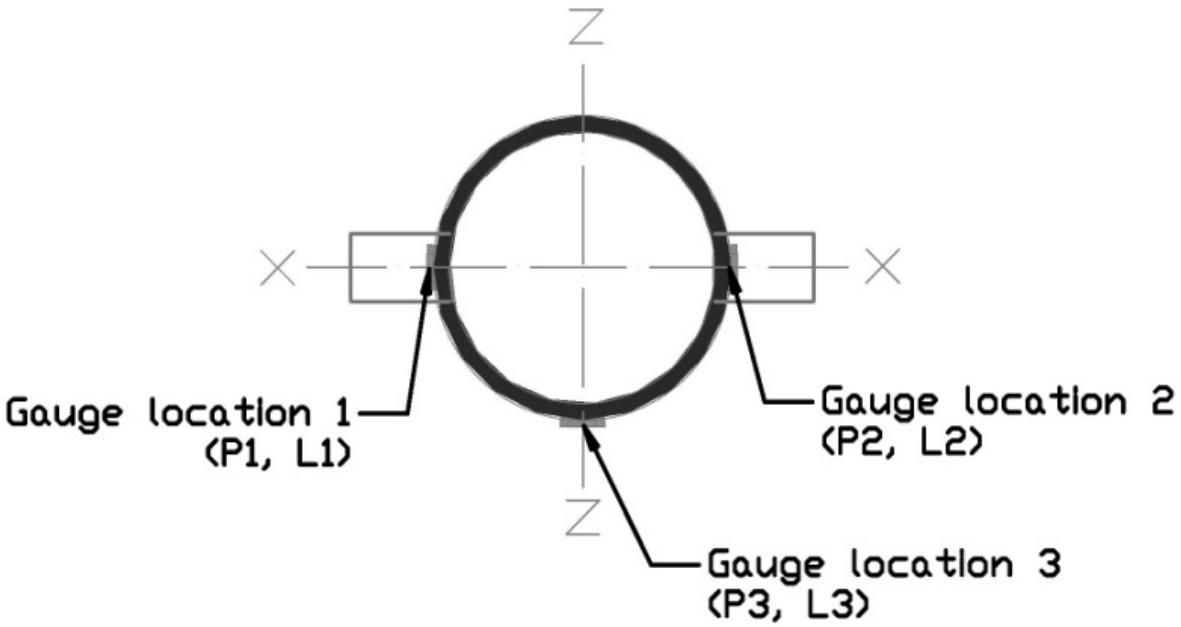

Figure 5: schematic of strain gage locations; “L” – longitudinal gage; “P” – Poisson gage

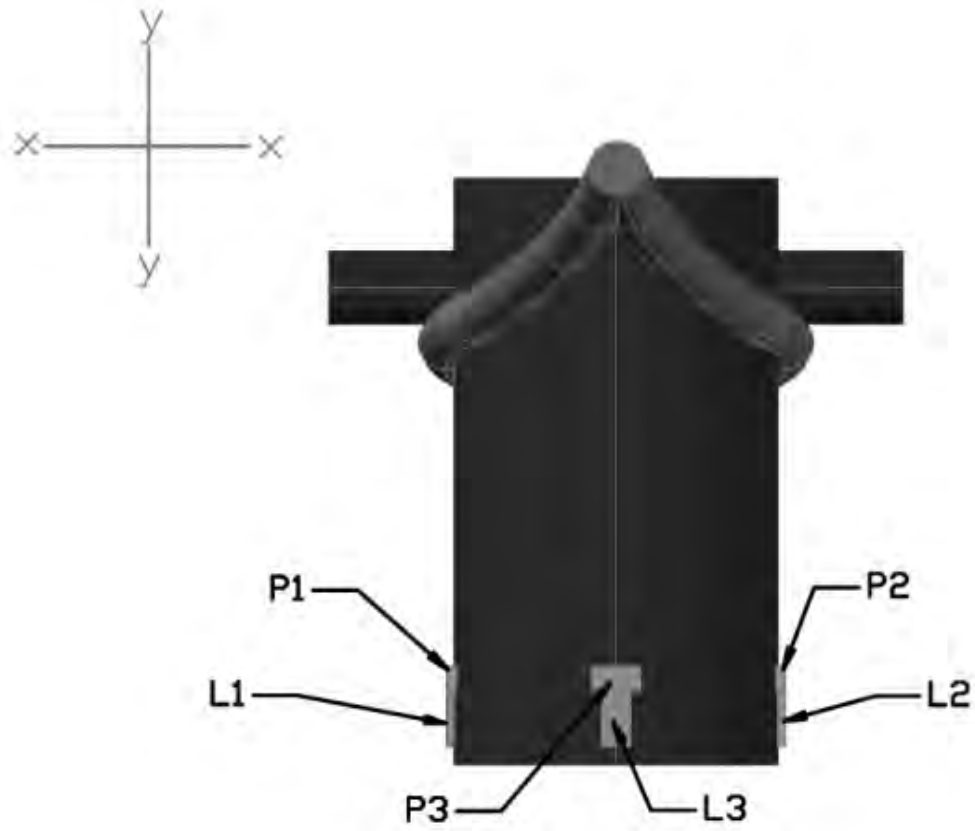

Figure 6: schematic of bollard, mooring line and strain gages from outboard of dock, looking shoreward

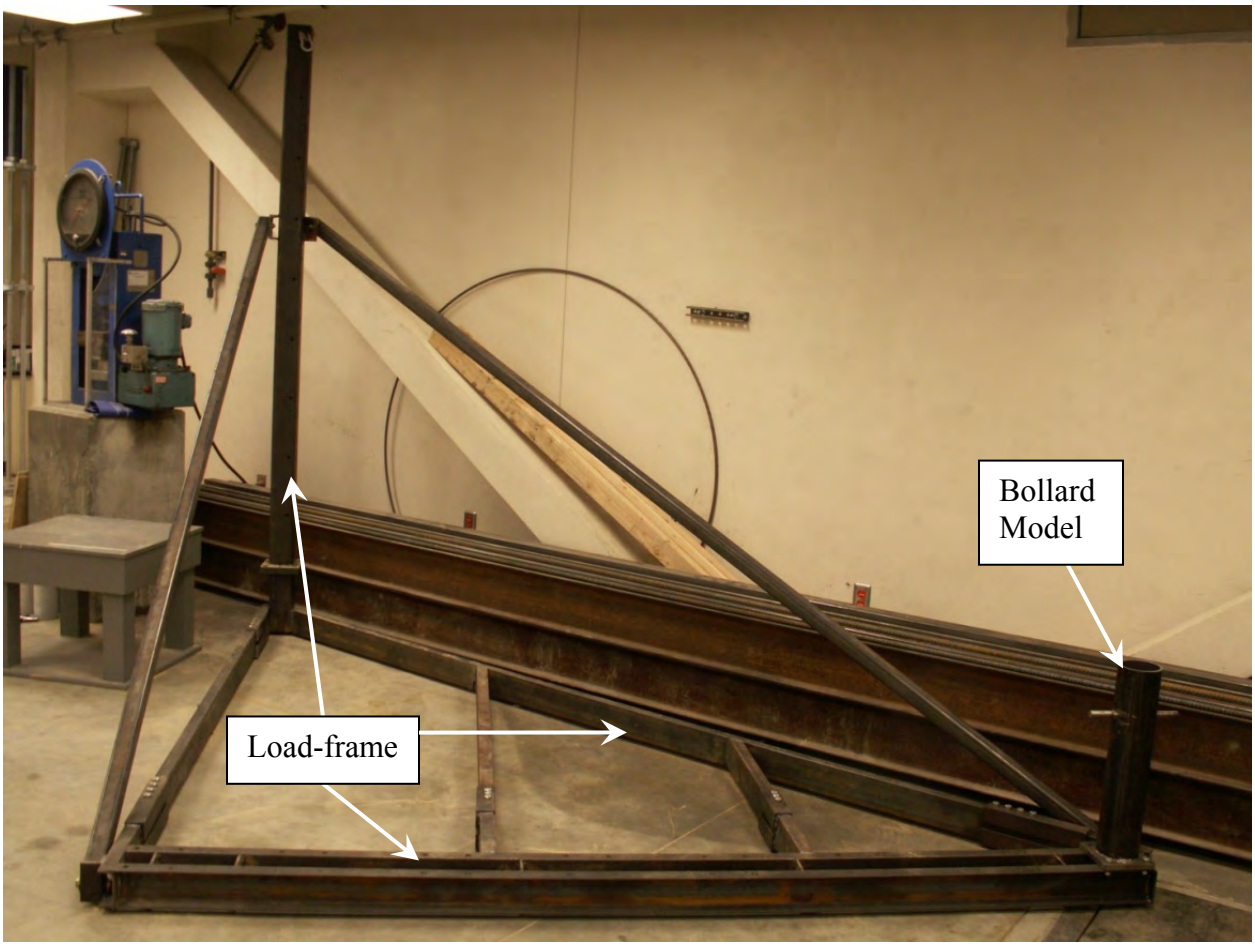

Figure 7: Load frame fabricated for study.

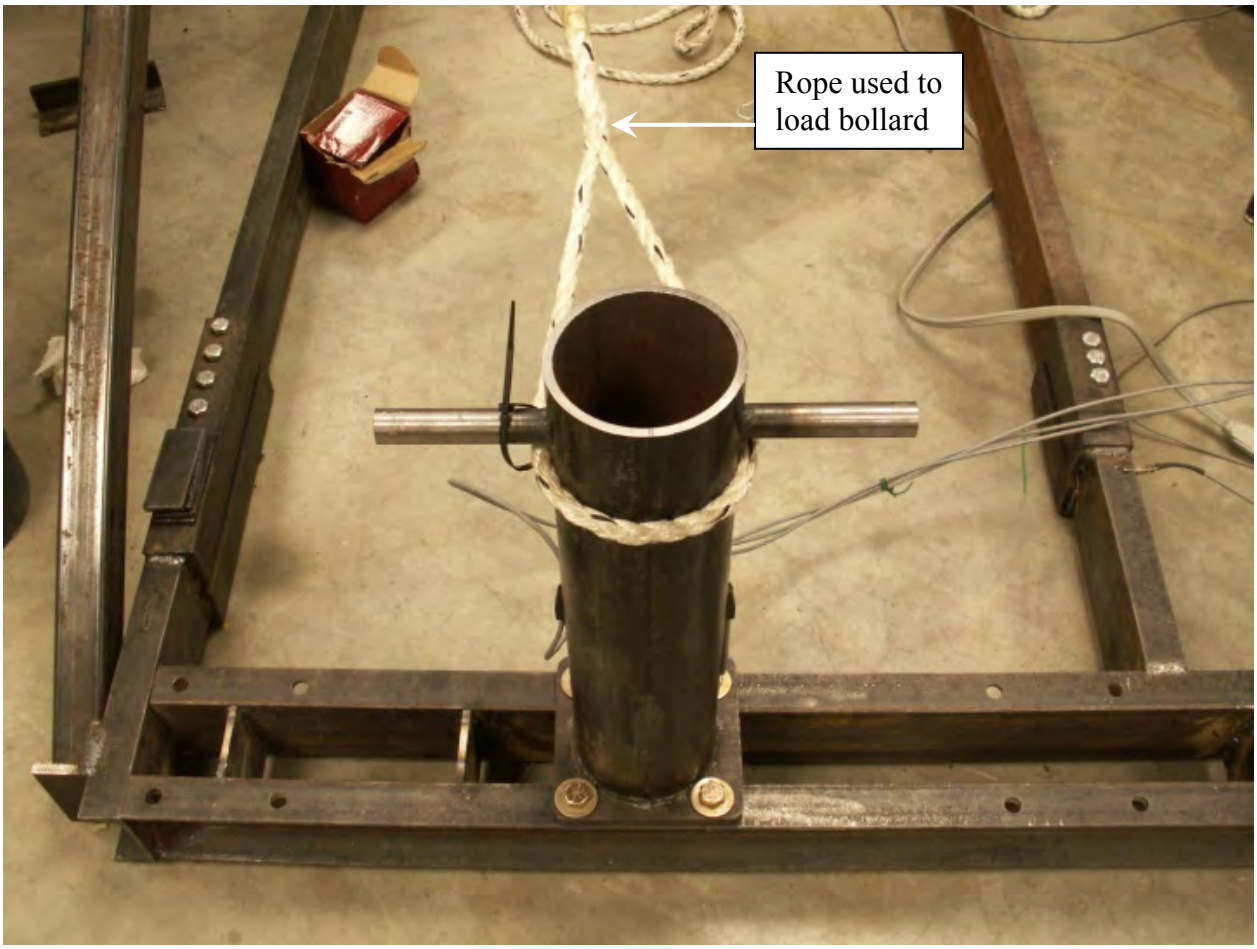

Figure 8: Pipe bollard mock-up

Figure 9: Typical bollard at Auke Bay ferry landing

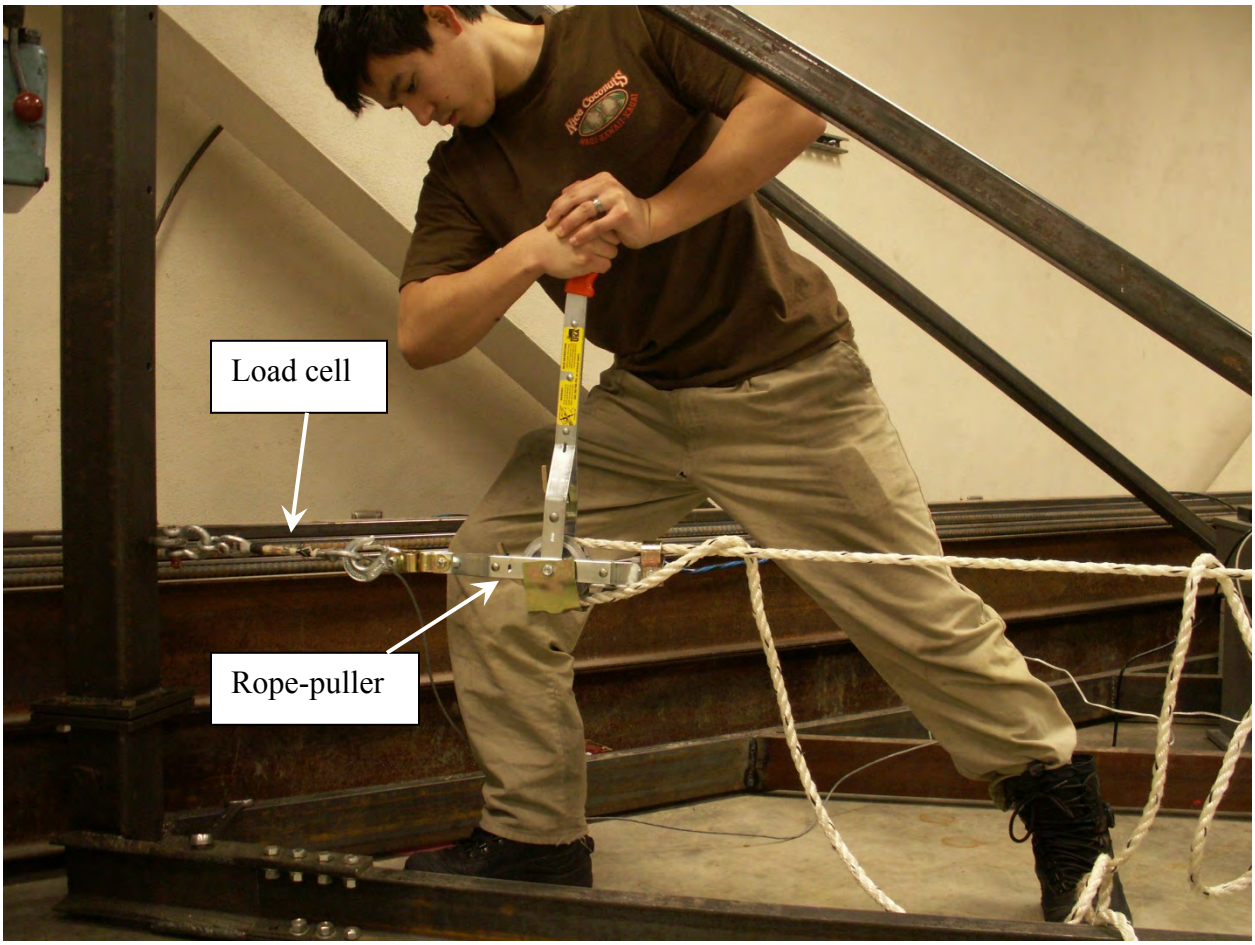

Figure 10: Application of load to the bollard mock-up.

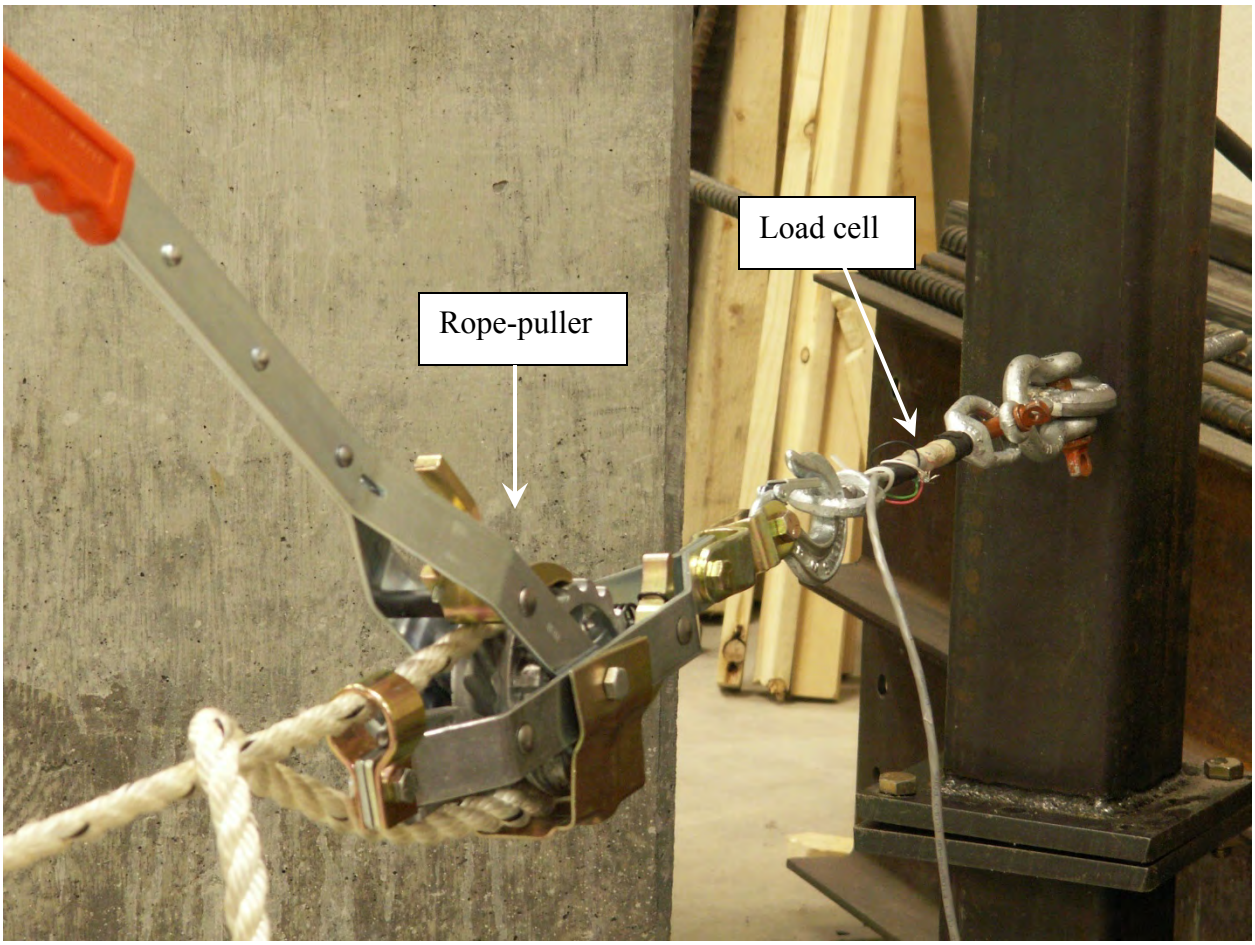

Figure 11: Rope-puller and homemade load-cell

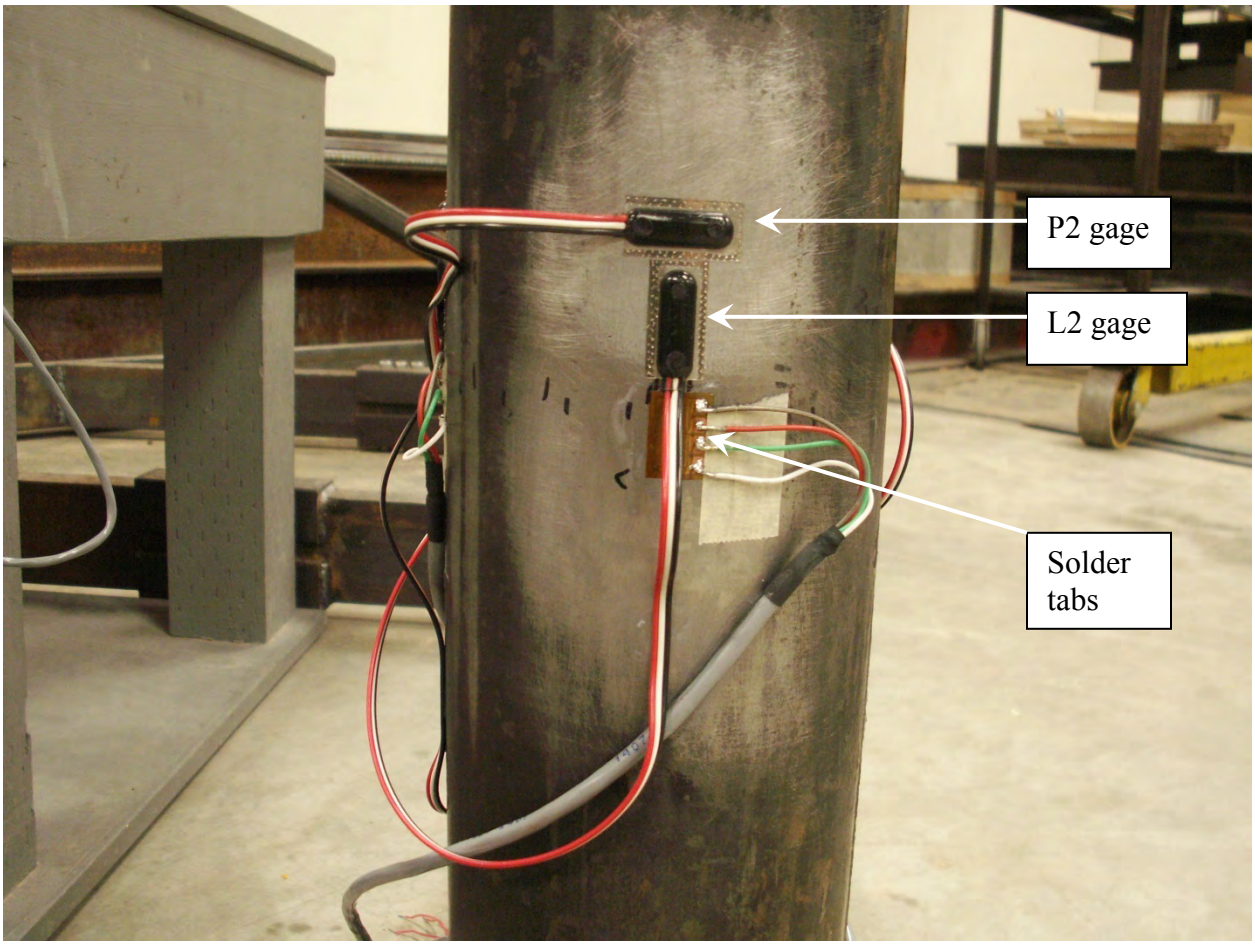

Figure 12: Bollard model showing Position 2 strain gages. (NOTE: solder tabs are from a previous stage when foil strain gages were adhered to the model. This was an intermediate step in the testing program not discussed in the manuscript. The intention was to validate the test apparatus.)

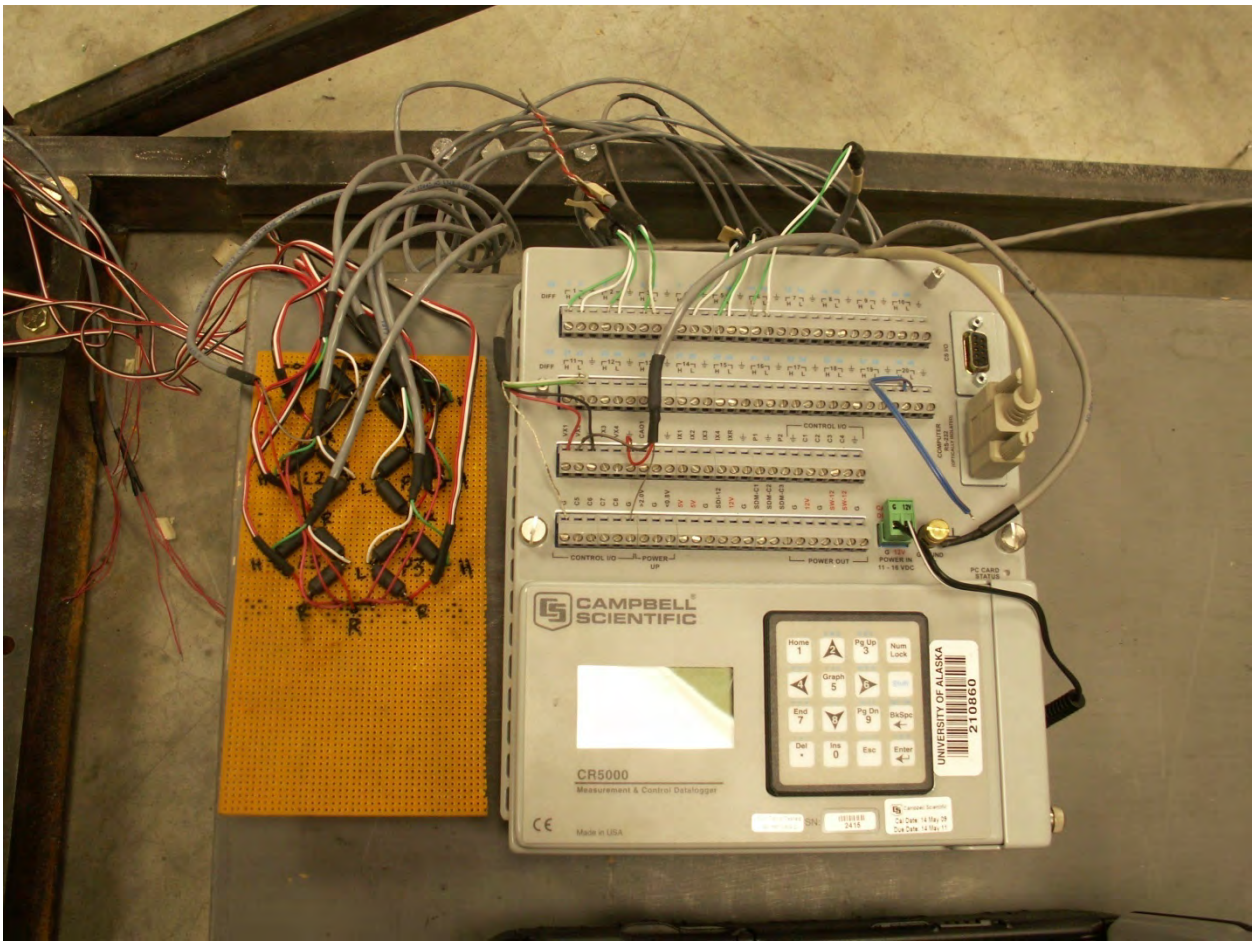

Figure 13: Completion bridges and datalogger

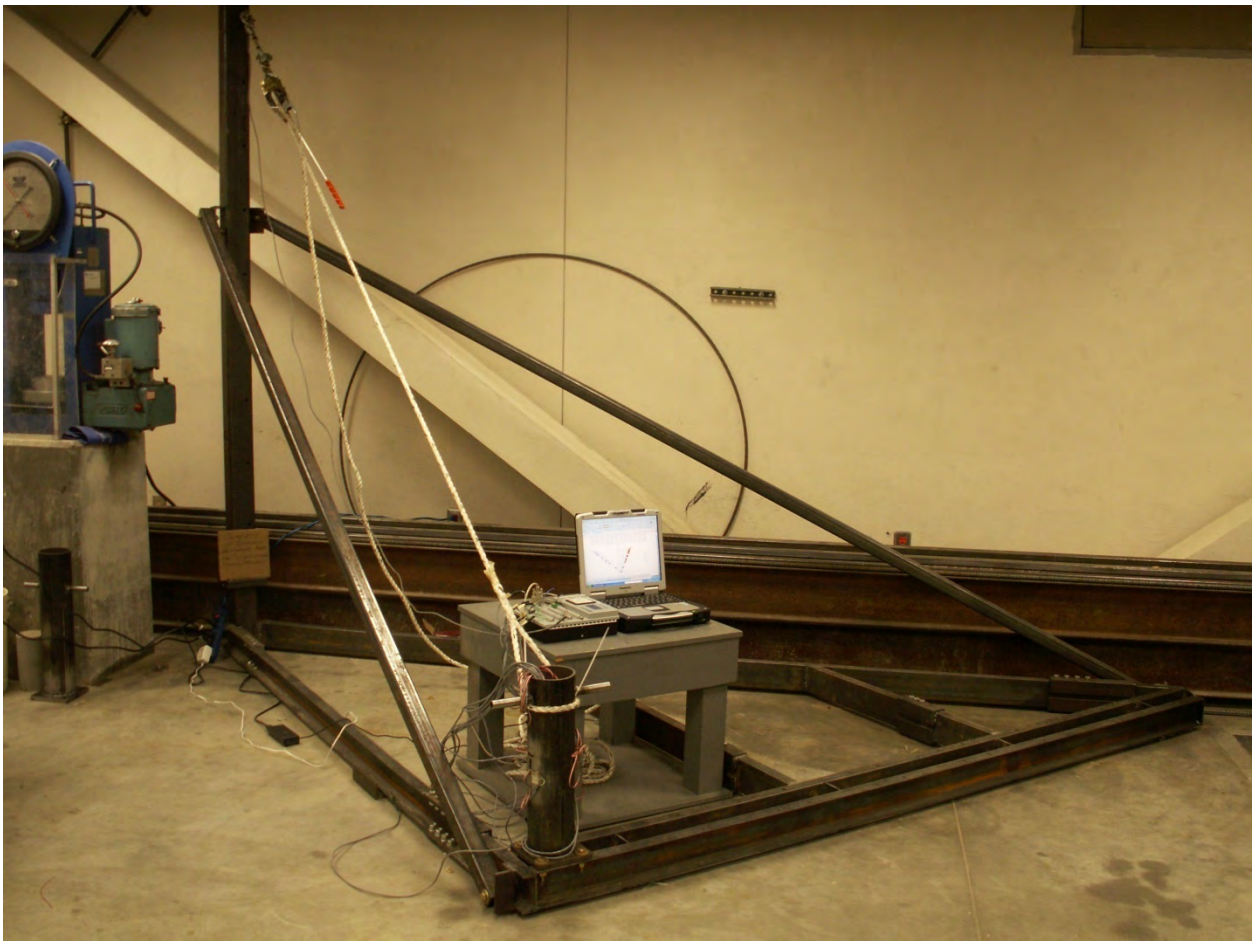

Figure 14: Entire testing apparatus

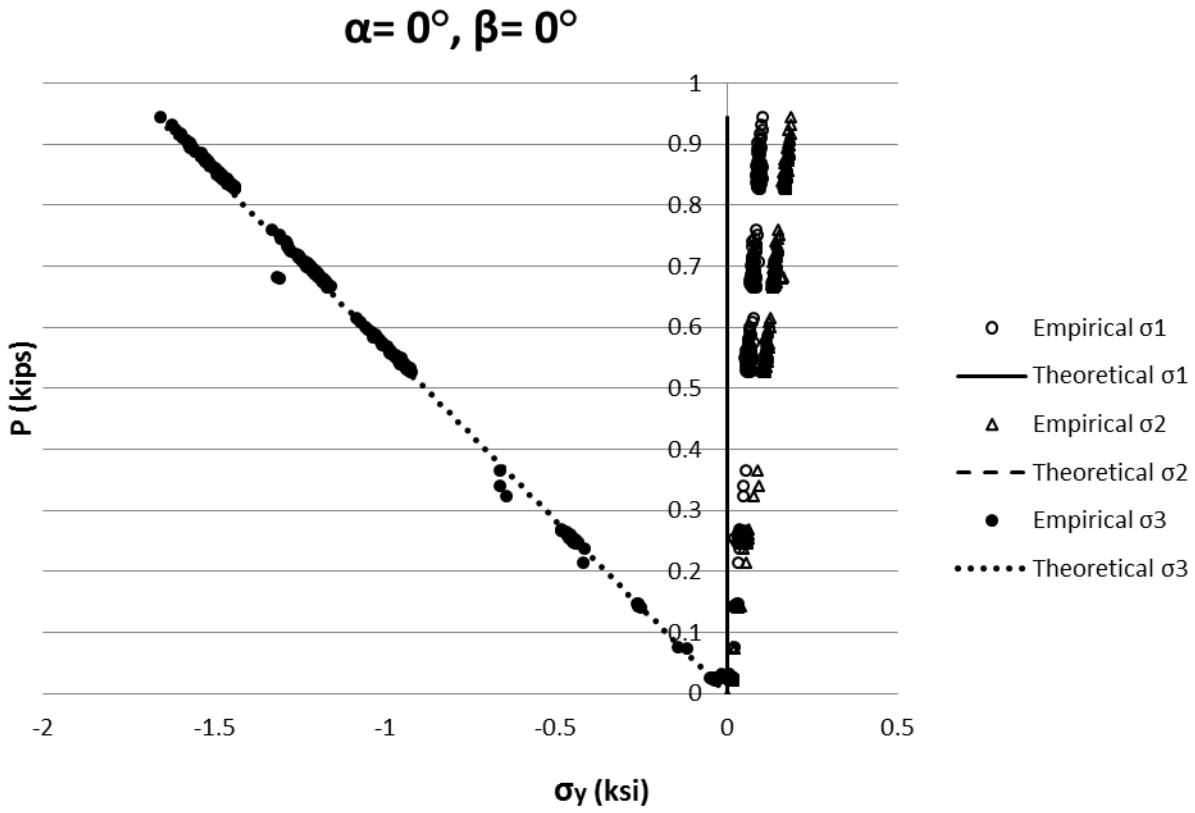

Figure 15: NOTE: Theoretical σ_1 and σ_2 are superposed on the vertical axis.

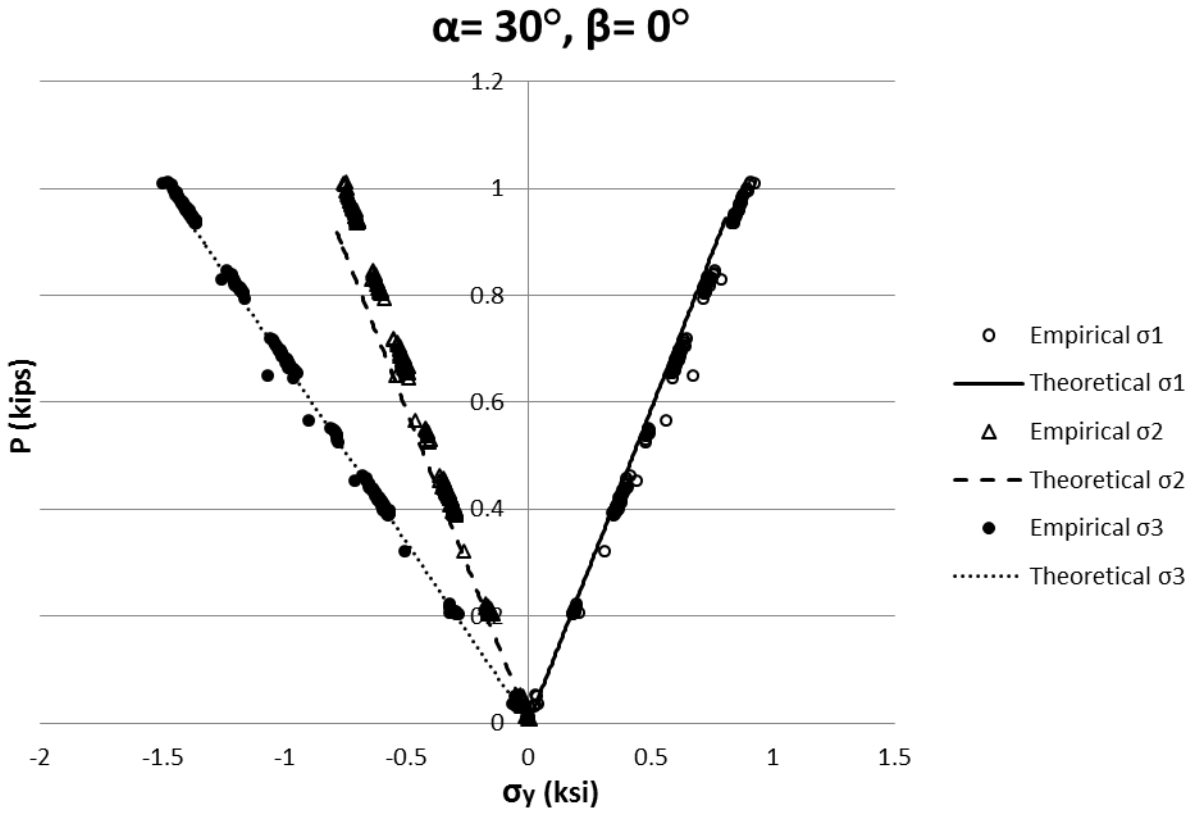
α= 30°, β= 0°
P (kips)
σy (ksi)
1.2
1
0.8
0.6
0.4
0.2
0
-2
-1.5
-1
-0.5
0
0.5
1
1.5
Empirical σ1
Theoretical σ1
Empirical σ2
Theoretical σ2
Empirical σ3
Theoretical σ3

Figure 16

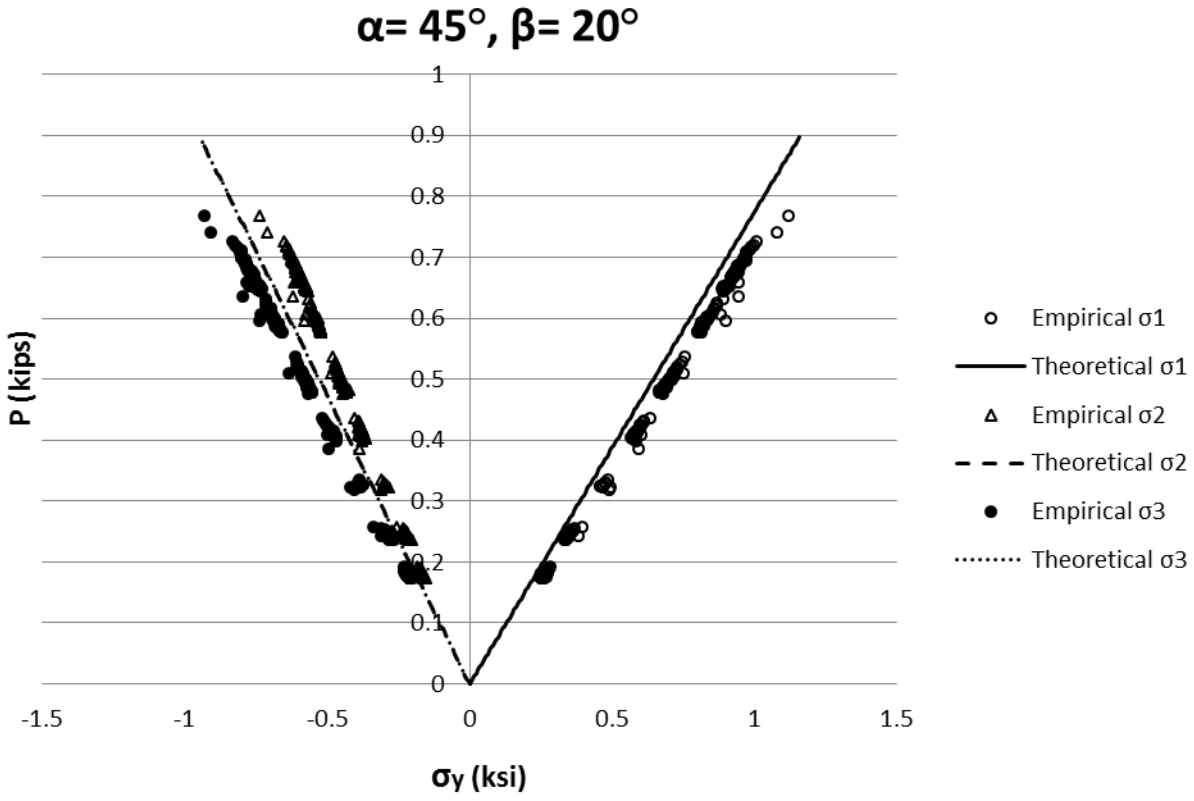

Figure 17: NOTE: Theoretical σ_1 and σ_2 are superposed, left of the vertical axis.

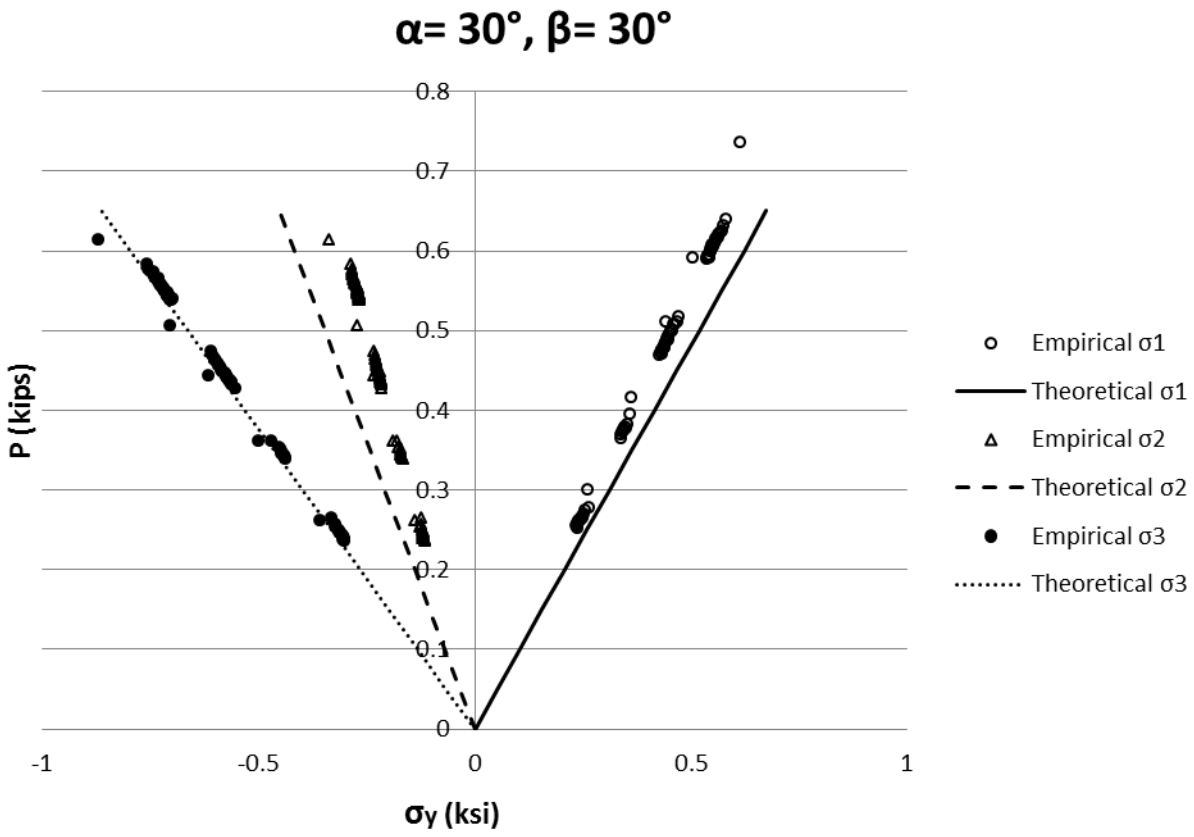
α= 30°, β= 30°
0.8
0.7
0.6
0.5
0.4
0.3
0.2
0.1
0
P (kips)
-1
-0.5
0
0.5
1
σy (ksi)
Empirical σ1
Theoretical σ1
Empirical σ2
Theoretical σ2
Empirical σ3
Theoretical σ3

Figure 18

Summary Test Results											
Empirical σ (psi)			Actual Force/Direction			Calculated Force/Direction			% Error/Difference		
θ_3	θ_2	θ_1	α°	β°	P (lbs)	α°	β°	P (lbs)	P	α	β
-1744.0	257.0	150.7	0	4	1016.3	-1.6	29.2	1,259.5	24%	2	25
-1456.3	295.5	229.1	0	12	877.1	-1.1	39.2	1,251.4	43%	-1	27
-716.5	-43.0	164.9	7	5	375.0	7.6	26.1	401.9	7%	-9%	21
-989.8	-229.2	363.4	15	5	533.0	15.6	21.1	541.2	2%	-4%	16
-829.4	-157.7	354.0	15	17	488.8	15.4	32.8	526.5	8%	-3%	16
-991.4	-503.3	607.6	30	0	673.0	28.0	12.8	683.9	2%	7%	13
-772.5	-361.6	558.1	30	20	509.1	27.8	32.2	535.4	5%	7%	12
-913.6	-394.1	685.5	30	25	656.2	27.0	37.7	691.6	5%	10%	13
-809.7	-331.3	632.4	30	30	601.5	26.7	41.5	660.1	10%	11%	12
-805.2	-803.0	810.8	45	0	645.5	44.9	1.0	621.3	-4%	0%	1
-692.8	-653.3	773.8	45	15	580.0	43.5	18.7	545.9	-6%	3%	4
-636.8	-573.2	799.6	45	30	608.5	42.4	35.1	571.7	-6%	6%	5
-266.7	633.3	-478.6	-60	20	411.1	-58.2	31.4	432.0	5%	3%	11

Table 1: Summary of laboratory results for select values of α, β, and P.